ERS ANNOUNCEMENT OF OPPORTUNITY

ALGERS: THE USE OF ERS SENSORS FOR THE STUDY OF THE DYNAMICS OF MODIFIED ATLANTIC WATER IN THE ALGERIAN BASIN (WESTERN MEDITERRANEAN SEA)

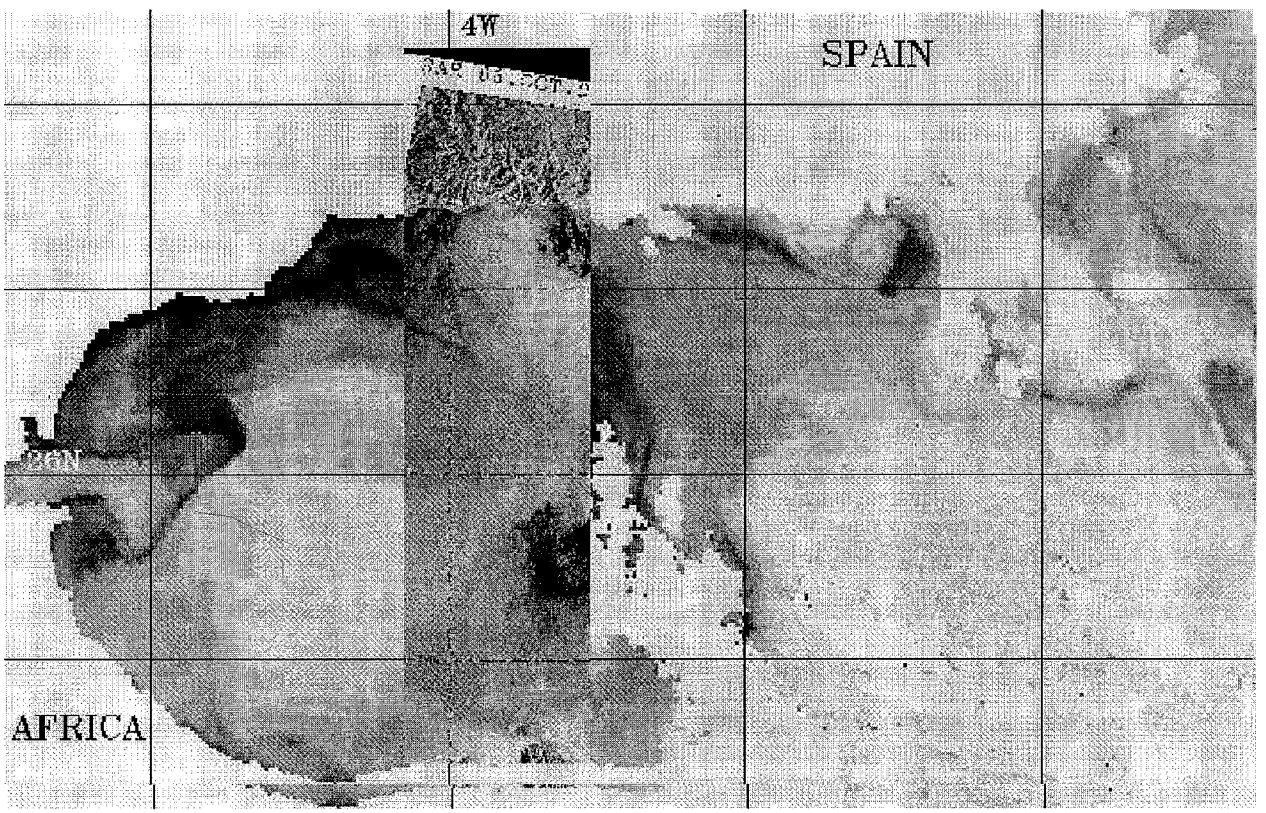

Proposal code: AO2.E102
PI: Jordi Font

R.6717

Barcelona, August 1998

FINAL REPORT

Project code: AO2.E102

Project title: ALGERS. The use of ERS sensors for the study of the dynamics of Modified Atlantic Water in the Algerian basin (western Mediterranean sea)

Report date: 31 August 1998

Author: Jordi Font, ICM-CSIC, Barcelona

Cover figure: *The jet of Modified Atlantic Water incoming in the Alboran Sea forms an anticyclonic gyre, as detected in NOAA SST and ERS-2 SAR images on 6 October 1996*

OBJECTIVES OF THE INVESTIGATION

Downstream the Alboran Sea, the jet of Modified Atlantic Water (MAW) incoming into the Mediterranean forms a well defined flow along the African coast: the Algerian current. The Algerian current does not permanently flow eastward along the Algerian slope nor smoothly spreads seaward. Due to hydrodynamic processes, mainly baroclinic instability, this alongslope current develops meanders near 0° - 1°E, that induce the formation of pairs of cyclonic and anticyclonic eddies. The cyclonic ones tend to disappear, while the anticyclonic can grow up to 50-100 km diameter, while translating eastwards along the coast at a few km/day. Large offshore anticyclonic eddies (100-200 km diameter), maybe later stages of the coastal eddies, have been observed to be quasi-steady for several months. These mesoscale structures play a major role in the configuration of the general circulation and the distribution of biogeochemical parameters in the Algerian basin. They appear to be able to deviate the flow of MAW to the north, and then have a major influence on the water mass exchanges in the Balearic channels, narrow passages that strongly constrain the meridional fluxes between the north- and south-western regions of the Mediterranean. Some of these eddies, near the Sardinia island, can interact with the vein of Levantine Intermediate Water (coming from the eastern Mediterranean) and hence strongly influence the distribution of intermediate waters throughout the whole western basin.

Satellite infrared imagery has demonstrated to be an adequate tool to identify and follow the evolution of such mesoscale structures for long periods. This is especially important for two reasons: very few *in situ* data have been collected in the Algerian basin (that is certainly the less studied region of the western Mediterranean), and the synopticity of remote sensing can provide the only experimental methodology to adequately sample and understand the turbulent nature of the regional dynamics. These big anticyclonic eddies, due to their dimensions and strength, are candidates to be resolved by present altimeters, what is not usually the case for most mesoscale features in the Mediterranean. SAR has demonstrated (see our first ERS AO proposal) to be able to identify, under certain environmental conditions, different kinds of surface mesoscale structures in the region.

Due to these circumstances, the ALGERS project (from ALGerian basin and ERS satellite) was proposed to the Second ERS Announcement of Opportunity with the general objective of using ERS sensors and other remote sensing data to study the dynamics of the surface layer in the Algerian

basin, in connection with an *in situ* experiment to be held in 1996. Specifically we proposed to investigate:

1) The generation and evolution of large anticyclonic eddies at a temporal scale of months

2) The drift of Modified Atlantic Water in relation to these large eddies

3) The identification of current shear mesoscale structures in the Algerian current

We include here the summary of the proposal as submitted to ESA in March 1994

DETAILED DESCRIPTION OF THE EXPERIMENT AND USE OF ERS DATA

As part of the European Union Marine Science and Technology Program, the MATER project (MAss Transfer and Ecosystem Response, MAS3-CT96-0051) was initiated in August 1996 as the second phase of the Mediterranean Targeted Project. This large project (more than 50 participant institutions from 15 countries) dedicated a specific task to the interdisciplinary study of the Algerian basin mesoscale instabilities, including several oceanographic campaigns, moored instrument arrays, drifting buoys, and analysis of satellite data. Another MAST project (OMEGA: Observation and Modelling of Eddy Scale Geostrophic and Ageostrophic circulation, MAS3-CT95-0001) implied field work in the Alboran Sea as well as studies on correlation between *in situ* and satellite data. With funds from these MAST projects and from the Spanish R+D National Plan (project AMB95-0901), a cruise took place in October 1996 on board the *RV HESPÉRIDES*. This cruise (leg 1: OMEGA-1, leg 2: ALGERS'96) covered the objectives announced in the ALGERS proposal for the field experiment.

Besides the oceanographic campaign, ALGERS proposal included activities in three other areas: variability of sea surface height studied with altimetry, SAR imaging of mesoscale structures, and study of the drift of MAW in the Algerian basin by surface drifters and infrared imagery.

1. *RV HESPERIDES* cruise

Several ERS SAR acquisition requests were made to cover the Alboran Sea and western Algerian basin for pre-cruise tests and identification of surface structures, and for further analysis of simultaneous *in situ* data acquired during the cruise. Conflicts with scatterometer acquisition in several ascending passes, and technical failures in some occasions, reduced the acquired passes to 13 over the Alboran Sea and 37 over the Algerian basin for the period from May to mid October 1996. 10 of them were from ERS-1 (May) and 40 from ERS-2. A total of 57 CD-ROMs were received in Barcelona from I-PAF until mid September and, after that date, 15 CD-ROMs were received in Bergen, where the NERSC team processed and analysed the images while the Spanish investigators were initiating the sea work. Under specific request, and thanks to an agreement within the OMEGA project that includes the participation of the Southampton Oceanography Centre (Dr. Trevor Guymer), from 21 September the British West Freugh satellite station recorded 15 SAR passes. As RAIDS QL5 products they were downloaded by NERSC at near-real time, analysed and transmitted by satellite link to the *HESPERIDES*.

The cruise with the Spanish *RV HESPERIDES* in the Algerian basin and Alboran Sea took place from 30 September to 21 October 1996. During the previous week a portable satellite HRPT station (Sea Space Terascan TS3000 system) was installed on board, and provided continuously infrared imagery from AVHRR/NOAA-12 and 14 until the end of the cruise. This and previous remotely sensed information was used in fine tuning the location of the ship track and sampling points.

The first leg of the cruise (30 September - 14 October) consisted mainly in 3 repeated surveys covering in less than 3 days a box of approximately 80 km by 100 km (11 parallel transects 10 km apart) on the northern boundary of the western anticyclonic Alboran gyre. The ship was continuously steaming at 8-9 knots and recording data from 3D and differential GPS, hull mounted RDI VM150 Acoustic Doppler Current Profiler, Simrad EK500 split beam multi-frequency echo-sounder and

SeaSoar towed undulating CTD, plus continuous surface water measurements and meteorological observations. Surface water samples for chemical and biological determinations were taken at regular intervals and mostly analysed on board. After that, a regular grid of CTD stations covered the same box and collected samples for chemical, biological and suspended particulate matter determinations in the upper 400 m. During this leg 3 descending ERS-2 SAR passes over Alboran (2, 6 and 9 October) were obtained in near-real time, as well as one pass (13 October) over the Algerian basin.

After unloading the SeaSoar system in Málaga, the second leg consisted in the intensive sampling of a coastal instability of the Algerian current, located between 0° and 1°E, that had been observed in the previous days by infrared imagery. In 30 stations CTD casts, together with water sampling for chemical and biological analysis, were performed down to 2700 m. In several transects perpendicular to the coast, underway ADCP current measurements and multi-beam echosounding were recorded, as well as 119 vertical profiles with XBT/XCTD probes. A total of 18 surface drifters were released upstream and in the centre of the sampled instability. One descending and 2 ascending ERS-2 SAR passes (16 and 19 October) were transmitted to the ship in near-real time.

Another cruise by the British *RSS DISCOVERY*, co-ordinated with the *HESPERIDES* cruise in the frame of OMEGA and MATER, covered in December the eastern Alboran Sea and western boundary of the Algerian basin. The results, also obtained with SeaSoar, ADCP and CTD, have been used in further analysis in comparison to ERS data.

2. Variability of sea surface height

Several tools for the processing and visualisation of altimeter data were developed, as indicated in the proposal. Some of them were completed during 1995 and reported in the final report of our previous ERS-1 project (AO E1). The algorithms for Complex Empirical Orthogonal Functions analysis, prepared at JPL, have been implemented in the computing facilities at ICM and UPC in Barcelona. For the merging of different altimetric products in objectively analysed maps of sea surface anomalies (ERS + Topex/Poseidon), it was decided to use the methodology developed at CLS/GRGS (Toulouse, France) made available to us through the joint participation in the MATER project.

A series of these maps, corresponding to the first period of coincidence of ERS-1 at 35 days repeat cycle and Topex/Poseidon (1992-1993), was used for a study of the propagation of mesoscale signals in the Algerian basin with the CEOF methodology. Results from this analysis were compared to infrared imagery (ATSR) and *in situ* data recorded near the Sardinia channel in November 1993.

Due to the specific dates it was not possible to locate any *HESPERIDES* sampling transect along altimeter tracks within few hours of the satellite pass. However, this was done in the second cruise in December on board the *DISCOVERY*. The Southampton Oceanography Centre has been analysing repeated ERS-2 tracks along these lines to follow the evolution of the detected mesoscale structures. The proposed technique of combining ADCP and hydrographic profiles, to derive the absolute surface geostrophic current perpendicular to the altimeter track, has been implemented by SOC. We have recently submitted a new proposal to ERS AO 3 to make these simultaneous *in situ* plus altimeter measurements in 1999-2000, and prepare an almost automatic computation of currents in forthcoming repeats of the same orbit.

3. SAR imaging of mesoscale structures

The examination of the SAR.PRI images previous to the cruise (May - October 1996) revealed that, in a considerable amount of scenes, mesoscale circulation structures were not observed, probably due to the prevailing wind conditions. We tried to have access to RADARSAT (through an ADRO project) wide and narrow ScanSAR images to have a synoptic view of a larger area, but due to technical and logistical reasons it was not possible. These images, as well as those received on near real time, were scarcely used for the guidance of the oceanographic cruise in comparison to infrared AVHRR imagery.

Different methodologies of identification of structures in two-dimensional images have been tested, but by now have not been applied to this SAR data set. Although beyond the present AO time frame, a new member of the ICM team, a postdoctoral student, will work on this subject from next autumn.

Unfortunately the number of time coincidences, even in a few days lag approximation, between SAR images and *in situ* measurements is very low. This, together with the commented problems on image formation due to very low winds, has strongly limited the proposed study on the comparison of both data sources. Only in one case, 6 October 1996, some results have been obtained. A more deep analysis of this case, including different data sets, is planned within the OMEGA project.

The proposed work on SAR data assimilation has not finally been undertaken within the framework of ALGERS.

4. Drift of Modified Atlantic Water

A preliminary study of MAW circulation in the Algerian basin focused on the area of the Sardinian channel was completed in 1996. An analysis of the time evolution of surface structures by altimetry and infrared imagery for the 1992-93 period has also been done. During the *HESPERIDES* cruise 18 surface drifters were released across a coastal meander. They were tracked by ARGOS during several months, and allowed a complete study of the evolution of some mesoscale eddies and the drift of MAW in conjunction with satellite infrared imagery. The easy access, and simple processing, to AVHRR images pushed us to mainly use these kind of products to compare with drifter trajectories instead of ATSR.

RESULTS AND CONTRIBUTION OF ERS DATA

The results obtained during the ALGERS project can be classified in three main topics:

1. The variability of surface circulation in the Algerian basin studied by altimetry

This study was mainly developed by Catherine Bouzinac, who carried out a PhD thesis work on this subject at the Institut de Ciències del Mar (Barcelona) from 1994 to 1998 under the direction of Dr. Jordi Font, and in close collaboration with other ALGERS Co-Investigators: Drs. Jorge Vázquez, Claude Millot and J.J. Martínez-Benjamin. She obtained her Doctoral degree at the Université Pierre et Marie Curie (Paris VI) in November 1997.

The combination of ERS (good spatial resolution) with Topex/Poseidon (good temporal resolution) altimeter data has been successful in the adequate sampling of the big mesoscale structures generated by instabilisation of the Algerian current. It has been possible to derive several characteristics of the dynamics of this region by analysing combined maps of sea surface anomalies.

The following is a part of Dr. Bouzinac's thesis that includes a comparison between altimetric Sea Level Anomalies with other satellite and *in situ* information, as well as a paper (Bouzinac et al., 1998) published in the Journal of Geophysical Research ERS special issue, that summarises the results of the Complex Empirical Orthogonal Functions analysis.

THESE de DOCTORAT

de l'université

PIERRE et MARIE CURIE (PARIS VI)

spécialité: OCEANOGRAPHIE PHYSIQUE

VARIABILITE SPATIALE ET TEMPORELLE DE LA CIRCULATION SUPERFICIELLE DANS LA REGION DU COURANT ALGERIEN

CATHERINE BOUZINAC

soutenue le 13 novembre 1997, devant le jury composé de:

Monsieur Jordi FONT	directeur de thèse
Monsieur Claude FRANKIGNOUL	président du jury
Monsieur Pierre DE MEY	rapporteur
Monsieur Jean-Claude GASCARD	rapporteur
Monsieur Claude MILLOT	examinateur
Monsieur Jorge VAZQUEZ	examinateur

Table of Contents

List of Tables

5. COMPARISONS OF ALTIMETRIC DATA WITH IN-SITU AND INFRARED DATA

5.1. INTRODUCTION

The combined altimetric data of ERS-1 and T/P have never been used before for a local study in a Mediterranean basin. *Ayoub et al.* (1997), the authors of the SLA maps, have observed the general patterns of the mesoscale variability in all the western Mediterranean sea, but they have not detailed their observations at the basin scale. It is thus necessary to know what are the smallest features detected in these maps of 0.2-degree resolution. Obviously, features smaller than 40 km are not resolved, but the objective analysis has also a smoothing effect. In order to estimate the spatial resolution of these altimetric data and to confirm some of the patterns they reveal, the SLA and GVA maps are compared with dynamic heights derived from the CTD data and with SST images, respectively. Then, in order to estimate the correspondence between SLA and SST, time correlation is computed in all the study area.

5.2. COMPARISON WITH CTD DATA

In this section, the SLA are compared with the dynamic heigths obtained from the four different CTD data transects of the PRIMO-1 experiment in 1993 presented in Section 3.1.1. The SLA are spatially interpolated on the exact position of each CTD cast. Three of the CTD transects, dated of 11-Nov-1993, are compared with the 11-Nov-1993 SLA data. The fourth transect dated of 12-Mar-1993 is compared with an interpolation in time of the 06-Mar-1993 and the 16-Mar-1993 SLA data.

Since the altimetric available data are anomalies from the annual mean sea level and not absolute sea surface heights, they cannot be compared directly to dynamic heights from hydrography. Actually, a correct comparison has to be performed with the SLA added to the annual climatological dynamic heights, using the method of *Hernandez et al.* (1995) with the climatological data of the Mediterranean Oceanographic Data Base (see Section 3.1.2). The problem is to choose an as good as possible reference depth, which is supposed to be a level of no motion, to compute the dynamic heights. In the T2S region, no constant level of no-motion can be really encountered since the circulation in the deep and intermediate layers is subject to significant spatial variations and are not negligible by place (*G.P. Gasparini*, personal communication). However, for each transect, the level of reference has been finally chosen as a compromise to have both a level of reference as deep as possible and sections wide enough to prevent extrapolation on the slopes. Assuming typical velocities of the order of 1 cm/s at the reference level and horizontal spatial scales of 10-100 km, the error due to the surface contribution of the missing deep component is of the order of 0.1-1 dyn. cm. In the same way, an error of the order of 1 dyn. cm is also assumed for the climatological dynamic heights calculated relative to the same reference level. Δa being the error associated to the SLA and Δb being the error associated to the climatological dynamic height, the total error is $\Delta c = \Delta a + \Delta b$.

It is worth noting that the SLA are relative to the 1993 mean, while the annual climatological hydrography is an average on various years. Therefore, the interannual variability of the sea level can have a significant effect on these comparisons. Also, hydrological measurements do not take into account the barotropic component of the sea level, which exists in the Mediterranean sea, mainly due to wind. Moreover, the SLA correspond to the real sea surface while the upper CTD are measured at the depth of 5 m. For example, in the case of a contraction of the mixed layer due to an homogeneous temperature decrease of 5 C induced by a cold wind burst, the 5 m superficial water column incurs a fall of about 0.5 dyn. cm (see Annex B).

North of Sicily (Figure 5.1)

In March 1993, north of Sicily (see Figure 3.2 and Table 10.2), the reference level of 800

dbar has been used. The mean slope of the rising surface near Sicily due to the eastward flow along the northern coast of Sicily is visible from the climatological data but appears like a narrow vein at 38.3°N from the CTD data. This feature is not detected by the SLA data and the associated errors given by the objective analysis are greater near the coast probably due to the bad quality of the ERS-1 altimeter data in that area. An offset of about 7 cm between the SLA and the dynamic heights from CTD is visible. It might be due to the steric effect of the seasonal cycle. Indeed, on 16 March 1993, the spatial mean seasonal signal is about -7 cm (see Figure 6.1), but this signal should be as well observed in the CTD data. This offset could thus be explained by a barotropic component not measured by hydrography, since in March, the strong winds are still quite frequent. The fact that the SLA maps are available on 6 and 16 March 1993 and the CTD are of 12 March 1993 could be the reason why, even after a translation of 7 cm, the weak slopes of the sea level from the altimetric and the in-situ data, on scales of 50 km, are not in agreement.

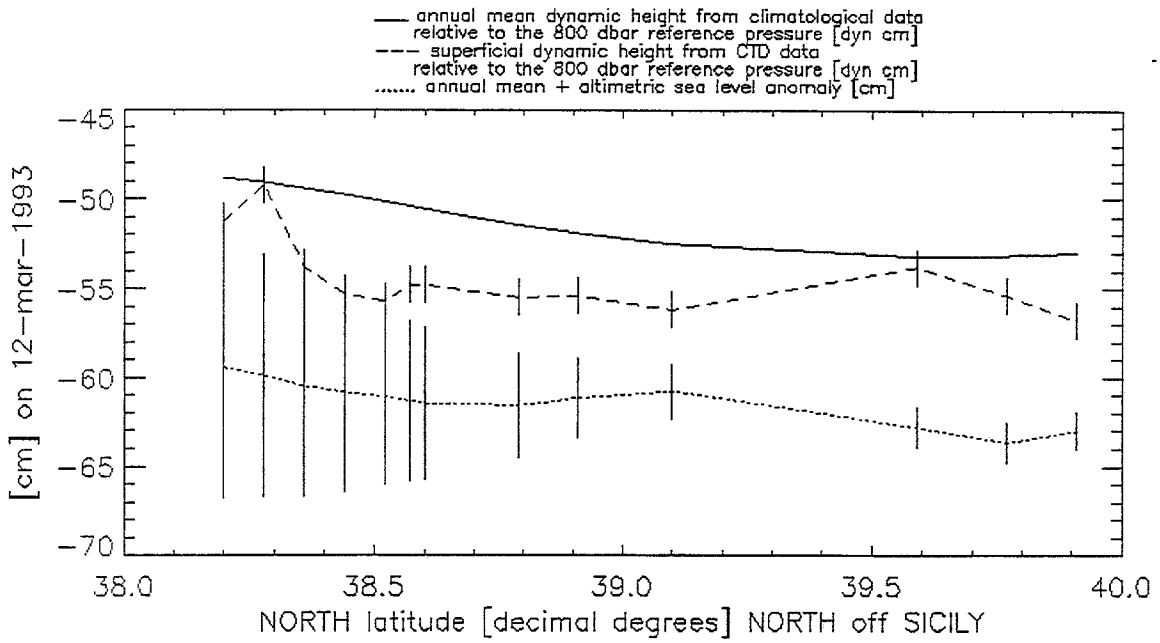

Figure 5.1: Dynamic heights relative to 800 dbar north of Sicily in March 1993. Full line corresponds to the annual mean dynamic height calculated from climatological data. Dotted line corresponds to the SLA added to the previous climatological height. Dashed line corresponds to the superficial dynamic height calculated from CTD data.

Strait of Sicily (Figure 5.2)

In November 1993, between Tunisia and Sicily (see Figure 3.3 and Table 10.4), the reference level of 180 dbar has been used. The mean slope of the rising surface near Tunisia due to the MAW southward flow through the strait is well visible on the three curves. The mean slopes from altimetry and hydrography are in good agreement. However, the CTD data display a sinusoidal shape of the dynamic sea level that is not evidenced by the SLA data and that could be due to two small eddies (cyclonic near Tunisia and anticyclonic near Sicily with diameters of about 50 km) of short time life.

Sardinia-Sicily section (Figure 5.3)

In November 1993, between Sardinia and Sicily (see Figure 3.3 and Table 10.3), the reference level of 500 dbar has been used. The altimetric SLA and the in-situ dynamic heights are in good agreement, except between 10.0°E and 10.5°E where the altimetry indicates a cyclonic anomaly, and near Sicily where the hydrography shows higher dynamic heights. This last feature has a spatial scale of about 30 km which is not resolved by the altimetric data. But the cyclonic anomaly has a diameter of about 80 km and is not visible in the CTD transect. However, looking at the climatological heights, the cyclonic tendency seems to be the usual situation. This indicates that

an anticyclonic anomaly is suggested by the CTD data. Thus, an anticyclonic eddy of short time life could be present at this place, but not sampled by the altimeters or deleted by the time smoothing effect of the objective analysis used to obtain the SLA map, as in the case of the strait of Sicily.

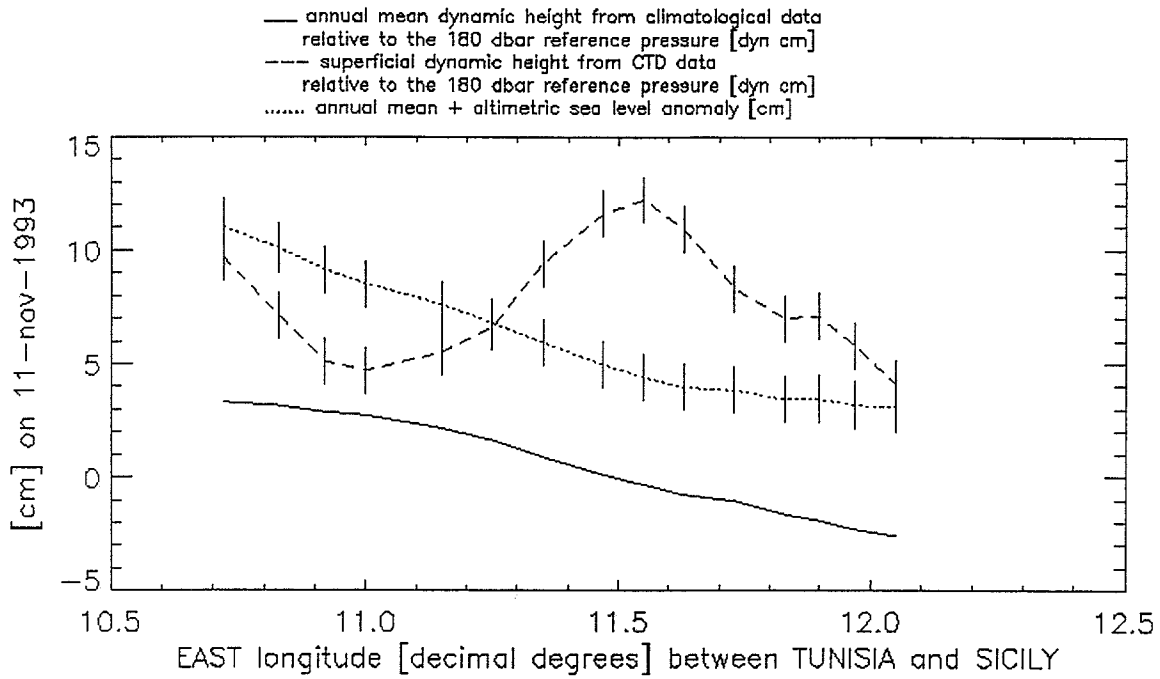

Figure 5.2: Dynamic heights relative to 180 dbar across the strait of Sicily in November 1993. Full line corresponds to the annual mean dynamic height calculated from climatological data. Dotted line corresponds to the SLA added to the previous climatological height. Dashed line corresponds to the superficial dynamic height calculated from CTD data.

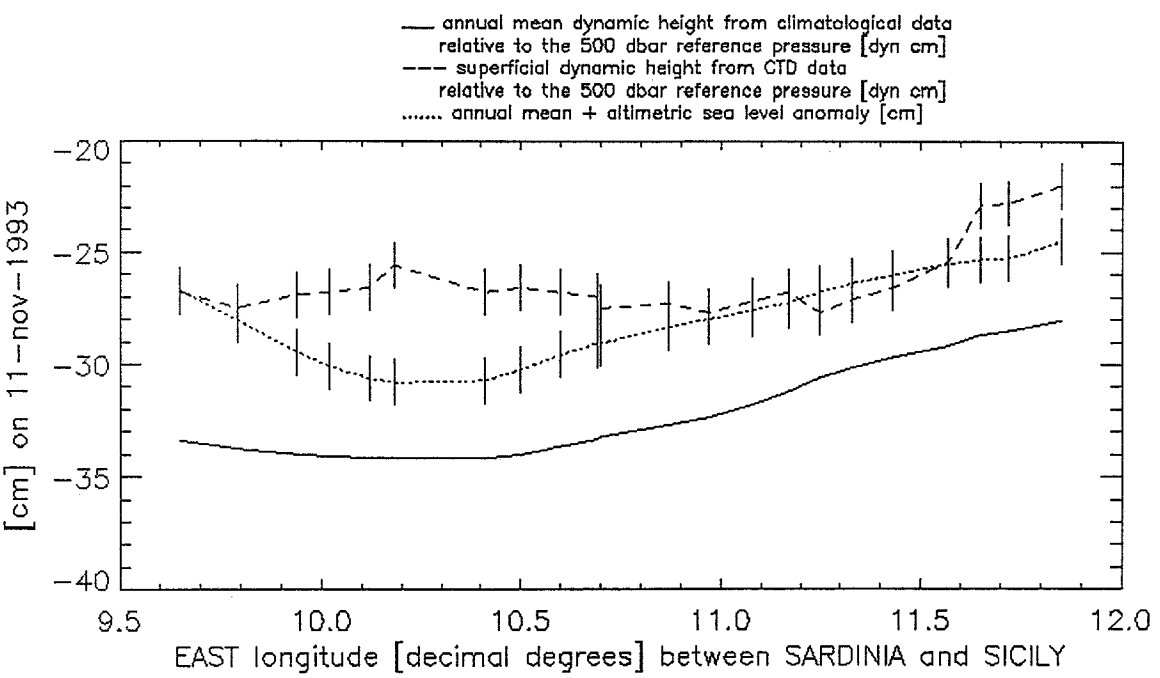

Figure 5.3: Dynamic heights relative to 500 dbar between Sardinia and Sicily in November 1993. Full line corresponds to the annual mean dynamic height calculated from climatological data. Dotted line corresponds to the SLA added to the previous climatological height. Dashed line corresponds to the superficial dynamic height calculated from CTD data.

Channel of Sardinia (Figure 4.8)

In November 1993, between Tunisia and Sardinia (see Figure 3.1 and Table 10.1)), the reference level of 800 dbar has been used. The altimetric SLA and the in-situ dynamic heights are in very good agreement. This may be attributed to the facts that no small circulation features are present and this section is oriented north-south with a better altimetric spatial resolution. The strong MAW eastward flow along the Tunisian shelf is well visible by an elevation of the sea surface of about 5 cm (see Section 4.4).

5.3. COMPARISON WITH ERS-1/ATSR/SST IMAGES

Nearly 90 ERS-1/ATSR/SST instantaneous images and the corresponding altimetric data have been examined from October 1992 to December 1993. Among all these images, only 13, presented here, are not too cloudy and evidence interesting SST gradients. On these images, the most contemporary GVA maps have been superimposed to see whether the SST gradients and the GVA currents coincide or not. On all the figures, blue and red correspond respectively to cooler and warmer waters and the 1000-m and 2000-m isobaths are shown. Flagged clouds are white and land is black. Some Algerian eddy characteristics, seemingly significant, are pointed out from these comparisons.

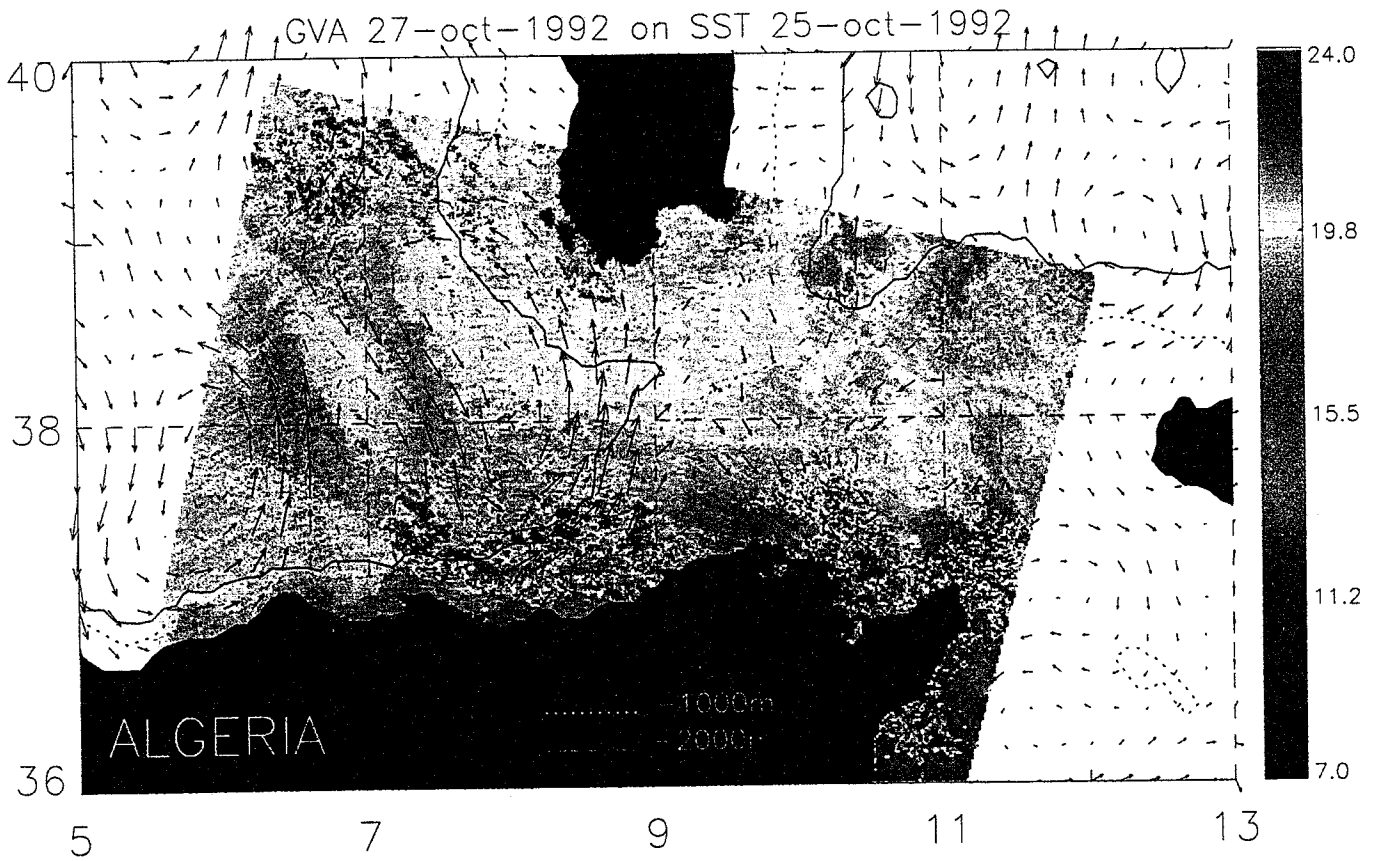

GVA map 27-Oct-1992 and SST image 25-Oct-1992 10h GMT (Figure 5.4)

On this SST image, an oval ring of warmer water is visible at about 7°E, 38.2°N. On the GVA map, it is located just between two large cyclonic anomalies. The jet from northwest to southeast, part of the eastern cyclonic anomaly west of the channel of Sardinia and the northward velocities of the western cyclonic anomaly seem associated with the warmer water. This could correspond to the beginning or the end of an anticyclonic warmer ring.

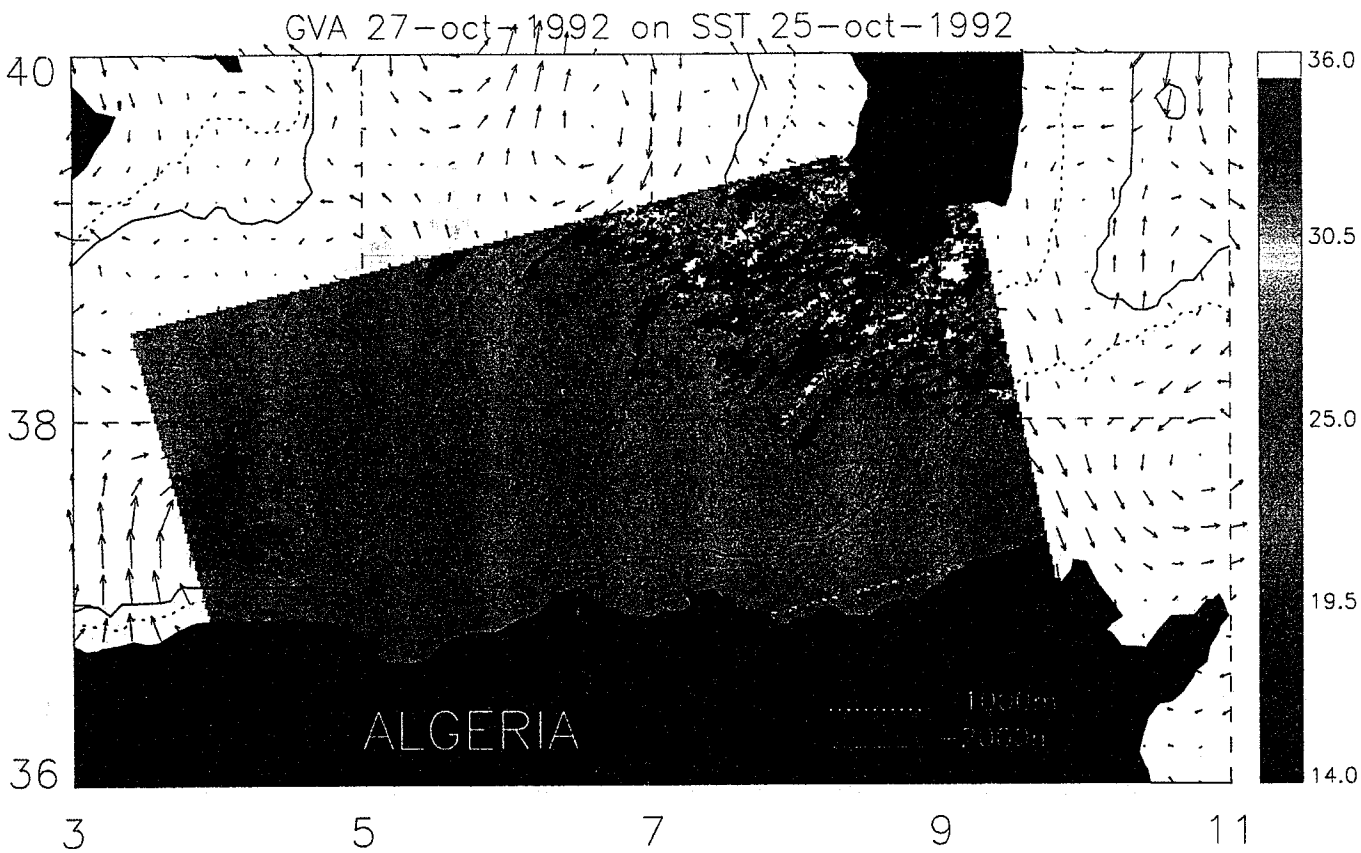

GVA map 27-Oct-1992 and SST image 25-Oct-1992 21h GMT (Figure 5.5)

An eddy of colder water is visible near the Algerian coast at 4-5°E. The GVA indicate that this eddy is anticyclonic, but its centre on the GVA map does not coincide with its centre on the SST image. However, the GVA suggest that the colder MAW of the Algerian current are first interacting with an anticyclonic eddy and then come back along the coast.

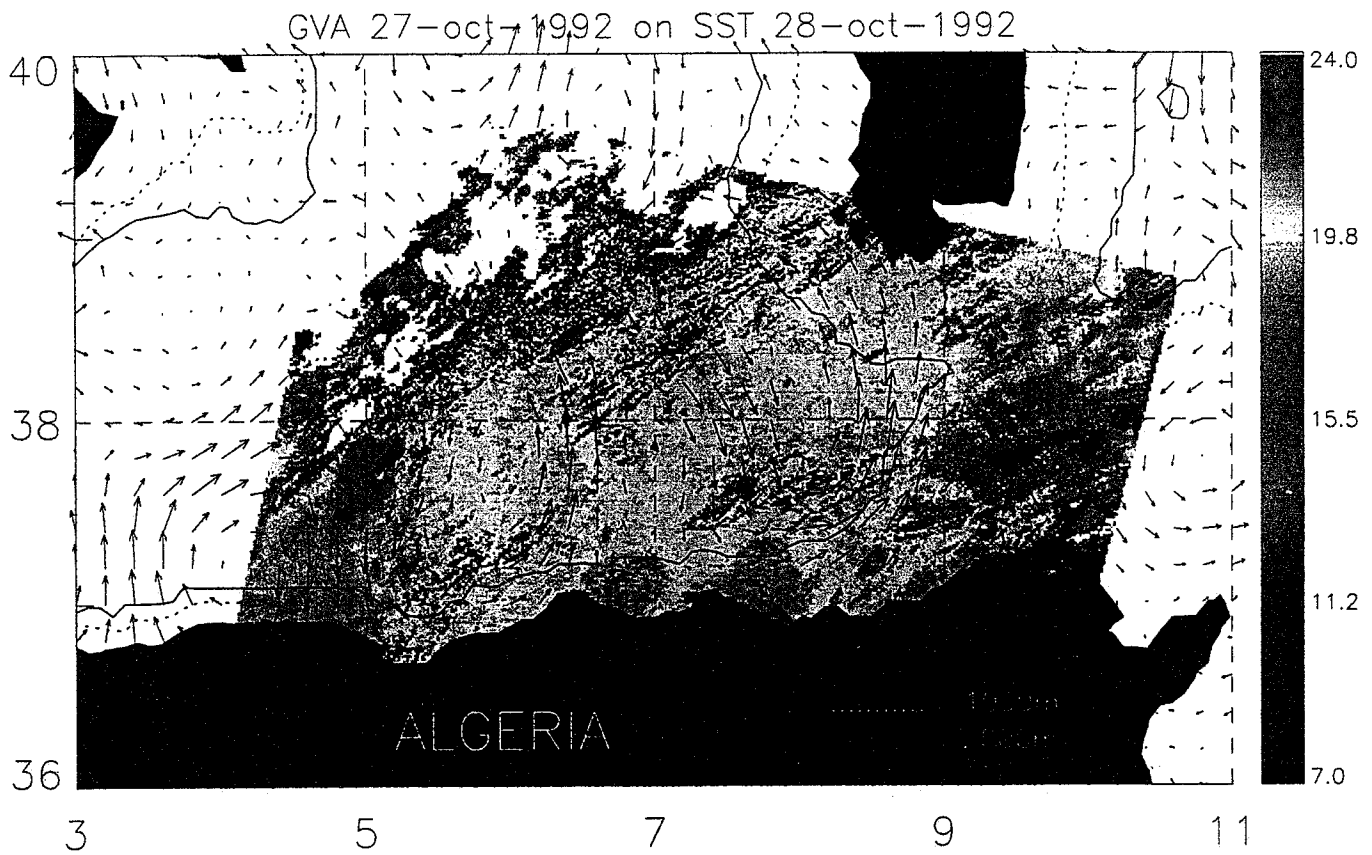

GVA map 27-Oct-1992 and SST image 28-Oct-1992 10h GMT (Figure 5.6)

This SST image shows three or four small meanders of warmer water due to the instability of the Algerian current along the coast with spatial scales less than 50 km. These features are not visible in the SLA map, probably because of their short time life and small size and also because of the bad quality of the altimetric data in the coastal zone.

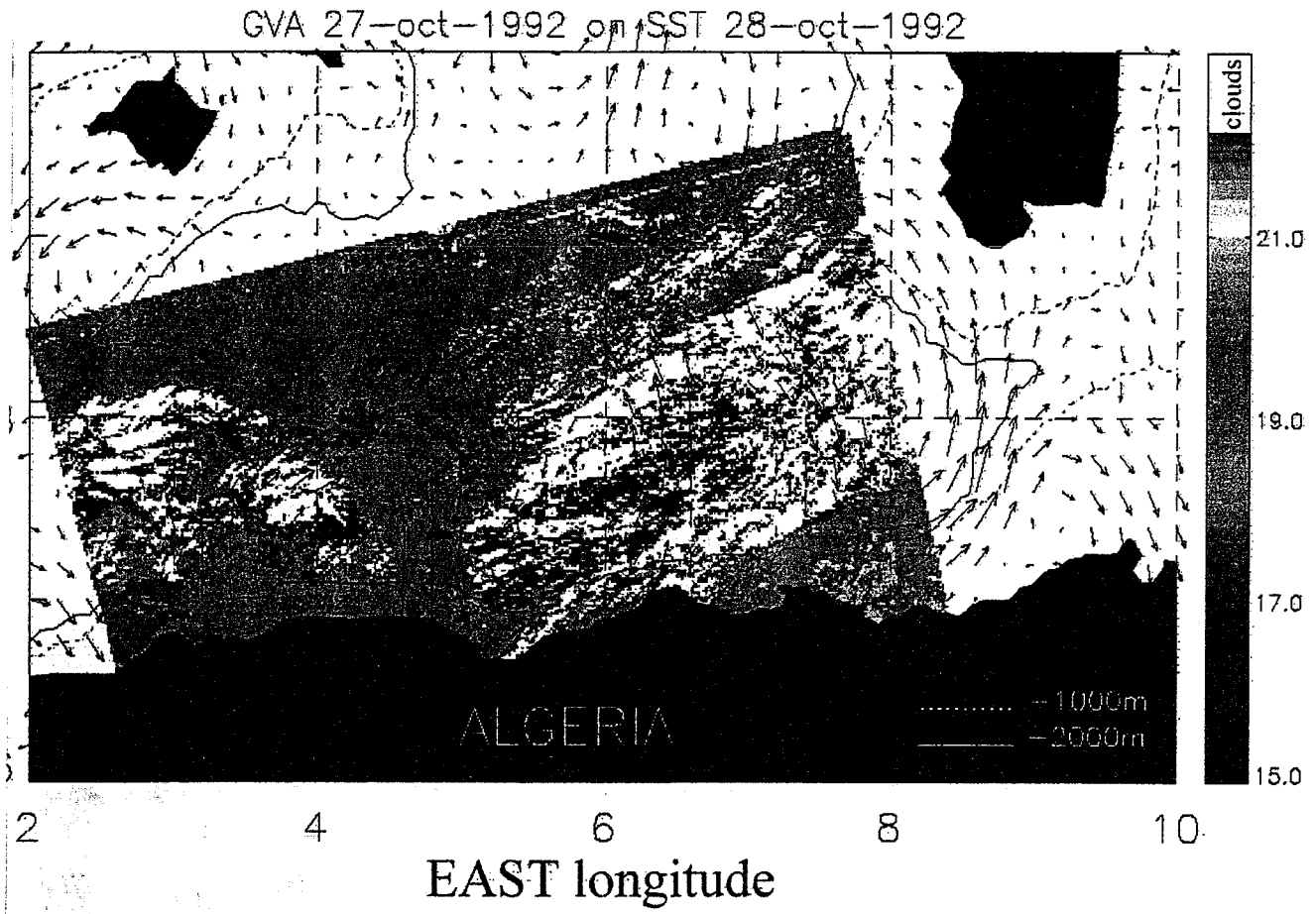

GVA map 27-Oct-1992 and SST image 28-Oct-1992 22h GMT (Figure 5.7)

The same anticyclonic eddy of cooler surface water, detected three days before, with warmer water trapped inside, is now clearly visible just between two masses of clouds, centered at about 4.5°E and 37.5°N with a diameter of about 100 km. At this location, the altimetric map does not display a well defined circular positive anomaly, but a rather oval one with a northeast extension overlying the cooler water of the picture. The resulting GVA eddy is centered at 4°E and 37 °N. The offset between the SST and the GVA may be due to the SLA mapping interpolation and to the motion of the eddy. The hypothesis that this eddy began as a meander of the current a few days before the 27th of October, then developed and moved eastward a few days after, could explain the resulting oval (and not circular) form in the altimetric signal. Nevertheless, between 25 and 28 October, the eddy does not seem to have moved; thus, its motion might be very slow. The strongest GVA is 32 cm/s at 3.8°E, 37.6°N for the western edge and 38 cm/s at 4.8°E, 37.4°N for the eastern edge. Both maxima are located in the coolest vein of the eddy. These velocities are of the same order of magnitude than the ones obtained by *Benzohra and Millot* (1995a) from hydrography who reported 30 cm/s eastward in the northern part of a smaller coastal anticyclonic eddy of about 50 km in diameter at 4°E. The evolution of this anticyclonic anomaly can be followed in consecutive maps of SLA. Even if this anomaly really corresponds to an eddy at the end of October as shown by the SST image, this cannot be asserted during the following months; that is why the word "anomaly" is employed here instead of "eddy". First, it moves eastward along the coast until the end of December 1992. Then, from January to February 1993, it deviates progressively toward the center of the basin at about 6°E and desappears. Unfortunately, no ATSR image free of clouds has been found between November 1992 and February 1993 to corroborate that this anomaly still corresponds to an anticyclonic eddy.

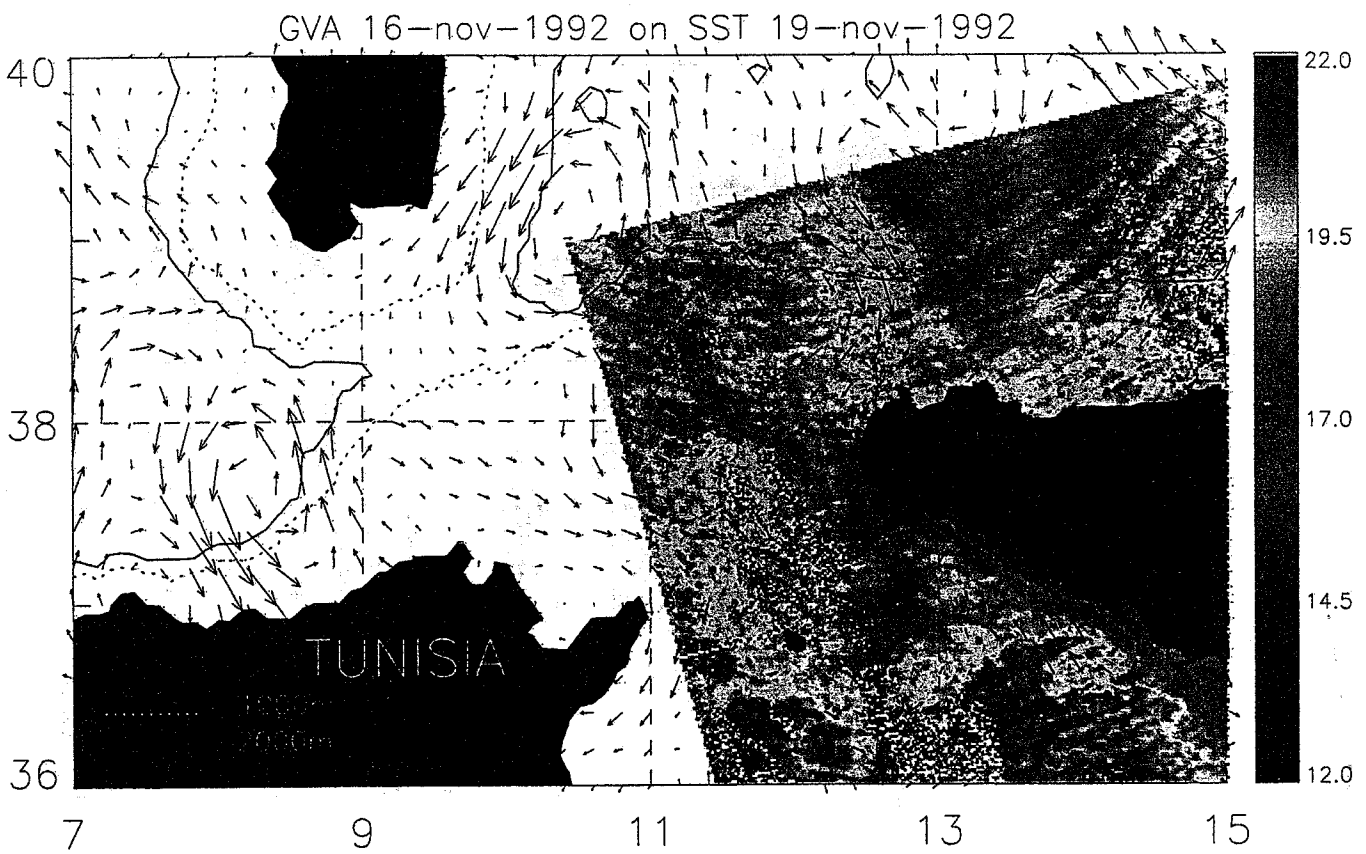

GVA map 16-Nov-1992 and SST image 14-Nov-1992 21h GMT (figure 5.8)

An anticyclonic anomaly northwest of Sicily contributes to a southward jet which seems to bring warmer water from the north toward the island. This warmer water follows the northern coast of Sicily in agreement with the GVA. Along the southwest coast, several tongues of cold water, which are wind-induced coastal upwellings (*Le Vourch et al.*, 1992), are visible on the SST image but they do not correspond to any GVA feature, except perhaps at the southern point of the island where the superficial current anomaly is coherent with the front associated with the upwelling.

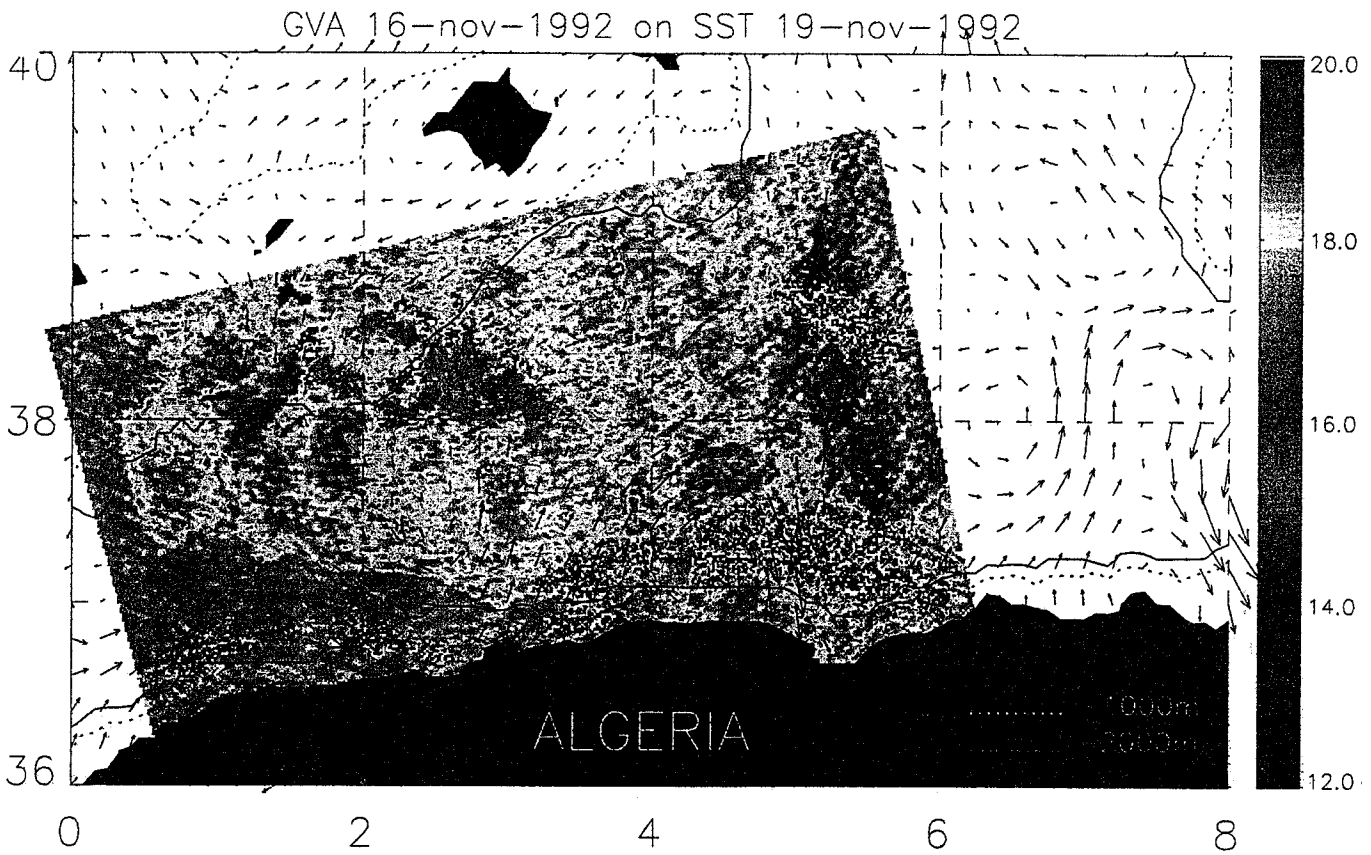

GVA map 16-Nov-1992 and SST image 19-Nov-1992 22h GMT (Figure 5.9)

An intensification of the Algerian current between 1°E and 3°E is associated with colder water flowing eastward along the coast. There, the GVA and SST are in very good agreement. On the contrary, just north of this jet, the SST image reveals a small cyclonic eddy (diameter of about 50 km) of warmer water that is not visible on the GVA map.

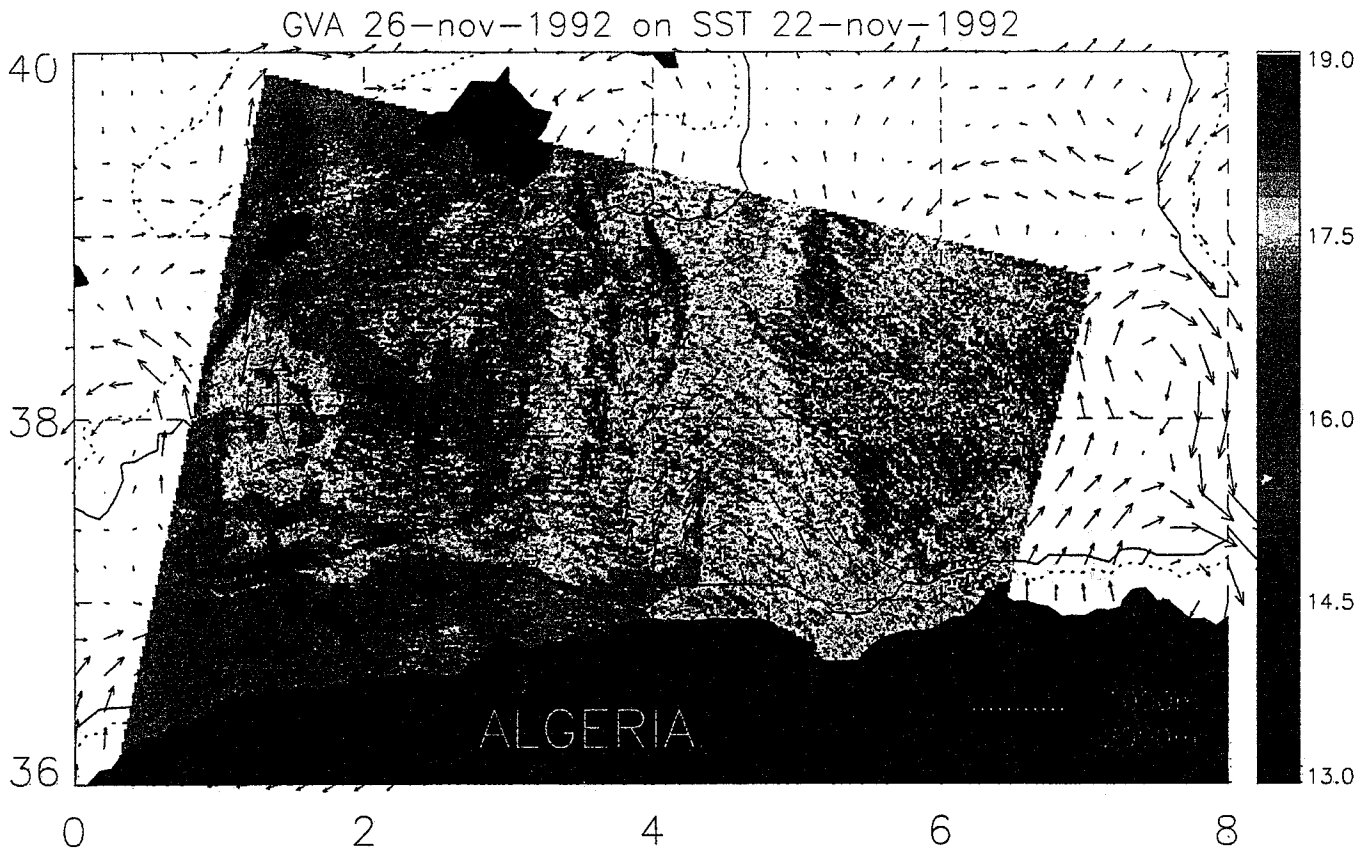

GVA map 26-Nov-1992 and SST image 22-Nov-1992 10h GMT (Figure 5.10)

In spite of the four days between the SST image and the GVA map, both data sets are in quite good agreement. A cold band seems carried along an anticyclonic anomaly due to a meander of the Algerian current, once again between 4°E and 5°E. The other parts of the image cannot be compared because of the presence of isolated clouds.

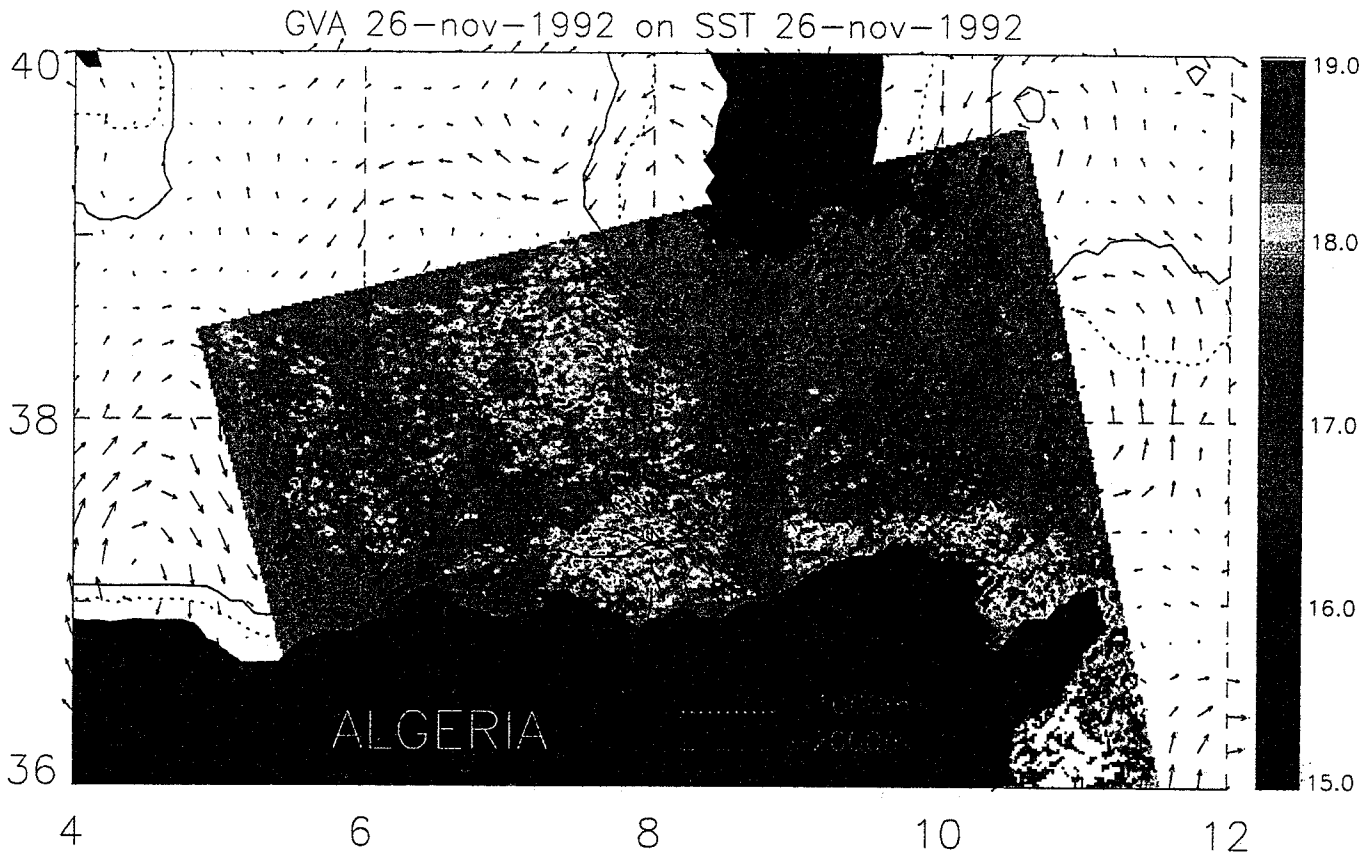

GVA map 26-Nov-1992 and SST image 26-Nov-1992 21h GMT (Figure 5.11)

Between 5°E and 7°E, colder water comes back toward the Algerian coast and then flows eatward. The greatest velocities are well superimposed on the lowest temperatures. Two anticyclonic anomalies in the western part of the Sardinia channel correspond with areas of warmer waters contrasting with colder water in the northern part of the channel. The northern anticyclonic anomaly could be a real anticyclonic eddy with warmer water in its center, while the southern anomaly could correspond to a large meander.

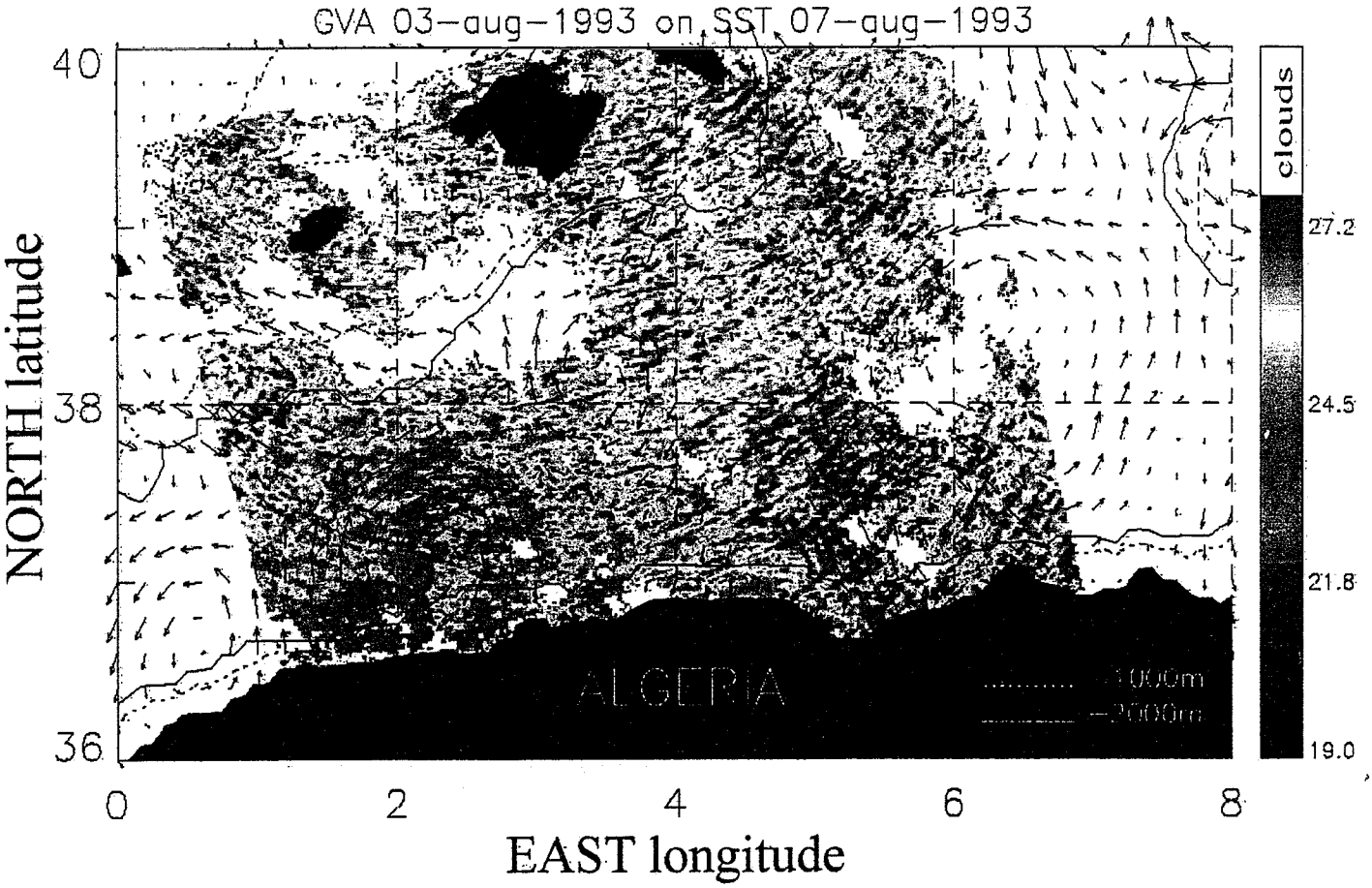

GVA map 03-Aug-1993 and SST image 07-Aug-1993 22h GMT (Figure 5.12)

Although the SST gradients are not very clear, a circular shape of cooler surface waters is detected near the Algerian coast at about 2-3°E, 37°N. The velocities reveal an anticyclonic eddy with a diameter of more than 100 km. The center of this eddy is 8 cm higher than the edge. The small shift between the eddy described by the GVA and the warmer centre visible on the SST picture, along with the 4 days separating the GVA and the SST data, suggest an eastward propagation of the eddy. The strongest velocity anomaly of 28.5 cm/s is located at 2°E, 37.4°N in the northwestern part of the eddy. Ten days later (13-Aug-1993, map not shown), the GVA maximum in this anticyclonic structure is 34 cm/s at 2.6°E, 37.4°N, in the northeastern part of the eddy. In twenty days, the eddy centre has drifted about 40 km eastward at 37°N. This gives a propagation velocity of about 2 km/day which is slightly weaker than 13 km/day observed by *Taupier Letage and Millot* (1988) during July 1984 in the same area and 3-5 km/day estimated by *Millot at al.* (1990) from IR imagery and current measurements.

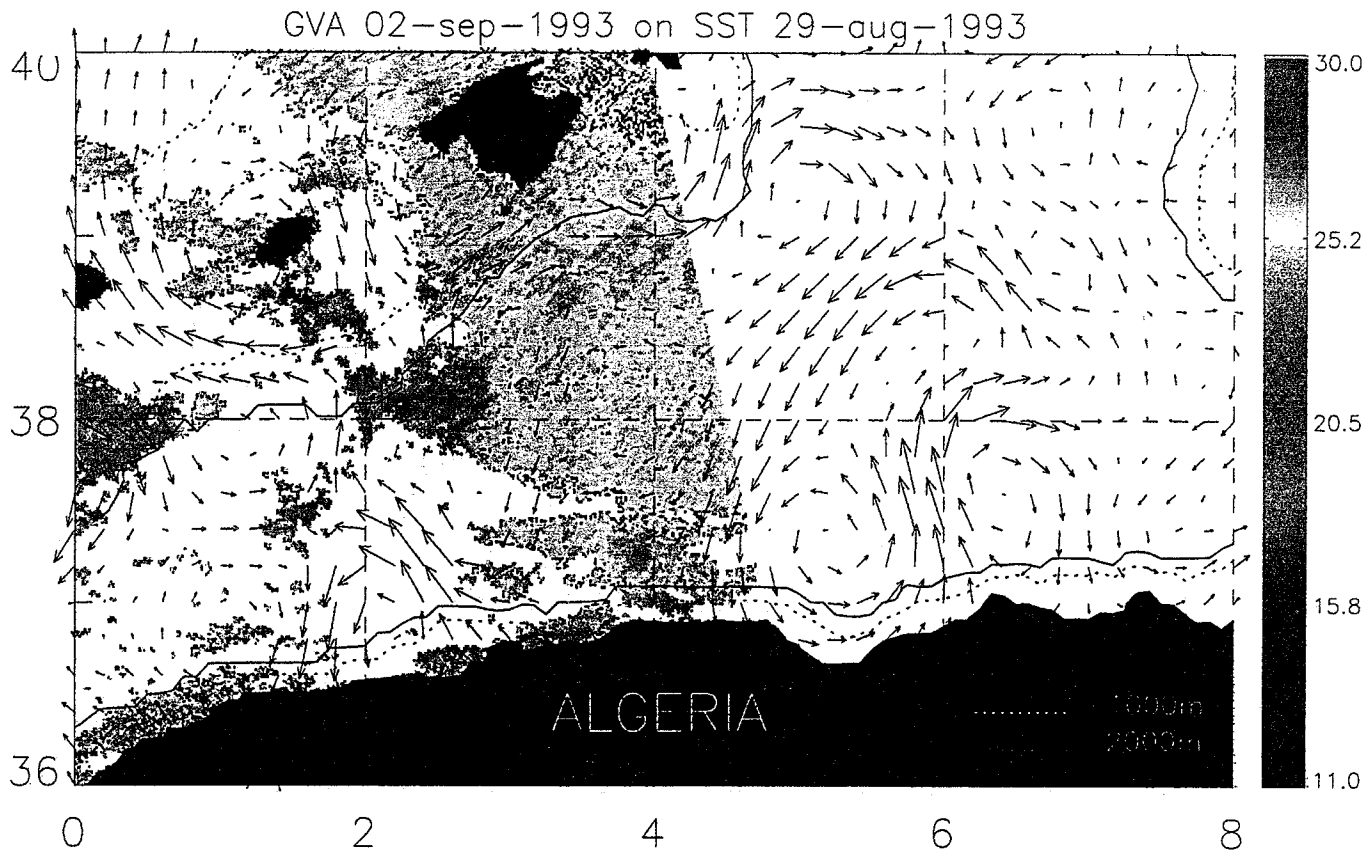

GVA map 02-Sep-1993 and SST image 29-Aug-1993 22h GMT (Figure 5.13)

In spite of the four days separating the SST image and the GVA map, it is interesting to note the eastward jet south of Mallorca that seems associated with colder water.

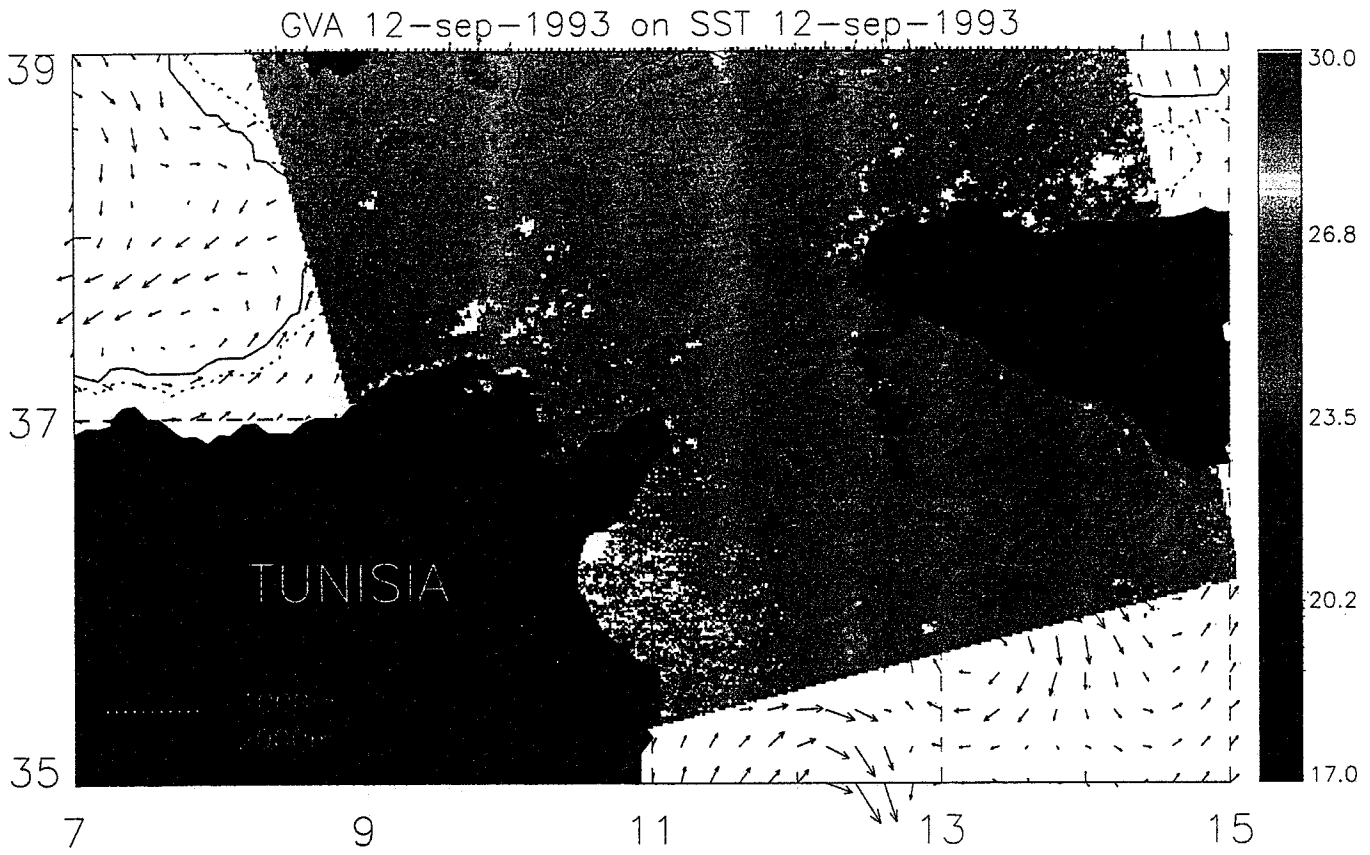

GVA map 12-Sep-1993 and SST image 12-Sep-1993 21h GMT (Figure 5.14)

In that special case, a lot of contrasts, gradients and fronts, are detected in the SST, but none seems associated to the superficial velocity anomalies, except, may be, at the southeast of Sardinia, where a weak anticyclonic anomaly could carry along colder water. Nevertheless, a typical coastal upwelling at the southwest of Sicily (*Le Vourch et al.*, 1992) could be enhanced and drawed by the strong anticyclonic anomaly occupying the strait of Sicily. While this colder water is driven southward, warmer water is driven northward on the other side of the anomaly, along the Tunisian coast.

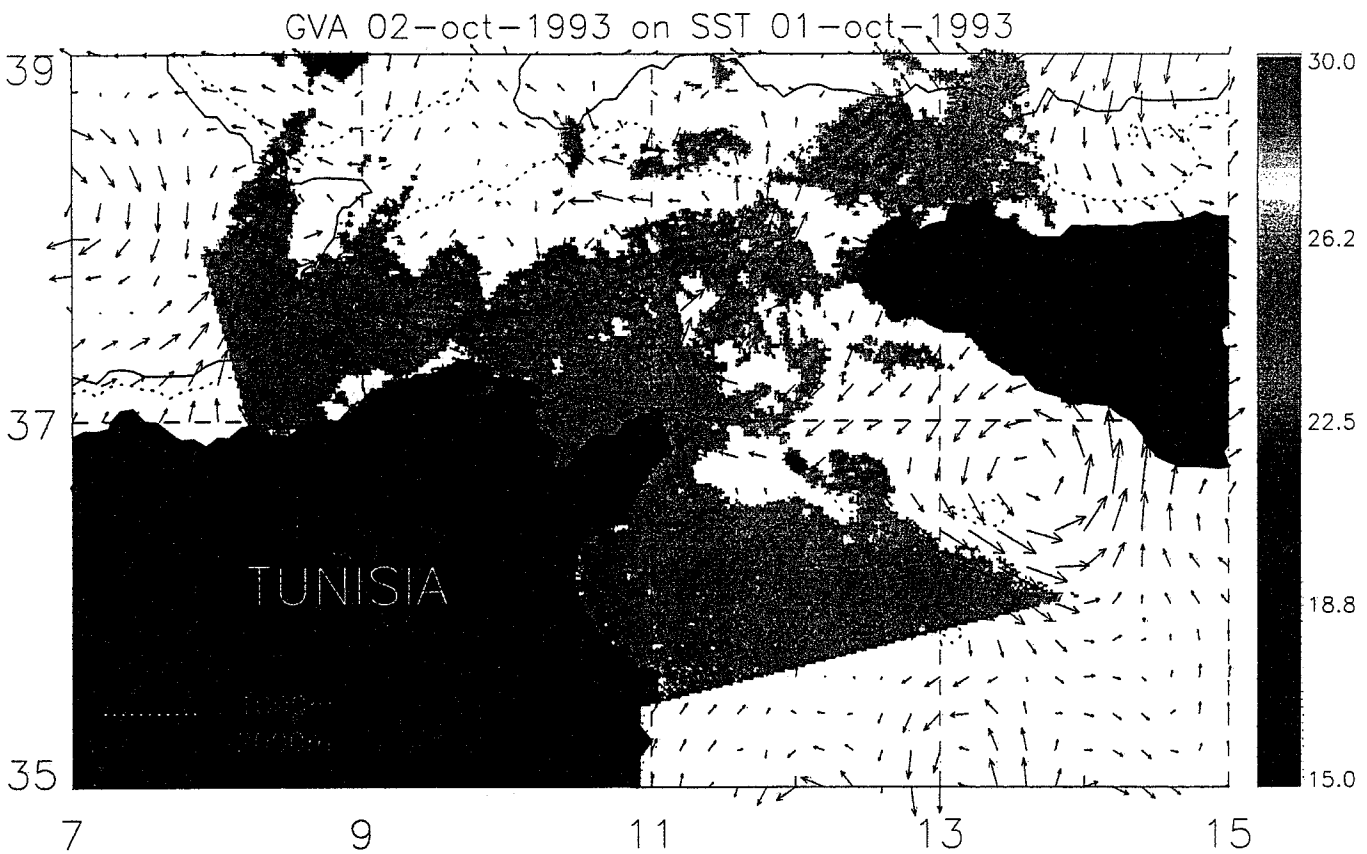

GVA map 02-Oct-1993 and SST image 01-Oct-1993 21h GMT (Figure 5.15)

East of Tunisia, a zonal thermal front separates colder waters at the north and warmer waters at the south at about 36.2°N and corresponds to an eastward zonal jet that brings warmer water from the south near the Tunisian coast. The steric difference between the warmer waters at the south and the colder waters at the north seems to induce a positive gradient of the sea level, giving eastward geostrophic components. Some filaments suggest small dynamic features inside the front.

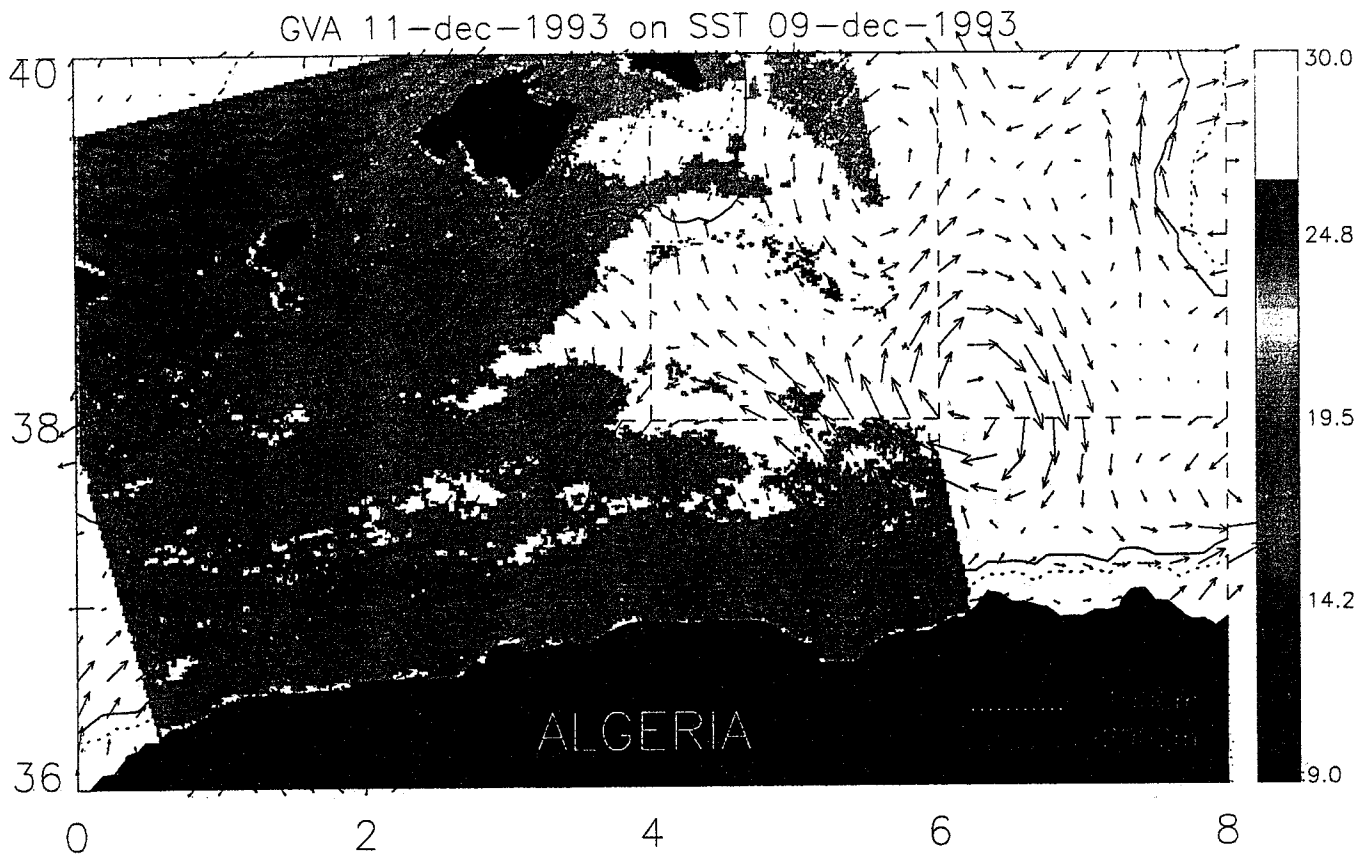

GVA map 11-dec-1993 and SST image 09-dec-1993 22h (Figure 5.16)

An intense thermal front is located between the Balearic basin and the Algerian basin (*Lopez-Garcia et al.*, 1994) but it does not coincide with any local jet or any inversion in the current direction. However, on the eastern edge of the image, the thermal front separates eastern velocities for the cold water and null velocities for the warm water. In the southwest part of the image, the Algerian current contrasts with colder temperatures that correspond with the higher velocities of a meander along the African coast.

5.4. CORRELATION WITH PATHFINDER SST MAPS

Several studies like the one of *Pattullo et al.* (1955) have shown that, at seasonal scale, the sea level faithfully records the thermal content in the mixed layer. However, at mesoscale, the relationship between SLA and SST is not trivial, since transient events can have sea level signature without thermal signature, as revealed in Section 5.3. Nevertheless, due to the different temperatures between the MAW and the surface Mediterranean waters from June to October (MAW is colder) and from January to February (MAW is warmer) (*Le Vourch et al.*, 1992), the mesoscale activity associated with the Algerian current is often visible in infrared pictures (*Taupier-Letage and Millot*, 1988). It is thus interesting to look at the correlation in time between SLA and SST in the high and low variability areas.

The 9-km Pathfinder day and night SST maps have been averaged on 10 days and 10 nights. Then, they have been spatially interpolated with an objective analysis on a grid of 0.2-degree resolution (see Section 3.3.2) to perform correlation calculations between SST and SLA maps with the same resolution in space and time. The 44 maps of the SLA time series can be considered as time independent measurements (*P.Y. Le Traon*, personal communication). However, due to some bad values due to clouds, almost all the SST time series at one point have between 40 and 44 values (Figure 5.17.a), except near the coasts where the atmospheric conditions impede a good retrieval of SST and only a few correct values are available. With 40 degrees of freedom, the 95% and 99% confidence levels are 0.30 and 0.39, respectively. For the SST, whose temporal behaviour is, by far, dominated by the seasonal variation, the number of degrees of freedom is much lower than for the SLA. The autocorrelation function gives about 6 degrees of freedom and the 95% and 99% confidence levels are then 0.71 and 0.83, respectively. The bad values of SST and the corresponding values of SLA have been removed from the time series to compute the Pearson correlation coefficient. In the case of complete time series (t=1,...,44), the Pearson correlation coefficient is:

$$P(H,T) = \frac{\sum_{t=1}^{t=44} (H_t - \overline{H})(T_t - \overline{T})}{\sqrt{\sum_{t=1}^{t=44} (H_t - \overline{H})^2 \sum_{t=1}^{t=44} (T_t - \overline{T})^2}},$$

with H standing for SLA and T for SST.

The overbar denotes the time average.

Correlation coefficient less than 0.5 is obtained in the Algerian current area until the channel of Sardinia (Figure 5.17.b). The lowest correlation is found in the centre of the basin and low correlations are also found near the coast at about 5°E and southwest of Sardinia. Only one small zone of the current shows a higher correlation of 0.6-0.7 at about 6°E near the coast. Northward, far from the current and its meanders, the correlation is higher with the maximum of 0.8 east of Minorca. This means that the variations of SST and SLA are less linked in the current area than in the surrounding zones. Figure 5.17.c and Figure 5.17.d display the best cross-correlation lag and the associated cross-correlation value, respectively. The lag is more than 50 days where the correlation is low, but even at that lag, the cross-correlation does not reach more than 0.6 in the central basin and the channel of Sardinia. An example of high correlation (0.86) is shown in Figure 5.18 for the location 5°E, 40°N (note that this SST time series has two bad values which were discarded). At this point, the cross-correlation is maximum with a lag of about 30 days. Another example of high correlation (0.76) is found at 2°E, 38.4°N (Figure 5.19), the cross-correlation is maximum with a lag of about 20 days. The comparison with an example of low correlation (0.20) at 5°E, 37°N (Figure 5.20) reveals that the difference comes from the higher variability of the SLA time series. At one point, the more variable the SLA, the lower the correlation with the SST. Actually, the correlation seems to be primarily based on the seasonal cycle because the SST is less sensitive to the mesoscale variability than the SLA. The ratio of the mesoscale variation on the seasonal variation appears to be smaller for SST (about 2/5, see also *Le Vourch et al.*, 1992 and *Picco*, 1990) than for SLA (about 5/10). Nevertheless, the highest correlation points indicate a lag of 20-30 days between the seasonal variations of the SST and the SLA, and roughly, the lowest correlations indicate notable mesoscale activity.

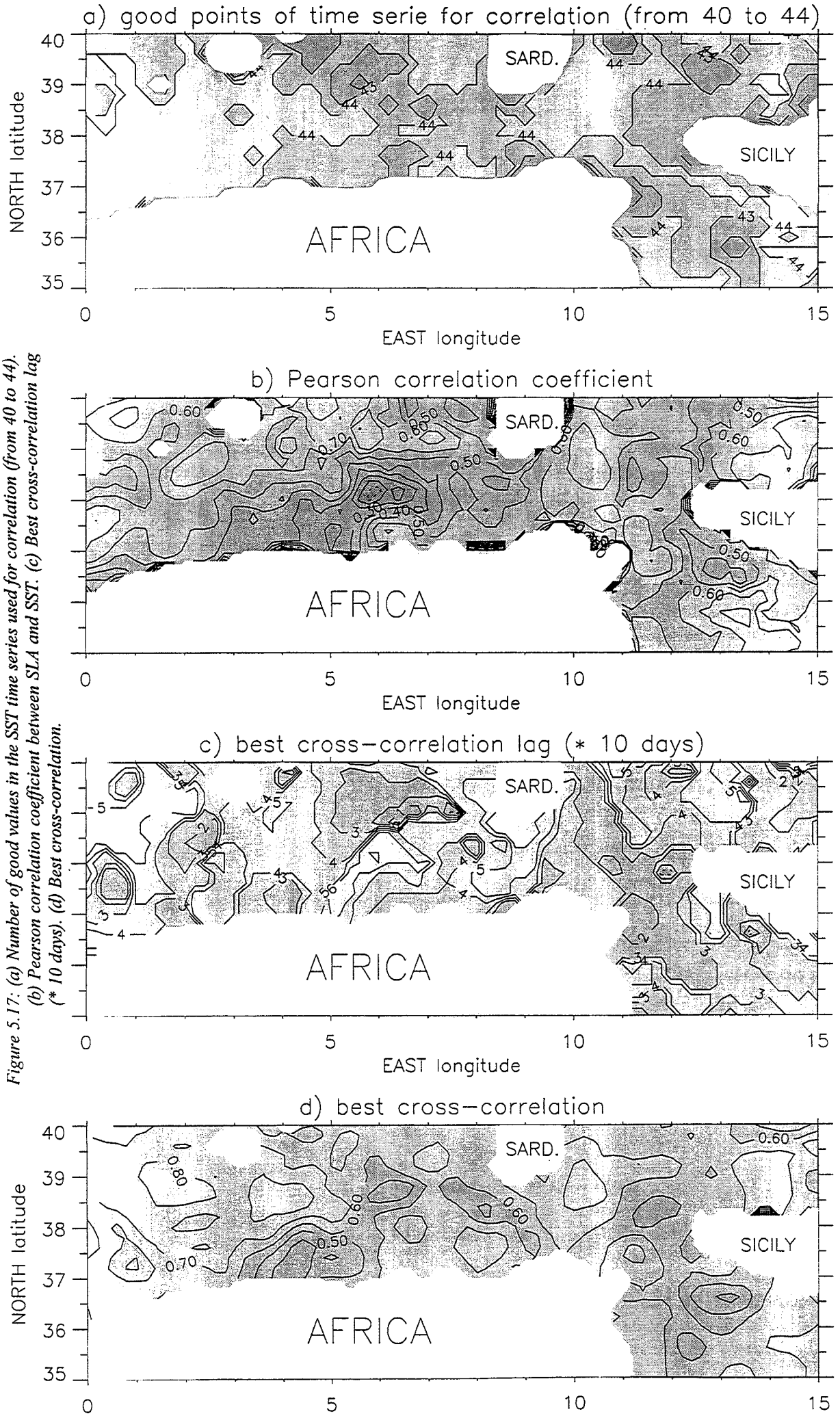

Figure 5.17: (a) Number of good values in the SST time series used for correlation (from 40 to 44). (b) Pearson correlation coefficient between SLA and SST. (c) Best cross-correlation lag (10 days). (d) Best cross-correlation.*

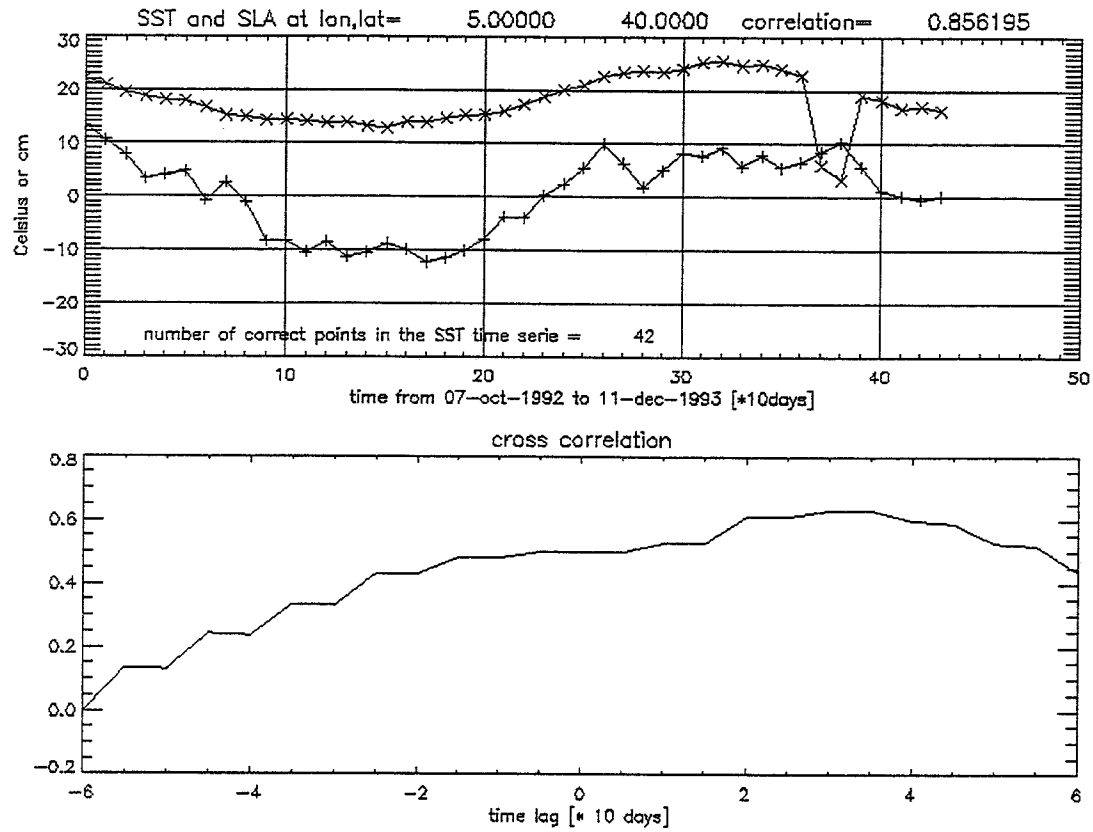

Figure 5.18: SST (C, x) and SLA (cm, +) time series at 5E, 40N and the corresponding cross-correlation function.

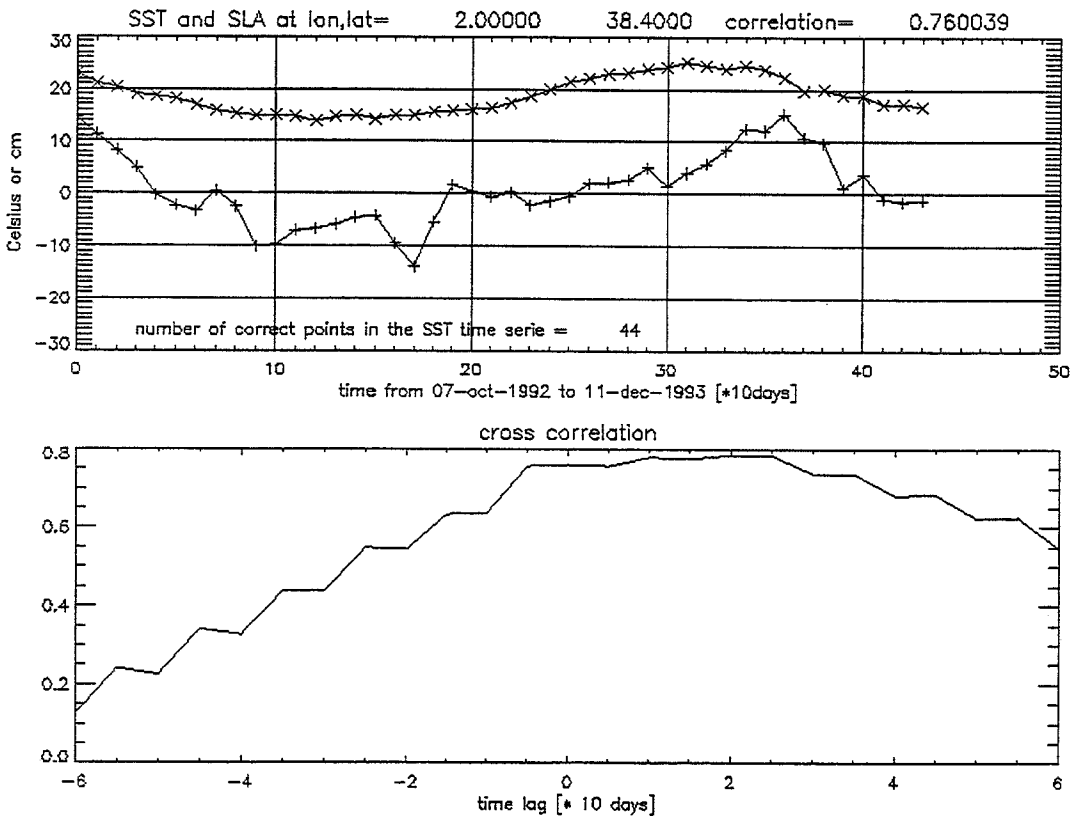

Figure 5.19: SST (C, x) and SLA (cm, +) time series at 2E, 38.4N and the corresponding cross-correlation function.

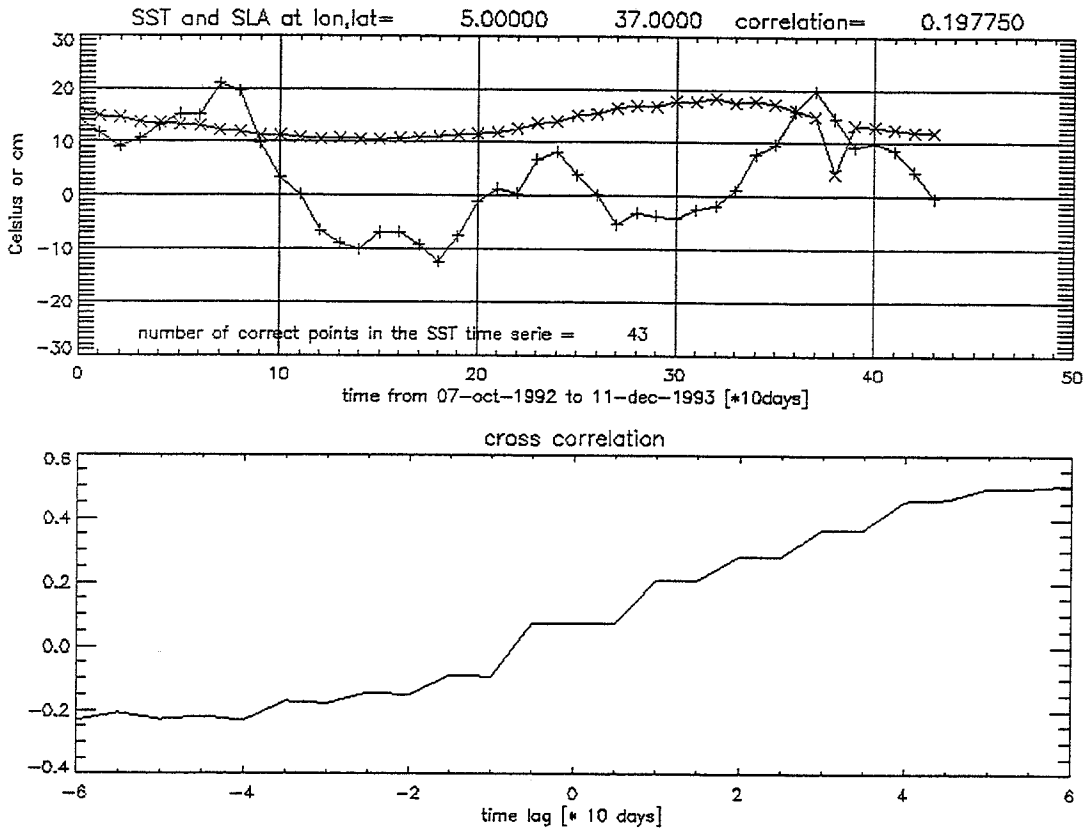

Figure 5.20: SST (C, x) and SLA (cm, +) time series at 5E, 37N and the corresponding cross-correlation function.

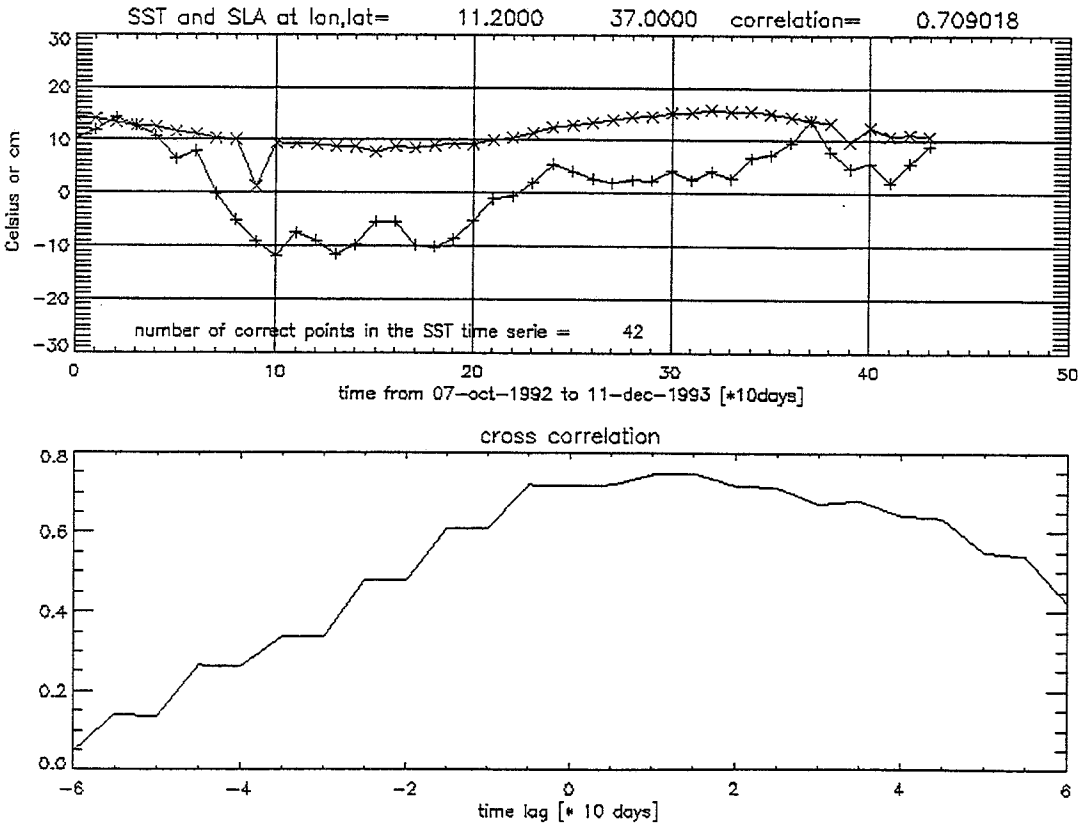

Figure 5.21: SST (C, x) and SLA (cm, +) time series at 11.2E, 37N and the corresponding cross-correlation function.

In the T2S area, the correlation is more than 0.5 almost everywhere, with the maximum (0.8) in the centre of the southern strait of Sicily. It reaches more than 0.7 northeast of Tunisia and southeast of Sardinia. An example of high correlation (0.71) is shown in Figure 5.21 for the location 11.2°E, 37°N. Here again, the lag of best cross-correlation is 10-20 days.

In the region of the Gulf Stream where the thickness of the mixed layer is about 200 m, the annual cycle at the surface leads that at the depth of 100 m by about two months (*Wang and Koblinsky*, 1996). This is consistent with a lag of 20-30 days in the western Mediterranean basin, considering that the mixed layer is only 40-50 m thick. Even if the MAW southward flow is quite turbulent near the Tunisian coast, the disturbances like meanders and rings have spatial scales of about 50 km (*Manzella et al.*, 1990) or less (see Section 5.2). This could explain the relatively small sea level variations observed at this point, compared with the ones observed at 5°E, 37°N (Figure 5.20). However, these variations are more visible in winter, with an amplitude of about 5 cm, than in summer, in agreement with the seasonal description of *Manzella et al.* (1990). Thus, the mesoscale activity is important in the T2S area but not detected as well as in the Algerian basin by the SLA maps due to smaller scales. As a consequence, the correlation between SST and SLA is better in the T2S area than in the southern part of the Algerian basin, even if both areas are subject to mesoscale variability.

5.5. CONCLUSION

As expected, the altimetric SLA are in quite good agreement with the in-situ dynamic heights on spatial scales larger than 50 km and in the absence of barotropic component. Obviously, the smaller and the short-lived features, especially in the T2S region, are not resolved by the altimetric maps. From the comparison between SST images and GVA maps, it appears that surface events can be suggested by altimetry and not by thermography, and vice-versa. However, the mesoscale features of the Algerian current are often detected with both the altimetric data and the IR data. Once again, the meanders smaller than 50 km with SST signatures are not resolved by the altimetric data because of the proper resolution of the SLA maps and probably also because of the bad quality of the altimetric data near the shore. Indeed, the time of locking on flying from land to sea for the ERS-1 altimeter is a few seconds and can give some bad data on the first 10-20 km after the coastline. Nevertheless, the observations of several anticyclonic eddies in the Algerian basin, with both altimetric and IR signatures, and the agreement of the associated GVA of 30-40 cm/s with previous in-situ velocity measurements demonstrate that it is possible to study the mesoscale activity in the Algerian basin with the combined SLA from ERS and T/P. The correlations between SLA and SST are better in the T2S area and far from the Algerian current than in the current region itself. Far from the current system where heat advection can be important, the steric component of the sea level variations is, by far, the dominant one. Moreover, these high correlations reveal a lag of 20-30 days between the SST and the SLA seasonal variations, the SST change being ahead of the SLA change. This phase lag is due to the fact that the steric changes in the sea level are the result of the thermal expansion and contraction of the upper water column, and the sea level height, unlike the SST, represents an integrated response of all the water column including the mixed layer, which requires 20-30 days in the Mediterraean sea. Finally, the low correlation between SST and SLA in the areas of high variability suggests that the SLA is a better indicator of the mesoscale events than the SST.

6. BASIC STATISTICS, KINETIC ENERGY AND REYNOLDS STRESS

6.1. INTRODUCTION

To get some preliminary and basic information on the sea level variability, statistics are performed on the SLA maps. Then, maps of Eddy Kinetic Energy (EKE) and Reynolds Stress (RS) are derived from the maps of GVA (u',v'), to gain more insight on the dynamical processes. Indeed, EKE, $(u'^2+v'^2)/2$, and RS, $\langle u'v' \rangle$, are two representative parameters of the mesoscale activity, especially in the case of meander and eddy generation (*Ikeda*, 1981; *Tai and White*, 1990).

6.2. BASIC STATISTICS ON SEA LEVEL ANOMALIES

The temporal evolution of the spatial mean SLA (Figure 6.1) shows the annual seasonal cycle of variability with a maximum value of +10 cm in fall (October 1992 and 1993) and a minimum value of -8 cm between winter and spring (February, March, April 1993). This curve is very similar to the one obtained by *Larnicol et al.* (1995) for all the western Mediterranean sea from two years of T/P data only. This means that the study area has a seasonal response quite identical to the mean response of the entire western basin. This temporal variation of the mean sea level is also in good agreement with the description of the seasonal variability of the Atlantic water inflow at the strait of Gibraltar made by *Ovchinnikov* (1974). From in-situ measurements and from salt conservation, he deduced that the sea level continuously increases from January to November and rapidly decreases between December and February.

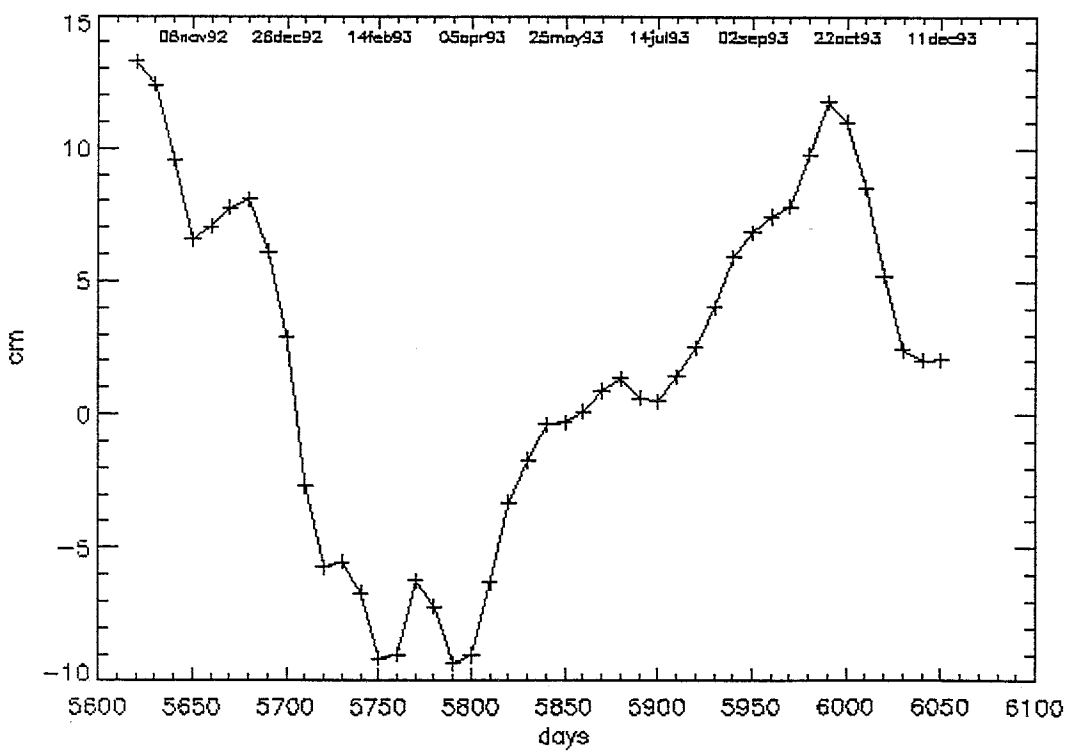

Figure 6.1: Temporal evolution of the spatial mean SLA from 07-Oct-1992 to 11-Dec-1993.

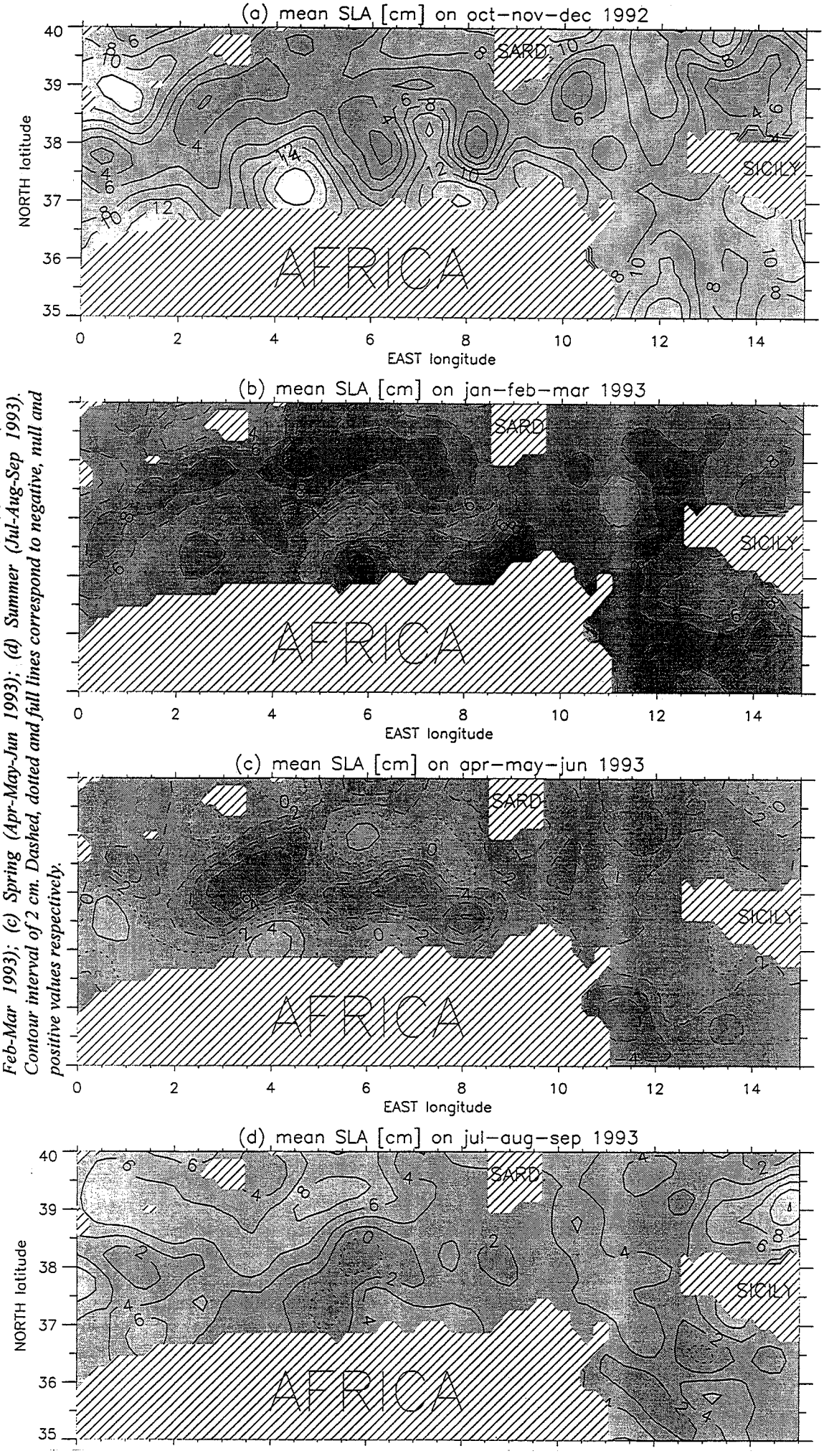

Figure 6.2: Seasonal mean Sea Level Anomalies. (a) Fall (Oct-Nov-Dec 1992); (b) Winter (Jan-Feb-Mar 1993); (c) Spring (Apr-May-Jun 1993); (d) Summer (Jul-Aug-Sep 1993). Contour interval of 2 cm. Dashed, dotted and full lines correspond to negative, null and positive values respectively.

The map of the seasonal mean SLA for the fall 1992 (Figure 6.2.a) shows various maxima along the African coast at 1-2°E, 4-5°E, 7-8°E, and 9-10°E with anomalies higher than 12 cm including a spatial mean anomaly of about 8 cm for this season. In spring 1993 (Figure 6.2.c), two similar maxima are observed at 4°E and 6-7°E with anomalies higher than 0 cm including a spatial mean anomaly is about -2 cm for this season. Whereas, in winter and summer 1993 (Figure 6.2.b and Figure 6.2.d), no such maxima can be seen along the African coast. This indicates that the Algerian current is subject to an important seasonal variability with strong positive level anomalies in fall and spring that could favour the formation of anticyclonic eddies. This temporal variability of the Algerian current will be detailed by the second mode of the CEOF analysis (Section 7.3.2).

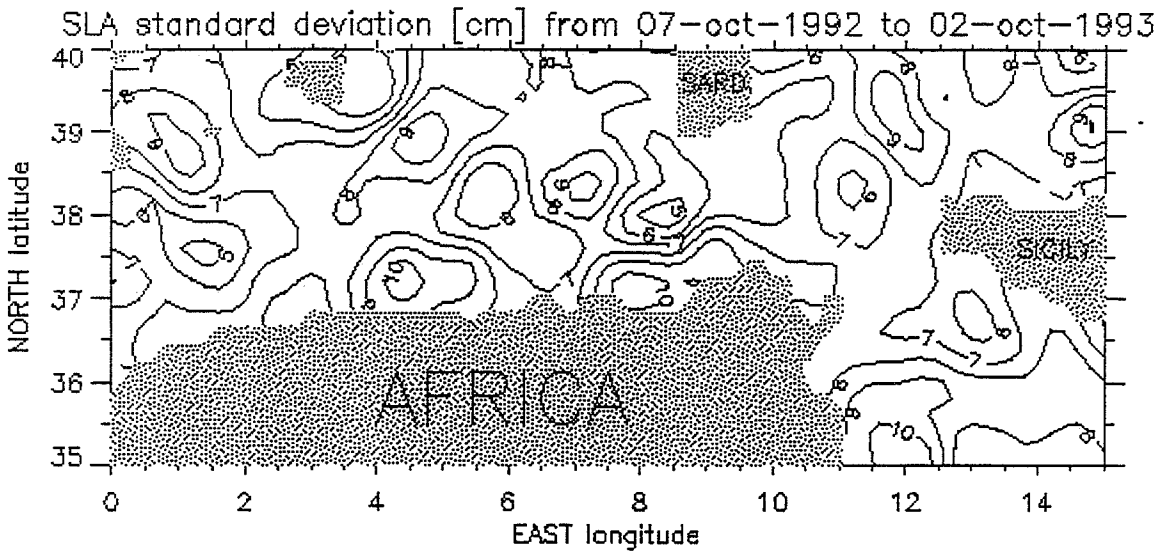

Figure 6.3: Map of SLA standard deviation for the annual period from 07-Oct-1992 to 02-Oct-1993. Contour interval of 1 cm.

The map of standard deviation for the annual period from 7-Oct-1992 to 2-Oct-1993 is shown in Figure 6.3. A large part of the standard deviation is due to the seasonal cycle of the sea level variations. This explains the relatively high background values (5-6 cm) found in the quietest areas. In order to compare, according to *Zlotnicki et al.* (1989), most of the world ocean has a variability below 8 cm *rms*, with uniform variability below 4 cm *rms* in some equatorial areas. Standard deviations higher than 10 cm are visible between 4°E and 5°E and between 8°E and 9°E near the African coast, revealing two intense variability points in the Algerian current. However, these two points roughly correspond to T/P tracks crossovers (Figure 3.4). The eastern one is really located on a crossover but the western one is centred between 4°E and 5°E, while the crossover occurs between 5°E and 6°E. Even if there is no standard deviation maximum on the other T/P crossovers, these two maxima could be partially induced by the geographic position of the T/P data and by some discrepancies between ERS-1 and T/P data corrections, like for instance the extrapolation of the ionospheric correction necessary to process ERS-1 data near the coast (*Ayoub et al.*, 1997).

There are obviously two distinct reasons for the altimetric sea level variability to be the highest in the area of the Algerian current. The first reason is that the axis of the current does not stay in a fixed position but shifts by about 50 km, mainly where the meanders develop. Thus at a fixed position, sea level rises and falls as the current axis moves on or off that position. This is also the reason why the current cannot be seen all along the Algerian coast, since its position does not shift enough and the lack of a geoid model allows one to measure only sea level variability, not absolute departure of the sea level from the geoid. The second reason for the increased variability approaching the Algerian current is the passage of eddies shed by instabilities of the current, as in the case of the Gulf Stream (*Zlotnicki et al.*, 1989).

6.3. EDDY KINETIC ENERGY AND REYNOLDS STRESS FROM GEOSTROPHIC VELOCITY ANOMALIES

The anticyclonic eddy detected in the SST image of 28-Oct-1992 (Figure 5.7) and the GVA map of 27-Oct-1992 has a maximum EKE of about 600 cm^2/s^2 in its eastern half with southward velocities. This anticyclonic anomaly is visible until the end of March 1993 in the altimetric data. Even if this anomaly really corresponds to an eddy at the end of October as shown by the SST image, this cannot be asserted for the following months; that is why the word "anomaly" is employed here instead of "eddy". Until the end of December, it moves eastward along the Algerian coast, its maximum EKE being always located in its eastern half. Then, from January to March, it detaches from the coast and moves northward until the centre of the basin where it vanishes. During these three months, its maximum EKE is located in its southern half, thus associated with westward velocities. The evolution of its maximum EKE is displayed in Figure 6.4 and reveals energy pulsations from 200 cm^2/s^2 to 1600 cm^2/s^2 with periodicity of 1-2 months. However, these pulsations coud be an artifact of the ERS-1 repetition cycle of 35 days, since the anomaly moves across the T/P+ERS-1 space-time sampling scheme.

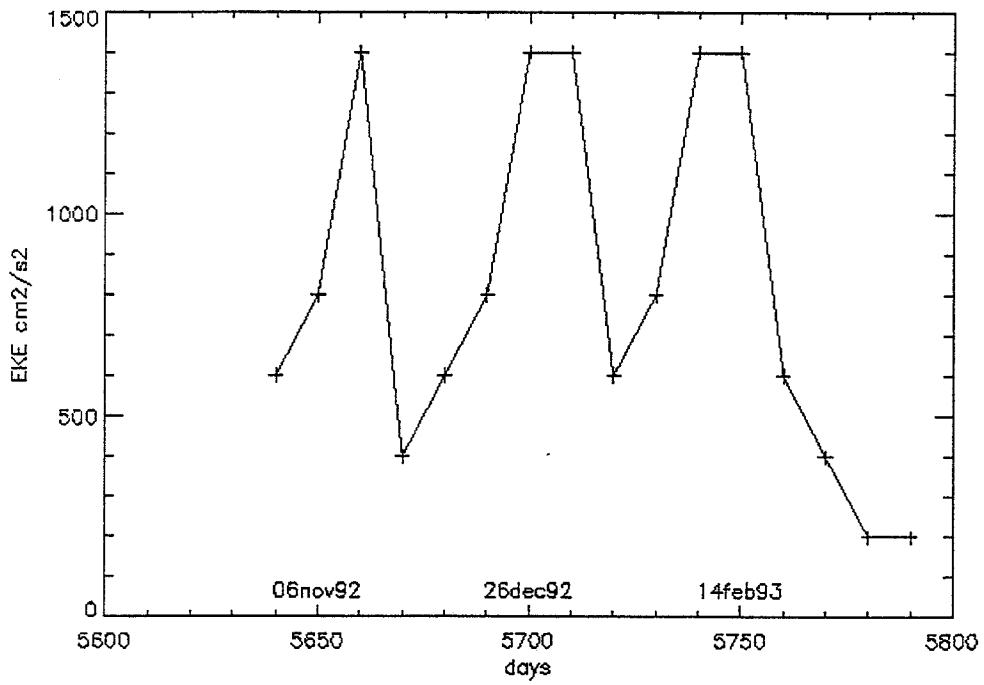

Figure 6.4: Time evolution of the EKE maximum of an anticyclonic anomaly between October 1992 and March 1993.

The anticyclonic eddy detected in the SST image of 07-Aug-1993 (Figure 5.12) and the GVA map of 03-Aug-1993 has a maximum EKE of 400 cm^2/s^2 in its northern half. This anticyclonic eddy is visible in the three altimetric maps of the month of August with a very slow eastward motion along the coast. At the end of the month, its maximum EKE is about 500 cm^2/s^2 in its eastern half.

During fall 1992, the seasonal mean EKE maxima are 700 cm^2/s^2 in the southwestern part of the channel of Sardinia and 500 cm^2/s^2 at 5°E near the Algerian coast. A secondary maximum of 300 cm^2/s^2 is located southeast of Sardinia (Figure 6.5). For winter 1993, only one maximum of 700 cm^2/s^2 is observed at 6°E, about 100 km away from the Algerian coast (Figure 6.6). In spring 1993, the mean EKE are lower with only 400 cm^2/s^2 as maximum in the western part of the channel and at 3°E, 60 km away from the coast (Figure 6.7). For summer 1993, no high mean EKE is encountered in the Algerian basin, neither in the T2S region (Figure 6.8). All these seasonal maxima are in correspondence with the SLA variability map shown previously in Figure 6.3. The seasonal EKE maxima are encountered in the area of higher mesoscale variability due to the Algerian current.

The seasonal maps of RS are more difficult to understand and have to be observed in relation with the seasonal EKE maps. Roughly, the RS extrema coincide with EKE maxima. In fall 1992, the western maximum is +200 cm^2/s^2 and the eastern minimum is -400 cm^2/s^2. Southeast of Sardinia, the RS is more than +200 cm^2/s^2 (Figure 6.9). With the help of Figure 6.2, one can see that these three maxima correspond to northeast, southeast and southwest GVA, respectively. For the mean of winter 1993, the RS minimum is less than -300 cm^2/s^2 and corresponds to southeast and northwest GVA in the centre of the Algerian basin (Figure 6.10). For spring 1993, both maxima are more than +250 cm^2/s^2 and correspond to northeastward GVA from the Algerian coast (Figure 6.11). Finally, in summer 1993, no extremum RS values are observed (Figure 6.12). According to the theories summarised in *Tai and White* (1990), the RS arises from two major sources. Near the jet, it is associated with the non-linear instabilities (meanders). The convergence or divergence of the eddy momentum flux gives rise to mean flow positive or negative acceleration. Away from the jet, it is the result of transient Rossby wave radiation. Thus, in the case of the Algerian current, strong meandering occur in fall 1992 and spring 1993 at about 4°E and 8°E, while eddy activity is found toward the centre of the basin at about 38°N during winter 1993.

6.4. CONCLUSION

The highest variability is found in the Algerian current with about 10 cm *rms*, whereas variability of 5-6 cm *rms* is found in the quietest areas, due to the seasonal variability. In fall 1992 and spring 1993, high positive SLA are observed along the Algerian coast and could correspond to the formation of large meanders induced by the instability of the Algerian current. These largest meanders could be the first stage of future anticyclonic eddies.

In the T2S area, no seasonal RS or EKE high values are observed, except southeast of Sardinia where the surface circulation around the island seems more intense during fall 1992 and fall 1993 (see also Section 4.4 and Figure 4.9). This suggests that the mesoscale variability has a quite homogeneous spatial distribution in the T2S region at seasonal scale and that the eddies are short-lived (in agreement with the results of comparisons and correlations made in Chapter 5), smoothed by the seasonal average. In the Algerian basin and close to the channel of Sardinia, EKE and RS are subject to seasonal variation with maxima in fall and spring, consistently with the seasonal SLA variability maps; but the time series of 15 months covers too short a period to conclude further. The examination of two anticyclonic eddies show that the maximum EKE encountered inside such an eddy is 500-1000 cm^2/s^2. However, the position of this maximum inside the eddy is variable. The maximum seasonal RS of the mesoscale events in the Algerian basin are ± 200-400 cm^2/s^2. In the large meanders of the Algerian current, the seasonal average of the eddy momentum flux is positive associated with northeastward velocities. All the EKE and RS values mentioned in this chapter can be useful for the validation of western Mediterranean numerical models.

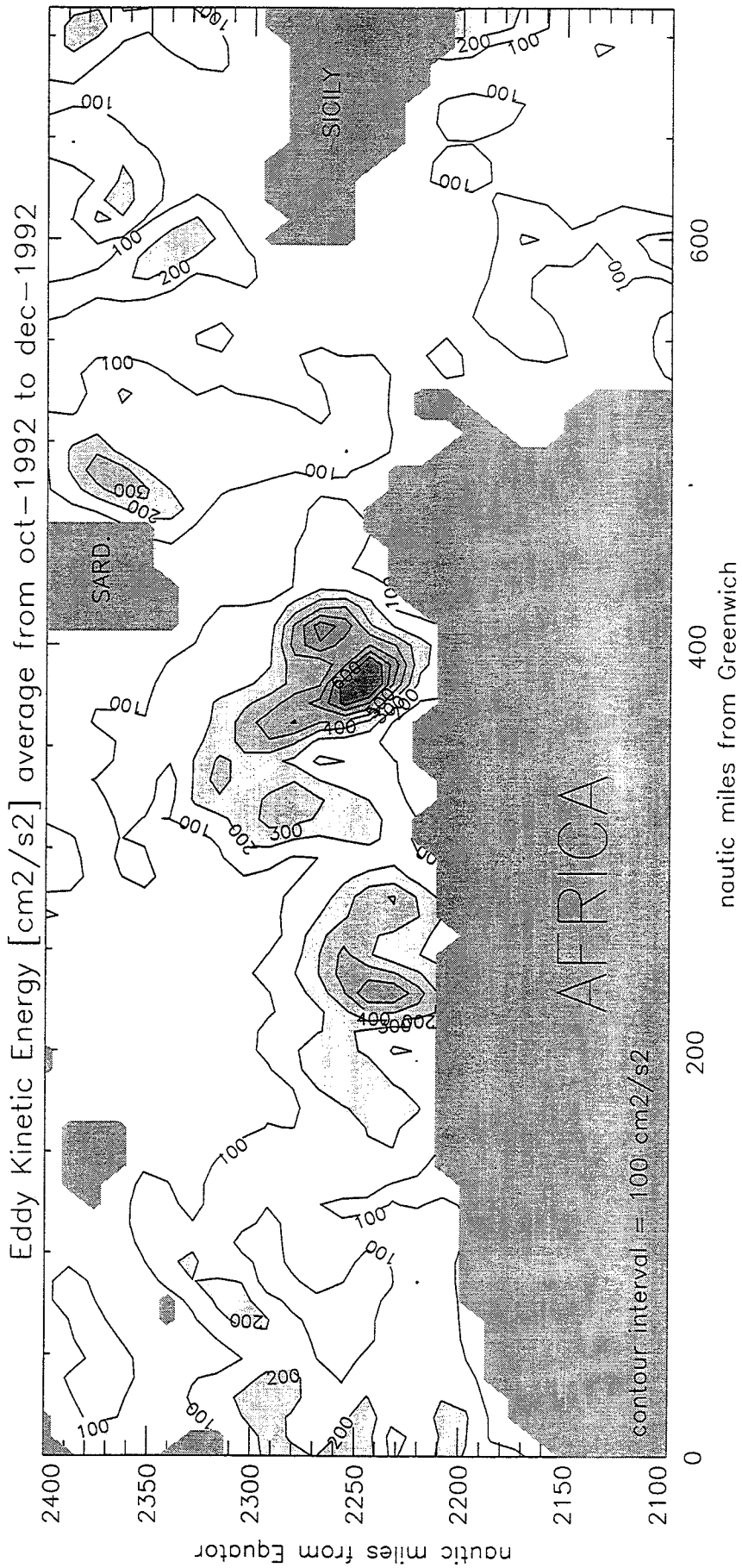

Figure 6.5: Mean EKE during Fall 1992.

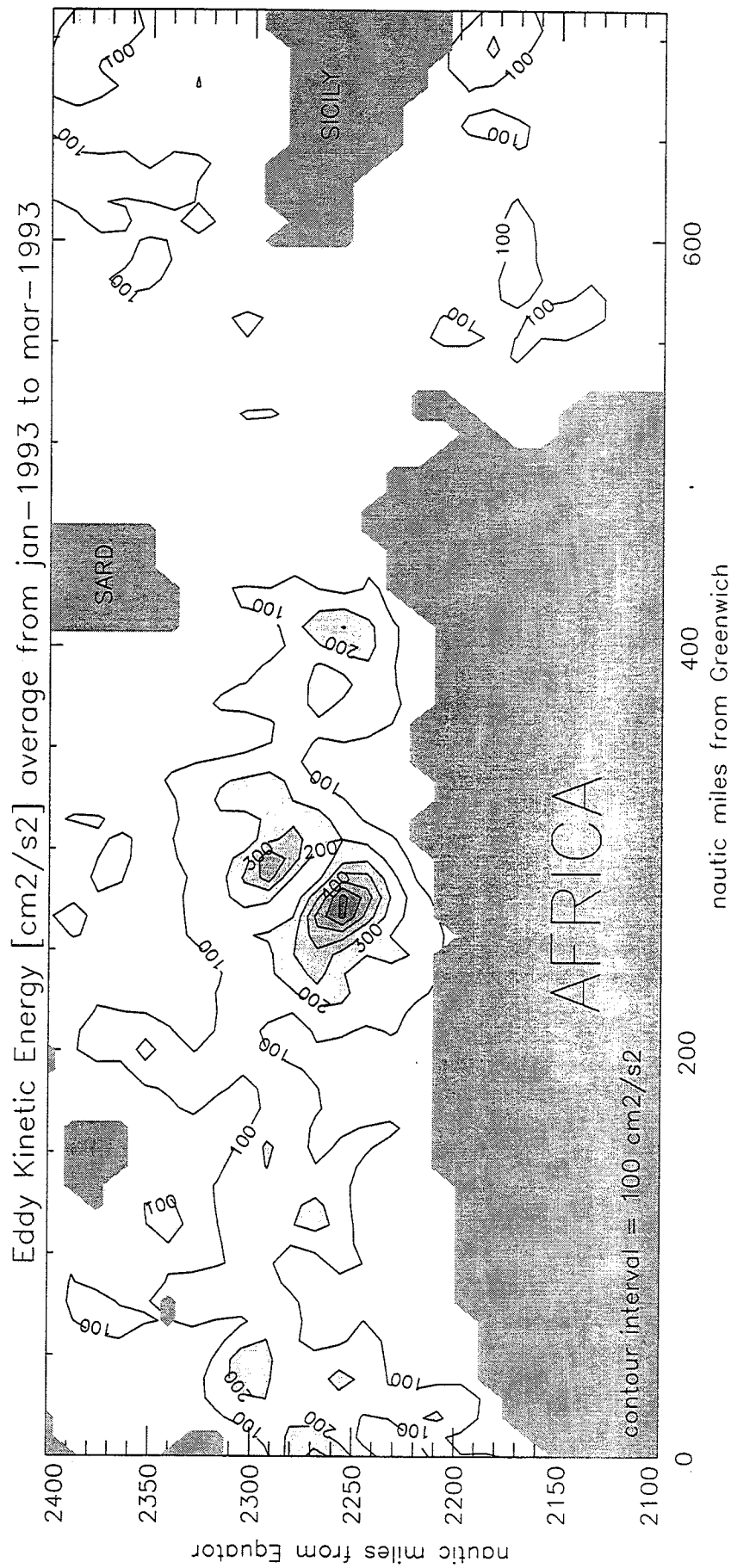

Figure 6.6: Mean EKE during Winter 1993.

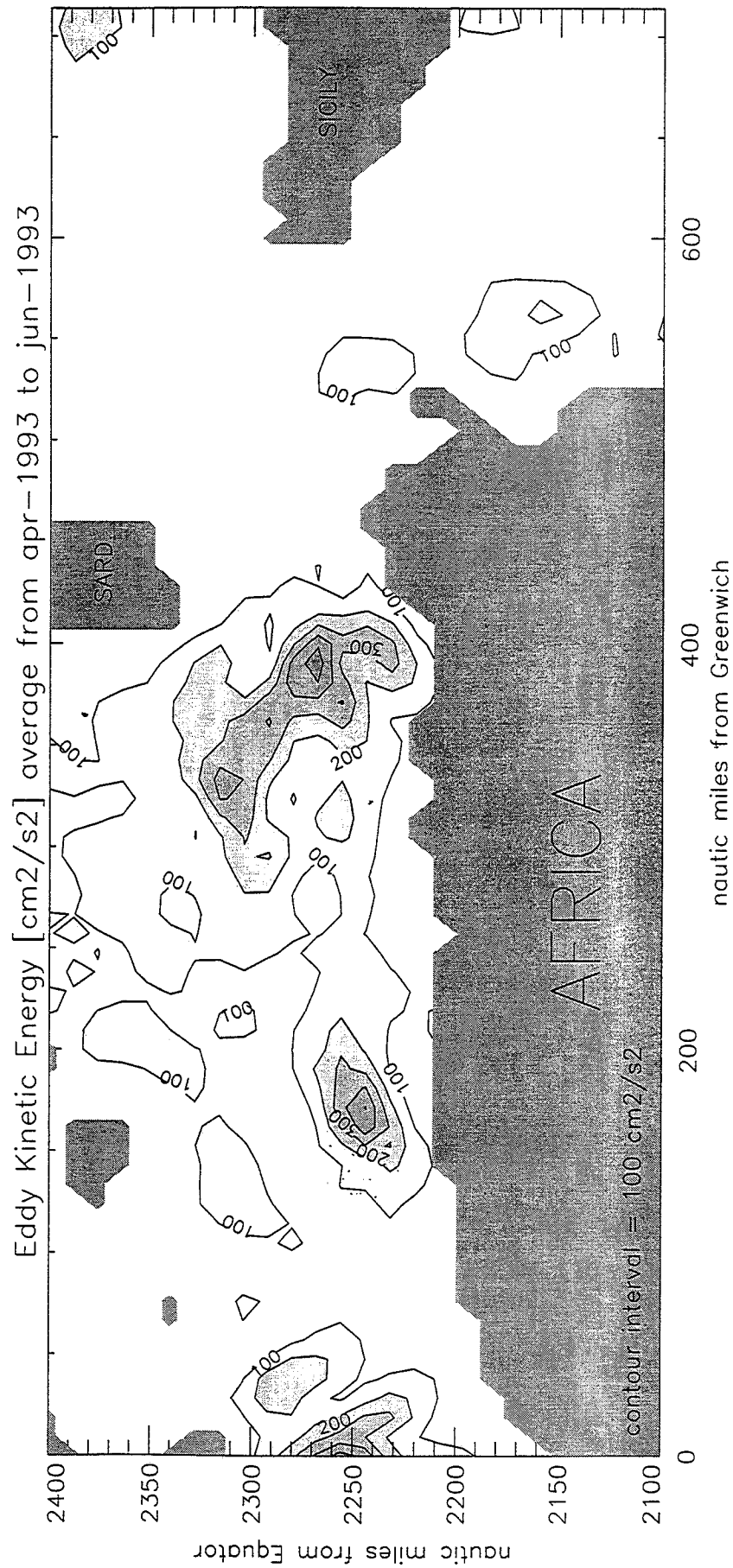

Figure 6.7: Mean EKE during Spring 1993.

Figure 6.8: Mean EKE during Summer 1993.

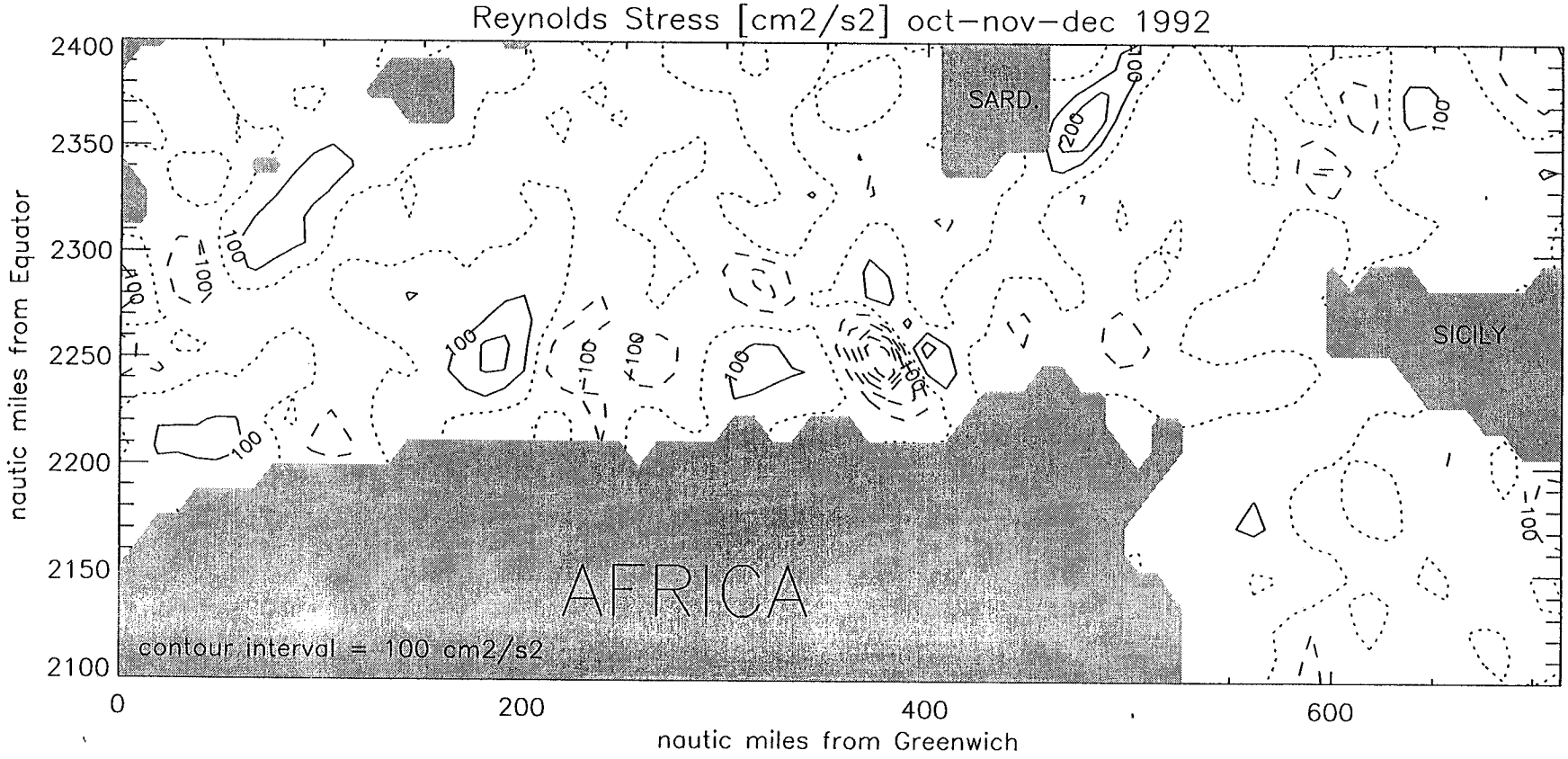

Figure 6.9: Mean RS during Fall 1992.

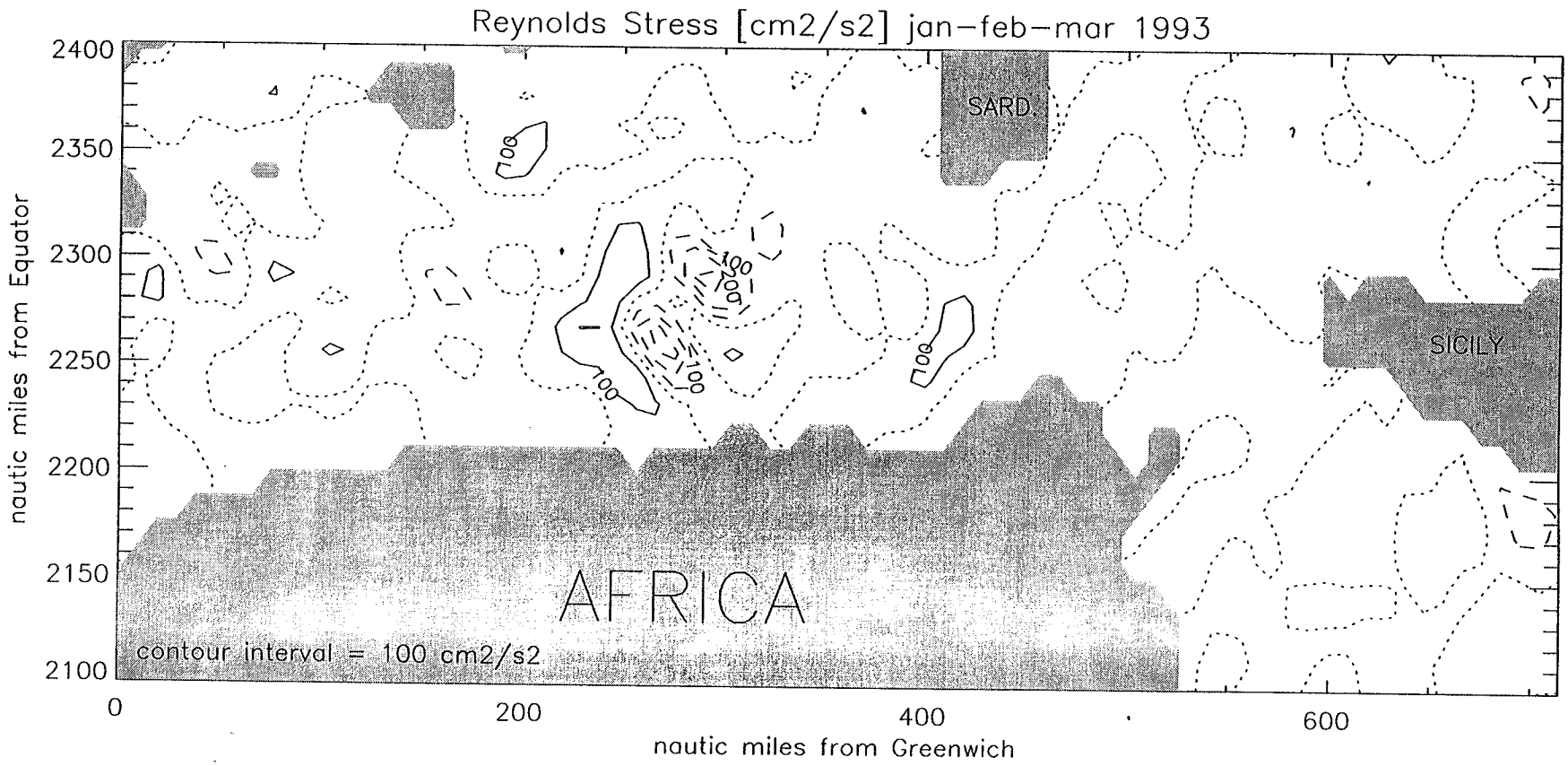

Figure 6.10: Mean RS during Winter 1993.

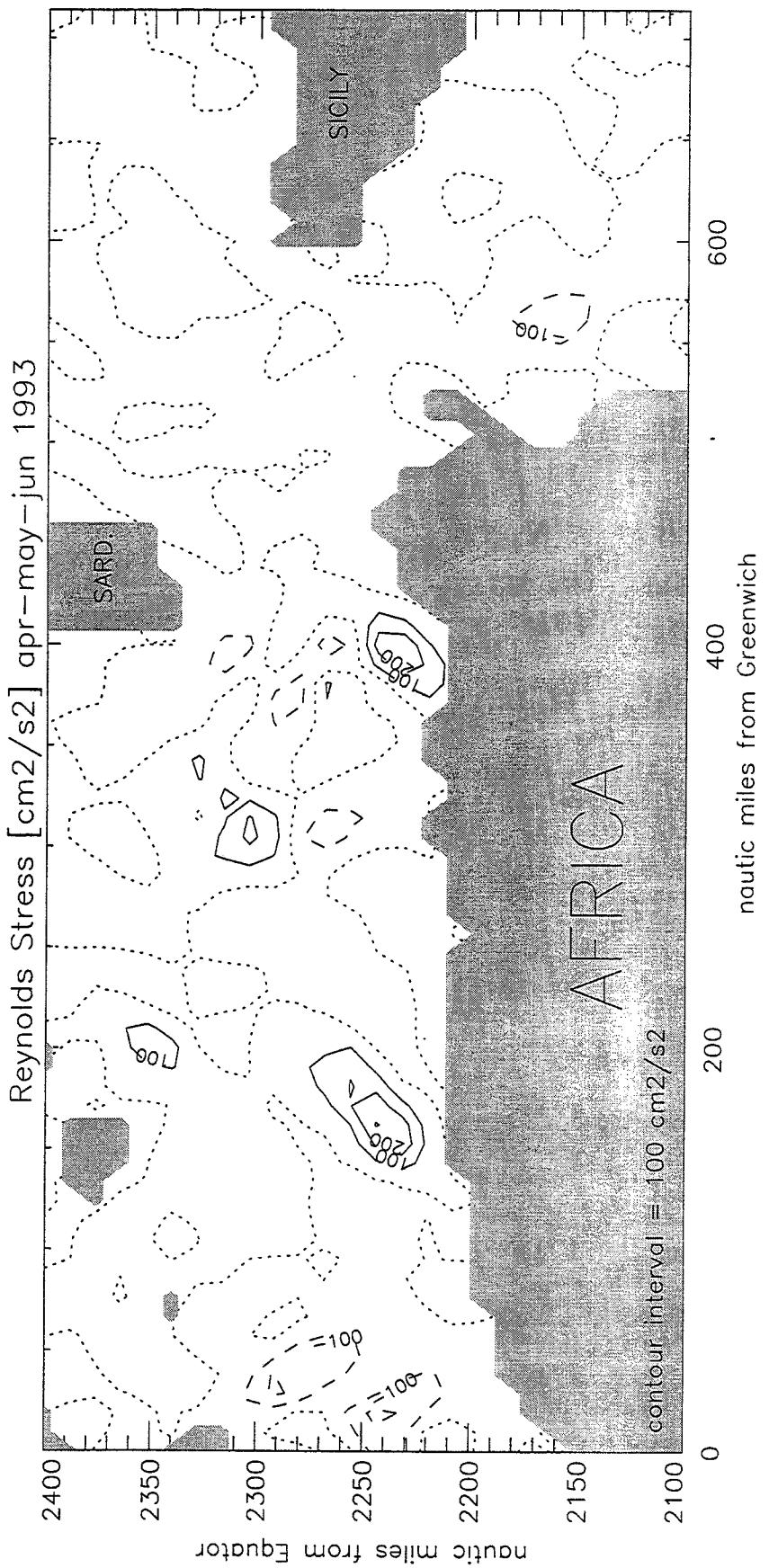

Figure 6.11: Mean RS during Spring 1993.

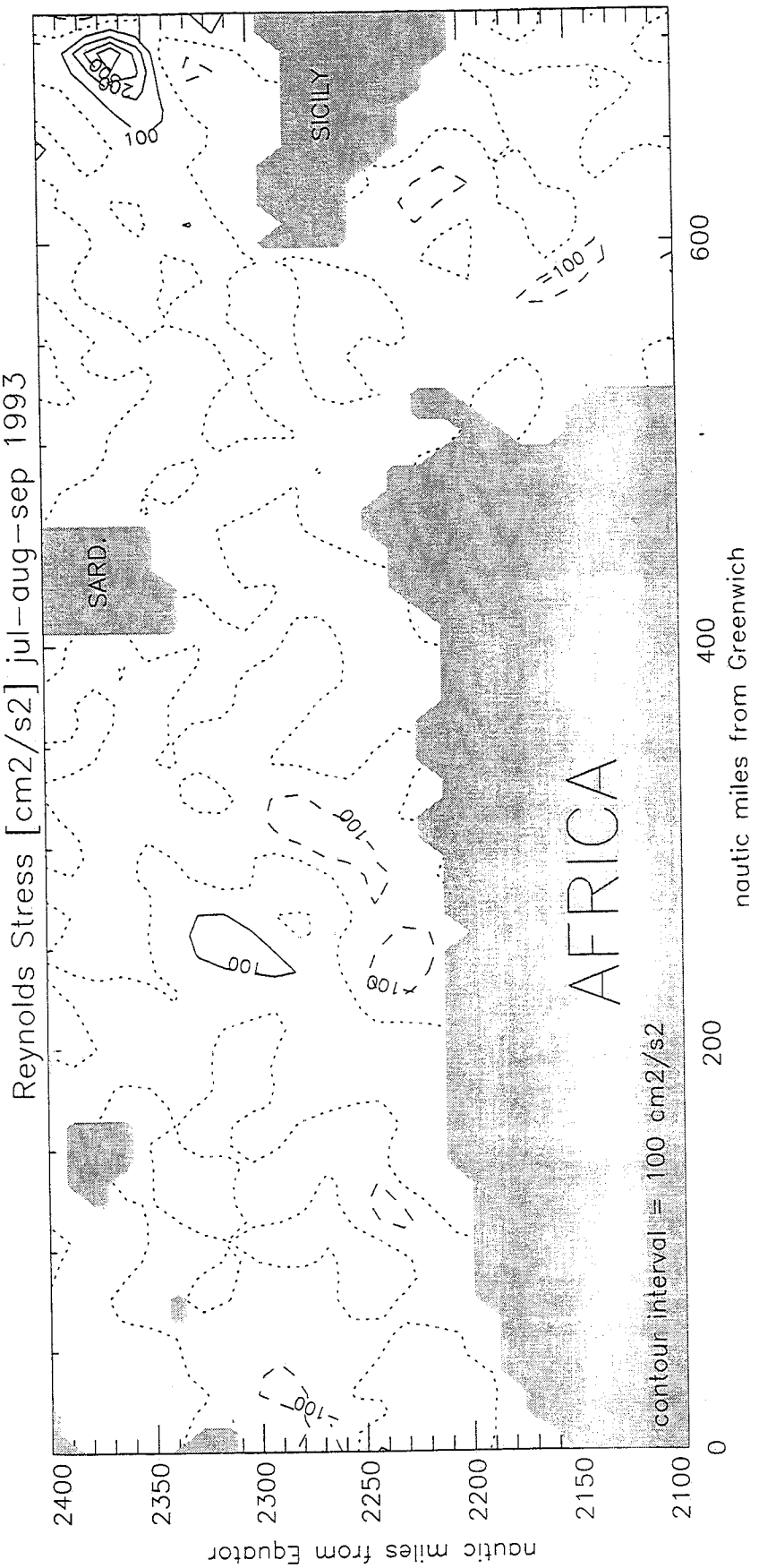

Figure 6.12: Mean RS during Summer 1993.

JOURNAL OF GEOPHYSICAL RESEARCH, VOL. 103, NO. C4, PAGES 8059–8071, APRIL 15, 1998

Complex empirical orthogonal functions analysis of ERS-1 and TOPEX/POSEIDON combined altimetric data in the region of the Algerian current

Catherine Bouzinac
Instituto de Ciencias del Mar, Consejo Superior de Investigaciones Cientificas, Barcelona, Spain

Jorge Vazquez
Jet Propulsion Laboratory, California Institute of Technology, Pasadena

Jordi Font
Instituto de Ciencias del Mar, Consejo Superior de Investigaciones Cientificas, Barcelona, Spain

Abstract. Maps of sea level anomalies (SLA) relative to the 1993 annual mean sea level combine the data from the two altimetric missions, ERS-1 and TOPEX/POSEIDON, during the overlap period (October 1992 to December 1993). These regular maps in space and time of residual sea level every 10 days on a 0.2° regular grid are used in the region of the Algerian current where the mesoscale eddies are of primary importance to the circulation of all the Mediterranean water masses. They are first compared with ERS-1 along-track scanning radiometer sea surface temperature images to get information on two anticyclonic eddies produced by instabilities of the Algerian current and visible in both infrared and altimetric data sets. Then, an analysis of complex empirical orthogonal functions (CEOFs) is performed on the SLA data set to see the correlation of the different dynamic features of the observed variability. The CEOF analysis is applied to the complex time series formed from the original SLA time series and their Hilbert transforms to separate the variability into spatially coherent modes. The spatially correlated signal in the study area (0–15°E and 35°–40°N) was found to be dominated by the first two CEOFs. These first two modes explain nearly 85% of the variability, with 80% of the total variance for the first one and 5% of the total variance for the second one. The temporal phase of the first mode indicates that a constant frequency of one cycle per year is clearly dominant, corresponding to the seasonal signal. The strongest amplitude is obtained in the southern part of the channel of Sardinia and south of the Strait of Sicily. The temporal amplitude and the temporal phase of the second mode show a periodicity of about 6 months which appears to be associated with the variability of the Algerian current as the phase isolines are parallel to the mean current path along the Algerian coast. The strongest amplitude of the second mode is located near the African coast at ~4°E and 8°E. These two points of high variability could correspond to eddy detachments from the main current.

1. Introduction

The Atlantic water enters the western Mediterranean Sea by the Strait of Gibraltar in the surface layer. In the Alboran basin it mixes with saltier Mediterranean waters and reaches the Greenwich meridian with a salinity >36.5 psu. This eastward flow of Modified Atlantic Water (MAW) then forms a well-defined jet along the Algerian coast called the Algerian current which is driven by the density difference between the Atlantic and the Mediterranean surface waters [*Millot*, 1985]. The Algerian current is hence a coastal current which flows eastward along the North African coast and drives the MAW from the Alboran basin to the channel of Sardinia and the Strait of Sicily. Meanwhile, part of the MAW spreads into the Algerian basin by instabilities of the current which begin to meander at 1° or 2°E (Figure 1) [*Millot*, 1987]. The meanders can then generate cyclonic and anticyclonic eddies. However, the cyclonic ones disappear rapidly, while the anticyclonic ones can develop as they propagate eastward with the current and may detach from the main current [*Millot*, 1994]. Indeed, large anticyclonic eddies with diameters of 200 km have been observed in the Algerian basin during several months [*Taupier-Letage and Millot*, 1988]. These huge eddies, which can occupy an extensive part of the basin as far as Sardinia, could be old stages of eddies generated by the instabilities of the Algerian current which may have drifted after being detached from the coast. During their residence they are able to deviate seaward a significant portion of the Algerian current [*Benzohra and Millot*, 1995a]. *Perkins and Pistek* [1990] described an eastward flow of MAW in the northern part of the channel of Sardinia and a westward flow in the southern part during June 1986. This situation seemed to be due to the presence of an anticyclonic eddy impeding the usual MAW eastward circulation

Copyright 1998 by the American Geophysical Union.

Paper number 97JC02909.
0148-0227/98/97JC-02909$09.00

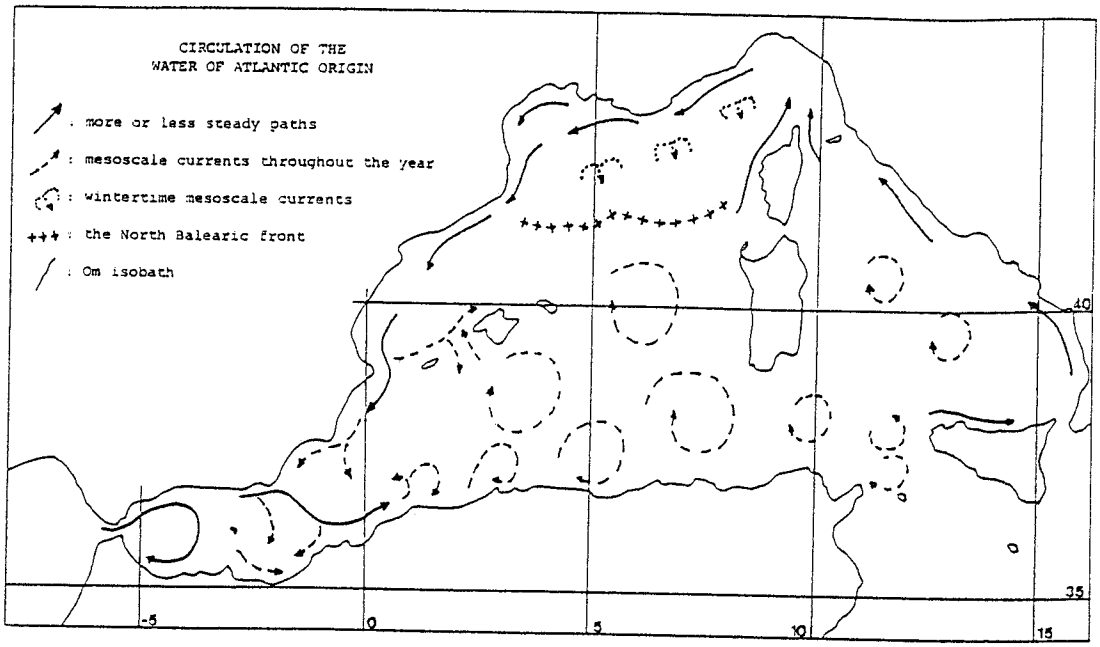

Figure 1. Modified Atlantic Water (MAW) circulation in the western Mediterranean Sea, from *Millot* [1987].

near the Tunisian coast. Recently, *Fuda et al.* [1997] have performed expendable bathy thermograph (XBT) sections between Tunisia and France. Their results show that at ~8°E near the channel of Sardinia some eddies detach quite periodically from the coast and drift northward and westward after reaching Sardinia, following the 2500 m isobath. This is supported by current-meter measurements in the western part of the channel during the Programme de Recherche Internationale en Mediterranee (PRIMO)-1 experiment (1993–1994), which revealed a 3 month long anticyclonic perturbation propagating northward at a depth of 200 m with a strong influence on the bottom circulation [*Bouzinac et al.*, 1997].

The Algerian eddies are hence of primary importance to the circulation of all the water masses in the western Mediterranean Sea [*Millot et al.*, 1990] because of their deep extension [*Benzohra and Millot*, 1995b]. In the surface layer the MAW circulation is affected by this mesoscale activity, and its temporal and spatial variability is thus very large. Its seasonal variability has also been observed in the Strait of Sicily by *Manzella et al.* [1990], who reported a summer flux of about one-half that of the winter. However, the variability scales of this surface circulation are still to be established.

Variability of the Mediterranean sea level has been studied using the data from TOPEX/POSEIDON (T/P) altimeters [*Larnicol et al.*, 1995], but the resolution of the gridding ground tracks of this satellite is too coarse (the distance between two tracks is 2.8° which is equivalent to about 250 km at the 38°N latitude) to observe the circulation in small basins such as the Mediterranean one where the mesoscale signals, of the order of 100 km, can be strong but not very large. The Algerian eddies have been clearly detected by T/P, but the space and time sampling of T/P is not dense enough to follow their evolution. The variability of the Alboran basin has been observed with the data of the European Remote Sensing (ERS-1) satellite altimeter [*Vazquez et al.*, 1996], but the resolution in time is low because of a 35 day satellite repetition cycle and does not allow a good estimation of the temporal variability of the anticyclonic gyres usually observed in this basin. It was therefore necessary to combine data from ERS-1 (with a repetition cycle of 35 days and a distance between two tracks of ~60 km) and T/P (with a repetition cycle of 10 days and a distance between two tracks of ~250 km) altimeters to study the variability of the Mediterranean sea level with adequate temporal and spatial resolutions.

The main goal of this study is to estimate the temporal and spatial scales of the mesoscale activity of the Algerian current from a synoptic point of view provided by the satellite altimetry. The frequency of the formation of the anticyclonic anomalies and their direction of propagation are investigated by means of a complex empirical orthogonal function (CEOF) analysis. The data set is described in section 2. Two sea surface temperature (SST) images of anticyclonic eddies are compared with the altimetric data in section 3. Basic statistics are performed on sea level anomaly (SLA) maps in section 4. The CEOF analysis and its results are presented in section 5. Conclusions are drawn in section 6.

2. Data Set

The T/P and ERS-1 altimeters provide complementary space and time sampling of the oceanic circulation, but they do not obtain data with the same accuracy. The accurate determination of the satellite geocentric position, and especially its radial component, is a basic requirement for accurate measurement of the sea level. The radial component of the T/P orbit is determined to within 5 cm, while ERS-1 orbits are only determined to within 15 cm. However, since T/P and ERS-1 are flying simultaneously, the more precise T/P data have been used to correct the ERS-1 orbit error [*Le Traon et al.*, 1995].

After applying the usual corrections including the inverse barometer effect the data of the first overlap period of the two altimetric missions, which begins on October 1992 and ends on December 1993, have been merged by *Ayoub et al.* [1996]. The lack of knowledge of the geoid impedes the use of the absolute

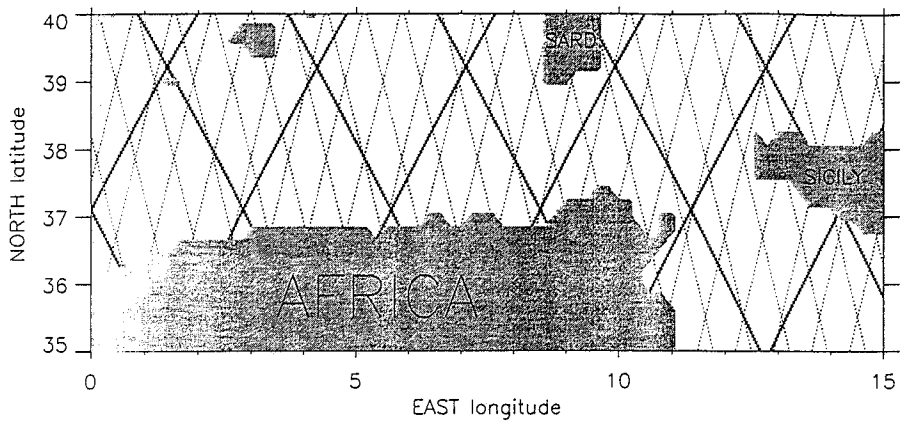

Figure 2. ERS-1 (dotted lines) and TOPEX/POSEIDON (bold lines) tracks in the study area.

heights of the sea level; hence only SLA are considered. They have calculated SLA relative to the annual mean sea level and not relative to the 15 months of the complete data set since the seasonal signal is very important in the Mediterranean Sea [*Larnicol et al.*, 1995]. Then, SLA maps have been created every 10 days with a spatial resolution of 0.2° using an objective analysis (spatial radius of 200 km and temporal radius of 20 days) with the correlation function of *Le Traon and Hernandez* [1992], the a priori errors being 10% and 15% for T/P and ERS-1, respectively.

For the present study the data from 0° to 15°E in longitude and from 35° to 40°N in latitude have been extracted to focus on the MAW flow between the Alboran basin and the eastern Mediterranean Sea. The ERS-1 and T/P tracks in the area are shown in Figure 2. The resulting 44 regular maps in time and space and their associated error maps also provide an excellent database to make comparisons with SST images from the along-track scanning radiometer (ATSR) of ERS-1.

The structures observed from the SLA maps are more or less circular forms of positive or negative anomalies that evolve in time and space with horizontal scales from 50 to 250 km in diameter. To allow a direct comparison with ATSR images by superimposition of the SST on the SLA, vector maps of surface turbulent geostrophic velocities or geostrophic velocity anomalies (GVA) have been calculated, computing the SLA gradient in both directions (east and north) at each grid point. The resulting vector ring structures are cyclonic for a local SLA minimum or anticyclonic for a local SLA maximum, as a consequence of the geostrophic balance. Even if the majority of the resulting GVA structures look like surface vortex circulation, they do not correspond necessarily to real closed cells or eddies. Here such ring structure is called an eddy only if its existence is confirmed by SST; otherwise, the term anticyclonic or cyclonic anomaly is used. However, in the regions where anticyclonic eddies have often been observed with infrared pictures the circular shapes of positive SLA probably correspond to such eddies.

3. Comparisons With ERS-1/ATSR/SST Images

Some Algerian eddy characteristics are pointed out here from the comparison between GVA maps and ATSR/SST instantaneous images, where the clouds are white and the land is black. Plate 1 presents an SST image taken on October 28, 1992, at 2200 UT with the GVA of October 27, 1992, superimposed. An anticyclonic eddy of cooler surface water is visible just between two masses of clouds, centered at ~4.5°E and 37.5°N with a diameter of ~100 km. At this location the altimetric map does not display a well-defined circular positive anomaly but a rather oval one with a northeast extension overlying the cooler water of the picture. The resulting GVA eddy is centered at 4°E and 37°N. The offset between the SST and the GVA may be due to the SLA mapping interpolation and to the motion of the eddy. The hypothesis that this eddy began as a meander of the current a few days before October 27, then developed, and moved eastward a few days after could explain the resulting oval (and not circular) form of the altimetric signal. The strongest GVA is 32 cm s^{-1} at 3.8°E, 37.6°N for the western edge and 38 cm s^{-1} at 4.8°E, 37.4°N for the eastern edge. Both maxima are located in the coolest vein of the eddy. These velocities are of the same order of magnitude as the ones obtained by *Benzohra and Millot* [1995a] from hydrography, who reported 30 cm s^{-1} eastward in the northern part of a smaller coastal anticyclonic eddy of about 50 km in diameter at 4°E. The evolution of this anticyclonic anomaly can be followed in consecutive maps of SLA. Even if this anomaly really corresponds to an eddy at the end of October as shown by the SST image, this cannot be asserted during the following months; that is why the word "anomaly" is employed here instead of "eddy." First, it moves eastward along the coast until the end of December 1992. Then, from January to February 1993, it deviates progressively toward the center of the basin at ~6°E and disappears. Unfortunately, no ATSR image free of clouds has been found between November 1992 and February 1993 to corroborate that this anomaly still corresponds to an anticyclonic eddy.

Plate 2 presents an SST image taken on August 7, 1993, at 2200 UT. Although the SST gradients are not very clear, a circular shape of cooler surface waters is detected near the Algerian coast at ~2°–3°E, 37°N. The nearest GVA map in time (August 3, 1993) is overlaid on this SST picture. The velocities reveal an anticyclonic eddy with a diameter of more than 100 km. The center of this eddy is 8 cm higher than the edge. The small shift between the eddy described by the GVA and the warmer center visible on the SST picture, along with the 4 days separating the GVA and the SST data, suggest an eastward propagation of the eddy. The strongest velocity anomaly of 28.5 cm s^{-1} is located at 2°E, 37.4°N in the northwestern part of the eddy. Ten days later (August 13, 1993; map

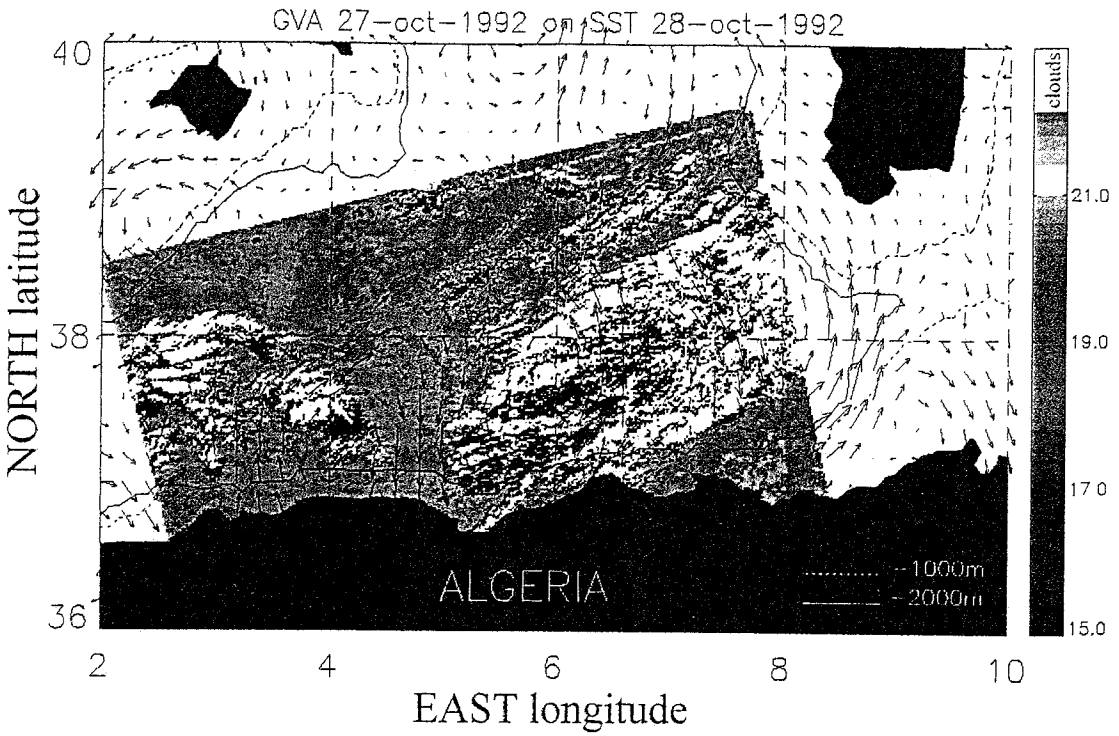

Plate 1. Sea surface temperatures (SST) of October 28, 1992, with geostrophic velocity anomalies (GVA) of October 27, 1992.

not shown), the GVA maximum in this anticyclonic structure is 34 cm s^{-1} at 2.6°E, 37.4°N in the northeastern part of the eddy. In 20 days the eddy center has drifted ~40 km eastward at 37°N. This gives a propagation velocity of ~2 km d^{-1} which is slightly weaker than the 13 km d^{-1} observed by *Taupier-Letage and Millot* [1988] during July 1984 in the same area and the 3–5 km d^{-1} estimated by *Millot et al.* [1990] from infrared imagery and current measurements.

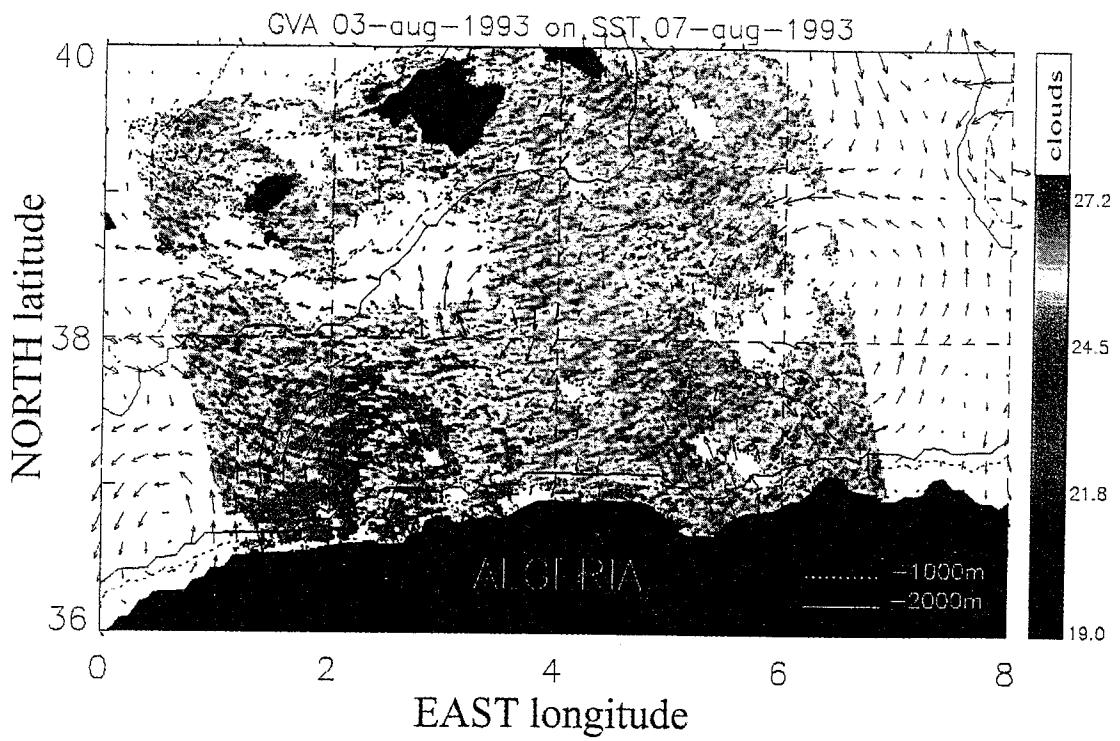

Plate 2. SST of August 7, 1993, with GVA of August 3, 1993.

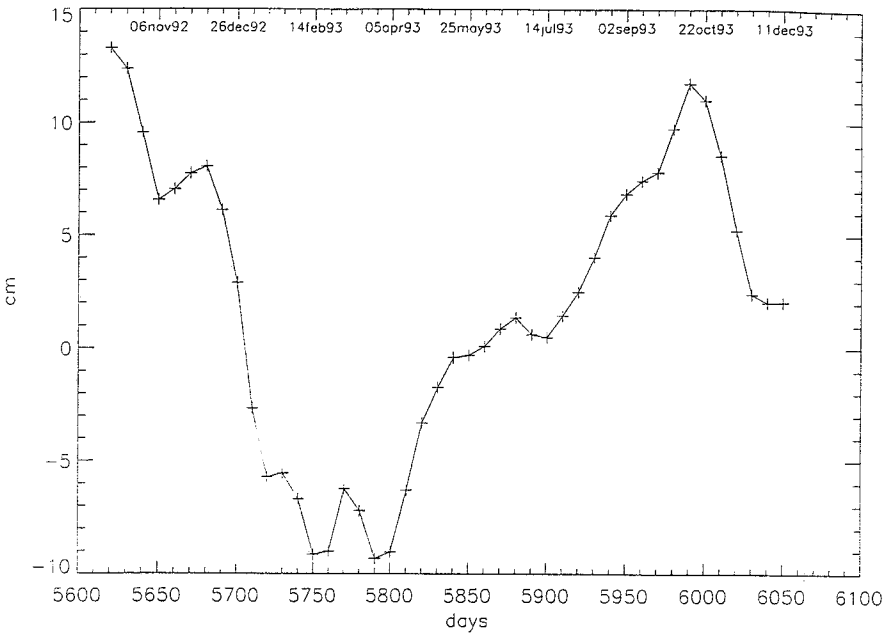

Figure 3. Temporal evolution of the spatial mean sea level anomaly (SLA) from October 7, 1992, to December 11, 1993.

4. Basic Statistics

The temporal evolution of the spatial mean SLA (Figure 3) shows the annual seasonal cycle of variability with a maximum value of +10 cm in the fall (October 1992 and 1993) and a minimum value of −8 cm between the winter and spring (February, March, and April 1993). This curve is very similar to the one obtained by *Larnicol et al.* [1995] for all the western Mediterranean Sea from T/P data only. This means that the study area has a seasonal response quite identical to the mean response of the entire western basin. This temporal variation of the mean sea level is also in good agreement with the description of the seasonal variability of the Atlantic water inflow at the Strait of Gibraltar made by *Ovchinnikov* [1974]. From in situ measurements and from salt conservation he deduced that the sea level continuously increases from February to November and rapidly decreases between December and February.

The map of the seasonal mean SLA for the fall of 1992 (Figure 4a) shows various maxima along the African coast at 1°–2°E, 4°–5°E, 7°–8°E, and 9°–10°E with anomalies higher than 12 cm including a mean anomaly of ~8 cm for this season. In the spring of 1993 (Figure 4c), two similar maxima are observed at 4°E and 6°–7°E with anomalies higher than 0 cm, while the mean anomaly is ~−2 cm during this season whereas in the winter and summer of 1993 (Figures 4b and 4d), no such maxima can be seen along the African coast. This indicates that the Algerian current is subject to an important seasonal variability with strong positive level anomalies in the fall and spring that could favor the formation of anticyclonic eddies.

The map of standard deviation for the annual period from October 7, 1992, to October 2, 1993, is shown in Figure 5. A large part of the standard deviation is due to the annual cycle of the sea level. This explains the relatively high background values (5–6 cm) found in the quietest areas. In order to compare, according to *Zlotnicki et al.* [1989], most of the world ocean has variability below 8 cm rms, with uniform variability below 4 cm rms in some equatorial areas. Standard deviations higher than 10 cm are visible between 4°E and 6°E and between 7.5°E and 9°E near the African coast, revealing two intense variability points in the Algerian current.

There are obviously two distinct reasons for the altimetric sea level variability to be highest in the neighborhood of the Algerian current. The first reason is that the axis of the current does not stay in a fixed position but shifts by ~50 km, mainly where the meanders develop. Thus, at a fixed position the sea level rises and falls as the current axis moves on or off that position. This is also the reason why the current cannot be seen all along the Algerian coast since its position does not shift enough and the lack of a geoid model allows one to measure only sea level variability, not absolute departure of the sea level from the geoid. The second reason for the increased variability approaching the Algerian current is the passage of eddies shed by the instabilities of the current, as in the case of the Gulf Stream [*Zlotnicki et al.*, 1989].

5. CEOF Analysis

5.1. Methodology

Oceanic phenomena are usually the combination of various parameters difficult to dissociate interacting at many different timescales and space scales. The decomposition into empirical orthogonal functions (EOFs) is advantageous because it is built on modes calculated from the data themselves, hence proper to the data set and not imposed. If the correlation between the data and the base functions is low, a high number of base functions will be necessary to describe the phenomena. That is why it is better to choose a set of orthogonal functions where the few first ones are sufficient. Hence the empirical eigen functions are useful in analyzing large data sets. Their principal virtues are that they provide the most efficient method of compressing data (they reduce the amount of data by keeping only the most significant phenomena), and they may be regarded as uncorrelated modes of variability of the

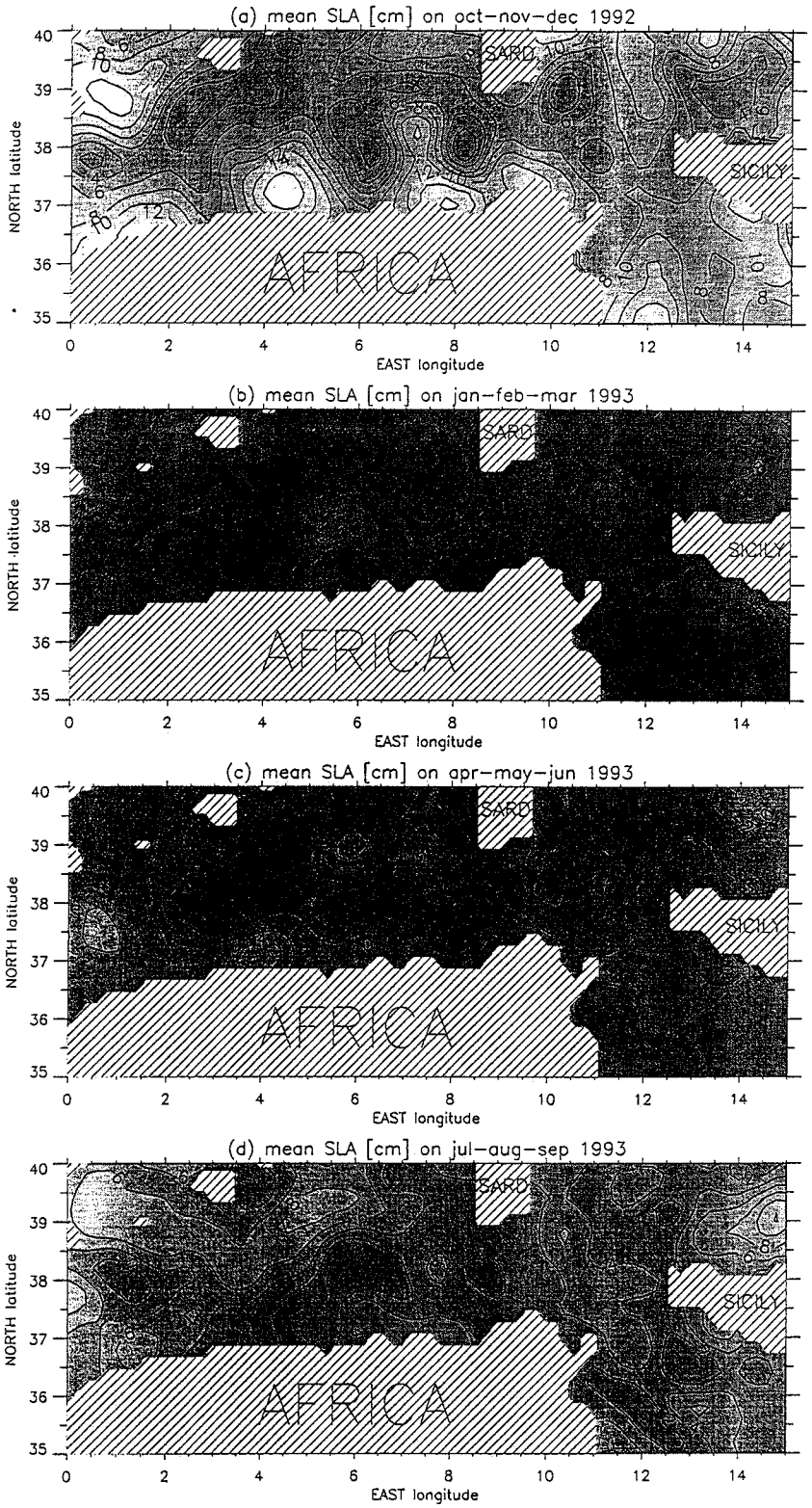

Figure 4. Seasonal mean SLA: (a) fall (October, November, and December 1992), (b) winter (January, February, and March 1993), (c) spring (April, May, and June 1993), (d) summer (July, August, and September 1993). The contour interval is 2 cm. Dashed, dotted, and solid lines correspond to negative, null, and positive values, respectively.

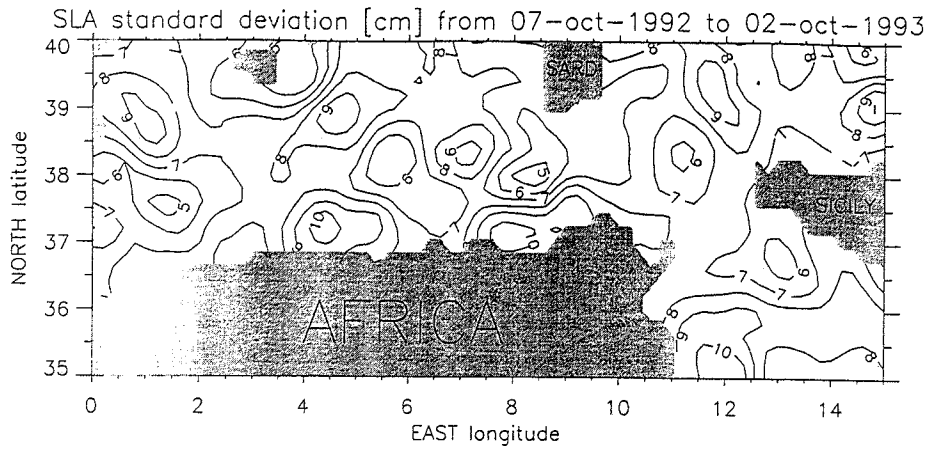

Figure 5. Map of SLA standard deviation for the annual period from October 7, 1992, to October 2, 1993. The contour interval is 1 cm.

field [*Davis*, 1976]. Unlike real empirical orthogonal functions where the modes represent standing wave patterns, complex EOFs can resolve propagating waves [*Horel*, 1984]. The decision to apply CEOFs instead of real EOFs is appropriate because of the wave propagation associated with the instabilities of the Algerian current. This method of analysis has given good results in the Gulf Stream [*Vazquez*, 1993] and on the surface circulation variability in the Alboran basin [*Vazquez et al.*, 1996]. Complex time series $H(x, y, t)$ are formed from the original time series and their Hilbert transforms. The real part of $H(x, y, t)$ is simply the value of the residual sea level at grid point (x, y) and time t, while the imaginary part is the Hilbert transform of the original data field where the amplitude remains unchanged but where the phase is shifted by $\pi/2$. In practice, an estimate of the Hilbert transform is obtained directly from the Fourier coefficients [*Barnett*, 1983] derived from fast Fourier transform (FFT) routines. This approach is subject to the problems that Fourier analysis normally presents (aliasing, end effects, etc). Hilbert transforms obtained from FFT routines are more strongly influenced by end effects than are the Fourier transforms themselves [*Horel*, 1984]. Hence each end (roughly 10% of the total time series) is cosine-tapered to eliminate this problem.

No assumption is made about phase propagation in either the x or y direction. The covariance statistics are applied in the spatial domain to extract the correlated orthogonal signal. Mathematically, the rest of the procedure is similar to real EOF analysis except that the statistics are performed on the complex time series $H(x, y, t)$. For detailed examples on the use of EOFs, see *Stidd* [1967] and *Davis* [1976]. Since the covariance matrix is Hermitian, it possesses real eigenvalues which give the variance associated with each mode. In the CEOF procedure the complex time series $H(x, y, t)$ is decomposed in terms of a set of orthogonal functions $F(x, y)$.

$$H(x, y, t) = \sum_{m=1}^{N} w_m(t) F_m^*(x, y)$$

where the asterisk is the complex conjugation, N is the total number of grid points in the sea ($N = 1306$) and $w(t)$ is the amplitude function. Thus both the eigenvectors $F_m(x, y)$ of the spatial covariance matrix and the temporal amplitudes $w_m(t)$ are complex and have an amplitude and a phase component. For each dominant mode m are plotted

The spatial amplitude

$$A_m(x, y) = \sqrt{NF_m(x, y) F_m^*(x, y)}$$

The spatial phase

$$\varphi_m(x, y) = \arctan \left\{ \frac{\mathrm{Im}\,[F_m(x, y)]}{\mathrm{Re}\,[F_m(x, y)]} \right\}$$

The temporal amplitude

$$w_m(t) = \sqrt{\frac{\sum_{x,y}^{N} H(x, y, t) F_m(x, y) \sum_{x,y}^{N} H^*(x, y, t) F_m^*(x, y)}{N}}$$

The temporal phase

$$\varphi_m(t) = \arctan \left\{ \frac{\mathrm{Im}\left[\sum_{x,y}^{N} H(x, y, t) F_m(x, y) \right]}{\mathrm{Re}\left[\sum_{x,y}^{N} H(x, y, t) F_m(x, y) \right]} \right\}$$

For plotting purposes the temporal (spatial) amplitude is divided (multiplied) by the square root of N.

5.2. Results

The spatially correlated signal in the study area was found to be dominated by the first two CEOFs. These two modes explain nearly 85% of the variability, with 80% of the total variance contained in the first one and 5% of the total variance in the second one (Table 1). It is readily seen that higher modes add little variance as the modal structure becomes quickly degenerate and are not significant. The question is whether the second mode, representing only 5% of the variability, is significant or not. A Monte-Carlo simulation analysis [*Overland and Preisendorfer*, 1982] was applied by running 100 simulations of the CEOF analysis on Gaussian random numbers with a standard deviation of 5. None of the resulting random modes explain >6% (Figure 6). This means that the

Table 1. Contributions (c(m)) of Each Complex Empirical Orthogonol Function (CEOF) Mode (m) in Percentage of the Total Variance

m	c(m)
1	79.92
2	5.00
3	2.89
4	2.27
5	1.89
6	1.38
7	1.21
8	0.96
9	0.74

Table 2. Amplitudes of the Input Propagating Waves (1 and 2) and Amplitude of the Input Noise (3) for Each Simulation and Percentages of the Total Variance Explained by Each Resulting CEOF

Simulation	Amplitude 1, cm	Percent 1	Amplitude 2, cm	Percent 2	Amplitude 3, cm	Percent 3
1	10	89.05	2	3.87	2	0.82
2	10	84.25	2.5	5.67	2.5	0.88
3	10	79.07	3	7.61	3	0.98
4	10	58.58	5	15.31	5	1.67
5	10	47.21	5	13.07	7	2.58

second mode of the present analysis could be considered a priori as noise and not significant. However, its temporal and spatial amplitudes do not display any random behavior, as displayed by the modes of the Monte-Carlo simulation. In order to verify that the CEOF analysis is able to separate a propagating wave and a noise background of the same amplitude the analysis was applied on various simulated fields, each one composed of the sum of three terms: a propagating wave of high amplitude (10 cm), a propagating wave of small amplitude (between 2 and 5 cm), and a Gaussian random noise of the same amplitude. The two propagating waves have different periods and wavelengths. The percent variance associated with each mode for each simulation and their respective amplitudes are displayed in Table 2. In every case the three features are spatially and temporally well resolved by the three lowest modes of the CEOF analysis, even in simulations 1 and 2 where the second modes represent <6% of the total variance. Since the rms error associated with the altimetric data set is ~3 cm [*Ayoub et al.*, 1997], the simulation closest to the real data is simulation 3 which shows that the second wave is completely separated from the noise. Even in the last case (simulation 5 in Table 2) where the noise rms is greater than the amplitude of the second wave, the period and the wavelength of the second CEOF are in agreement with the period and the wavelength of the second input wave, and the variability explained by the second CEOF is higher than the one explained by the third CEOF. Thus one can assert that the second mode of the present analysis is the representation of a weak but coherent phenomenon.

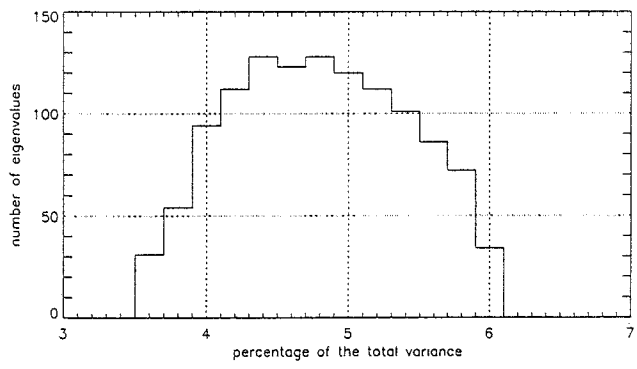

Figure 6. Histogram of all eigenvalues representing >3% of the total variance for 100 simulation runs of CEOF analysis using a Gaussian random number generator with standard deviation of 5.

5.2.1. The first mode (CEOF 1). The temporal phase of the first mode (Figure 7b) indicates a constant frequency of one cycle per year corresponding to the seasonal variability. The strongest signal is observed in the southern part of the channel of Sardinia, south of the Strait of Sicily near the Tunisian coast, at the entrance to the Tyrrhenian basin, and southeast of Mallorca (Figure 8a). The spatial phase (Figure 8b) is homogeneous, indicating a stationary seasonal oscillation in all the study area. The normalized temporal amplitude (Figure 7a) does not show a clear annual cycle, but its multiplication by the cosine of the temporal phase gives back the seasonal curve of Figure 3.

According to *Larnicol et al.* [1995], who analyzed 2 years of T/P data in the whole Mediterranean Sea and characterized changes in the mean level, roughly half of the seasonal signal

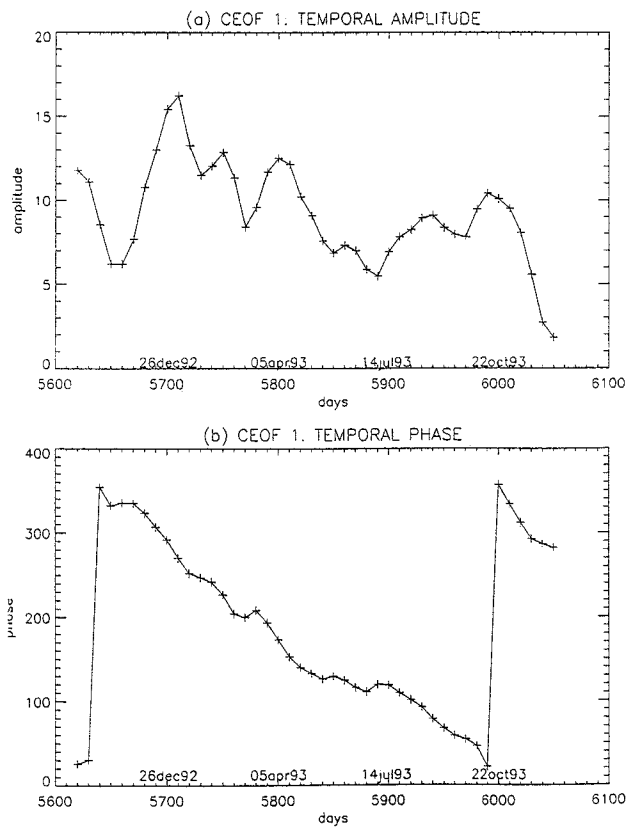

Figure 7. (a) Temporal normalized amplitude and (b) temporal phase in degrees of complex empirical orthogonal function (CEOF) 1.

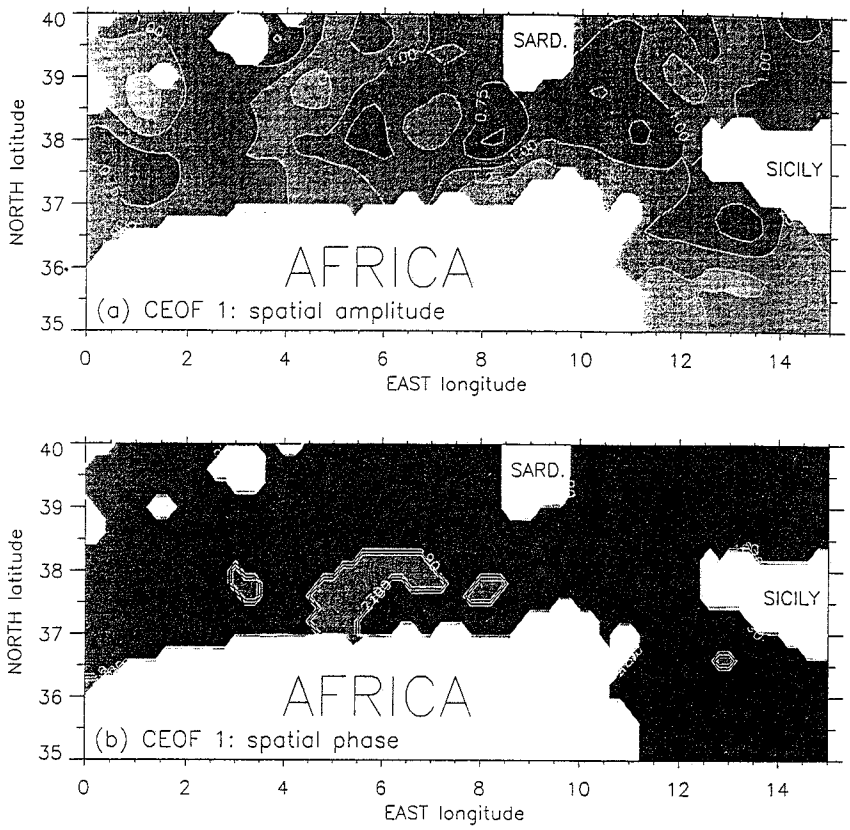

Figure 8. (a) Spatial normalized amplitude with a contour interval of 0.25 and (b) spatial phase with a contour interval of 90° of CEOF 1.

is related to the steric effect of contraction and dilatation of the surface waters due to the heat exchanges at the ocean-atmosphere interface. The other half could be due to a slight seasonal imbalance between inflow and outflow at the Straits of Gibraltar and Sicily and between evaporation and precipitation. These contributions to the seasonal sea level variations are still an important subject of investigation on the Mediterranean Sea [*Manzella and La Violette*, 1990; *Millot et al.*, 1992] which will not be discussed here.

5.2.2. The second mode (CEOF 2).

The temporal normalized amplitude (Figure 9a) and the temporal phase (Figure 9b) of the second mode show a periodicity of ~6 months which appears to be associated with the variability of the Algerian current as the phase isolines are parallel to the mean path along the Algerian coast up to the channel of Sardinia (Figure 10b). The strongest amplitudes of the second mode are located near the African coast between 4°E and 6°E and north of Sicily (Figure 10a). This map is very similar to the map of SLA standard deviation (Figure 5). This indicates that the second CEOF represents the mesoscale activity. The phase isolines all along the coast (Figure 10b) show a deviation offshore at 4°E that corresponds to a maximum in amplitude. From this point the spatial phase decreases northeastward. In the western part of the channel of Sardinia (8°–9°E) the amplitude presents a secondary maximum, and the spatial phase decreases from south to north.

The real spatial amplitudes (centimeters) of the second mode bimonthly average (Figure 11) present the same situation in October–November 1992 and April–May 1993 as a consequence of the 6 month periodicity. The highest values are

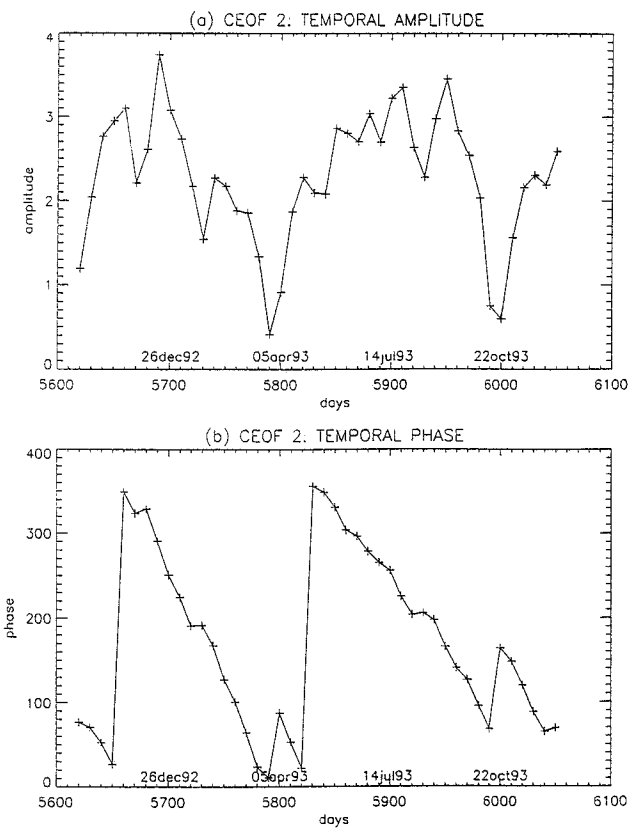

Figure 9. (a) Temporal normalized amplitude and (b) temporal phase in degrees of CEOF 2.

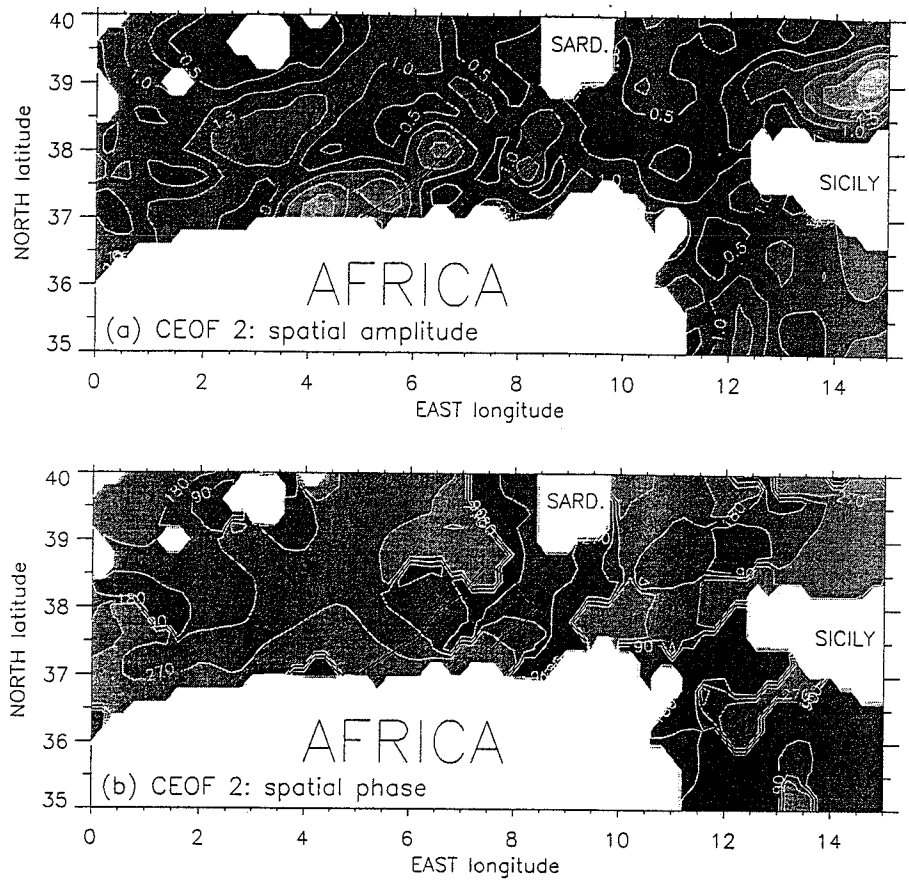

Figure 10. (a) Spatial normalized amplitude with a contour interval of 0.5 and (b) spatial phase with a contour interval of 90° of CEOF 2. The two black lines are the sections used for the time-latitude diagrams plotted in Figure 12.

located at 4°E near the coast and at 8°–9°E in the southern part of the channel. In December–January 1993 the former has progressed eastward, while the latter has moved northward across the channel. In February–March 1993 both positive anomalies have weakened and moved to more northerly positions. This cycle repeats from April to May 1993 with an evolution slightly longer than 6 months as the amplitudes are still significant in August–September 1993 but vanish in October–November 1993 (this last map is not shown). Looking at the amplitude maps of this mode every 10 days like a movie, both areas of maximum variability evoke wave propagation eastward and northward, since positive and negative anomalies alternate, with wavelengths of 140 ± 30 km and phase velocities of 1 or 2 km d^{-1}. The propagation from the two high-variability points is also visible on the time-latitude diagrams shown in Figures 12a and 12b. Figures 12a and 12b display the time evolution of the second-mode amplitude along the two sections drawn on Figure 10. In Figure 12a the propagation is northeastward between the Algerian coast and Sardinia. Pulsation of the propagating anomaly amplitude is observed with a period of ~60 days. In Figure 12b the propagation follows approximately the deep isobaths (~2000 m) with the same period of pulse. Both wave propagations end in the same area, southwest of Sardinia.

After comparison with the map of satellite tracks (Figure 2) it can be stated that the two areas of maximum variability roughly coincide with the two T/P track crossover points at 37°N and could be due to an artifact of the mapping routine. However, the other T/P crossover points do not present any variability maxima. One can also remark that the northward propagation near the channel of Sardinia is nearly parallel to ERS-1 descending tracks for one half and parallel to ERS-1 ascending tracks for the other half and could be due to temporal aliasing between measurements of adjacent or crossing tracks. However, the northeastward propagation from the Algerian coast (5°E) is not parallel to any tracks. In more general terms, no coherent relationship has been found between the CEOF results and the sampling of the original data or the mapping analysis used to create the SLA data set. Thus the CEOF patterns do not seem to be due to any artifact of the procedure.

6. Discussion and Conclusion

A CEOF analysis performed on 15 months of combined altimetric SLA from T/P and ERS-1 shows that the variability in the region of the Algerian current is dominated by two modes which are the annual cycle and an almost semiannual cycle. Because of their respective periodicity, the second CEOF could be a harmonic of the first CEOF, but the similarity between the map of SLA standard deviation (Figure 5) and the amplitude map of the second mode (Figure 10a) supports the fact that the two modes are associated with two very

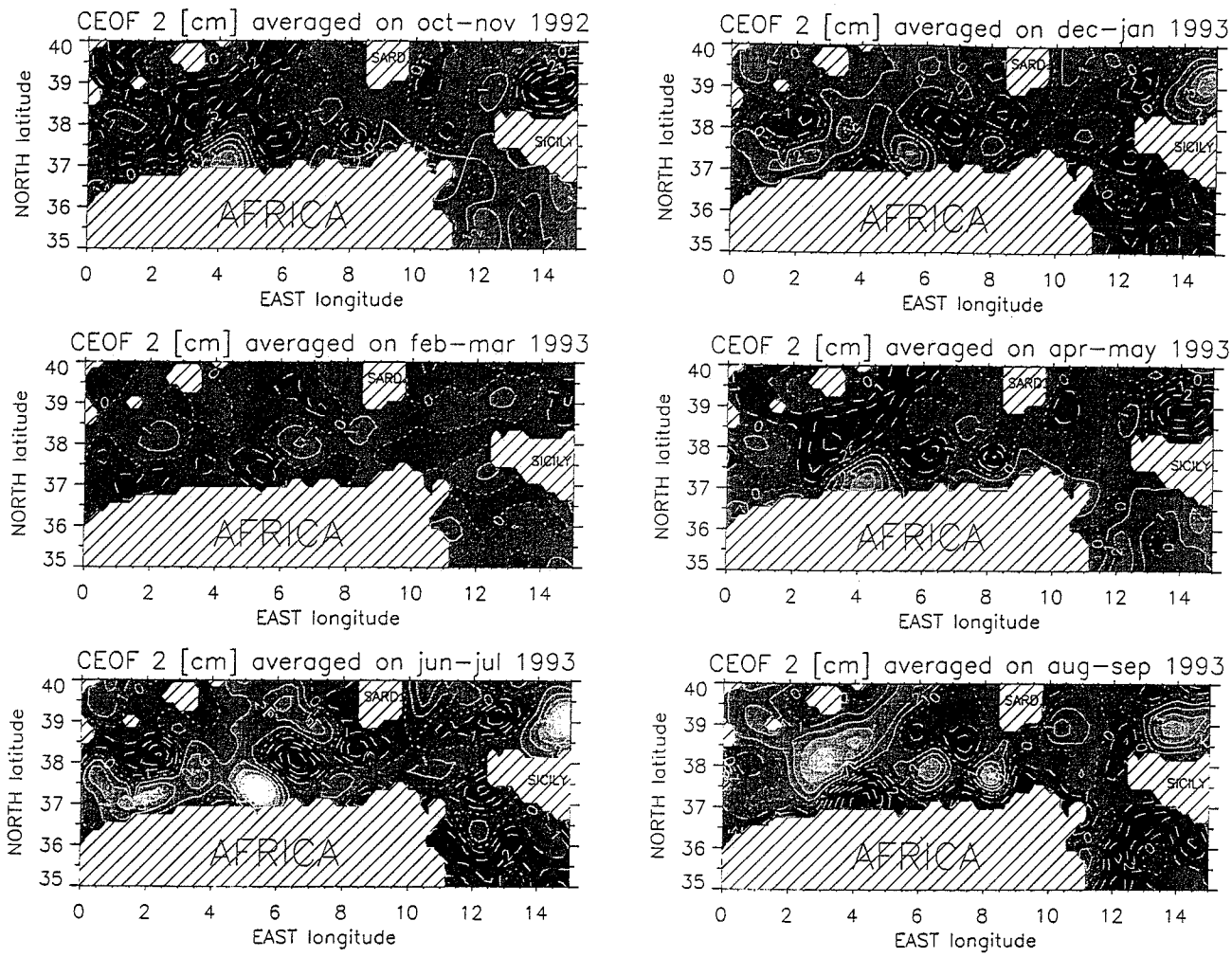

Figure 11. Bimonthly averaged amplitudes of CEOF 2. The contour interval is 1 cm. Dashed, dotted, and solid lines correspond to negative, null, and positive values, respectively.

different physical phenomena which are the seasonal steric effect and the mesoscale variability.

The path of the Algerian current in the southern channel of Sardinia could be strongly affected by the seasonal variability as the first CEOF amplitude is higher in this area with the maximum seasonal mean value obtained in the fall of 1992 and fall of 1993. This can be related to the seasonal variability of MAW flux observed in the Strait of Sicily by the fact that these positive SLA (visible in Figure 4a) could be linked to a stronger MAW circulation around the northeast cape of Tunisia and a direct path toward the Strait of Sicily. This is in agreement with the recent observations of *Astraldi et al.* [1996], who report a wide MAW flow, as broad as the strait, in the winter and a narrow vein close to Tunisia during the summer and fall. However, the in situ data in the Strait of Sicily are sparse, especially along the Tunisian coasts, and according to *Manzella et al.* [1990], the maximum MAW flow occurs during the winter and not during the fall. Even if the seasonal variation of the mean sea level is similar to the one described by *Ovchinnikov* [1974], the 15 month time series of altimetric data used in this study is too short to get any solid conclusion on the annual seasonal variability locally represented by the first CEOF pattern.

The second CEOF reveals two points of higher variability along the Algerian current path. The decreasing phase from south to north across the western opening of the channel of Sardinia could correspond to the propagation of eddies described by *Fuda et al.* [1997] or by *Bouzinac et al.* [1997], who report an anticyclonic eddy evolving between June and August 1994 in the same area. This is in agreement with the hypothesis that some anticyclonic eddies could detach from the African coast at the entrance of the channel, following the deep bathymetry, because of their vertical extension, as events of ~6 months between the formation and the complete disappearance of the eddy. In the same way such detachments could occur between 4° and 6°E if one assumes that positive anomalies correspond to real anticyclonic eddies. The amplitude and phase isolines imply a northeast propagation of the eddies. This is supported by the anticyclonic eddy observed at the end of October 1992 (Plate 1), which is part of the second CEOF features (Figure 11a).

The pulsation of ~2 months observed in the amplitude of the second CEOF may be related to the growth rate of the baroclinic instabilities in the Algerian current which have been modeled by *Beckers and Nihoul* [1992]. Indeed, they obtained a development time of a few weeks for the perturbations to affect the whole current. However, the fact that this pulsation is visible in all the basin cannot be explained.

The 6 month periodicity of the mesoscale activity does not

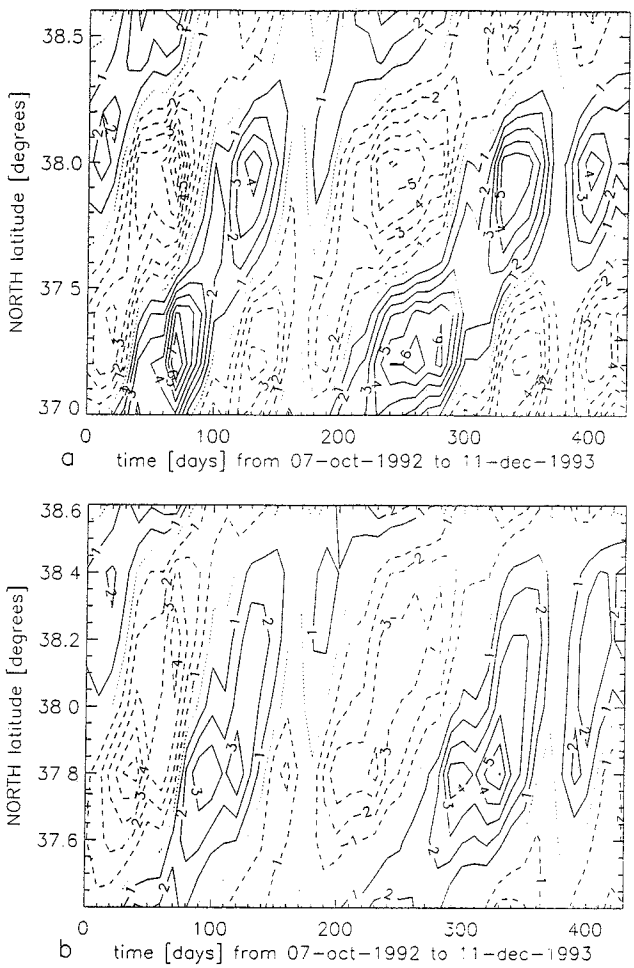

Figure 12. Time-latitude diagrams of the CEOF 2 amplitude (centimeters) (a) between 5°E, 37°N and 7.4°E, 38.6°N and (b) between 7.6°E, 37.4°N and 7.6°E, 38.6°N. These sections are shown in Figure 10.

appear in the previous studies of the Algerian current from in situ and infrared observations. Anticyclonic eddies have been detected in the spring, summer, and fall [*Taupier-Letage and Millot*, 1988], and the largest ones have lasted more than 6 months [*Millot et al.*, 1990]. This periodicity could also be a specific feature of the year 1993. It is therefore impossible to confirm this periodicity revealed by the second mode of the CEOF analysis whereas the propagation path and the propagation speed of 1 or 2 km d^{-1} fit quite well with in situ observations near the channel of Sardinia. In the future it would be necessary to monitor these eddies on a longer time period with the same almost continuous synoptic maps to ascertain whether the mesoscale variability is subject to a semi-annual cycle. This will be possible using the combined altimetric data of T/P and ERS-2.

Acknowledgments. This research has been undertaken in the framework of the Mediterranean Targeted Project (MTP) phase II-MATER (contribution MTPII-MATER/004). We acknowledge support from the European Commission's Marine Science and Technology Programme (MAST III) under contract MAS3-CT96-0051. C. Bouzinac benefited from financial support from Ministerio de Asuntos Exteriores in the frame of the Franco-Spanish exchange. We are grateful to N. Ayoub (CLS, Toulouse) who provided the altimetric SLA maps and to the Centre de Supercomputació de Catalunya (CESCA) whose CRAY YMP was used for CEOF computation. We warmly thank C. Millot, F. Martel, and E. García for their helpful comments. This study is a contribution to ESA ERS Announcement of Opportunity project ALGERS (E102/0). The Spanish National Program on Marine Sciences and Technology (CICYT) gave economic support to the research through project MAR95-1861.

References

Astraldi, M., G. P. Gasparini, S. Sparnocchia, M. Moretti and E. Sansone, The characteristics of the water masses and the water transports in the Sicily channel at long time scales, edited by F. Briand, *Bull. Inst. Océanogr.*, *17*, 95–115, 1996.

Ayoub, N., P. Y. Le Traon, and P. De Mey, A description of the Mediterranean surface variable circulation from combined ERS-1 and TOPEX/POSEIDON altimetric data, *J. Mar. Syst.*, in press, 1997.

Barnett, T. P., Interaction of the monsoon and Pacific trace wind system at interannual time scales, The equatorial zone, *Mon. Weather Rev.*, *111*, 756–773, 1983.

Beckers, J. M., and C. J. Nihoul, Model of the Algerian current's instability, *J. Mar. Syst.*, *3*, 441–451, 1992.

Benzohra, M., and C. Millot, Characteristics and circulation of the surface and intermediate water masses off Algeria, *Deep Sea Res.*, *42*, 1803–1830, 1995a.

Benzohra, M., and C. Millot, Hydrodynamics of an open Algerian eddy, *Deep Sea Res.*, *42*, 1831–1847, 1995b.

Bouzinac, C., C. Millot, and J. Font, Hydrology and currents observed in the channel of Sardinia during the PRIMO-1 experiment from November 1993 to October 1994, *J. Mar. Syst.*, in press, 1997.

Davis, R. E., Predictability of sea surface temperature and sea level pressure anomalies over the north Pacific ocean, *J. Phys. Oceanogr.*, *6*, 249–266, 1976.

Fuda, J. L., C. Millot, I. Taupier Letage, and X. Bocognano, XBT sections across the western Mediterranean sea, *J. Mar. Syst.*, in press, 1997.

Horel, J. D., Complex principal component analysis: Theory and examples, *J. Clim. Appl. Meteorol.*, *23*, 1660–1673, 1984.

Larnicol, G., P. Y. Le Traon, and P. De Mey, Mean sea level and variable surface circulation of the Mediterranean Sea from 2 years of TP altimetry, *J. Geophys. Res.*, *100*, 163–177, 1995.

Le Traon, P. Y., and F. Hernandez, Mapping of the oceanic mesoscale circulation; validation of satellite altimetry using surface drifters, *J. Atmos. Oceanic Technol.*, *9*, 687–698, 1992.

Le Traon, P. Y., P. Gaspar, F. Bouyssel, and H. Makhmara, Using TOPEX/POSEIDON data to enhance ERS-1 data, *J. Atmos. Oceanic Technol.*, *12*, 161–170, 1995.

Manzella, G.M.R., and P. E. La Violette, The seasonal variation of water mass content in the western Mediterranean and its relationship with the inflows through the straits of Gibraltar and Sicily, *J. Geophys. Res.*, *95*, 1623–1626, 1990.

Manzella, G.M.R., T. S. Hopkins, P. J. Minnett, and E. Nacini, Atlantic water in the strait of Sicily, *J. Geophys. Res.*, *95*, 1569–1575, 1990.

Millot, C., Some features of the Algerian current, *J. Geophys. Res.*, *90*, 7169–7176, 1985.

Millot, C., Circulation in the western Mediterranean Sea, *Oceanol. Acta*, *10*, 143–149, 1987.

Millot, C., Models and data: A synergetic approach in the western Mediterranean sea, in *Ocean Processes in Climate Dynamics: Global and Mediterranean Examples*, pp. 407–425, Kluwer Acad., Norwell, Mass., 1994.

Millot, C., I. Taupier Letage, and M. Benzohra, The Algerian eddies, *Earth Sci. Rev.*, *27*, 203–219, 1990.

Millot, C., G.M.R. Manzella, and P. E. La Violette, Correction to "The seasonal variation of water mass content in the western Mediterranean and its relationship with the inflows through the straits of Gibraltar and Sicily" by G. M. R. Manzella and P. E. La Violette, *J. Geophys. Res.*, *97*, 17,961–17,962, 1992.

Ovchinnikov, I. M., On the water balance of the Mediterranean Sea, *Oceanology*, *14*, 198–202, 1974.

Overland, J. E., and R. W. Preisendorfer, A significance test for principal components applied to a cyclone climatology, *Mon. Weather Rev.*, *110*, 1–4, 1982.

Perkins, H., and P. Pistek, Circulation in the Algerian basin during June 1986, *J. Geophys. Res.*, *95*, 1577–1585, 1990.

Stidd, C. K., The use of eigenvectors for climatic estimates, *J. Appl. Meteorol.*, *6*, 255–264, 1967.

Taupier-Letage, I., and C. Millot, Surface circulation in the Algerian basin during 1984, *Oceanol. Acta*, *9*, 79–85, 1988.

Vazquez, J., Observations on the long period variability of the Gulf Stream downstream of Cape Hatteras, *J. Geophys. Res.*, *98*, 20,133–20,147, 1993.

Vazquez, J., J. Font, and J. J. Martinez Benjamin, Observations on the circulation in the Alboran Sea using ERS-1 altimetry and sea surface temperature data, *J. Phys. Oceanogr.*, *26*, 1426–1439, 1996.

Zlotnicki, V., L. L. Fu, and W. Patzert, Seasonal variability in global sea level observed with GeoSat altimetry, *J. Geophys. Res.*, *94*, 17,959–17,969, 1989.

C. Bouzinac and J. Font, Instituto de Ciencias del Mar, Consejo Superior de Investigaciones Cientificas, Paseo Juan de Borbon, 08039 Barcelona, Spain. (e-mail: cath@icm.csic.es; jfont@icm.csic.es)

J. Vazquez, Jet Propulsion Laboratory, California Institute of Technology, 4800 Oak Grove Drive, Pasadena, CA 91109-8099. (e-mail: jv@pacific.jpl.nasa.gov)

(Received December 19, 1996; revised October 3, 1997; accepted October 10, 1997.)

2. The detection of mesoscale structures in SAR images

During our previous ERS AO project (1991-1995) interesting results were achieved in the domain of identifying mesoscale current features in the western Mediterranean, and in relating them to oceanographic phenomena measured *in situ* and to atmospheric conditions (Font et al., 1996; Shirasago and Font, 1997). It was expected during ALGERS to increase this knowledge and develop new techniques to correlate *in situ* with SAR information. However, as indicated before, the results in this subject have been poorer than expected. The temporal and spatial coverage of the western Algerian basin by SAR images has appeared to be too low for an adequate detection and tracking of the anticyclonic eddies that dominate the regional circulation. The strong dependence of the imaging capability of SAR on the wind conditions would require a high frequency sampling to make it a useful tool, comparable to satellite infrared imagery. The proposed use of RADARSAT, with a significantly larger swath, has not been feasible. It was expected to incorporate colour imagery (SeaWiFS) into the study of the Algerian eddies, but this was frustrated by the continuous delay in the satellite launch.

As explained, the only case of spatial and almost temporal coincidence between SAR and *in situ* sampling (6 October, Alboran Sea) will be the subject of a specific analysis within the OMEGA project, co-ordinated by another ALGERS Co-I, Dr. Joaquim Tintoré.

The near real time access of SAR imagery to the scientific team on board the research vessel has been a success. Quick looks of the SAR scenes, as well as the corresponding features identification performed at NERSC Bergen, were received on the *HESPERIDES* the day following the ERS-2 overpass. Due to the circumstances enumerated above, this information was less used in the guidance of the vessel sampling than the NOAA SST maps directly received and processed on board. The following is a series of all the images and interpretations for the pre-cruise and cruise periods (5 September - 16 October) and a paper (Chic et al., 1997) presented at the 3rd ERS Symposium that summarises this aspect of the ALGERS results.

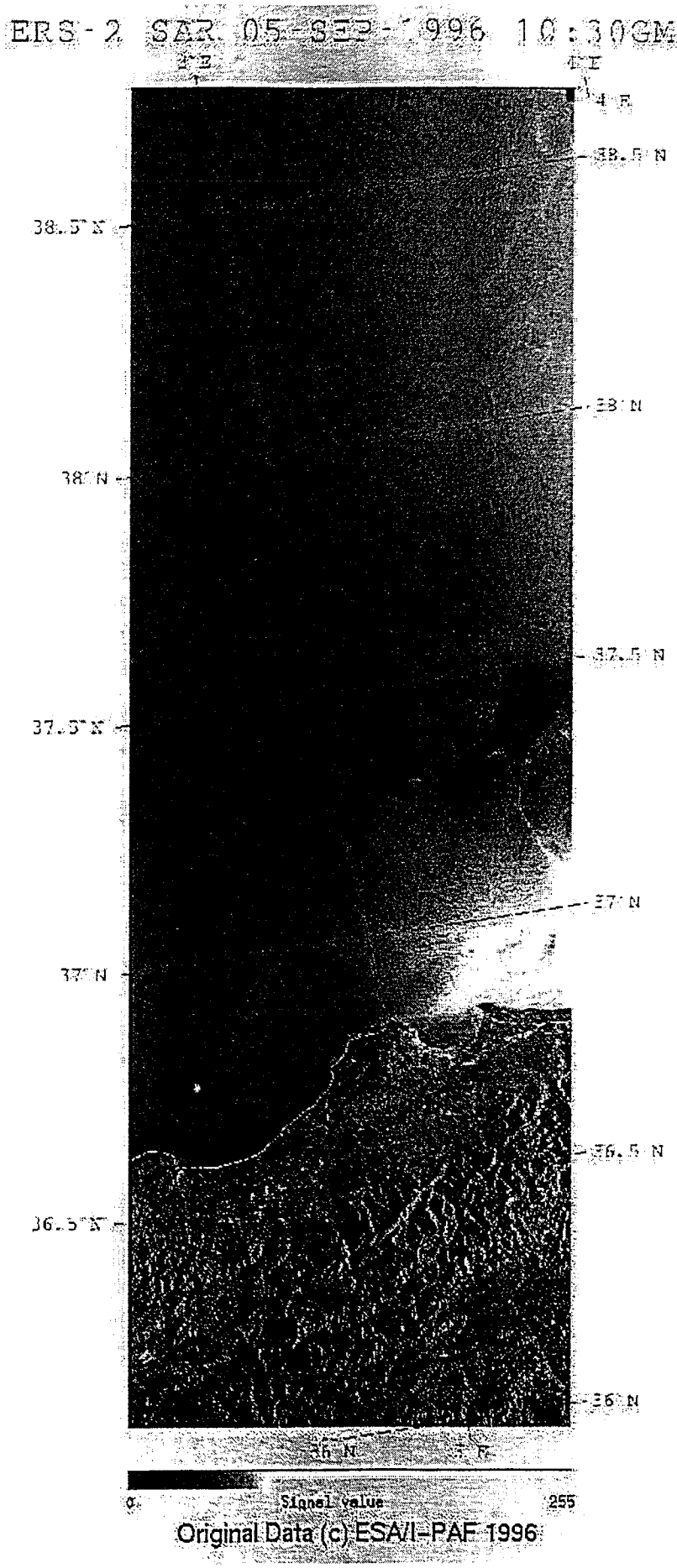

i960905d.jpg

ERS-2 SAR 05-SEP-1996 10:30GMT

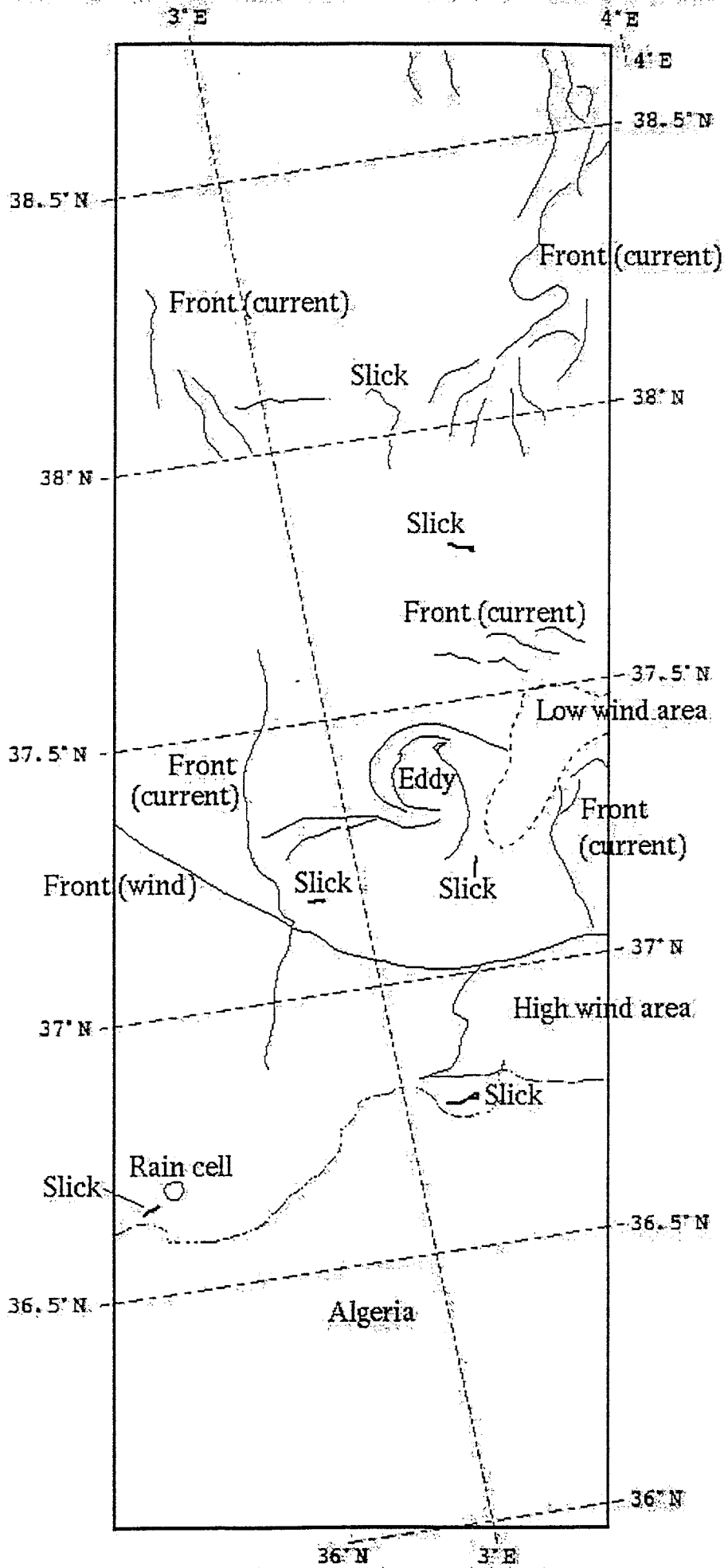

Image Interpretation by NERSC

ERS-2 SAR 08-SEP-1996 10:36GMT

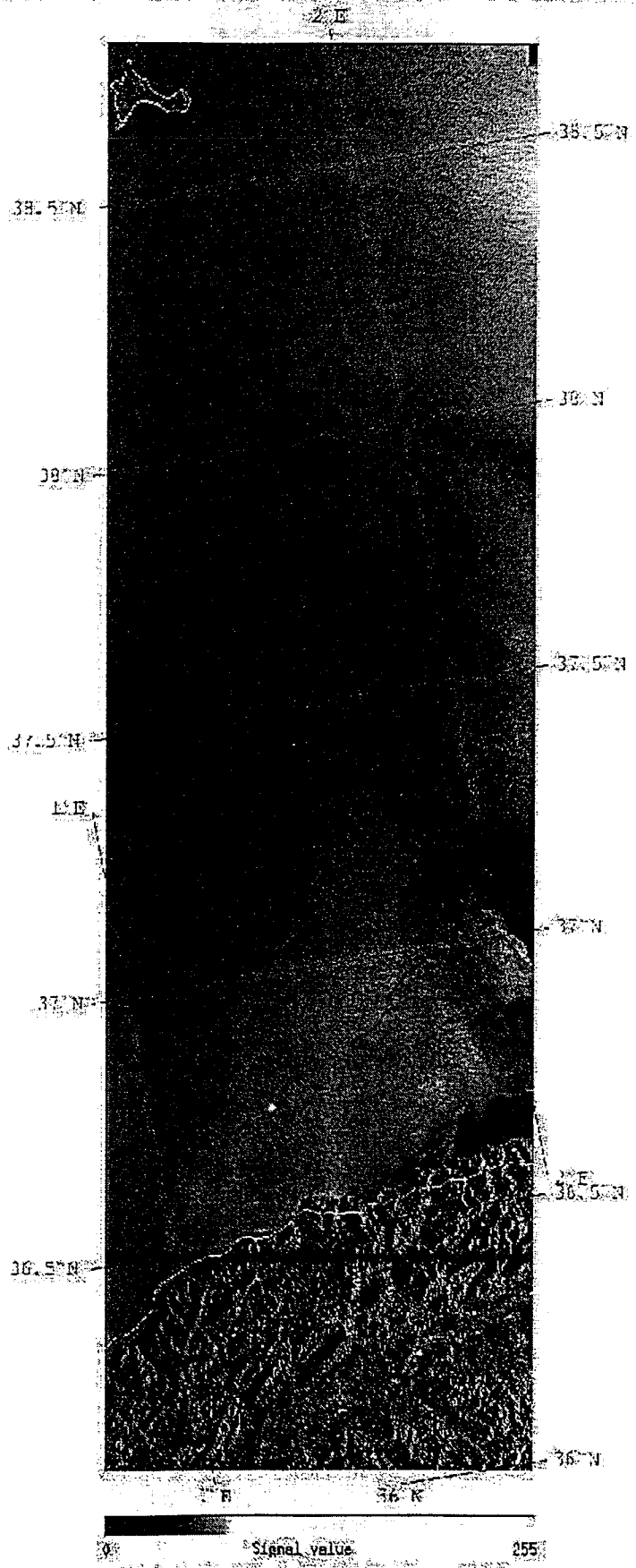

i960908d.jpg

ERS-2 SAR 08-SEP-1996 10:36GMT

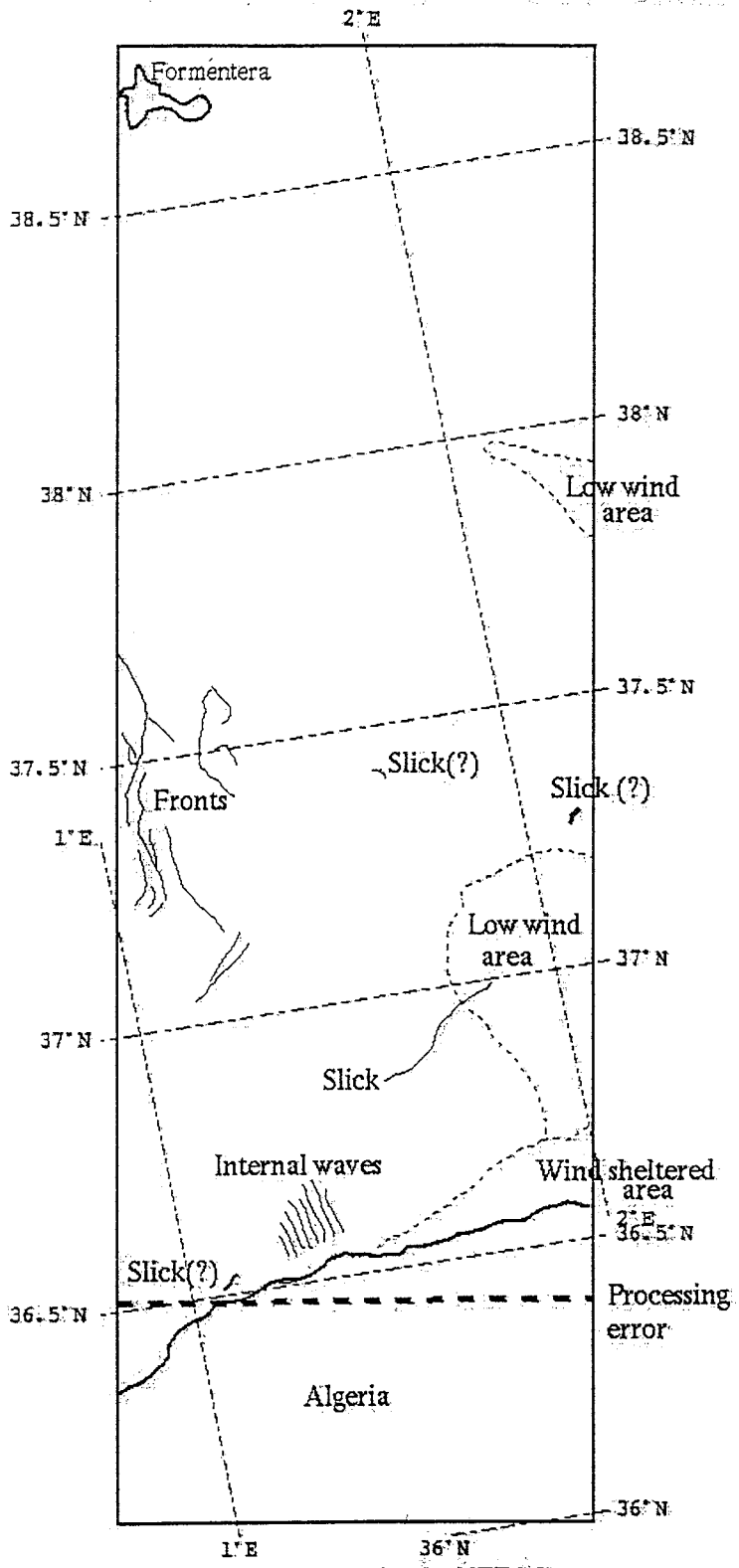

Image Interpretation by NERSC

a960908d.jpg

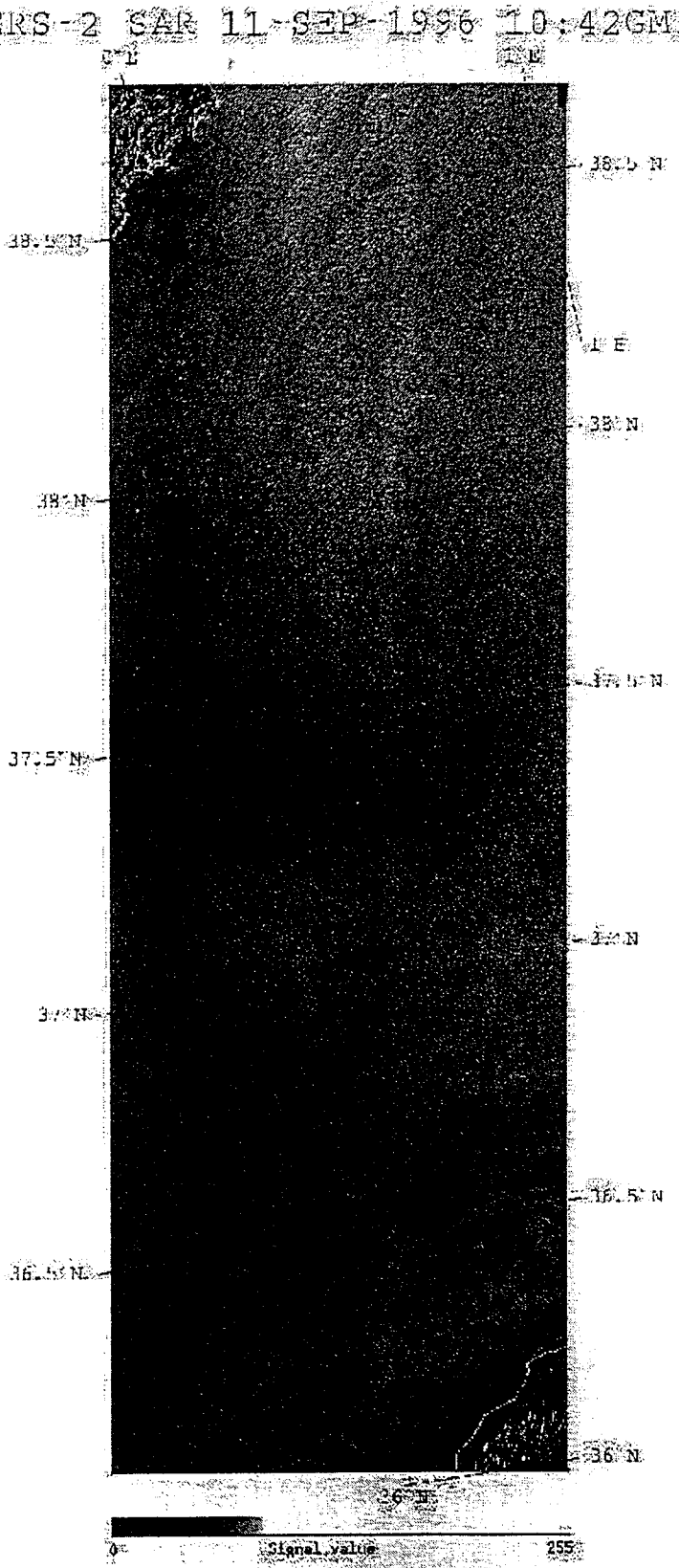

i19609112.jpg

ERS-2 SAR 11-SEP-1996 10:42GMT

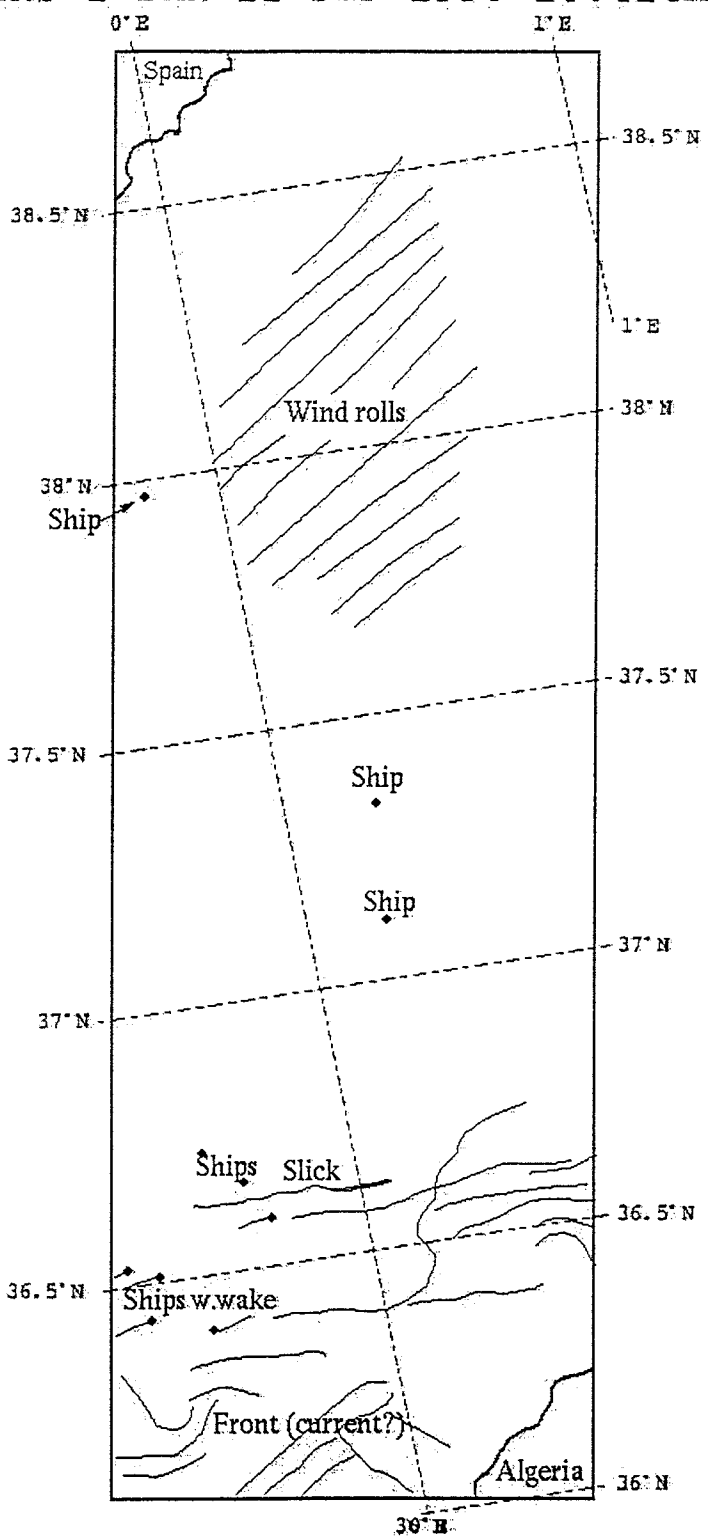

Image Interpretation by NERSC

a960911a.jpg

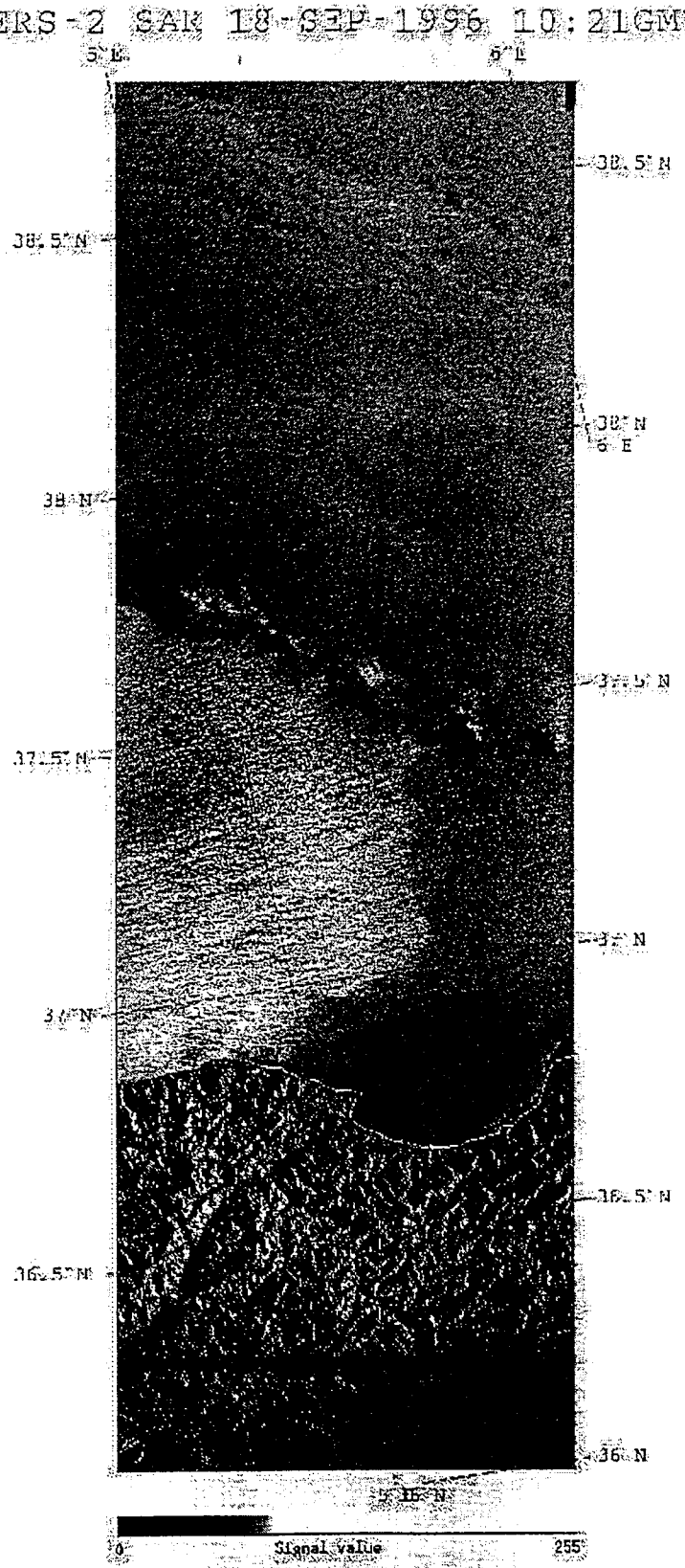

Original Data (c) ESA/I-PAF 1996

i960918d.jpg

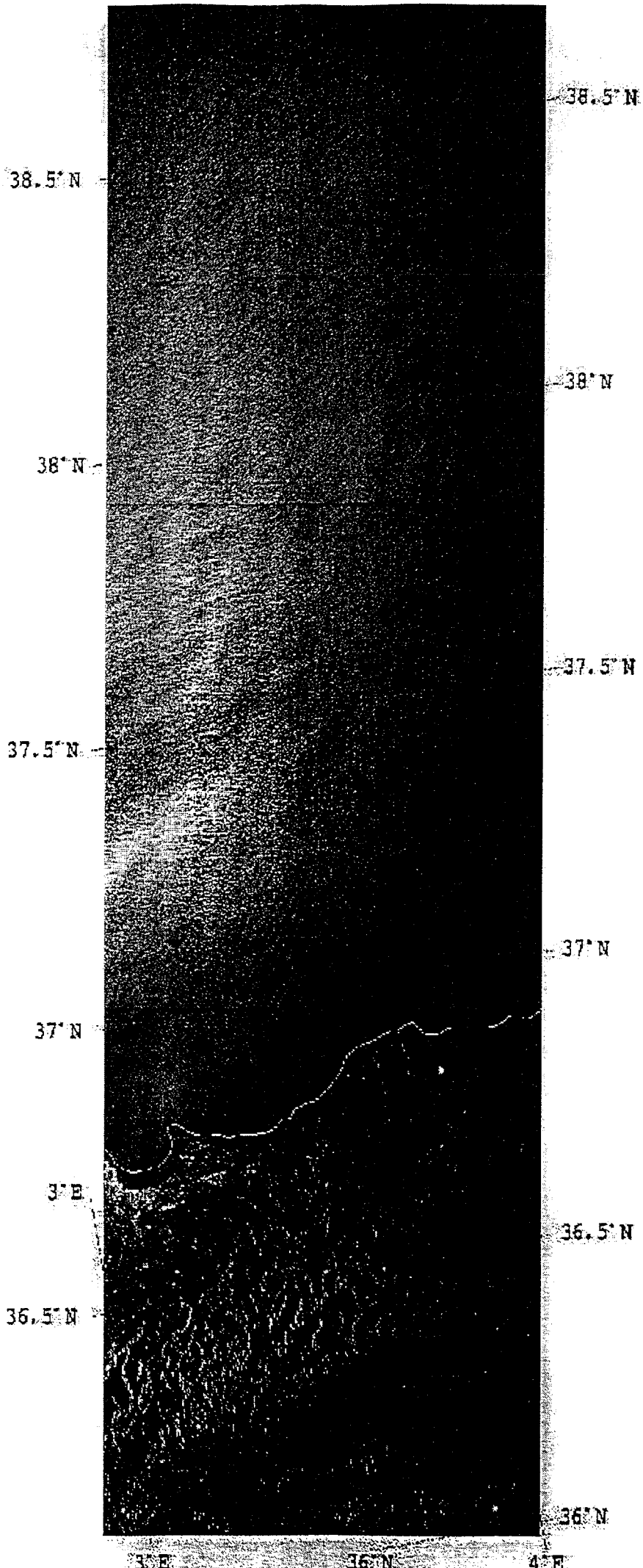
38.5°N
38.5°N
38°N
38°N
37.5°N
37.5°N
37°N
37°N
3°E
36.5°N
36.5°N
36°N
3°E
36°N
4°E

ERS-2 SAR 21-SEP-1996 10:27GMT

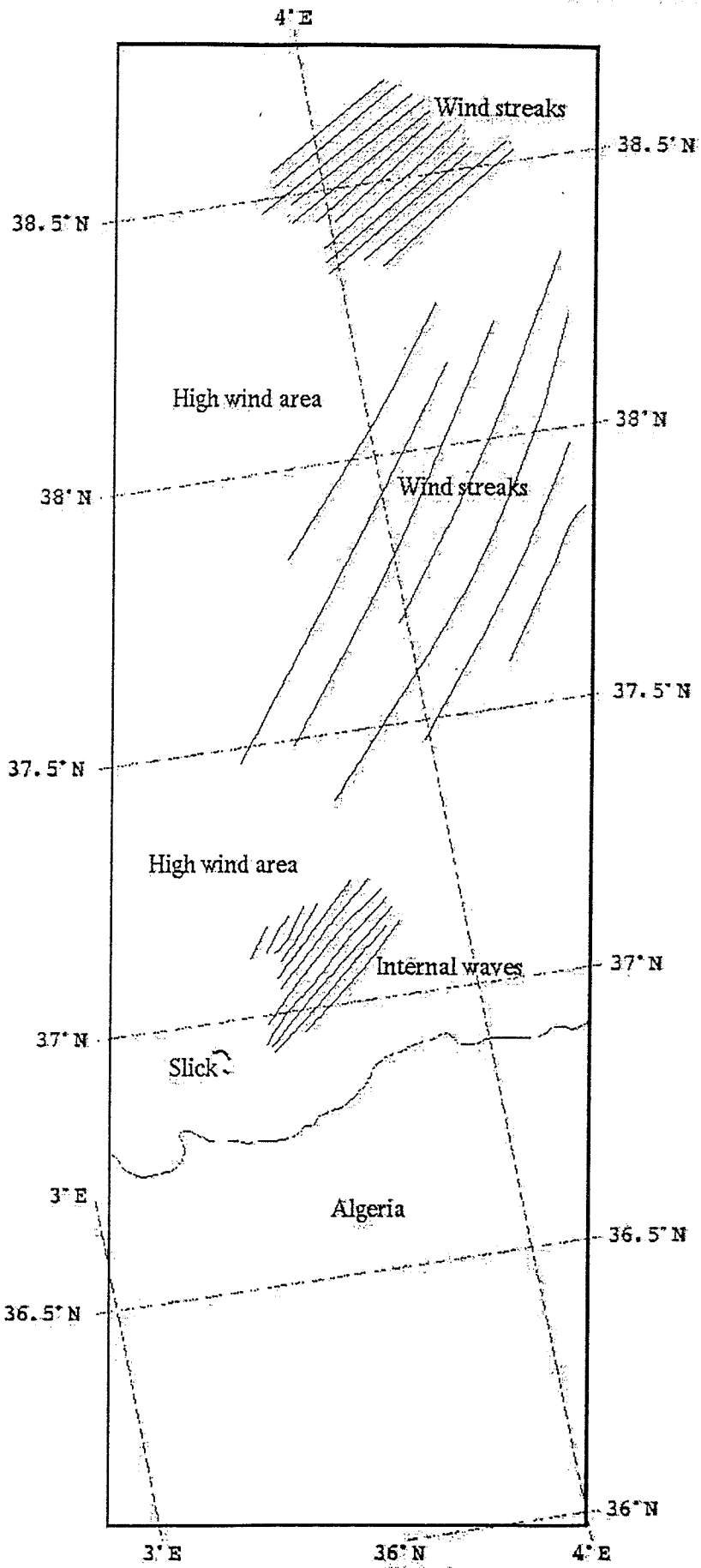

Image Interpretation by NERSC

970921d.jpg

ERS-2 SAR 24-SEP-1996 10:33GMT

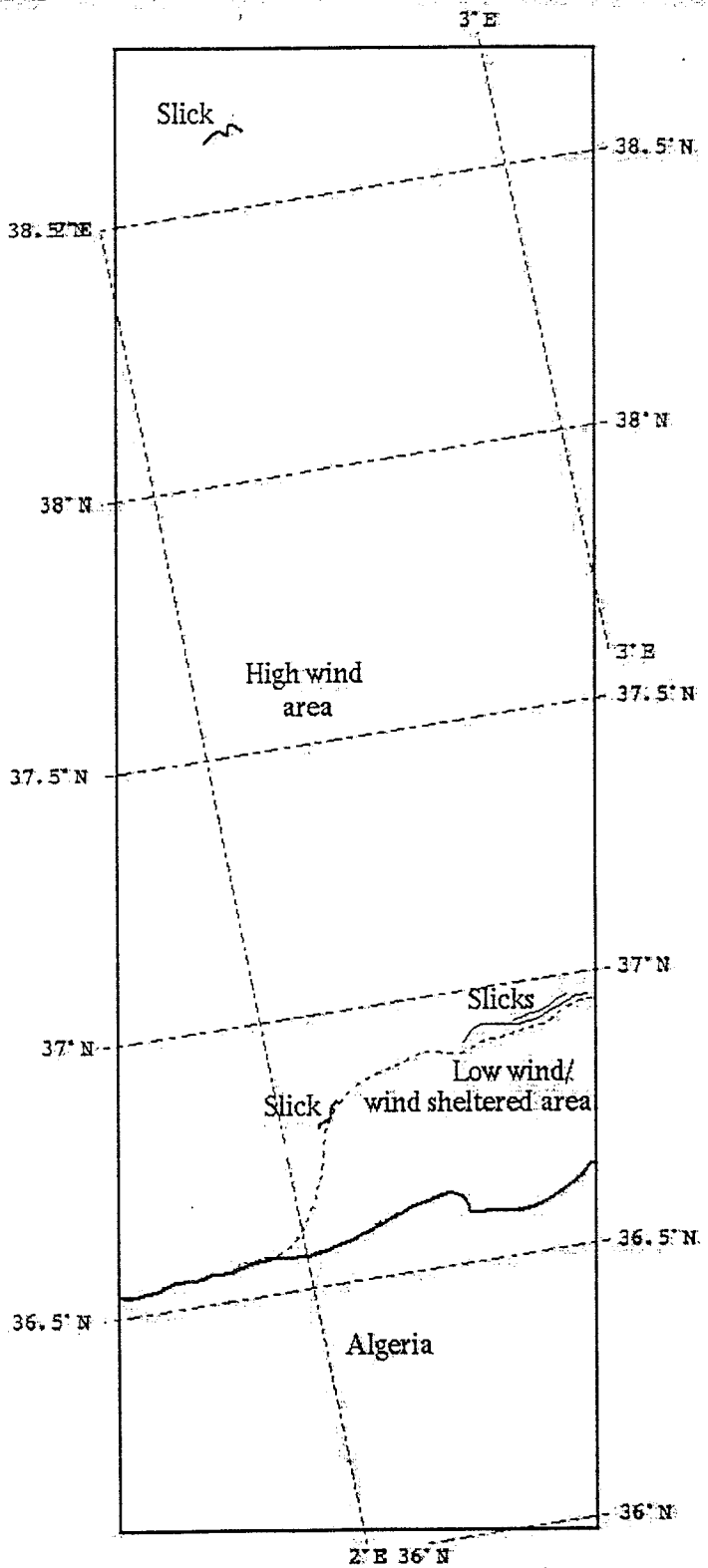

Image Interpretation by NERSC

a960924a.jpg

ERS-2 SAR 27-SEP-1996 10:38GMT

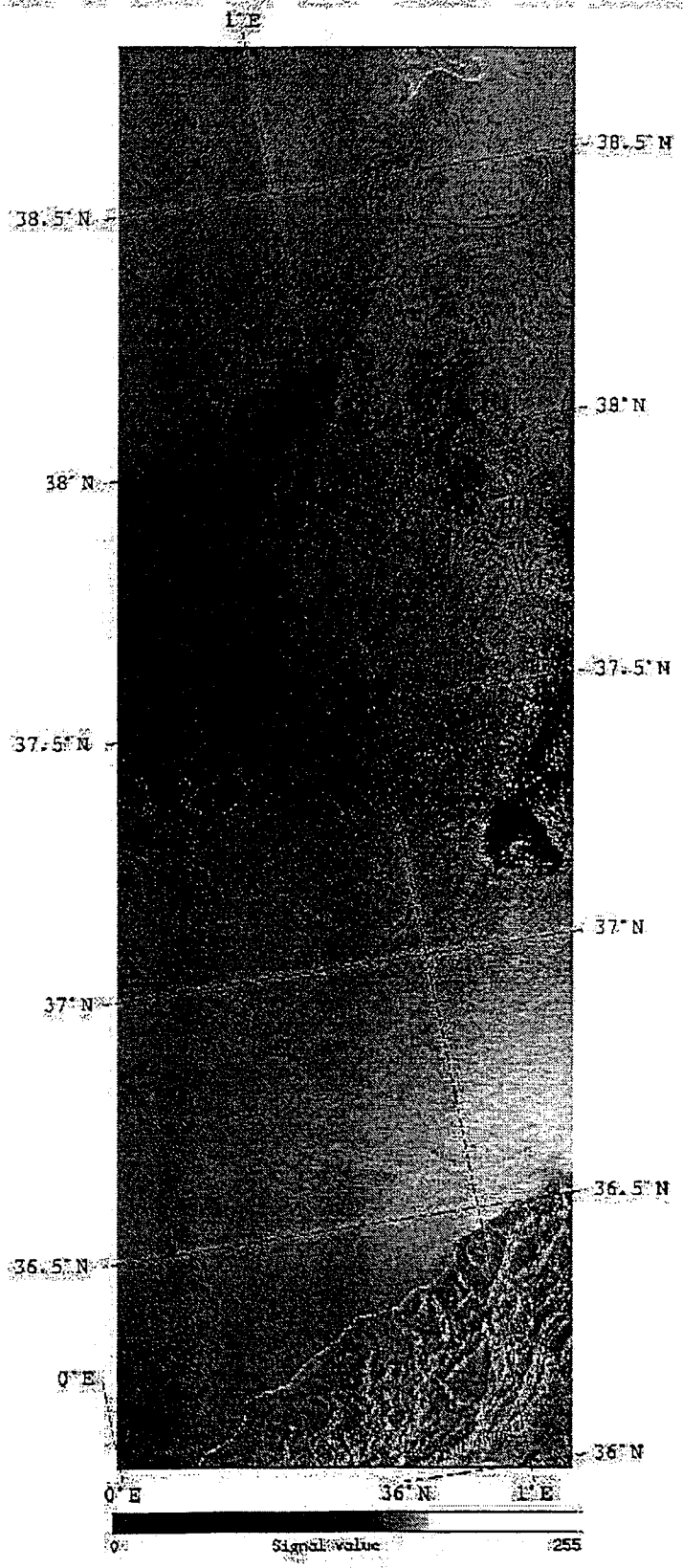

Original Data (c) ESA/West Freugh 1996

i960927d.jps

ERS-2 SAR 27-SEP-1996 10:38GMT

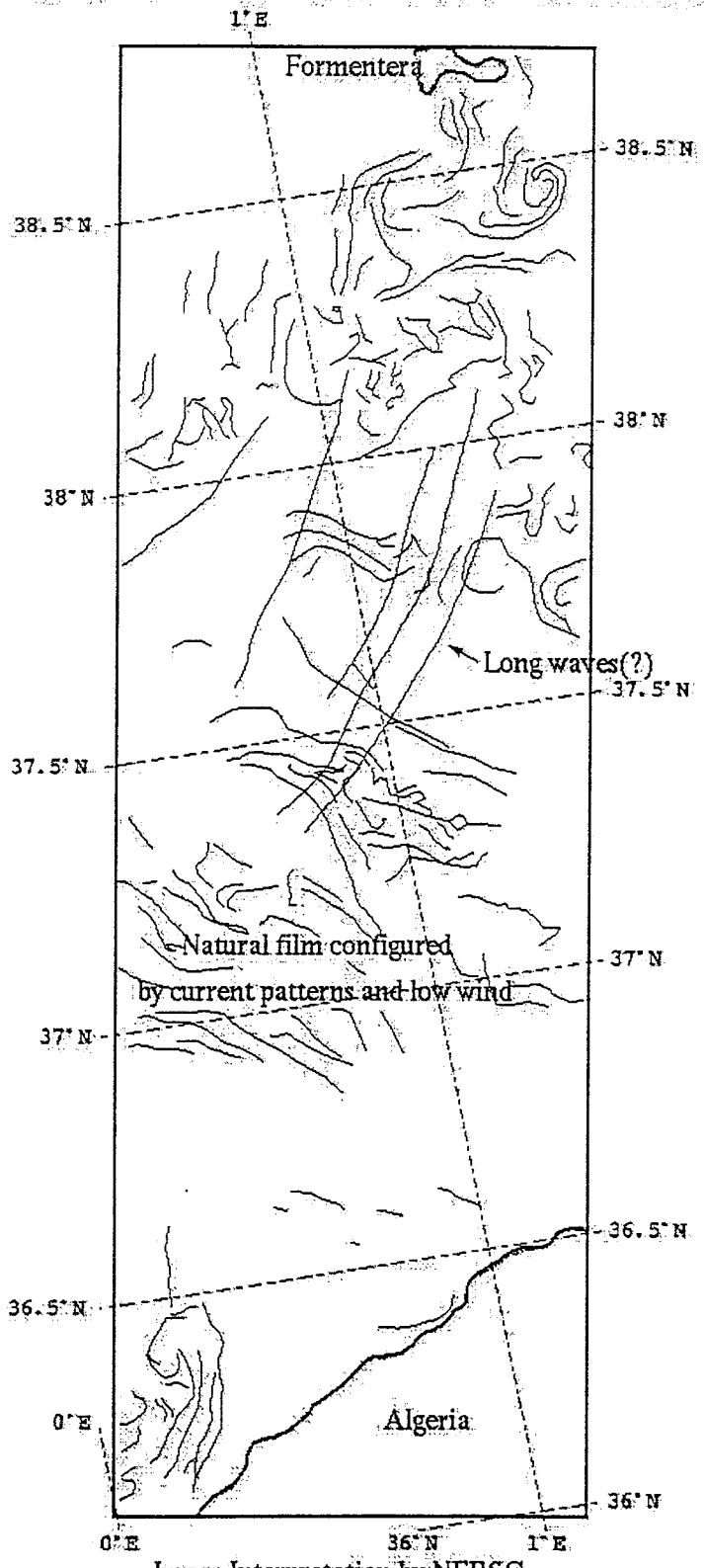

Image Interpretation by NERSC

a960927d.jpg

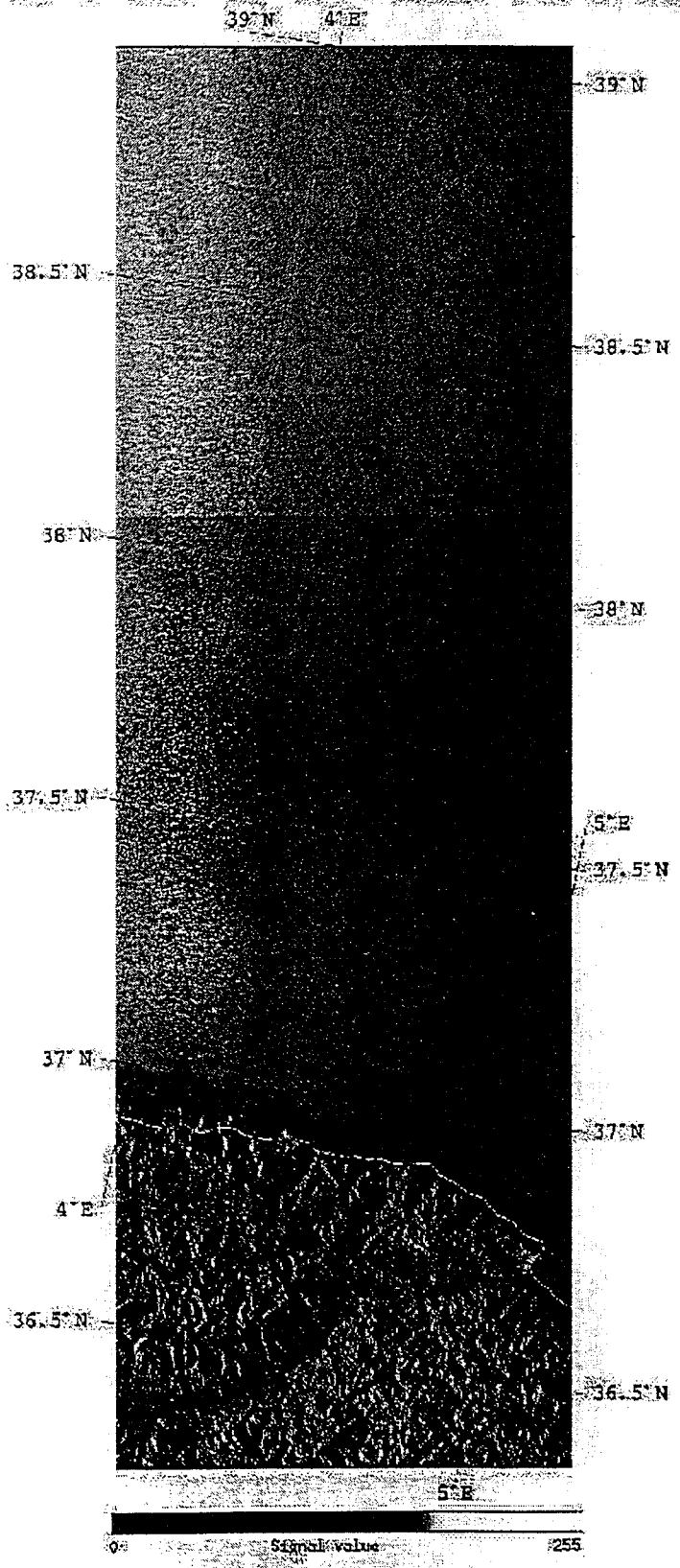

i960930a.jpg

ERS-2 SAR 30-SEP-1996 21:59GMT

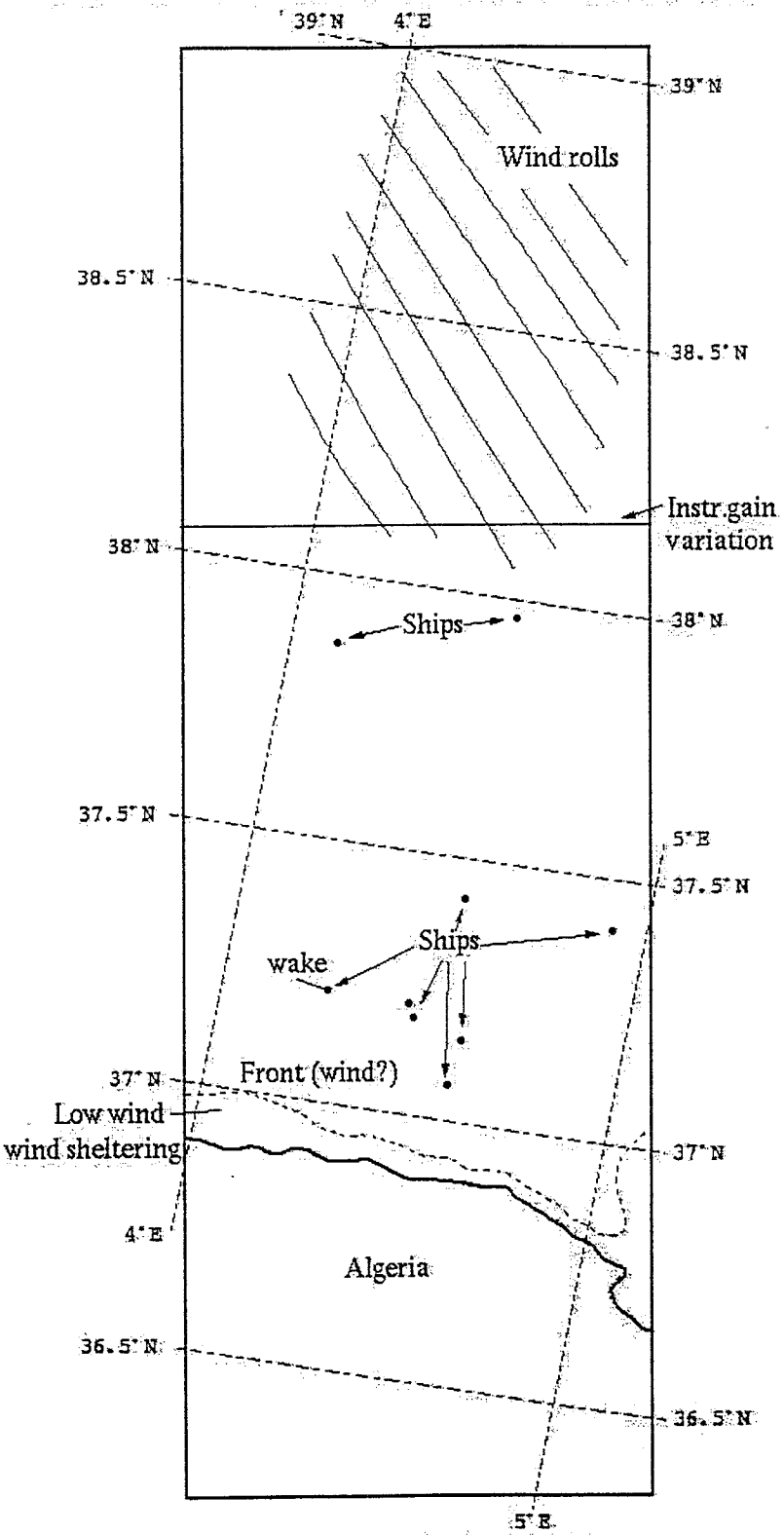

Image Interpretation by NERSC

a960930a.jpg

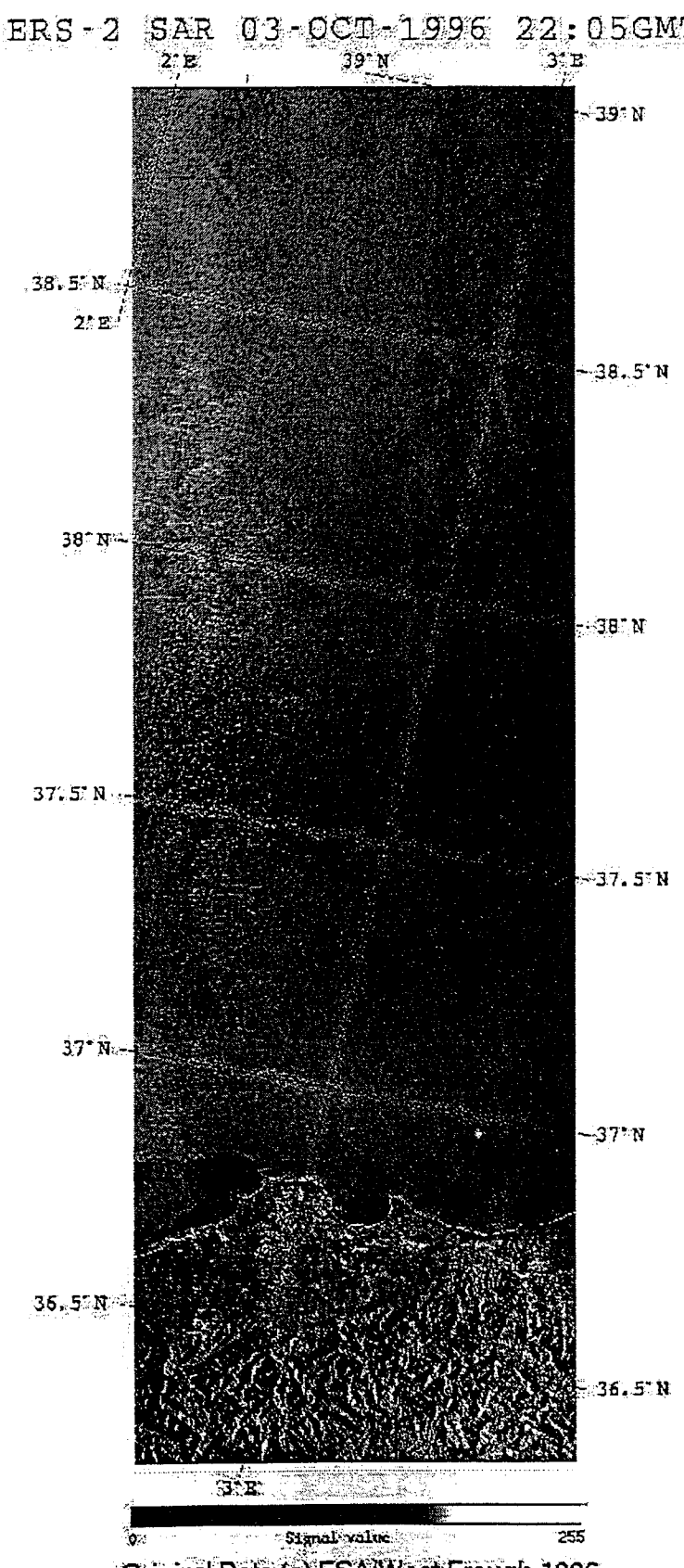

Original Data (c) ESA/West Freugh 1996

i961003a.jpg

ERS-2 SAR 03-OCT-1996 22:05GMT

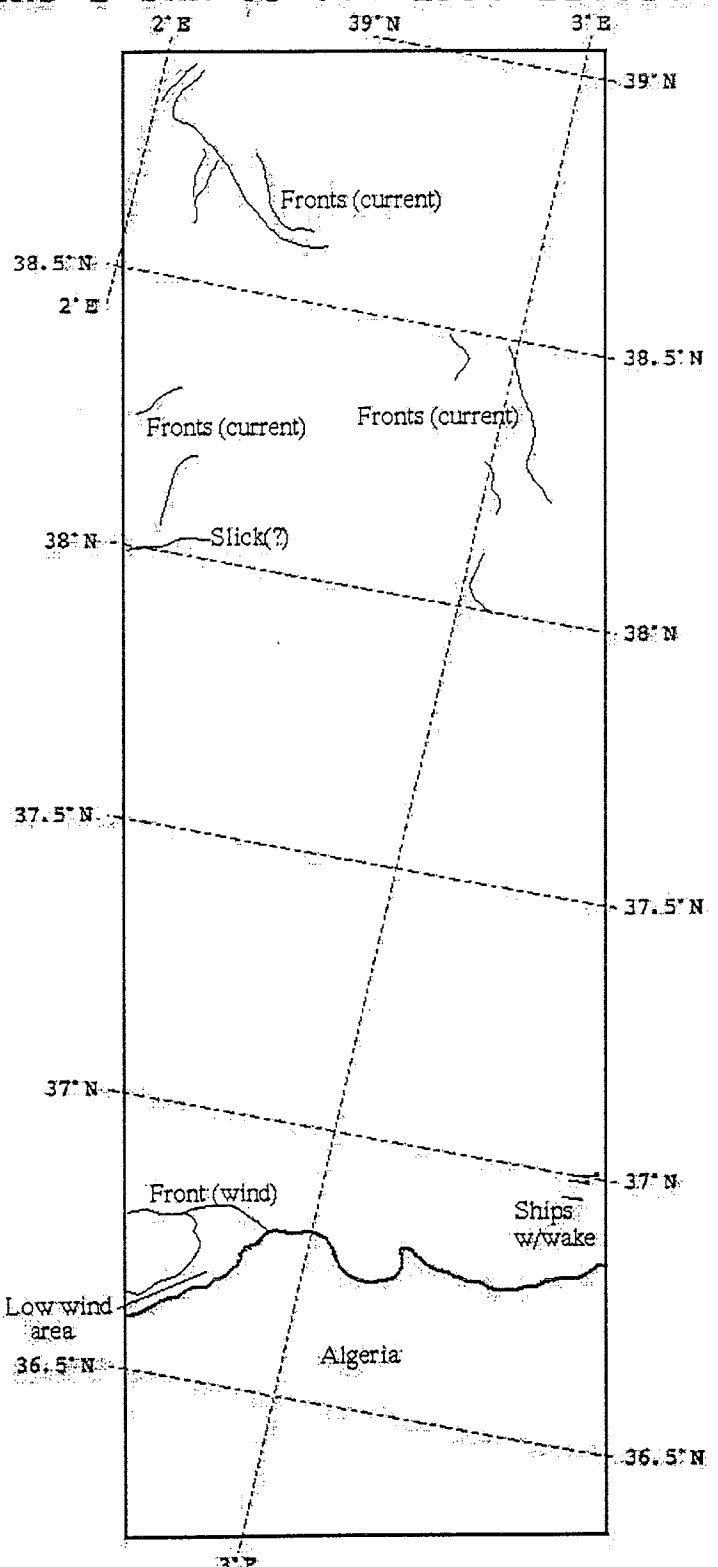

Image Interpretation by NERSC

a961003a.jpg

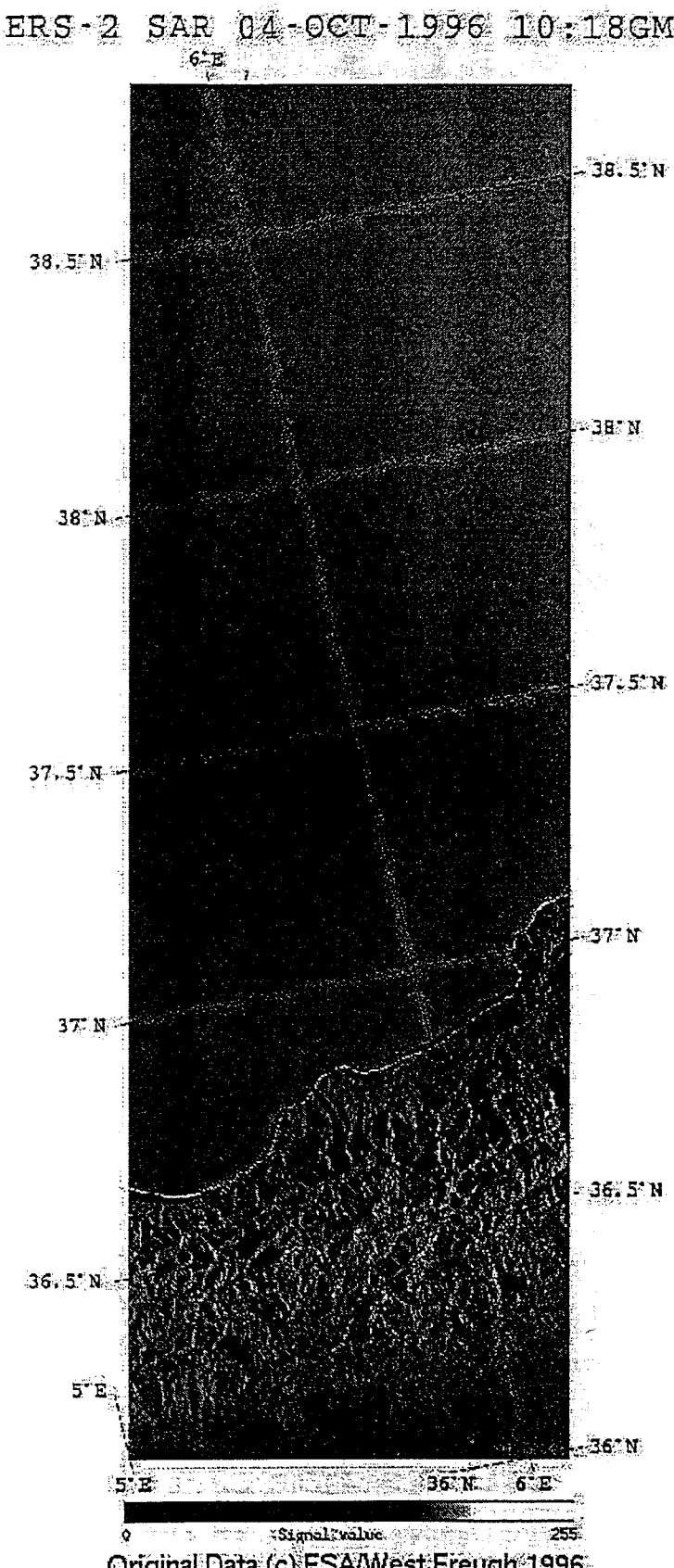

i961004d.jpg

ERS-2 SAR 04-OCT-1996 10:18GMT

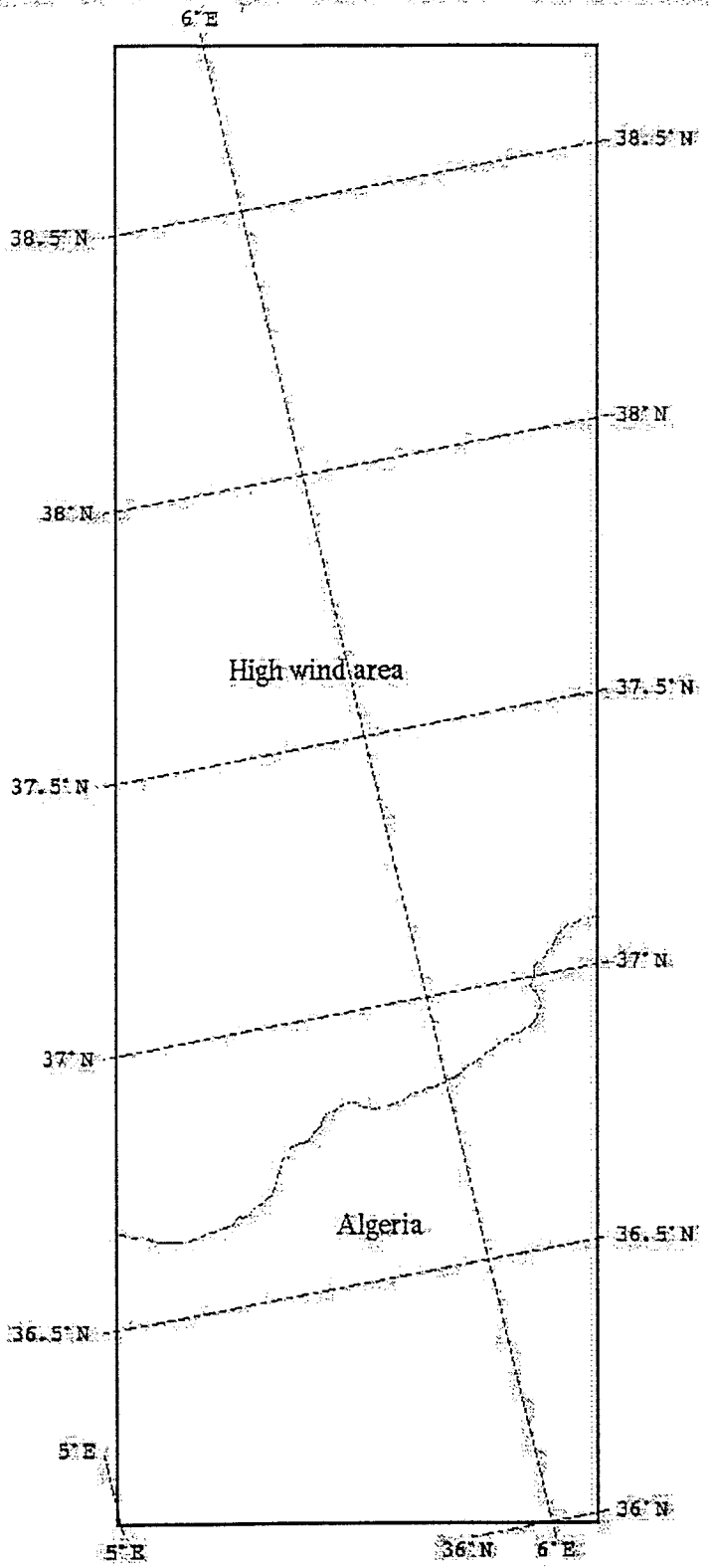

Image Interpretation by NERSC

a961004d.jpg

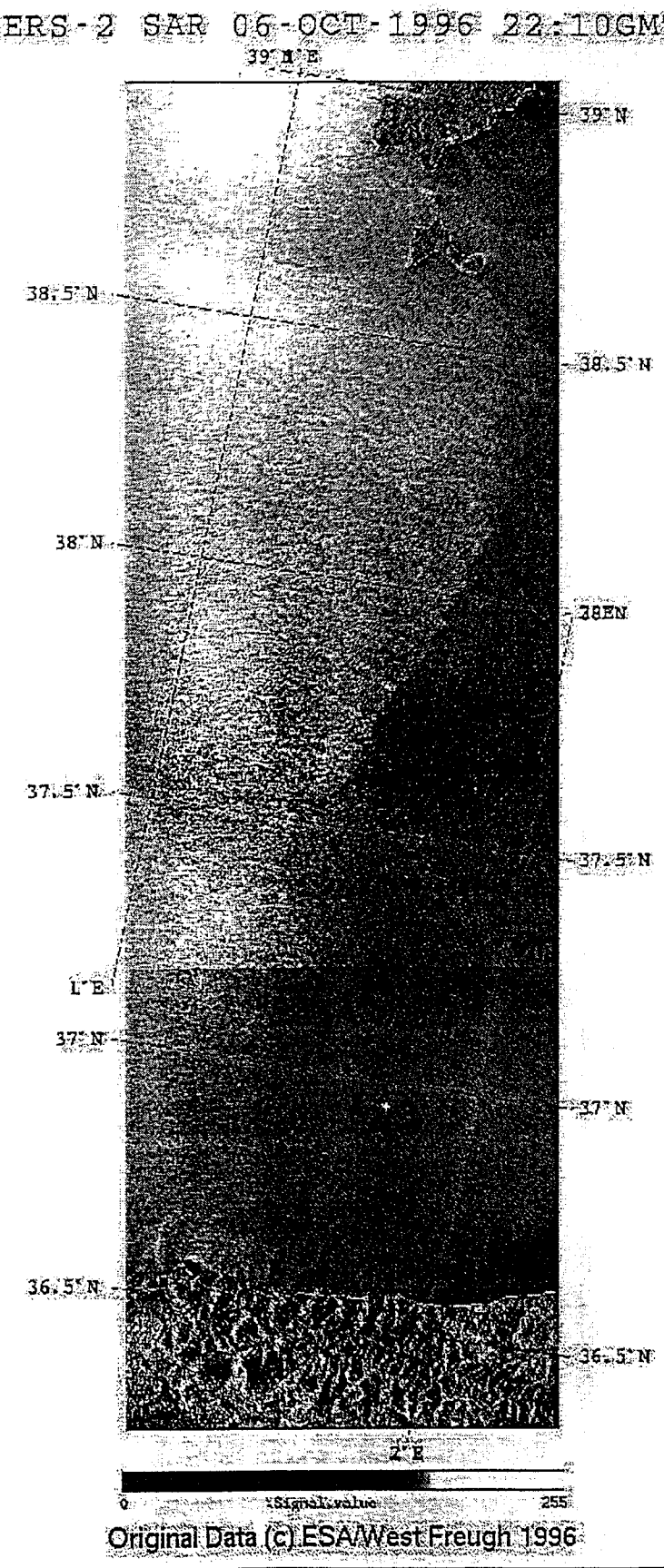

i961006a.jpg

ERS-2 SAR 06-OCT-1996 22:10GMT

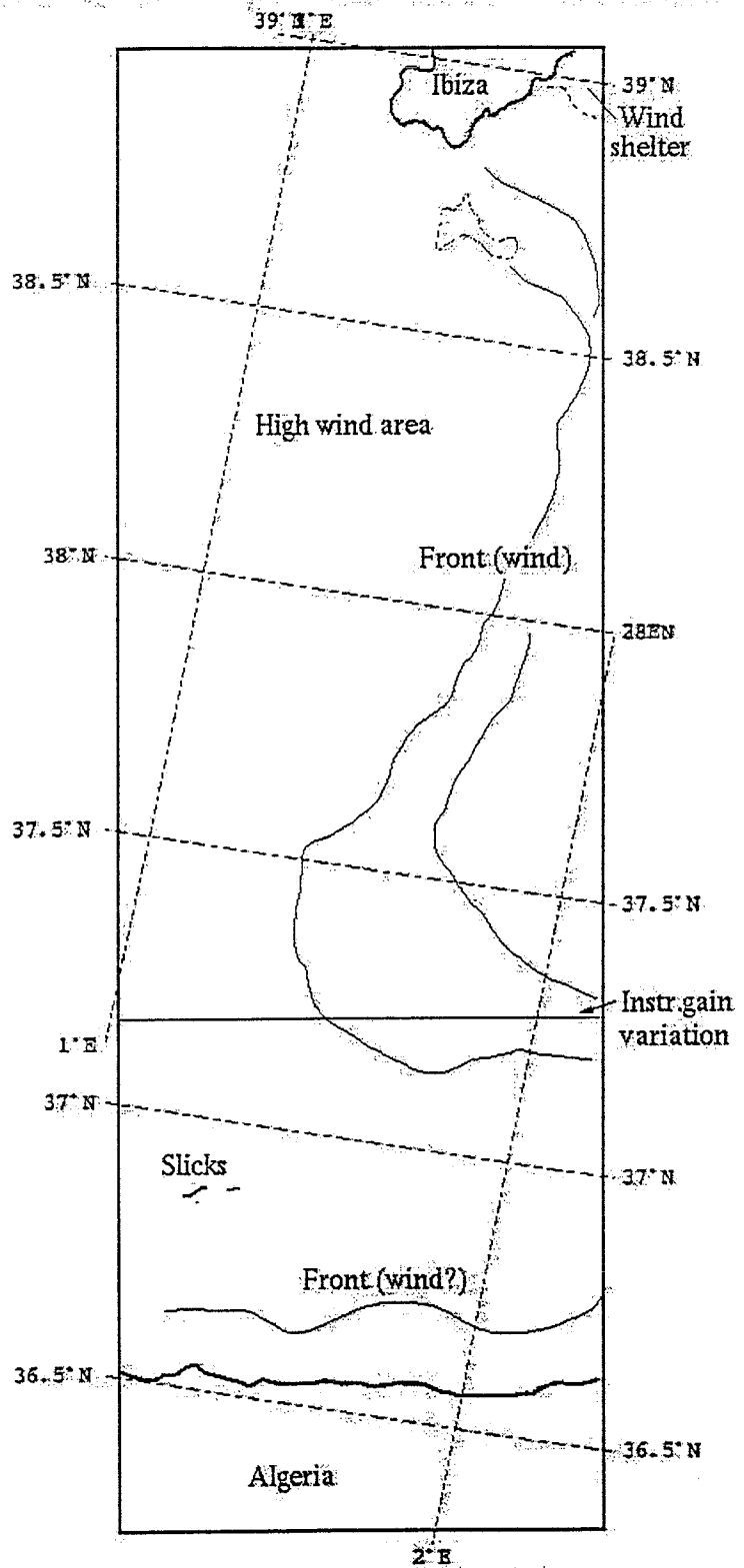

Image Interpretation by NERSC

a961006a.jpg

ERS-2 SAR 07-OCT-1996 10:24GMT

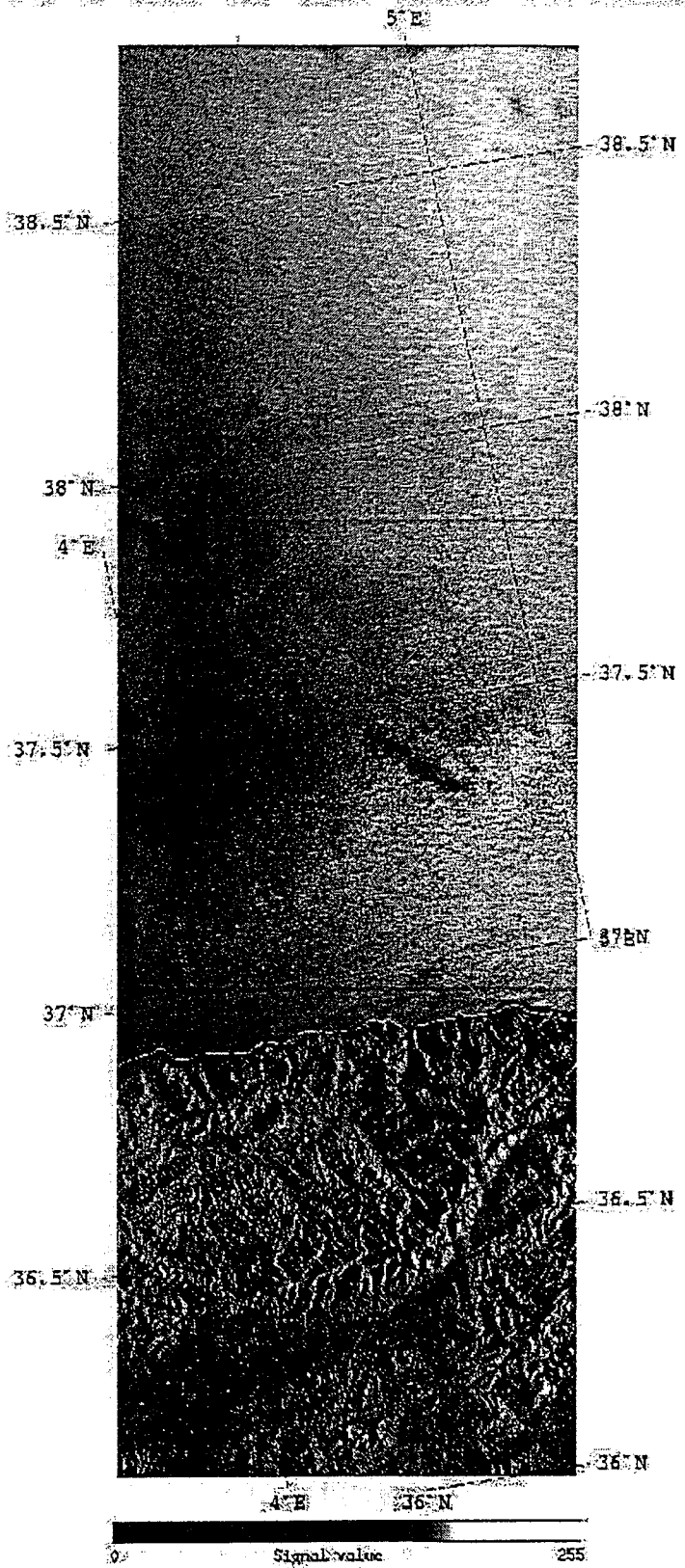

Original Data (c) ESA/West Freugh 1996

: 9610072.jpg

ERS-2 SAR 07-OCT-1996 10:24GMT

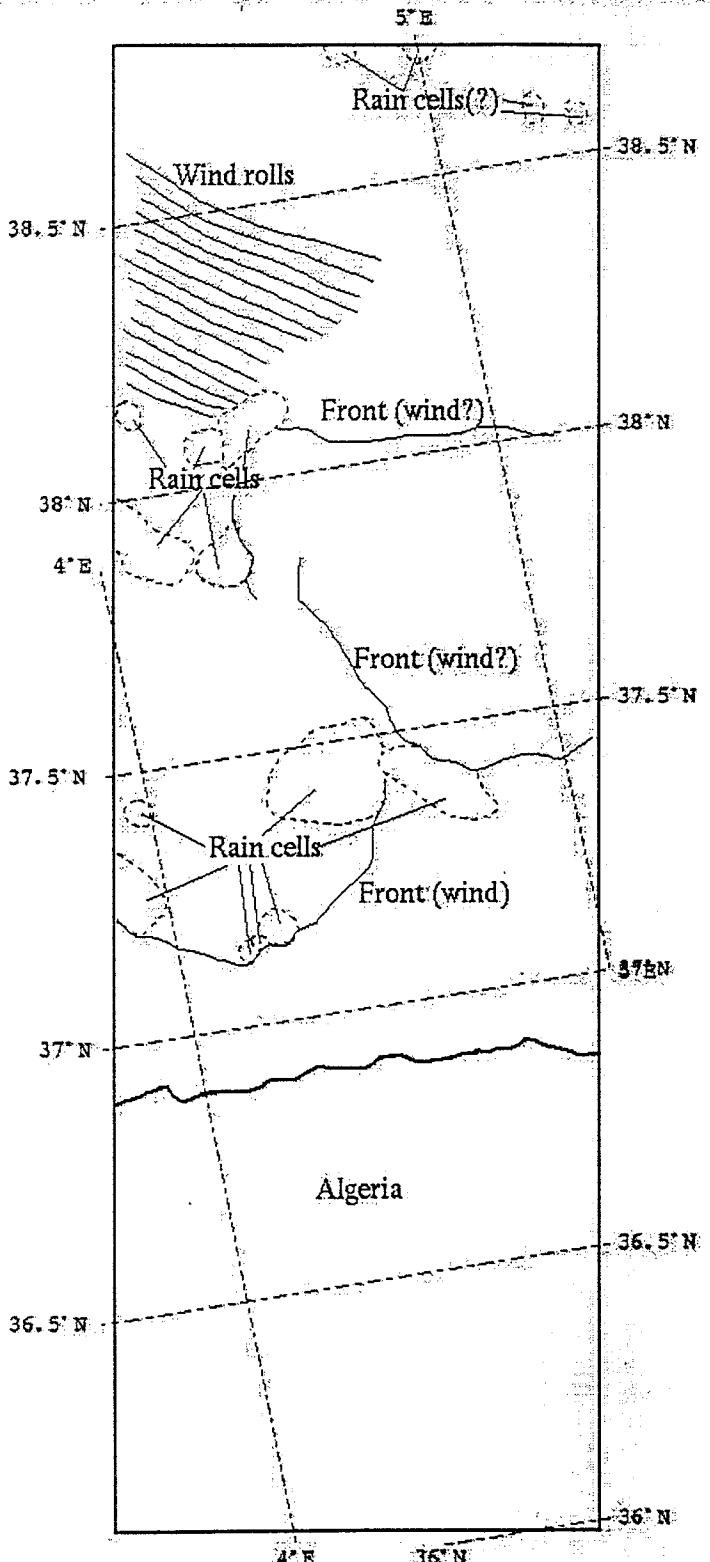

Image Interpretation by NERSC

a961072.jpg

ERS-2 SAR 09-OCT-1996 22:16GMT

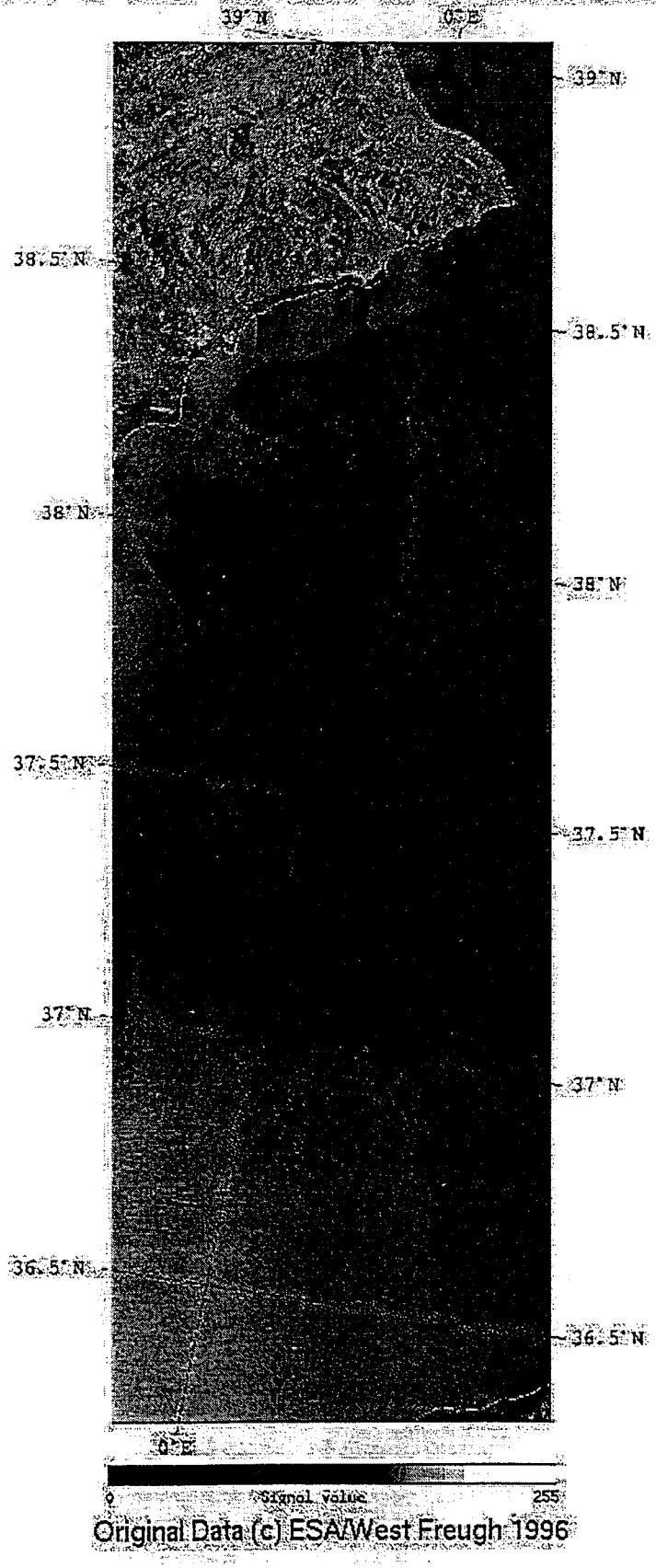

Original Data (c) ESA/West Freugh 1996

i961009a.jpg

ERS-2 SAR 09-OCT-1996 22:16GMT

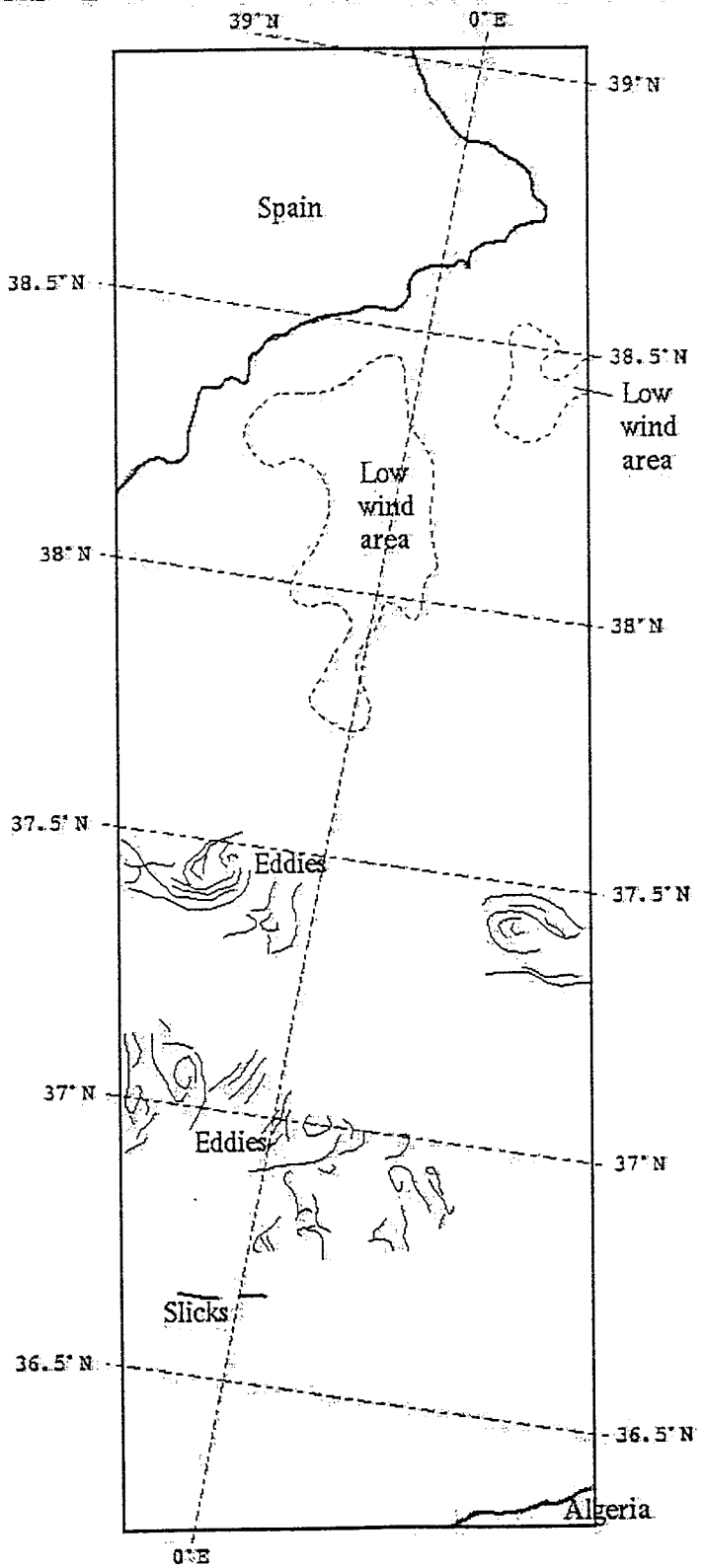

Image Interpretation by NERSC

a961009a.jpg

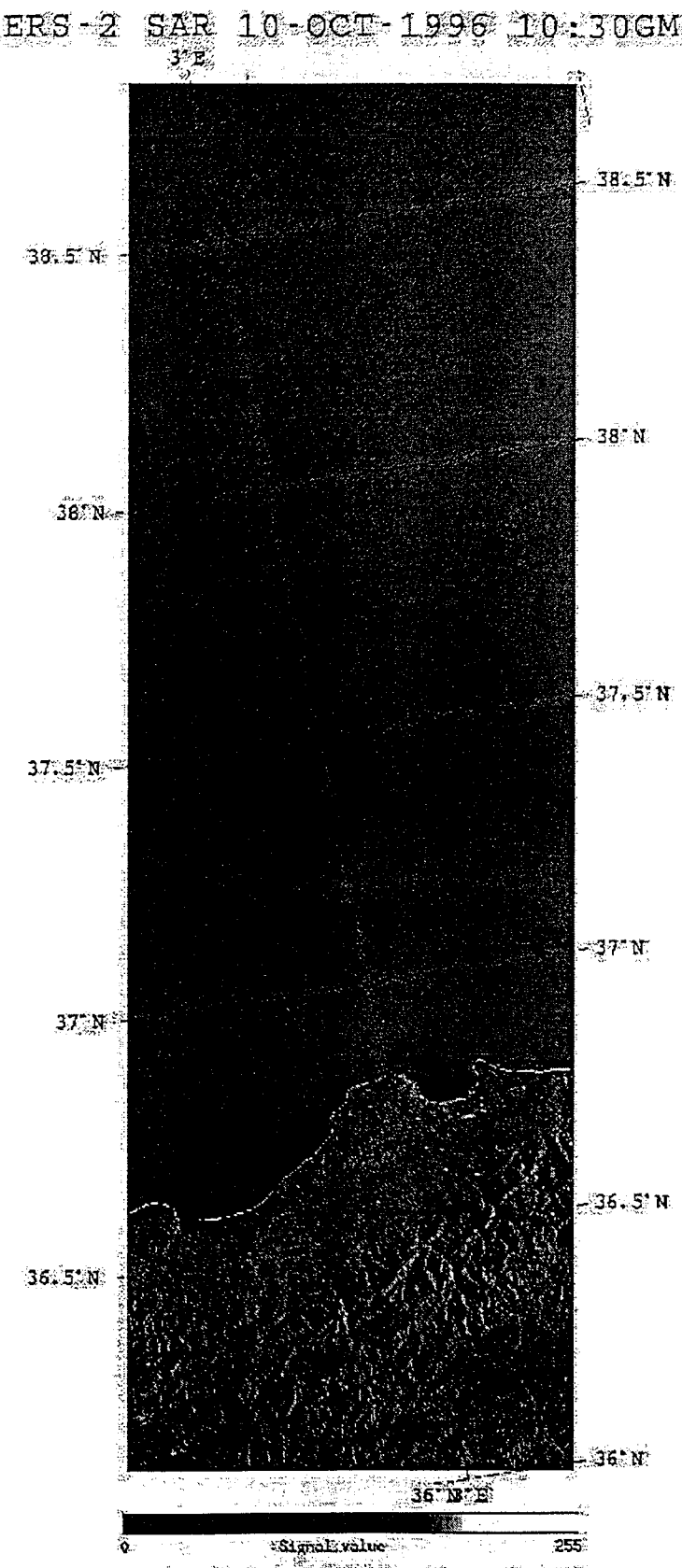

i961010a.jpg

ERS-2 SAR 10-OCT-1996 10:30GMT

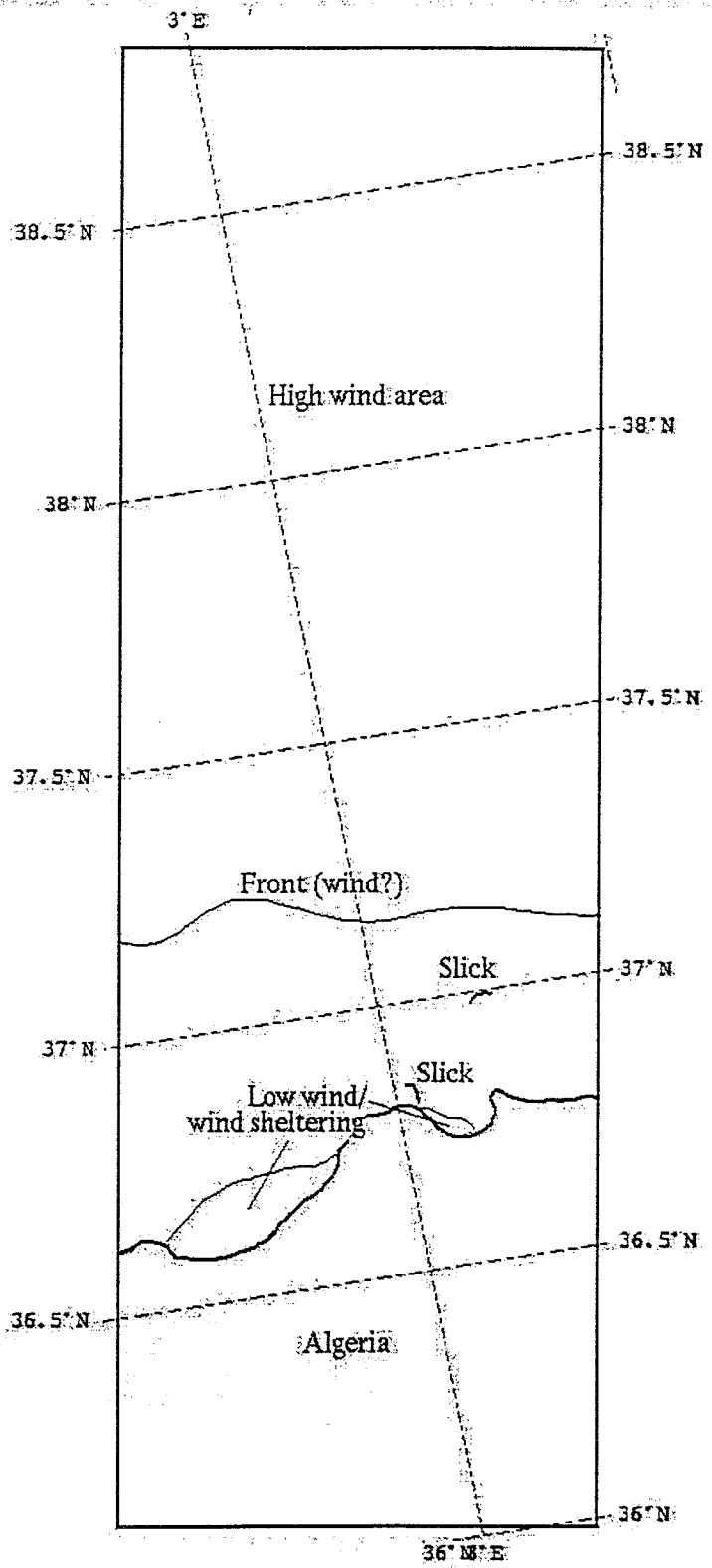

Image Interpretation by NERSC

a9610102.jpg

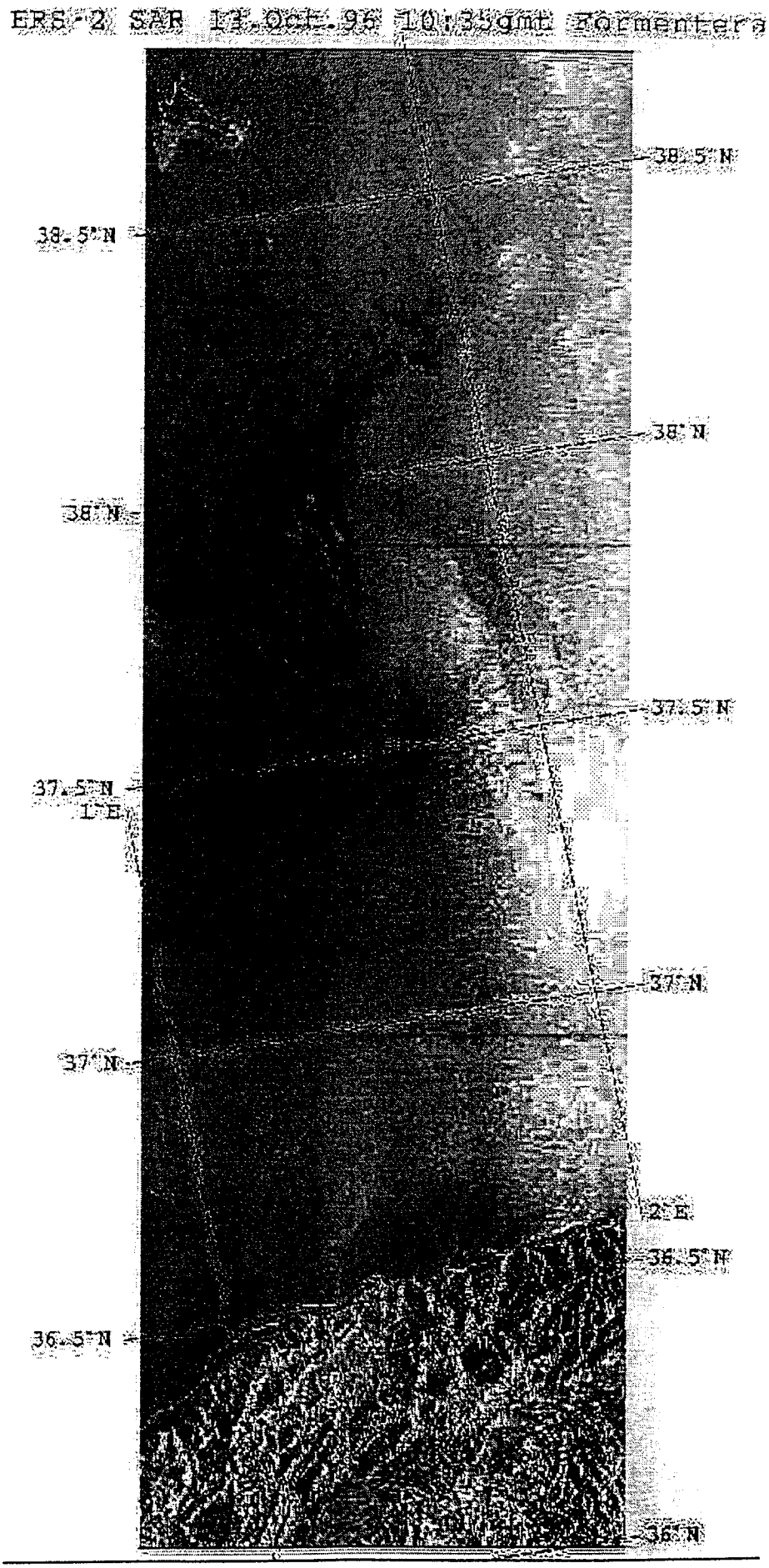

i961013d.jpg

ERS-2 SAR 16-OCT-1996 10:41GMT

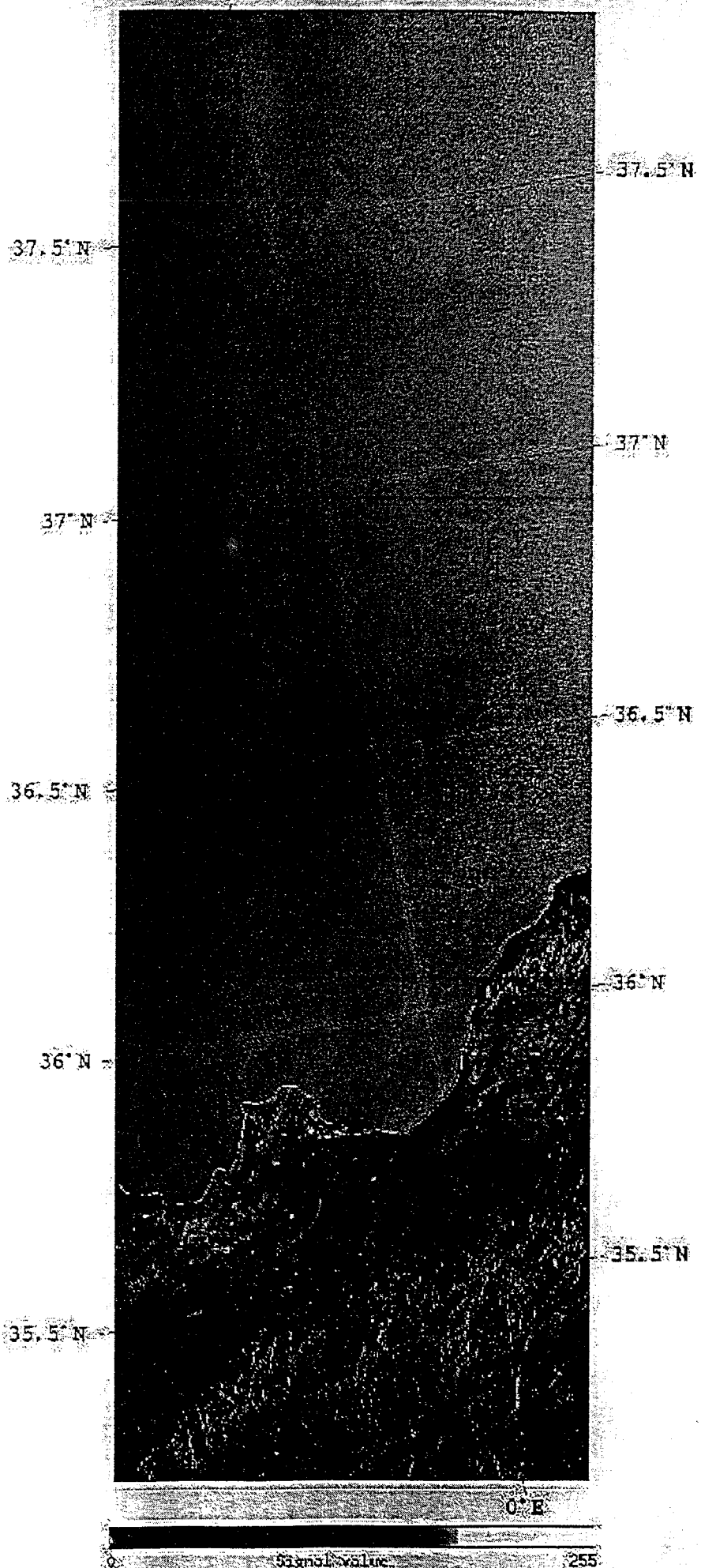

19961016d.jpg

Original Data (c) ESA/West Freugh 1996

ERS-2 SAR 16-OCT-1996 10:41GMT

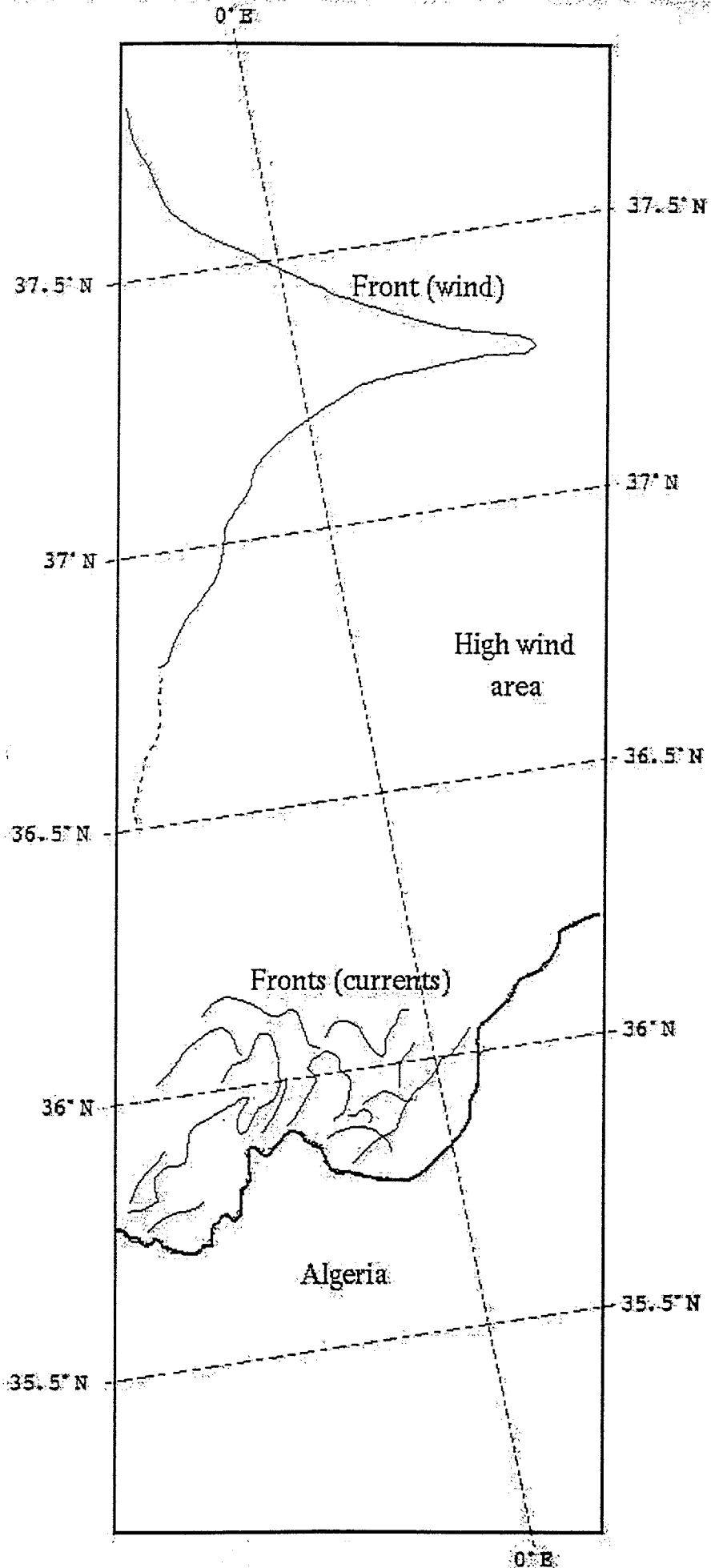

Image Interpretation by NERSC

a961016d.jpg

ERS ANNOUNCEMENT OF OPPORTUNITY

Proposal: **ALGERS**

Summary of Main Points of the Proposal

i) Investigation theme

The use of ERS sensors for the study of the dynamics of Modified Atlantic Water in the Algerian basin (western Mediterranean sea)

ii) Principal investigator

Jordi Font
Head Dept. Oceanography
Institut de Ciències del Mar (C.S.I.C.)
P. Joan de Borbó s/n, E-08039 Barcelona, Spain
Phone: ++34 3 2216450 Fax: ++34 3 2217340 Email: jfont@masagran.uab.es

iii) Co-Investigators

Paul Budgell
Research Director
Marine Monitoring and Remote Sensing
Nansen Environment and Remote Sensing Center
Edvard Griegsvei 3a, N-5037 Solheimsvik-Bergen, Norway
Phone: ++47 55297288 Fax: ++47 55200050
Email: budgell@fram.nersc.no

Johnny André Johannessen
Research Director
Marine Monitoring and Remote Sensing
Nansen Environment and Remote Sensing Center
Edvard Griegsvei 3a, N-5037 Solheimsvik-Bergen, Norway
Phone: ++47 55297288 Fax: ++47 55200050
Email: johnny@nanvax.nersc.no

María José López
Departament de Geografia
Universitat de València
Ap. 22060, E-46080 Valencia, Spain
Phone: ++34 63864230 Fax: ++34 63864249

Juan José Martínez Benjamín
Profesor Titular
Departament de Física Aplicada
Universitat Politècnica de Catalunya
Modul B5, Campus Nord, Jordi Girona Salgado s/n, E-08034 Barcelona, Spain
Phone: ++34 34017057 Fax ++34 34016801
Email: benjamin@etseccpb.upc.es

Claude Millot
Directeur de Recherche CNRS
Centre d'Océanologie de Marseille
Antenne C.O.M. - c/o IFREMER
B.P. 330, F-83507 La Seyne, France
Phone: ++33 94304884 Fax: ++33 94301372
Email: cmillot@toulon.ifremer.fr

Ian S. Robinson
Head of Oceanography Department
University of Southampton
Southampton SO9 5NH, UK
Phone: ++44 703595000 Fax:++44703593059
Email: @soton.ac.uk

Joaquin Tintoré
Profesor Titular
Departament de Física
Universitat de les Illes Balears
Crtra. Valldemossa km 7.5, E-07071 Palma de Mallorca, Spain
Phone: ++34 71173227 Fax: ++34 71173426
Email: dfsjts0@ps.uib.es

Jorge Vázquez
Oceanography Group
Jet Propulsion Laboratory
California Institute of Technology
M/S 300/323, 4800 Oak Grove Drive, Pasadena, CA 91109, USA
Phone: ++1 8183548168 Fax:++18183936720
Email: jv@foggy.jpl.nasa.gov

iv) Abstract of proposal

The objective of the ALGERS proposal is to use ERS sensors and other remote sensing data to study the dynamics of the surface layer in the Algerian basin in connection with a Spanish in situ campaign to be held in 1996. This objective is considered in the framework of investigating the physical processes that determine the marine circulation in the western Mediterranean (MAST Mediterranean

Targeted Project). Specifically we propose to investigate:

1) The generation and evolution of large anticyclonic eddies at a temporal scale of months
2) The drift of Modified Atlantic Water (MAW) in relation to these large eddies
3) The identification of current shear mesoscale structures in the Algerian current

The research will be conducted through the following activities:

1. Field experiment

An oceanographic campaign (CTD, ADCP) plus current meter moorings and Argos lagrangian drifters to identify mesoscale eddies in the Algerian basin and to study their interaction with the mean current and topography.

2. Altimeter study of sea surface height variability

2.1 Development of processing algorithms for treatment of satellite altimetry data along with implementation of new analysis and visualisation techniques

2.2 Validation, including comparison of altimetry data with current meter, ADCP and SST

2.3 Circulation and variability studies by objective mapping of ERS and Topex/Poseidon data plus complex empirical orthogonal functions analysis

2.4 Use of altimeter data in numerical modelling effort of the W Mediterranean circulation

3. SAR imaging of mesoscale structures

3.1 Identification of mesoscale current structures in SAR images of the Algerian basin

3.2 Comparison of SAR signatures with measured current shear (ADCP) during the oceanographic campaign

3.3 SAR data assimilation into an eddy-resolving isopycnic coordinate ocean model

4. Monitoring of the Eastward/Northeastward drift of Modified Atlantic Water in the Algerian basin with ATSR data combined with surface height maps and drifters trajectories. Ocean colour (SeaWifs) will be integrated in this study.

It is expected to achieve an important contribution to the knowledge of the dynamics of the Algerian basin, especially in the domain of mesoscale/large scale interaction. The synopticity of ERS measurements and the availability of long periods of altimeter and ATSR data are powerful tools to investigate the influence of processes taking place in the Algerian basin on the adjacent Mediterranean basins, as for example the effect of migrating anticyclonic eddies on the large scale spreading of MAW. A fundamental issue will be the implementation of some working methods to improve the use of ERS sensors for surface layer mesoscale dynamics.

The development of analytical techniques as well as the archiving of long period altimeter, ATSR and SAR data series will be initiated during 1994-1995. The oceanographic campaign is scheduled for spring/summer 1996, and after that the major effort on data analysis and numerical studies will take place. It is expected to complete the proposed research by 1998.

v) Summary of the required data

Altimeter and ATSR-SST global coverage of the Algerian basin will be requested for the whole duration of the experimental part of the proposal: 1994, 1995, 1996. Altimeter OPR at a continuous basis. If available both ERS-1 and ERS-2 data sets will be used. A number of 500-600 ATSR-precise SST 500 x 500 km images has been calculated to cover the study area every 5 days.

SAR 100 x 100 km PRI images are required for two different purposes: an archive of data acquired in the region from mid 1995 to 1996 (some 50 scenes), and an exhaustive coverage of the area of the oceanographic campaign during 40 - 50 days (approx. 150 - 200 scenes). A part of these last images should be transmitted at near-real time to be received on board the research vessel.

Data other from ERS will be obtained from several sources.

ERS-2 SAR NEAR REAL TIME DATA USED IN THE SAMPLING STRATEGY OF AN OCEANOGRAPHIC CRUISE IN THE WESTERN MEDITERRANEAN

Oscar Chic, Jordi Font

Institut de Ciències del Mar, CSIC
P. Joan de Borbó s/n, E-08039 Barcelona, Spain
phone: 34 3 2216416, fax: 34 3 2217340
e-mail: ochic@icm.csic.es, jfont@icm.csic.es

Stein Sandven

Nansen Environmental and Remote Sensing Center
Edvard Griegsvei 3a, N-5037 Solheimsvik, Norway
phone: 47 55 297288, fax: 47 55 200050
e-mail: stein@nanvax.nrsc.no

ABSTRACT

Near-real time remote sensing has been used to guide the *in situ* sampling in an oceanographic cruise on board the Spanish *RV Hespérides* in the western Mediterranean (October 1996). NOAA AVHRR was collected by a portable HRPT station, and ERS-2 SAR acquired by West Freugh (Scotland) station, analysed at NERSC (Norway) and transmitted to the ship few hours after the satellite pass. Mesoscale circulation structures evolve rapidly and require daily updated synoptic information to achieve the best efficiency in field measurements. The different characteristics of SAR and AVHRR in what concerns swath, revisiting time and dependence on atmospheric conditions, and the specific circumstances at the moment of the experiment, resulted in a much higher use of infrared information. At present SAR, although it can better resolve some features, is not yet an operational tool to drive the measuring strategy of an oceanographic ship in latitudes like the Mediterranean Sea. A future constellation of lower resolution and wider swath SARs could be an optimal solution to complement infrared radiometers in an efficient daily monitoring of ocean mesoscale structures.

INTRODUCTION

During the last decade, remote sensing and in situ studies have evidenced that mesoscale variability plays a major role in the Mediterranean Sea dynamics. The generation and evolution of meanders, eddies and filaments (time scales of days-weeks and spatial scales of few tens of km) are not only powerful mechanisms for shelf/slope exchanges, but can strongly influence and even modify the basin scale circulation. This is especially evident in the southern region of the western basin, where large anticyclonic eddies off Algeria can have life times of several months (Millot, 1994).

ERS-1 SAR was used in the western Mediterranean in a preliminary study carried out under an ERS-1 Announcement of Opportunity project ("Evaluation of ERS-1 microwave sensors capability in the study of oceanic fronts", code AO.E1, PI J. Font). In October 1992, *in situ* sampling, quasi-simultaneous to ERS-1 SAR acquisition, showed that surface signatures of mesoscale circulation features can be identified in SAR images of the Alboran Sea. A very good correlation was found between shear lines in the border of large gyres and the direction of the corresponding frontal jet measured by an Acoustic Doppler Current Profiler (ADCP) from the *R/V García del Cid* (Font et al., submitted).

The high spatial resolution offered by SAR could be used for fine positioning of *in situ* measurements in mesoscale dynamics studies. This implies the need of an almost-real time satellite data acquisition and transmission to the research vessel, what can be easily done for infrared radiometers with a portable HRPT station, but is much more difficult for SAR. Studies performed by the Nansen Environmental and Remote Sensing Centre (NERSC, Bergen) in the Norwegian Sea achieved such near-real time SAR imagery availability on board: ERS-1 data were acquired at Tromsö satellite receiving station, rapidly processed at Bergen, and interpreted images faxed to *R/V Håkon Mosby* three hours after acquisition (Johannessen et al., 1992).

The encouraging results in detecting frontal structures in the Mediterranean, and the experience acquired in obtaining near-real time SAR images, were the reason for proposing an ERS-2 project in the southern region of the western Mediterranean. "ALGERS. The use of ERS sensors for the study of the dynamics of Modified Atlantic Water in the Algerian basin" (code AO2.E102, PI J. Font) was organised, among other objectives, to

provide pre-cruise, post-cruise and near-real time SAR coverage to an interdisciplinary experiment to be done with the *R/V Hespérides* in the Alboran Sea and Algerian basin in autumn 1996. Simultaneous satellite synoptic information could strongly help in designing the *in situ* sampling of mesoscale structures

OMEGA-ALGERS CRUISE

The cruise took place from 30 September to 21 October 1996 in two legs on board the Spanish research vessel *Hespérides,* to fulfil the objectives of OMEGA project in the western Alboran gyre area, and to initiate the interdisciplinary study of the Algerian basin included in MATER project. OMEGA ("Observations and modelling of eddy scale geostrophic and ageostrophic circulation") and MATER ("Mass transfer and ecosystem response") are research projects of the Marine Science and Technology programme of the European Union.

During OMEGA, a box of 100 x 80 km in the northern half of the western Alboran gyre was sampled three times by undulating SeaSoar (CTD, fluorometer, light sensor, infrared backscatter sensor), ADCP and multibeam Simrad EK500 echosounding, and once in a regular grid of CTD (+oxygen, fluorescence, light transmission) stations. Differential and 3D GPS were used for precise navigation data. Water samples were taken for chemical and biological measurements: salinity, oxygen concentration, nitrite, nitrate, silicate, phosphate, ammonia, aliphatic and aromatic hydrocarbons, total chlorophyll, pigment speciation (HPLC), cytometry analysis (cyanobacteria, picoplankton, nanoplankton), yellow substances, particles size distribution and transmissometry, and image analysis of phytoplankton. During ALGERS, a mesoscale meander developed in the Algerian current near 1°E, previously tracked by remote sensing, was sampled along cross-shelf sections. The sampling methodology was quite similar, plus launching of expendable XBT and XCTD probes, primary productivity and radiotracers determinations, and deployment of surface drifters to be tracked by satellite.

REMOTE SENSING REAL TIME ACQUISITION

The availability of simultaneous satellite data was considered to be fundamental for both legs of the cruise: the optimal location of the OMEGA surveys in relation to the western Alboran gyre, and the permanent tracking of an evolving instability during ALGERS.

The remote sensing information acquisition during the cruise included infrared and SAR imagery. A SeaSpace portable HRPT satellite receiving station (Terascan TS300) was installed on board the *Hespérides* and obtained NOAA AVHRR infrared imagery four times a day all along the cruise. Sea Surface Temperature was computed, the images were georeferentiated and made immediately available to the oceanographers for analysis in comparison to field measurements. Figure 1 shows the study areas on this kind of images.

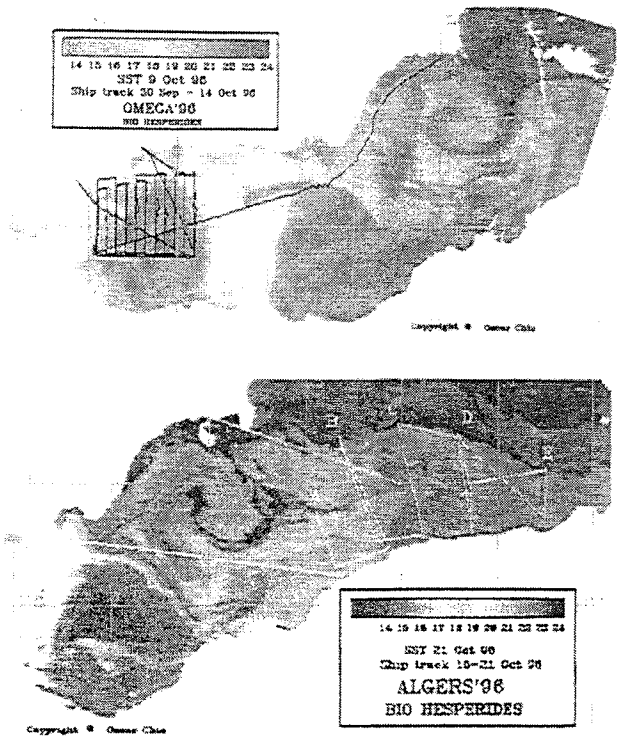

Figure 1. Alboran sea and western Algerian basin. NOAA sea surface temperature and ship track for both legs of OMEGA-ALGERS cruise in October 1996

The SAR acquisition was arranged with the British Defence Research Agency Satellite Ground Station, West Freugh (Scotland), through the Southampton Oceanography Centre, one of the OMEGA partners. SAR acquisition for both areas during the cruise had been requested to ESA within the ALGERS AO2 project. When ERS-2 SAR was observing the study area, data were especially recorded by West Freugh, that immediately generated QL5 products (50 m pixel size), then downloaded and analysed by NERSC at Bergen, and finally transmitted by Inmarsat link to the *Hespérides.* Compacted files of the SAR images, together with features detection analysis, were received on board during the day following the satellite pass. From 21 September to 21 October a total of 17 ERS-2 passes were recorded with this procedure. Figure 2 is one example of these transmitted files. The same features detection analysis was done off-line by NERSC with other SAR data sets received from ESA during September.

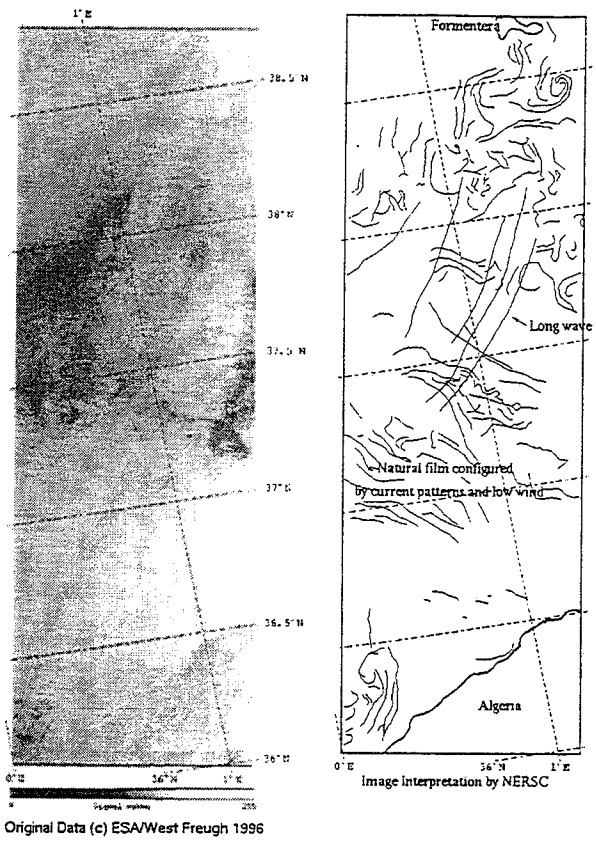

Figure 2. ERS-2 SAR image and its analysis received in near-real time on board *RV Hespérides* (orbit 7520, 27 September 1996)

Two specific cases studied during the cruise are presented here

CASE 1: THE WESTERN ALBORAN GYRE

The Alboran Sea is the region of the western Mediterranean in contact with the Atlantic ocean through the strait of Gibraltar. A surface inflow of light Atlantic water occurs as a narrow northeastward jet that later forms a wave-like front, usually coupled to two large anticyclonic gyres and mesoscale eddies developing along the edge of these gyres. The very active front in the surface 0-200 m layer along the edge of the western gyre gives rise to a three-dimensional ageostrophic circulation at mesoscale, and then provides an enhanced transport route for heat, nutrients and biomass. Surface features (water mass distribution, roughness patterns) reflect the presence of this intense dynamics. The objective of OMEGA is to determine the three-dimensional motion in such an area.

The continuous reception of AVHRR during the weeks previous to the cruise allowed a monitoring of the Atlantic water jet, and hence a precise positioning of the oceanographic sampling to better capture the area of intense mesoscale circulation. The scarce SAR coverage for this pre-cruise period prevented from using it in fine tuning the sampling strategy.

Figure 3 presents the results of the second underway SeaSoar and ADCP survey on 6-8 October (Allen et al., 1997). Both the density distribution and current vectors at 100 m indicate the presence of the anticyclonic gyre and its associated jet in the surface layer. The infrared images for this period clearly show the stability of the western gyre, with surface warm water accumulating in its center on the lighter side of the front.

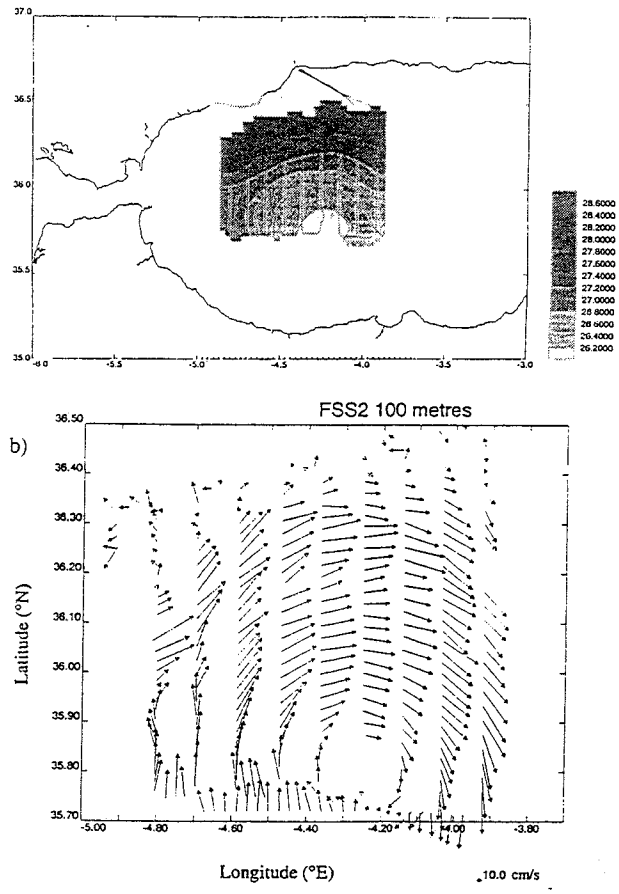

Figure 3. Sigma-theta (density) distribution and currents recorded by ADCP at 100 m during the second OMEGA survey on 6-8 October 1996

On 6 October one ERS-2 SAR image of the area was acquired (orbit 7649). In the NOAA-14 SST map of the same date, cold water entrained from the coastal area traces the location of the jet along its N and NE borders. A pulse of Atlantic water can also be detected in the thermal image, and this was corroborated in situ by visual observation of colour and roughness differences in surface water. The SAR image, formed under a wind intensity of 2.5 m/s, shows the presence of bright and dark lines in its NE area, that could be initially interpreted as the signature of internal waves. A precise georeferentiation allows an overlay of both images (fig. 4) and the identification of these sea

surface roughness singularities as shear lines depicting the frontal jet along the western Alboran gyre.

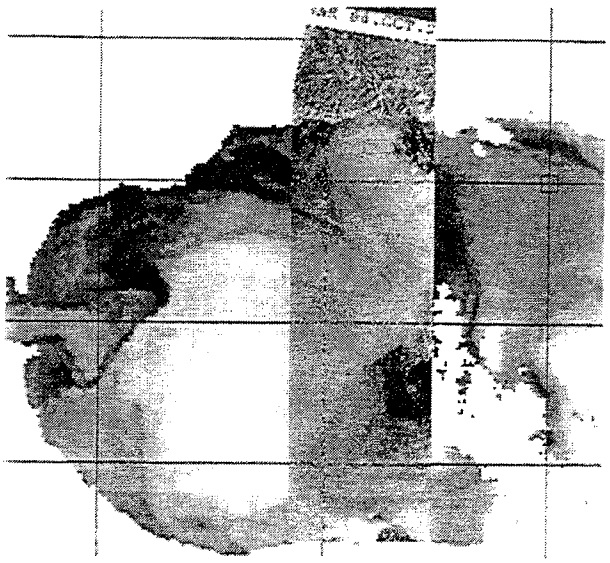

Figure 4. Overlay of NOAA SST and ERS-2 SAR images of the western Alboran sea on 6 October 1996. © ESA / West Freugh 1996

CASE 2: ALGERIAN CURRENT INSTABILITIES

Downstream the Alboran Sea, the jet of Modified Atlantic Water forms a well defined flow along the African coast: the Algerian current. Due to hydrodynamic processes, not yet fully understood, this alongslope current becomes unstable and develops meanders. These induce the formation of cyclonic and anticyclonic eddies, that can grow and play a major role in the configuration of the general circulation in the Algerian basin (Millot, 1994).

Until the end of September, 27 ERS-1 and ERS-2 passes with SAR acquisition (received from ESA) and daily AVHRR SST maps (retrieved from the German DLR ISIS server) were used to identify instabilities of the Algerian current and choose the most suitable area for the field work. In the weeks previous to the cruise a mesoscale meander was developed near 1°E. It appeared like an usual coastal anticyclonic eddy, with a well-marked secondary cyclonic circulation. Once the HRPT station was operative on the *Hespérides*, and thanks to the dominant clear weather, this specific structure was continuously monitored, and the *in situ* sampling organised to take the maximum advantage of the measurements for the best description of the phenomenon.

Figure 1 shows the ship tracks over the surface thermal signature of this mesoscale instability. obtained on 21 October. Besides some cloud covering during the cruise, the navigation and sampling sites were continuously updated from the satellite information. The different cross-shelf sections were located to fully intersect the alongslope current upstream, downstream and in key positions of the cyclonic and anticyclonic parts of the instability. An authorisation to work in Algerian waters allowed a complete sampling of the coastal zone.

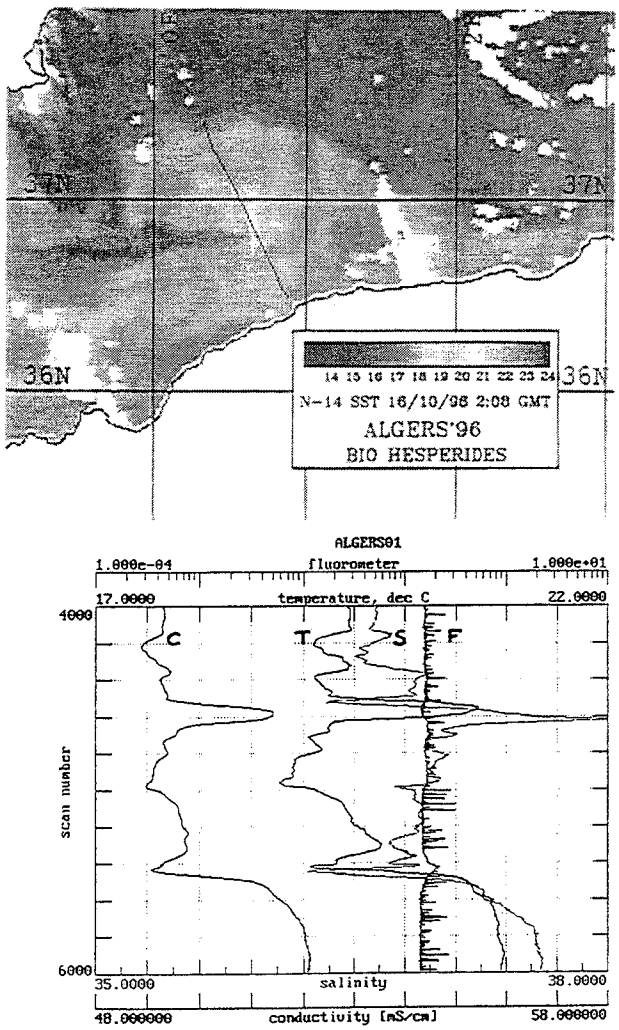

Figure 5. a) NOAA SST image of the Algerian current instability on 16 October 1996 with the ship track on 17 October. b) Surface variables recorded along this track from 13:48 (top) to 19:21 GMT (bottom)

On 16 October a cloud free image of the complete instability was obtained (fig. 5), as well as one SAR image of its western part (fig. 6). One of the sampling transects was situated to cross the core of the cyclonic eddy on the afternoon of 17 October (no cloud free image available for this date). An examination of the surface water temperature and salinity record along this transect from the coastal zone to offshore waters (fig. 5) indicates a perfect match between the *in situ* decription of the vein of Atlantic water (colder and fresher than the ambient water) and its remotely sensed signature.

cific hydrographic stations, to collect water at :ral depths, were positioned to coincide with dima or minima of surface variables (alongslope :ent, inner edge of the cyclonic eddy, cold core, :r edge). The corresponding SAR image (orbit 2), as received on board, does not seem to highlight surface structure related to the instability, maybe to too high wind intensity, 10 m/s from the NNE. l resolution (SAR.PRI) images provided by ESA l now be processed to improve the information on surface roughness.

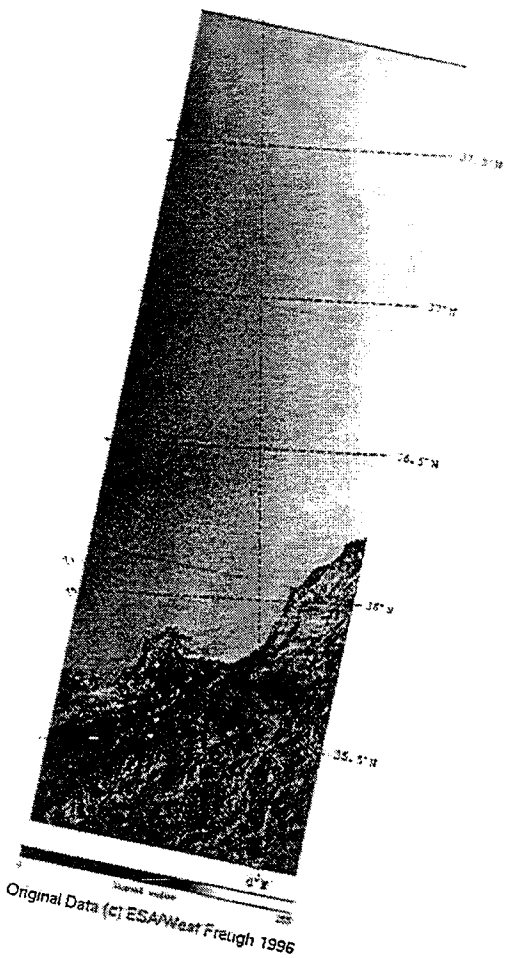

gure 6. ERS-2 SAR image of the western part (0°) of : studied instability on 16 October 1996

CONCLUSIONS

ıe use of near-real time remote sensing has proved to very efficient in the daily updating of sampling ategy for mesoscale circulation studies. The different aracteristics of SAR and AVHRR in what concerns ath, revisiting time and dependence on atmospheric nditions, and the specific circumstances at the moment the experiment, resulted in a much higher use of rared information to guide the in situ sampling. At esent SAR, although it can better resolve some features, is not yet an operational tool to drive the measuring strategy of an oceanographic ship in latitudes like the Mediterranean Sea.

For this kind of mesoscale studies, a SAR with lower spatial resolution (probably of the order of 50-100 m) but wider swath, would be of great help. An optimum solution would be an operational constellation of space borne radars to have a daily coverage of any ocean region. This could complement the lower resolution, and cloud depending, infrared radiometers, and allow a real all-weather all-time synoptic view of the ocean surface, a key issue for mesoscale dynamics.

Acknowledgements. This study is a contribution to projects ALGERS (code ERS AO2.E102), OMEGA (contract MAS3-CT95-0001) and MATER (contract MAS3-CT96-0051). ESA and West Freugh station provided ERS data. The Spanish R+D National Plan funded the oceanographic cruise (grant AMB95-0901-C02-02). The authors thank the *RV Hespérides* crew and participants in the cruise, and colleagues from ICM and NERSC that contributed to different aspects of the present work, especially Zacarías García, Torill Hamre, Kjell Kloster, Miquel Pancorbo and Morten Stette.

REFERENCES

Allen JT, Smeed DA, Crisp N, Ruiz S, Watts S, Vélez P, Jornet P, Rius O & Castellón A, 1997, Upper ocean underway operations on *BIO Hespérides* cruise OMEGA-ALGERS using SeaSoar and ADCP, *Southampton Oceanography Centre Internal Document* 17, 29 pp. + figures

Font J, Shirasago B & García-Górriz E, Surface large scale circulation and mesoscale variability in the Alboran Sea: SAR imaging of frontal structures, submitted to *J. Geophys. Res.* ERS special section

Johannessen JA, Shuchman RA, Davidson K, Frette O, Digranes G & Johannessen OM 1992, Coastal ocean studies with ERS-1 SAR during NORCSEX'91, *Proceedings First ERS Symposium, ESA SP-359*, 113-117

Millot C, 1994, Models and data: a synergetic approach in the western Mediterranean sea, P Malanotte-Rizzoli, AR Robinson (eds.) *Ocean Processes in Climate Dynamics: Global and Mediterranean Examples*, Kluwer Academic Pub., 407-425

3. The evolution of mesoscale structures in the Algerian current studied by surface drifters and infrared images

Satellite infrared images have been in the past a key observational tool to understand the role of mesoscale variability in the Mediterranean circulation. It is not easy to carry out *in situ* observations able to track the evolution of mesoscale structures at adequate temporal and spatial scales. Surface Lagrangian drifters can be a useful mean to complement satellite remote sensing in the study of mesoscale circulation over large areas, and in addition to quantify some characteristics of this circulation. An experiment with surface drifters was initiated during ALGERS'96 cruise: Thanks to real-time reception of satellite imagery, 18 units were released near 0° across the Algerian current and tracked for several months. Besides providing large-scale information on the spreading of recent Modified Atlantic Water (Font et al., 1998) the drifters' trajectories have been analysed jointly with SST maps to characterise and quantify several aspects of the evolution of mesoscale eddies linked to the Algerian current (Salas et al., 1998). Due to a much easier availability, the SST maps used in this study come from AVHRR/NOAA and not from ATSR/ERS.

Here we enclose the two unpublished papers cited above.

SM 1395

SCI. MAR., 00 (0): 000-000 SCIENTIA MARINA 0000

The drift of Modified Atlantic Water from the Alboran Sea to the eastern Mediterranean*

J. FONT[1], C. MILLOT[2], J. SALAS[1], A. JULIÀ[1], and O. CHIC[1]

[1]Institut de Ciències del Mar (CSIC), Barcelona, Spain.
[2]Laboratoire d'Océanographie et de Biogéochimie, COM-CNRS, La Seyne, France.
Corresponding author address: Dr. Jordi Font, Institut de Ciències del Mar CSIC, Passeig Joan de Borbó s/n, 08039 Barcelona, Spain, E-mail: jfont@icm.csic.es

SUMMARY: The Algerian basin is a region of the western Mediterranean with a highly variable circulation structure, including the eastward transport of Modified Atlantic Water (MAW) in its surface layer. An experiment with satellite tracked Lagrangian drifters was performed in 1996-97 to analyse the mesoscale circulation of the Algerian current. The complete trajectories of 18 drifters indicate that, at basin scale, all the surface flow occured along the coast from the Alboran Sea to the strait of Sicily. At that time, no portion of the inflowing MAW was driven to the central or northern regions.

Key words: western Mediterranean circulation, Algerian basin, Lagrangian drifters

RESUMEN: EL DESPLAZAMIENTO DEL AGUA ATLANTICA MODIFICADA DESDE EL MAR DE ALBORÁN HASTA EL MEDITERRÁNEO ORIENTAL. La cuenca Argelina es una región del Mediterr·neo occidental con una estructura de circulación altamente variable, incluyendo el desplazamiento hacia el este del Agua Atlántica Modificada (MAW). En 1996-97 se realizó un experimento con flotadores Lagrangianos seguidos por satélite para estudiar la circulación de mesoescala de la corriente Argelina. El conjunto de las trayectorias de 18 flotadores indican que, a gran escala, todo el flujo superficial se produjo a lo largo de la costa desde el mar de Alborán hasta el estrecho de Sicilia. Durante este período no hubo ningún transporte neto de MAW hacia el centro y norte de la cuenca.

Palabras clave: circulación en el Mediterr·neo occidental, cuenca Argelina, flotadores Lagrangianos

INTRODUCTION

Modified Atlantic Water (MAW) is initially made as a result of the mixing of comparatively fresh Atlantic water (S<36.5) flowing via the strait of Gibraltar into the Mediterranean Sea with the surface waters of the Alboran Sea (Gascard and Richez, 1985). The resulting water mass occupies the southern part of Alboran Sea and, entrained by an intense jet coupled to a wave-like front (La Violette, 1990; Viúdez *et al.*, 1996), exits the eastern end of this sub-basin either along the African coast (Viúdez and Tintoré, 1995) or along the

*Received . Accepted May 5, 1998.

Almeria-Oran front (Tintoré *et al.*, 1988). Near Oran, the MAW jet forms the Algerian Current (Millot, 1985; Arnone and La Violette, 1986) that flows eastward along the African continental slope, and is one of the most important and less known current systems in the western Mediterranean. At basin scale, MAW driven by the Algerian Current both penetrates into the eastern Mediterranean through the strait of Sicily, and circulates cyclonically all around the western basin (Millot, 1998). In its cyclonic circulation in the basin, it can be identified by a surface salinity minimum that is progressively smoothed by mixing with surrounding waters. In fact, all the basin surface layer (100-200 m) is occupied by the minimum salinity MAW whose minimum is dependent on the different degrees of mixing due to residence times, until reaching salinities above 38.0 in the open sea of the northwestern region. López-Garcìa *et al.* (1994) named the fresher MAW found in the Alboran Sea and along the Algerian coast as "recent MAW" to distinguish it from older MAW occupying the western and central regions of the western basin.

Thus, the traditional picture of a widespread eastward and northeastward flow in the Algerian basin (Ovchinnikov, 1966), has been replaced by the image of an alongslope coastal current subject to very intense mesoscale activity (Millot, 1998). However, some climatological and numerical studies (e.g. Tzipermann and Malanotte-Rizzoli, 1991; Pinardi and Navarra, 1993) still indicate the existence in the western Algerian basin of a widespread flow to the northeast (to the Balearic islands). This, despite the strong indication by satellite images evidence that the presence of recent MAW in this northern areas is not due to a general smooth flow of the Algerian Current, but to the interaction of the current with strong mesoscale eddies (Taupier-Letage and Millot, 1988; López-Garcìa *et al.*, 1994). The lack of hydrographic and current data in the Algerian basin with adequate horizontal and vertical resolution has till now prevented a complete explanation of this dynamical process.

To help in overcoming this deficiency, two projects have been instigated. The first one - "ALGERS: the use of ERS sensors for the study of the dynamics of Modified Atlantic Water in the Algerian basin (western Mediterranean sea)" - is a research project that utilizes data from the European Space Agency ERS satellites, and includes, as one of its objectives, the investigation of the drift of MAW in relation to the regional mesoscale eddies. The second project - "MATER: mass transfer and ecosystem response" - is the second phase of the Mediterranean Targeted Project of the European Union Marine Science and Technology (MAST) program. One of the MATER tasks is to study the mesoscale circulation in the Mediterranean using surface Lagrangian floats released at the Alboran's eastern boundary.

As a contribution to ALGERS and MATER, a surface drifter experiment was initiated as part of the ALGERS'96 cruise aboard the Spanish research vessel Hespérides in October 1996. We present here the first general results of this experiment, with the trajectories of all the drifters tracked by satellite for the several months they were operative.

THE LAGRANGIAN DRIFTERS

Two models of drifters were used (A111 and A104), both manufactured by Brightwaters Instrument Co., New York, USA. Model A111 is a simple cylindrical drifter that contains an ARGOS transmitter, an antenna and batteries, with a small wheel on top as floatation element. Only the antenna emerges from the sea surface, which minimises the wind drag effect. A secondary surface float attached to the drifter gives the necessary buoyancy for the subsurface drogue. This was a TOGA-WOCE standard holey sock, 10 m long with a 5 m tether, so the main drag was centred at 10 m below the surface with a subsurface-surface drag ratio close to 70. Model A104 is a bigger drifter, with a mechanical structure based on the popular Davis surface drifter (Davis *et al.*, 1982), that besides the ARGOS tracking equipment hosts a GPS (Global Positioning System) receiver and antenna, with both internal recording and data transmission through ARGOS. A temperature sensor is also included. Only the two antennas and the top of five small floats emerge from the sea surface. The A104 drifters also carried the same model of sock drogue, with dimensions adapted to produce a similar drag ratio as the A111. In all, 15 units of A111 and 3 units of A104 were deployed during the experiment. The A104 units were programmed to record the GPS position every 30 minutes. All the drifters were located by ARGOS on average 6-8 times a day.

THE DRIFTERS EXPERIMENT

The ALGERS'96 cruise aboard the RV Hespérides in October 15-21, 1996 was carried out in the western Algerian basin, close to where the Algerian Current is normally formed. The main objective of the cruise was to exhaustively sample the three-dimensional structure of a mesoscale instability of the Algerian Current from the dynamical, geochemical and biological point of view.

In the period prior to the cruise, satellite infrared imagery was used to identify the specific area to be sampled. By the end of September 1996, the satellite imagery indicated a mesoscale instability of the Algerian Current developing near 1°E, close to the eastern boundary of the Alboran Sea. The instability appeared as a meander of the current surrounding a coastal anticyclonic eddy, and associated with a secondary cyclonic eddy, upstream and seaward from the crest of the meander (Figure 1). This mesoscale feature was chosen as the instability to be studied during ALGERS'96. To maintain continuity between the features seen in the satellite images and ship's cruise work, a Sea Space portable satellite receiving station (Terascan TS-300 system) was installed aboard the Hespérides. This station provided the shipboard scientists with NOAA AVHRR infrared imagery four times a day. This continuous remote sensing monitoring was critical in guiding the in situ sampling, by daily updating the location of the main thermal gradients and hence the position of the boundaries of the evolving instability.

The deployment pattern and specific positions of the drifters discussed in this paper were derived from a coupled analysis of this satellite data and in situ underway measurements: surface temperature and salinity (SeaBird SBE21 thermosalinograph) and vertical profiles of temperature (expendable XBT probes Sippican T-7) and velocity (Acoustic Doppler Current Profiler RD Instruments VM0150).

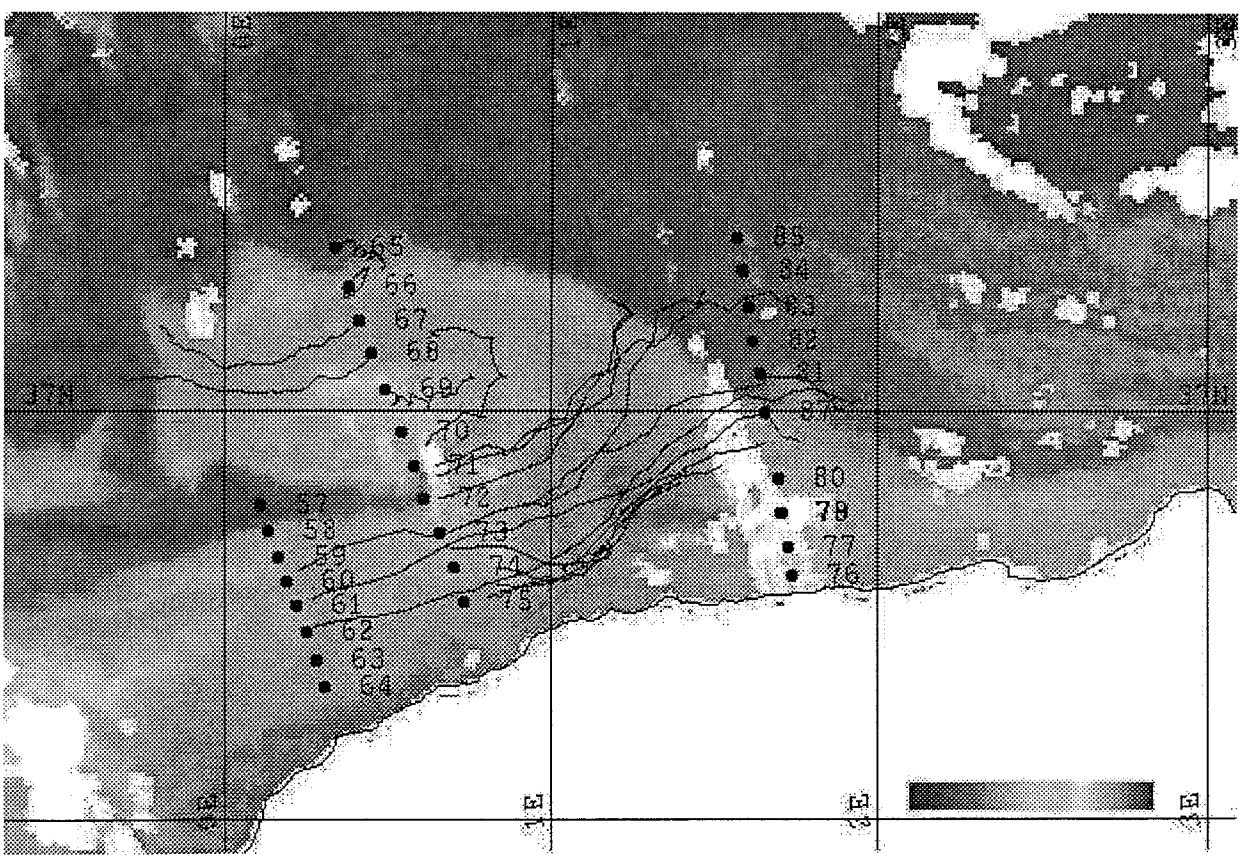

FIG. 1. – NOAA AVHRR image of the ALGERS'96 area on 16 October 1996, with the location of several CTD stations and trajectories of the 18 Lagrangian drifters until 21 October. The trajectories illustrate precisely the alongslope current and its offshore displacement to contour the coastal anticyclonic motion appearing between 1(and 2(E, that was growing and slowly migrating eastwards. The six outer drifters followed the motion of the cyclonic eddy, that was rapidly deforming, elongating to the west.

During the early hours of 17 October 1996, the A104 drifters were launched at three consecutive hydrographic stations, five nautical miles apart, in the core of the Algerian current upstream from the coastal instability (see Figure 1 and Table 1). It was planned to leave these drifters at sea for a few days for small scale measurements related to the evolution of the coastal structure, and recover them before the end of the cruise. Because of an unexpected reduction of cruise length due to technical problems, the drifters were not recovered and they were left to drift till the end of their battery life. The following day (18 October), the 15 A111 drifters were released at intervals of 5 miles, or 2.5 miles in the core of the current, along a straight line across the coastal current and the centre of the well developed cyclonic part of the instability, offshore the meander (Figure 1 and Table 1). The shipboard satellite receiving station, when receiving NOAA data, could retrieve the positions of the ARGOS transmitters located by the satellite during each overflight. In this manner, the drifters trajectories were tracked throughout the cruise. After the cruise, a daily on-line access to the ARGOS system was used to derive the complete trajectories of the drifters.

The drifters experiment was planned to last 12 months, and the batteries of the instruments (except for the three A104) were sufficient for the platforms to transmit during 400 days. However, they ceased to transmit much more rapidly than expected, in most cases near the coast. We believe the high failure rate in these regions was due to the instruments, or at least their antennae, being damaged on reaching the shore line. The life lengths of the 18 drifters span from 1 day to 5.5 months, as also detailed in Table 1. After the last position indicated in the table, drifter #18715 still continued to transmit for an additional eight weeks near the coast of Libya, but the localisations were scarce and were of poor quality. Figure 2 presents the whole set of drifters trajectories from their release points near 0(- 1(until their last ARGOS localisation.

RESULTS AND DISCUSSION

The experiment strategy was to deploy the Lagrangian drifters in an area influenced by the MAW jet outflowing from the Alboran Sea, and then to track them as they drifted about the Mediterranean basin (Figure 2). Besides characterising the mesoscale motion in the Algerian basin, the information would be used to study the MAW drift at large scale. An analysis of several portions of drifters trajectories in conjunction with satellite infrared imagery is being completed, in a separate study (Salas *et al.*, 1998), as a first contribution to the primary objective of the experiment, the mesoscale circulation study.

TABLE 1. – Deployment information and last localisation for the three A104 (ID 20700 series) and the 15 A111 (ID 18700 series) Lagrangian drifters used for the experiment

Drifter PTT ID	Launch date	Time	Launch position (N-E)	End position (N-E)	End date	Days tracked
20779	17/10/96	02:52	36.61-00.22	37.13-11.24	18/11/96	31
20780	17/10/96	04:06	36.52-00.22	36.78-02.02	24/10/96	6
20781	17/10/96	05:48	36.45-00.25	36.73-02.67	26/10/96	8
18724	17/10/96	20:53	37.39-00.34	38.08-14.45	18/02/97	124
18723	17/10/96	22:58	37.30-00.38	36.70-01.97	11/11/96	24
18715	18/10/96	02:01	37.21-00.41	32.53-14.65	31/03/97	165
18717	18/10/96	03:42	37.13-00.44	36.95-11.11	30/01/97	104
18725	18/10/96	06:44	37.04-00.49	37.21-09.18	02/12/96	45
18719	18/10/96	09:01	36.93-00.55	38.76-07.16	24/12/96	67
18722	18/10/96	12:20	36.86-00.63	38.10-12.70	12/01/97	86
18718	18/10/96	12:40	36.83-00.62	37.46-07.22	13/01/97	87
18721	18/10/96	14:49	36.78-00.64	37.66-12.51	07/01/97	81
18716	18/10/96	15:39	36.74-00.64	36.94-01.14	19/10/96	1
18727	18/10/96	18:08	36.70-00.67	37.03-06.31	01/12/96	44
18713	18/10/96	18:30	36.66-00.67	35.84-14.54	14/03/97	147
18714	18/10/96	19:58	36.62-00.70	37.03-08.92	03/12/96	46
18726	18/10/96	20:18	36.57-00.71	43.20-10.53	18/02/97	123
18720	18/10/96	20:39	36.53-00.73	37.14-04.36	18/11/96	31

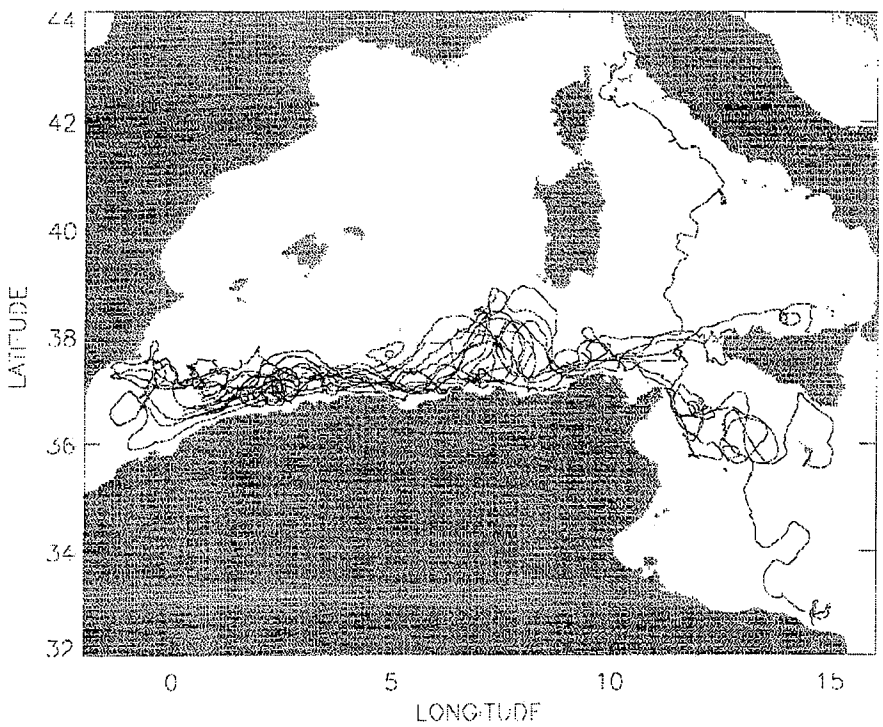

FIG. 2. – Complete trajectories (consecutive ARGOS locations) for all the Lagrangian drifters from October 1996 to March 1997. The release zone is between 0(and 1(E, 36(30' and 37(30'N, near the western limit of the Mediterranean area included in this figure.

The first relevant result to be noticed in Figure 2 is that all of the drifting buoys drifted eastwards in the southern part of the Algerian basin. This included those that were deployed in the cyclonic part of the meander and that initially drifted to the west almost reaching the Spanish coast. In spite of the strong mesoscale variability, as indicated by the numerous loops in the individual tracks (Figure 3), none was deflected to the north. We conclude therefore, that there was no widening or smoothing of the Algerian Current during the period of the experiment. We further conclude that no portion of the recent MAW went directly to the Balearic basin due to mesoscale motion. In essence, all the surface water that was leaving Alboran in October 1996 flowed to the east and with at least a portion reaching the Sardinia Channel by the end of December at a mean speed of almost 10 km/day.

The drift pattern disclosed by these 1996 drifter trajectories is very different from the one observed in an earlier drifter experiment in the same area (Millot, 1991). In June 1986, four surface floats were released in the Algerian Current (1(50' and 4(E) and, after drifting eastward, were abruptly entrained to the north near 5(E. None of these 1986 drifters progressed east of 5(40', and all either ceased transmission in the Algerian basin or reached the Ligurian Sea after drifting between the Balearic islands. This disruption of the alongslope flow indicated by these 1986 drifter trajectories appears to have been related to a big offshore anticyclonic eddy noted by concurrent satellite images and current measurements. The joint analysis of both Lagrangian data sets supports the hypotheses that the presence of recent MAW in the Balearic area (Font *et al.*, 1988; Pinot *et al.*, 1994) has to be due to the interaction of the alongslope Algerian Current with energetic mesoscale eddies, as documented by López-García *et al.* (1994) and other satellite imagery sets, and not to a permanent branching of the current from its beginning. A similar explanation could account for the presence of MAW in the western Corsican Current.

All these facts emphasize the need for an effective implementation of mesoscale motion (eddy-resolving) in the Mediterranean general circulation models, to reproduce a realistic time evolution of the main features and to find dynamic explanations for the mean current-eddy interactions.

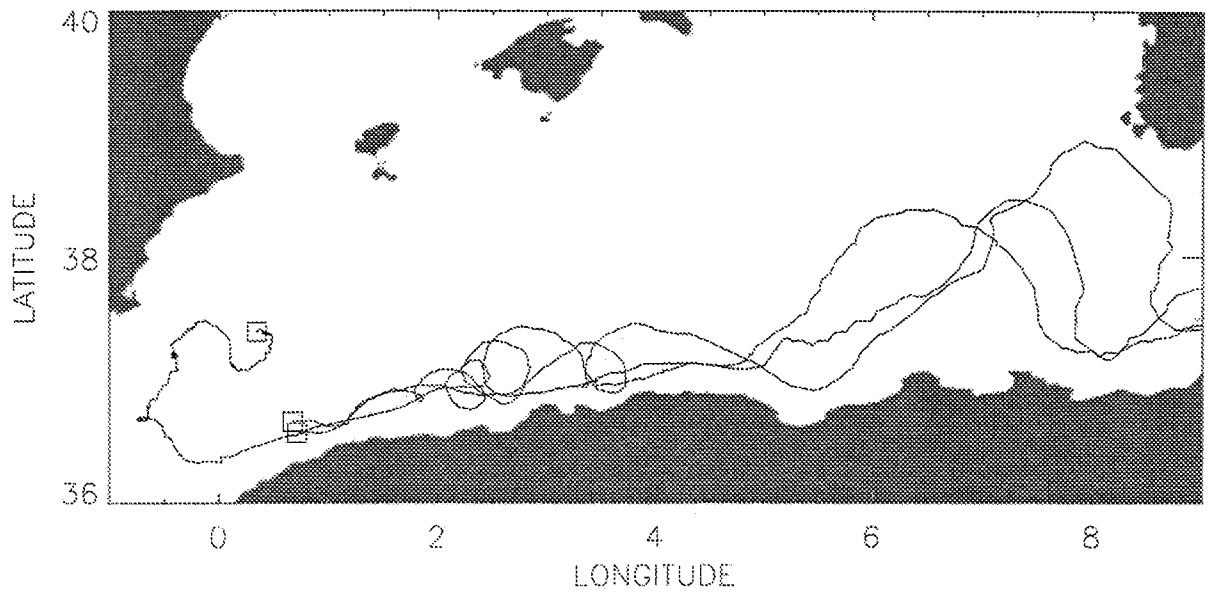

FIG. 3. – The trajectories of three of the ALGERS'96 drifters from their release location until they crossed the Sardinia Channel show how, despite any mesoscale perturbations, the net MAW drift is to the east along the Algerian coast.

Another relevant result of our experiment is that all the drifters that crossed the Sardinia Channel, the seven of them that were still transmitting after the first week of January 1997, did so close to the Tunisian coast. That is, the Algerian current was still an alongslope flow at that longitude (9(E), after having been subject to intense eddy motion southwest of Sardinia (Salas *et al.*, 1998). This situation is similar to the one that has been recorded for several months in 1993-94 during the first phase of the Mediterranean Targeted Project (Bouzinac *et al.*, 1998).

All these surviving Lagrangian drifters continued eastwards as far as the Strait of Sicily, where two of them went ashore on the westernmost coast of the island. Three other drifters passed through the strait into the eastern Mediterranean, and finished their trajectories in different locations of the western Ionian sea after having initially circulated following a southeastward path. This coincides with what Moretti *et al.* (1993) describe as a jet-like meandering flow in an analysis of several years of hydrographic data, and with trajectories of Lagrangian drifters released in several occasions in this region (Poulain, 1998). The remaining two drifters meandered into the Tyrrhenian sea, indicating a high variability of the MAW flow in the entrance of the strait. One of them initiated a cyclonic path along the slope, but went ashore in the north-eastern coast of Sicily. The last one crossed the southern Tyrrhenian and then followed the Italian peninsula slope as far north as the Corsican Channel (Figure 2).

The complete trajectories are now offered to the whole MATER community through the MATER www server (http://www.cetiis.fr/mtp/mater/), and can be used by the different teams working in the Algerian, Tyrrhenian and Ionian regions.

ACKNOWLEDGEMENTS

ALGERS'96 cruise on board the R/V Hespérides was part of project INTERMESO funded by the Spanish National Program on Environment and Natural Resources (AMB95-0901), and a contribution to the European research projects MATER (funded under contract MAS3-CT96-0051) and ALGERS (ERS AO E102/0). We are grateful to the Hespérides crew and master, and to all the colleagues on board and land who contributed to the drifters experiment, and to the Algerian authorities which allowed us to work in their national waters. J. Salas acknowledges a fellowship from the Mexican Comisión Nacional de Ciencia y Tecnologìa. This is MATER publication number MTP II-MATER/014

REFERENCES

Arnone, R. and P.E. La Violette.- 1986. Satellite definition of the bio-optical and thermal variation of the coastal eddies associated with the African current, J. Geophys. Res., 91: 2351-2364

Bouzinac, C., J. Font, C. Millot.- 1997. Hydrology and currents observed in the channel of Sardinia during the PRIMO-1 experiment from November 1993 to October 1994. J. Mar. Sys. (in press)

Davis, R.E., J.S. Dufour, G.J. Parks, M.R. Perkins.- 1982. Two inexpensive current-following drifters, Scripps Institution of Oceanography, 82-28, 54 pp.

Font, J., J. Salat, J. Tintoré.- 1988. Permanent features of the general circulation in the Catalan Sea, Oceanol. Acta, vol. sp. 9: 51-57

Gascard, J.C., C. Richez.- 1985. Water masses and circulation in the western Alboran Sea and in the Strait of Gibraltar, Progr. Oceanogr., 15: 157-216

La Violette, P.E.- 1990 The Western Mediterranean Circulation Experiment (WMCE): Introduction, J. Geophys. Res., 95: 1511-1514

López-Garcìa, M.J., C. Millot, J. Font, E. Garcìa-Ladona.- 1994. Surface circulation variability in the Balearic basin, J. Geophys. Res., 99: 3285-3296

Millot, C.- 1985. Some features of the Algerian current, J. Geophys.Res, 90: 7169-7176

Millot, C.- 1991. Mesoscale and seasonal variabilities of the circulation in the western Mediterranean, Dyn. Atm. Oceans, 15, 179-214

Millot, C.- 1997. Circulation in the western Mediterranean Sea. J. Mar.Sys., (in press)

Moretti, E., E. Sansone, G. Spezie, A. De Maio.- 1993. Results of investigations in the Sicily channel (1986-1990). Deep-Sea Res.,II, 40: 1181-1192

MACROAUTO ENBib Ovchinnikov, I.M.- 1966. Circulation in the surface and intermediate layers of the Mediterranean. Oceanology, 6: 48-59.

Pinardi, N., A. Navarra.- 1993. Baroclinic wind adjustment processes in the Mediterranean Sea, Deep-Sea Res.,II, 40: 1299-1326

Pinot, J.M., J. Tintoré, D. Gomis.- 1994. Quasi-synoptic mesoscale variability in the Balearic Sea. Deep-Sea Res., 41: 897-914

Poulain, P.M.- 1998. Lagrangian measurements of surface circulation in the Adriatic and Ionian Seas between November 1994 and March 1997. Rapp. Comm. int. Mer Médit., 35 (in press)

Salas, J., E. Garcìa-Ladona, J. Font, C. Millot.- 1998. Drifter and satellite thermal observations of the Algerian current in Autumn and Winter 1996-97. Rapp. Comm. int. Mer Médit., 35 (in press)

Taupier-Letage, I., C. Millot.- 1988. Surface circulation in the Algerian basin during 1984. Oceanol. Acta, 9: 79-85

Tintoré, J., P.E. La Violette, I. Bladé, A. Cruzado.- 1988. A study of an intense density front in the eastern Alboran Sea: The Almeria-Oran front, J. Phys. Oceanogr., 18: 1384-1397

Tzipermann, E., P. Malanotte-Rizzoli.- 1991. The climatological seasonal circulation of the Mediterranean Sea, J. Mar. Res., 49: 411-434

Viúdez, A., J. Tintoré.- 1995. Time and space variability in the eastern Alboran Sea from March to May 1990, J. Geophys. Res., 100: 8571-8586

Viúdez, A., J. Tintoré, R.L. Haney.- 1996. Circulation in the Alboran Sea as determined by quasi-synoptic hydrographic observations. Part I: Three-dimensional structure of the two anticyclonic gyres, J. Phys. Oceanogr., 26: 684-705

Submit Journal of Physical Oceanography

LAGRANGIAN SURFACE OBSERVATIONS IN THE ALGERIAN CURRENT

José Salas[1], Claude Millot[2], Jordi Font [1] and Emilio García-Ladona[1]

[1] Instituto de Ciencias del Mar, CSIC, Barcelona, Spain.

[2] Laboratoire d' Océanographie et de Biogéochimie/Centre d' Océanologie de Marseille, CNRS, La Seyne, France.

Abstract

During autumn and winter of 1996-97, several mesoscale structures in the Algerian basin, which are closely linked to the meandering of the Algerian Current, were documented for the first time by a combination of Lagrangian trajectories and temperature images. Using clustered buoys, the sequential evolution of a coastal anticyclonic eddy, the propagation and detachment from the coast of another coastal anticyclonic eddy and smaller eddies generated in the eastern boundary of the Alboran sea were observed. The birth of the eddy began with an instability of the Algerian current at 0-1°E. The current meandered on its eastward way surrounding an anticyclonic eddy, with a cyclonic circulation offshore of its crest. The coastal meander had a 100 km amplitude, and a wavelength ranging 180-230 km. The anticyclonic eddy reached its mature stage in 10 days after the instability of the current with a diameter of 120 km. It moved eastward with the main flow for one and half months, continuing its eastward migration with a diameter of less than 50 km to cross the Sardinia channel. The cyclonic one tends to diffuse rapidly westward. Small scale eddies and plumes were generated in the confluence of the meander's cyclonic flow and the flow of the incoming Atlantic waters. Throughout the trajectories of these buoys, small oscillatory motions were superimposed. Another coastal anticyclonic eddy was detected between 5°E-8°E with a diameter of 120-140 km and an average translation speed of 10 $Km\,d^{-1}$. While this eddy was near the coast, the route of the main flow along the coast was disrupted and flowed around the eddy. The eddy's detachment process began at 7°E, and at this time the main flow between the eddy and the coast was reestablished. It finally followed a northwestward circuit.

1.Introduction

Studies of the Algerian Current (hereafter AC) have recently emphasized the role of instabilities in forming mesoscale eddies along the Algerian coast (Millot, 1985).

The AC begins from the Almería-Oran jet near 1°W, and then flows along the Algerian coast carrying Modified Atlantic Water (MAW) (Millot, 1987; Taupier-Letage and Millot, 1988). Between 0° and 1°E, the AC is seen to be affected by instability processes, mainly of baroclinic nature, which begin as an undulation of the stream that evolves developing paired eddies (Fig.1). Usually, the cyclonic part of the instability tends to vanish in a few days, while the anticyclonic part may persist as an eddy that strongly interacts with the main flow. This eddy propagates downstream at a few $km\ d^{-1}$ with diameters ranging between 30-100 km. Series of satellite images taken over an extended time period show eddy lifetimes of at least several months (Benzohra and Millot, 1994). During its life, the eddy can follow a cyclonic circuit in the Algerian basin (Millot 1985), as a later stage of a coastal anticyclonic eddy (Fuda et al, 1997). But there are some cases in which the eddy doesn't complete the circuit, because it can cross the Sardinia channel enveloped by the AC, or, it can detach from the coast to the basin and stay there gyring for several days, months or years, until it interacts with another eddy or with the main flow. As consequence of eddies' interaction with the main flow, small cyclonic eddies can be generated along the Algerian coast and also exchanges of water between the Algerian and the Liguro-Provenzal basins can be induced (Taupier-Letage and Millot, 1988).

In 1985, Argos buoys were used for the first time in the Algerian basin, during the Mediprod-5 experiment, to study of the flow structure of the AC and its mesoscale of variability (Millot, 1991). Buoys were released in an eddy located at 1°50'E and another one at about 4°E. Their initial trajectory indicate an eastward flow of the current, then buoys turned northward, by the presence of one big anticyclonic eddy. Some of them were drifted in the Algerian basin under the influence of several mesoscale events and other passed between the Balearic Islands. The long-term motion and destiny of the Algerian eddies during this experiment was poorly know, in comparation with our Argos buoys trajectories which measured the sequential evolution of several mesoscale events.

The rich space-time mesoscale variability, measured with our ARGOS buoys trajectories offered us a great opportunity to focus this study on learning where those eddies go, what their eventual destiny is and how they can modify the flow of the AC along the coast. A sequential film of the Algerian eddies evolution is revealed in this paper combining satellite-tracked ARGOS surface buoys and a series of sea surface temperature (SST) to describe the movement and histories of three mesoscale events.
On studies of mesoscale variability, buoy trajectories escape from the current in several cases, it is important to combine it with surface temperature images to identify and understand the evolution of the surface current. Buoy trajectories combined with surface temperature images constituted a valuable information, which contributes to a kinematic understanding of mesoscale processes and suggests pathways of water parcels.
In the following section, instruments and buoy deployment strategy are described. The methodology used in this study was described in section 3. An overview of the buoy trajectories is shown in section 4. Evidence of small eddies are presented in section 5, and the results are discussed and concluded in section 6.

2.Data-set

The database for this study derives from eighteen ARGOS satellite-tracked surface buoys deployed during the ALGERS'96 experiment aboard the Spanish R/V Hésperides in the Western Mediterranean Sea in October 1996 and images of Sea Surface Temperature (SST).

Instruments

The Brightwaters Models A104 and A111 were used in this study to obtain data on mesoscale circulation. The Model A104 external design is similar to that of the Lagrangian current-following drifter developed by Davis (1982). A Davis-type Lagrangian drifting buoy is the synergy of the GPS (Global Positioning System)-ARGOS drifter combination, which resulted in several advantages over previous designs. Position time series are stored internally and telemetered through the ARGOS satellite system. The antenna supports the GPS receiver and a half-wave ARGOS antenna, which are completely encased in PVC to prevent corrosion. The two antennas

and the top of five floats rise from the sea surface. A water temperature sensor was added.

The main body of Model A111 is a rod-wheel buoyant from ARGOS transmitter rise over the sea surface, avoiding the wind drag effect. One float on short line is attached to the top rod-wheel, and supported a TOGA-WOCE standard sock, 10 m long with a 5 m tether, hangs centered at 10m below the surface water. Model A104 was held with drogue used in Model A111. The effective drag ratio of the drogue is 70.During the experiment three A104 and fifteen A111 buoys provided data 6-8 positions per day. The buoys with GPS were programmed to transmit positions every 30 minutes.

The SST maps represent 1-day and week averages. They were obtained from NOAA Advanced Very High Resolution Radiometer (AVHRR) images, using the GISIS (Graphical Interface to the Intelligent Satellite Data Information System) Internet facility from DLR (German Aerospace Research Center). In the images used, dark colors refer to warm waters, grey colors correspond to colder waters and white is reserved for clouds and land. During the cruise, both buoy positions and AVHRR images were received on board using a HRPT receiving station (Terascan TS 300 system from Sea Space).

SST images are composed according the maximum temperature value given at every pixel's position to minimize cloud coverage. Weekly images are derived from the daily maximum images using the average at every pixel's position.

Deployment strategy

Previous days to the cruise began; SST images displayed intense mesoscale variability along the Algerian coast. The Infrared image of October 16 showed the existence of an energetic mesoscale instability at the beginning of the AC near 0° and highlighted a mature eddy centered on 5°E. The instability appeared as a meander of the current surrounding a coastal anticyclonic eddy and associated with a strong cyclonic eddy upstream and seaward of the meander. This mesoscale structure was chosen as the specific area sampled during the ALGERS'96 experiment (Fig.2).

The deployment strategy began on October 17, with the launching of three buoys 8-10 km apart in the core of the AC and upstream of the meander. Fifteen more buoys were released along a line that crossed the center of the well-developed cyclonic part of the structure, i.e. upstream from the meander. Of these 15 buoys, 8 buoys were launched 3-

6 km apart in the inner part of the meander and 7 buoys, 8-11 km apart, in the cyclonic part (Fig.2).

3. Methodology

We will concentrate in this paper on data from the period October through January 1997 and on drifters that were in the area encloses within the box (Fig.3). The whole set of trajectories, were used to illustrate the general drift of MAW in the Western Mediterranean Sea in a separate study (Font et al, 1998).

In this study we investigate the mesoscale variability of the AC along the Algerian basin. Three main events were identified along the Algerian coast. Instability evolved into a coastal anticyclonic eddy (1) was observed inside of box II. On box III, a mature eddy (2) and small eddies were identified in box I.

Combining buoy trajectories with SST images, the evolution of these mesoscale events was study. This methodology consist in clustered buoy trajectories describing similar spatial structures in a time period of one week as maximum to correlate it with the structures observed on daily images. Sometimes daily complementary images were of poor quality (cloudiness) and the interpretation of the mesoscale evolution was difficult to do. To avoid this problem week-composite images were used in those cases in that the mesoscale events evolved slowly allowing correlating with buoy trajectories.

In this study, the buoy trajectories were clustered in similar times of mesoscale evolution featured in the following description. These time periods are divided into 12 segments of 7 days that begin on October 17 and finish on January 12. Throughout the study, cluster buoys at different time-periods were identified with colors (table 1). The circles in the trajectories represent segments of every 7 days. Crossed circles and triangles indicate first and last positions, respectively.

4. Buoy trajectories

4.1 Eddy 1

The birth of the first coastal anticyclonic eddy appeared in SST images as a meander of the current surrounding a coastal anticyclonic motion, associated with a secondary

cyclonic eddy, upstream and seaward from the crest of the meander. The buoy trajectories illustrate precisely the along-slope current and its offshore displacement to contour the anticyclonic structure (between 1° and 2°E), that was growing and slowly migrating downstream. Six buoys were entrained in the cyclonic eddy, the shape of which rapidly changed and became elongated (Fig.4). In the following days, this eddy mixed with the flow of the eastern Alboran gyre generating small eddies (farther on described), while the coastal anticyclonic structure continued growing. During October 17-24, the shape of the meander was clearly traced by the first group of trajectories, composed of five buoys (1-5) (Fig.5a). Their trajectories had wave-like shapes, between 0° and 3°E, with wavelengths ranging from 180 km-230 km and phase speed of $1 kmd^{-1}$. The growth-rate of the instability (10 days), its speed of propagation downstream (a few kilometers a day) and wavelengths of 160 km appear to be in good agreement with others observational and numerical studies (Millot et al., 1990; Mortier, 1992).

Then they followed the mean flow of the AC (Fig.5a). The mean velocity and standard deviation computed from daily positions of the buoys while in the instability event are in the E-W and N-S directions $\overline{u} = 20 - 29\ cms^{-1}$, $\overline{v} = 2 - 5\ cms^{-1}$ and $\sigma_u = 3 - 9\ cms^{-1}, \sigma_v = 2 - 5\ cms^{-1}$, clearly showed that in the initial phase of eddy generation it attain lower variance amplitudes mainly northward. As the eddy evolves, the variance amplitude tender to increase, until the eddy reach its mature state.

After October 24, two of these buoys, 1 and 2, ceased to transmit downstream the meander. Over the next six days, the remaining three buoys moved eastward with the main flow. Two of them (4-5) traveled eastward at about 30 cms^{-1} Buoy 3 moved faster than other buoys with a mean daily velocity of $38 cms^{-1}$. Further east the three buoys featured the structure of the second coastal eddy, documented in section 4.2.

From October 25, the meander sharpened near 2°E, becoming about 130 km in diameter on October 31, getting its mature stage. Our new eddy is comparable in surface dimensions and thermal structure with the eddy studied by Benzohra and Millot, (1995).

The second cluster of trajectories composed by four buoys (6-9) described two anticyclonic circuits during 14 days (Fig.5b). Two of them completed one revolution in 7 days with a diameter of about 40km and azimuthal velocities of14 cms^{-1}. Over the next week, November 1-7 the coastal eddy had continued its eastern migration. The two other buoys completed one revolution in 8 days with a diameter of about 50km (Fig. 5b)

and similar azimuthal velocities. The shorter rotation period of buoys, and its permanence on the eddy, suggest that they were near of the core of the eddy. Benzohra and Millot, (1995) found the zone of solid-body rotation in the core of the eddy (13.2-13.6°C) for radius of (20-30 km) and periods less of 6 days, similar wit our results.

Buoy 10 moved eastward at 16 cms^{-1}, contouring the edge of the eddy. On November 7 the same group of buoys exited the eddy, and moved eastward into a notable main flow in which speeds ranged from 19 cms^{-1} to 40 cms^{-1}. The second cluster of buoys converged to the coast near 4°E, and drifted parallel to it for about 150 km. Eventually the motion of the buoy 7 completely stopped in the vicinity of 37.14° N-4.36° E. The four remaining buoys of the second cluster farther on described the detachment process of the older eddy, presented on section 4.2.

During the following days November 8-23 the coastal eddy was reabsorbed within the AC. Subsequent images show it attached to the coast, with a diameter smaller than 50 km. As this eddy was propagating further east, the AC recovered its widespread eastward flow along the coast. Further eastward it meanders around the same surface eddy.

Between, 0-3°E, the flow bring together to the Algerian basin, between Nov 8-29, the third cluster of buoys (11-16) deployed in the cyclonic part of the meander and that initially drifted to the west and which almost reaching the Spanish coast. They drifted with the along-slope coastal current with an average speed of $30 cms^{-1}$ until some trajectories meandered and looped on its eastward way by the presence of the first coastal anticyclonic eddy which continued propagating eastward inside the AC, which keeping constant its size on its drift (Fig. 5c). The motion of buoy 14, relative to the eddy (1) (Fig.5c) shows that it made one loop around the eddy in eight days (December) at a diameter of 30 km and with azimuthal speed of $25 cm\, s^{-1}$. The buoy did not stay trapped in this eddy but drifted away from the coast to the southwestern corner of Sardinia Island (by the presence of eddy 2) and made two small cyclonic loops on its northward way, before it failed on the sea.

In the eastern migration of the main flow, buoy 12 moved offshore in a think anticyclonic arc that indicate a meander of the AC over the eddy. Other two buoy trajectories (15-16) followed a similar trajectory of buoy 12. They clearly showed a train of anticyclonic motions, result from a superposition of the azimuthal velocity of the anticyclonic eddy and the translation towards the east by the AC. At the arrows, the

drifters are at the southeastern side of the eddy, moving against the AC; halfway between arrows it is in the northwestern side, where the eddy velocity and the AC have the same direction. The center of the eddy is located between these extremes, indicates that our eddy translate with a uniform speed of 8 $km\,d^{-1}$ which is similar to the translation velocity $3\,km\,d^{-1}$ estimated with mooring-arrays in one meander enclosing a surface coastal anticyclonic eddy.

Further eastward, between 8-10°E, the trajectory of buoy 15 contour another eddy left the coast. On January 13 buoy completely had crossed the Sardinia channel at the same time in which buoy 12 stopped signaling in the Algerian basin. There was the last evidence of the eddy's migration using buoys. Later on the eventual destiny of eddy (1), was followed with thermal features extracted from SST images. The IR used, were collected from January to February of 1997. They indicated that the coastal eddy continued moved downstream within the main flow interacting with another eddy (located 9°E) until it disappeared or crossed the Sardinia channel within the AC. It is possible that it crossed the channel because its diameter was lesser than the cross-effective section of the channel. Millot et al (1997) made a surface schematic interpretation from SST images of the propagation of one coastal anticyclonic eddy, clearly similar with eddy 1 of this study. Supported on this study and the size of our eddy we are convinced that eddy (1) crossed the Sardinia channel.

This is an important result, because in the circulation diagram of Millot (1998), eddies describe a cyclonic circuit. At least in this study the eddy generated close 0°E not completed the proposed cyclonic circuit by Millot (1998).

The reestablishment of the AC flow (between 0-2°E) after the generation of one coastal anticyclonic eddy does not appear reported in previous studies of in situ and infrared observations. In this study was supposed that another eddy could be generate again near 0°, by an instability process. Because images from the first days of November clearly showed an small eddy centered at 0° upstream of the first eddy and apparently rotating in an anticyclonic sense (Image of November 2, not shown here). In the following days it become visible in the SST images disappearing then of twenty days. Its possible that mixing between the incoming Atlantic water and the water of the cyclonic eddy not permit introduce the necessary amount of energy to feed these eddy. In the eastern boundary of the Alboran Sea, daily images of November, showed how of the incoming

Atlantic waters was mixing with the waters of the cyclonic eddy. As consequence of the mixing small vortices were generated in the area, farther on are presented on section 5. Bouzinac et al (1998) revealed a 6 month periodicity of eddies generation during 1993. However theirs results are not corroborated for other years. Its necessary to focus further studies on the periodicity of Algerian eddies generation if it really has a periodic signal.

4.2 Eddy 2

The second interesting event was a mature eddy centered near 6.5°E. It could be an older stage of one coastal anticyclonic eddy generated near 0°E. During its eastward drift the old eddy leaves the coast, thus becoming what Millot (1994) called an "open sea eddy". The main effect of the eddy is to trap MAW and disrupt the main flow of the AC along the coast. On the SST image, the eddy core showed relatively warm MAW than its background fluid. This thermal structure supports an anticyclonic rotation that has been observed directly with the four cluster of buoys composed by buoys from clusters one (3-5) and two (6,8-10) (Fig.6a).

On October 30 buoy 4 arrived at 5° E, when the MAW leaving the coast bypasses this surface eddy, with a mean eastward velocity of 17 $cm\,s^{-1}$ before reaching again the coast and following it. More northward on November 3, the motion of buoy 3 relative to the eddy center at a diameter of 120 km, close to the one inferred from the satellite image of November 5, completed an anticyclonic loop in 13 days with azimuthal speed of $30\,cms^{-1}$. The longer rotation period, of buoy 3, suggest that it be outside the core of the old eddy. From buoys, an important feature observed in eddies is that its inner part rotating much more rapidly than its outer part, similar as the observed in a solid body rotation. The coastal eddy translated eastward at about $7\,km\,d^{-1}$, have been separated from the surface current at 7°E. The detachment point location found in this study is closely with that reported in the Fuda's et al (1998) study. However, such detachment could occur at about 4-5°E (Bouzinac et al, 1998). Here, an interesting question raise: ¿Why, are there different detachment eddy's points along the Algerian coast. Numerical studies need to explain the dynamics processes, which induce the detachment of eddies at different places of the Algerian coast.

Three trajectories from cluster four showed us three stages of eddy's detachment processes, with a visible enlargement to the north of their trajectories, which produced a cross-stream standard deviation larger than the along-stream one (Fig.6b).

The first stage occurs, when the eddy becomes attached to the current and the main flow is diverted and flow around the eddy (buoy8). In the second stage, documented with buoy 10, the eddy center opens to the north of the main flow, which is in a form of an open meander. During the first two stages both buoys, from the period of 22-28 November drifted at a mean speed of $30 cm s^{-1}$ and $35 cm s^{-1}$ respectively. Then this eddy is seen at a more seaward location, thus reopening, along the coast, the eastward route of the AC. Buoy 6 (November 20-28) moved eastward between the open sea eddy and the coast at an average velocity of $20 cm s^{-1}$, before it failed on December 3

Finally, in the third stage it is possible for the meander to then dissipate or to come away as another eddy. Buoy 5 showed that a new eddy was formed. On the northwest edge of the open meander water from the eddy was observed to be exit into the Algerian basin from 29-08 December, just in front of the southwestern part of the Sardinia Island. The region near the Sardinia channel is particularly complicated one. There was evidence for a semipermanent eddy-meander in this region. Several buoys of cluster five moving eastward with the AC became entrained for various periods of time in this structure (Fig.6c). On 29-5 December buoy 11 traced half part of an anticyclonic eddy becomes attached to the AC moves downstream. Then the same buoy completed a cyclonic trajectory between December 6-11 with a small diameter of approximately 40km. From December 12 it changed, its course northward at a mean speed of $50 cm s^{-1}$ completed on December 19 an elliptical trajectory, with axis of size of 70 km x 110 km until it again turned eastward. It is clear eddy was leaving the AC to move northward, showed a form of an open meander. From December 13-26 buoy 13 entrained in the core of the eddy completed completes an anticyclonic loop in 7 days, at a mean daily speed of 42 $cm s^{-1}$. This new eddy was interacting with the old eddy, described with cluster 4. Thus there is evidence of eddy-eddy-AC interaction. On last days of December buoy 12, was deflected to the northwestward as consequence of the old eddy initiate a northwest circuit, proposed by Millot (1985) and confirmed by Fuda et al (1997). This process can be clearly observed in the surface waters with the satellite image of December 21 (Fig.7). Based on drifting buoys and satellite infrared images, its possible that eddies play an important role in the exchange of heat by transporting warm

water from its warm core to the open Algerian basin. The transport may occur when an open eddy is deflecting northwestward and when the eddy interacts with the AC and exchanges water with it. Those evidence are added to that Fuda et al (1997) and Buozinac et al (1997) that region near the Sardinia channel is one in which large meanders and eddies are produced.

Finally, completed the drift of the buoy trajectories from cluster 4 and cluster 5 which escapes from the influence of the most energetic mesoscale events to continue their journey along the Tunisian coast. As buoys approached at the entrance of Sardinia channel, from the east with a speed of $20 cm\, s^{-1}$, $10 cm\, s^{-1}$ slowed displayed an anticyclonic meander, surrounded a small anticyclonic eddy along the Tunisian coast. It was crossing the channel gradually. On the first days of January, the eddy completely crossed the Sardinia channel to vanish south of the Tyrrhenian Sea. On the next days, other buoys drifted along the Tunisian coast, free of mesoscale activity. Confirmed that eddy crossed completely the Sardinia channel with the AC (Fig. 6b,c). Evidences from the drifting buoys suggest that the entrance of Sardinia channel is an area of strong mesoscale variability.

5. Small eddies

After the few days of the cruise, the cyclonic eddy was elongated to the west, mixed its water with the incoming Atlantic water from the west. In the confluence zone of the water and along of the edge of the cyclonic eddy, there were small-scale instabilities that appear to have been born in the flow of the eddy, evolved in cyclonic and anticyclonic vortices. Those kinds of structures were well tracked by one group of six buoys.

Throughout the trajectories of the group of buoys, small oscillatory motions were superimposed upon the longer period flow. They can related with inertial waves, the most energetic phenomenon measurable in the drifter data (Poulain et al, 1996).

On October 25 buoy 15 followed an elliptic anticyclonic path (40 km x 20 km) which closed on November 2 (Fig.8a) In the next 18 days the buoy motion changed to an anticyclonic rotation. Around November 16 the buoy began to proceed to the north with the waters from the Spanish coast, turned southwest and then back to the east, closing a cyclonic loop in 7 days. From its deployment position, buoy 14 was entrained in the

flow of the cyclonic eddy. It then moved westward along the northern side of it. By the end of October 1996, it circulated along the edge of a small anticyclonic vortex developed from the cyclonic eddy. On November 8 near of 1°W this buoy turned southward, executing oscillations of a shorter period. Finally on November 22, it took and eastward direction parallel to the Algerian coast (Fig.8b).

While buoy 16 turned northeast it completed a cyclonic loop on November 30, with a mean speed of $9\,cm\,s^{-1}$. A complete revolution was accomplished in 28 days. Forty-two days later, it turned back at 20 km north of its deployment position and began to move to the east. The buoy meandered to the east from December 16-26. It then continued to drift eastward along the Algerian coast (Fig.9a). Two other trajectories, from buoys 11 and 12, are also presented in Fig. 9b. After leaving the flow of the cyclonic eddy they diverged on 1° W. Buoy 11 over the next 15 days executed a cyclonic loop, whose center was located at approximately 1.3°E and 36.6°N.At the north of this eddy, buoy 12 developed a cyclonic curvature to its path in the form of a wild gyrating motion.

Besides following the path of the cyclonic eddy, buoys in figure 10 could escape from the eddy to enter a filament path at 1° E. The motion of the buoys was initially cyclonic, although on November 1, buoy 13 began to proceed eastward again along the Algerian coast.

The trajectories of the surface drifters in the eastern boundary of the Alboran sea showed several small eddies with seemingly similar nature with those discrete eddies reported at 700m of depth in the Gulf stream (Rossby et al, 1983). In the Gulf Stream, the trajectories of surface buoys and SOFAR buoys at different depths generally show a vertical coherent structure with the surface (Schmitz, et al, 1981).

However the small eddies reported in this work apparently are transient, unlike of those reported in the Gulf stream, which are long-lived. In the Mediterranean Sea, the mechanisms of small-eddies are still obscure.

6.Discusion

For the first time, buoy trajectories of Algerian eddies have been obtained in the AC. These data give first estimates of the long eddies last and the first evidences of eddy eventual destiny and its role in the perturbation of the MAW flow.

The buoys used in this study clearly follow the path of MAW proposed in a circulation diagram by Millot (1985) and observed by Font et al (1998) in the trajectories of surface buoys. However, we found that the cyclonic circuit proposed for him is not following by the eddy formed near of 0°E.

During the first days, the trajectories described the meandering of the AC between 0° and 3°E. They had a wave-like shape with wavelength ranging from 180 km to 230 km. During 5 days, the mean along-stream component was from 20 cms^{-1} to 29 cms^{-1} and larger than the standard deviation, suggesting that the mean flow was stronger than the eddy flow. The meander evolved into a coastal anticyclonic eddy with 120-140 km in diameter and a revolution period of 7-8 days. The standard deviation of the two horizontal velocity components became larger than the mean values, suggesting a dominance of the eddy motions. In its final stage, after one month, the eddy merges completely with the main flow, which is in a form of a coastal meander, which crossed the Sardinia channel.

The open sea eddy observed at 6°E had a diameter of 120 km. Some buoys trapped in it completed one loop in 7 to 13 days. Between 6°E and 7°E, the buoys allowed us to observe in detail the detachment and interaction of this eddy with a meander during 40 days. The cross-stream standard deviation increased as a consequence of the detachment of the eddy that deflected some buoy trajectories towards the north. Algerian eddies usually, moved northwestward when they are not touching the AC and eastward when they are attached to it. Frequently eddies become attached to the AC and are advected parallel to the current in a downstream direction. This eastward movement can be quit fast.

The main effect of this eddy is to trap MAW and to disturb the main flow of the AC. Part of the current is deflected in the detachment period and the other part flows between the eddy and the coast. Small scale eddies were generated in the eastern Alboran Sea by mixing processes.

Acknowledgments: The efforts of the crew of the Hésperides ship during the buoy deployment cruise are gratefully. Thanks to Agustí Julia for his technical support in preparing the buoys. Oscar Chic provided the satellite infrared images. Assistance from many members of ALGERS'96 group is gratefully acknowledged. This research was supported by the European Union MAST program (MATER Mediterranean Targeted

Project phase II, contract MAS3-CT96-0051) and Spanish CICYT (MAR95-1861), and is a contribution to ALGERS project (ERS AO2 E102) of the ESA Earth Observation program. This work was completed while the author held a doctoral fellowship of México through CONACYT (Consejo Nacional de Ciencia y Tecnología).

References

EUROMODEL Group, 1995: Progress from 1989 to 1992 in understanding the circulation of the Western Mediterranean Sea. Oceanol. Acta, 18, 2: 255-271.

2- Millot, C., 1985: Some features of the Algerian current, J. Geophys.Res, 90, C4: 7169-7176.

3- Arnone, R., D.A. Wiesenburg and K. Saunders, 1990: The origin of the Algerian current, J. Geophys. Res., 95, C2: 1587-1598.

4- Millot, C., 1987: Circulation in the western Mediterranean Sea. Oceanol. Acta, 10: 143-149.

5- Taupier-Letage, I. and C. Millot, 1988: Surface circulation in the Algerian basin during 1984. Oceanol. Acta, 9: 79-85.

Figure captions

Figure 1. Circulation diagram, of the Modified Atlantic water inn the Algerian basin.

Figure 2. NOAA/AVHRR SST image of 16 October, showed the meander evolution and the deployment of the ARGOS buoys.

Figure 3. "Spaghetti" diagram of all 18 buoys. The boxes showed the three major features identified along the study. Box I, small scale eddies. Box 2, a meander evolving in a coastal anticyclonic eddy. Box 3, and old eddy left the current and interacted with another one.

Figure 4. NOAA/AVHRR SST image of 16 October with superimposed buoy tracks of the first three days.

Figure 5. Clustered buoys showed the meander evolution into a coastal anticyclonic eddy.

Figure 6. Clustered buoys showed the old eddy left the coast and interacting with another eddy.

Figure 7. Northwestward circuit, of the old eddy leaving the coast.

Figure 8. Clustered buoys showed the small scale eddies in the eastern boundary of the Alboran Sea. a) Buoy 15. b) Buoy 14.

Figured 9. Clustered buoys showed the small scale eddies in the eastern boundary of the Alboran Sea. a) Buoy 16. b) Buoy 11 and buoy 12.

Figure 10. Buoy 13 showed a plume in the edge of the cyclonic eddy.

Table 2.

Cluster	Tim-period covered	Color
1	17-24 Oct	Black
2	25-31 Oct	Reed
3	01-07 Nov	Green
4	08-14 Nov	Blue
5	15-21 Nov	Yellow
6	22-28 Nov	Cyan
7	29-05 Dec	Magenta
8	06-12 Dec	Maroon
9	13-19 Dec	Sea Green
10	20-26 Dec	Purple
11	27-02 Jan	Coral
12	03-12 Jan	Thistle

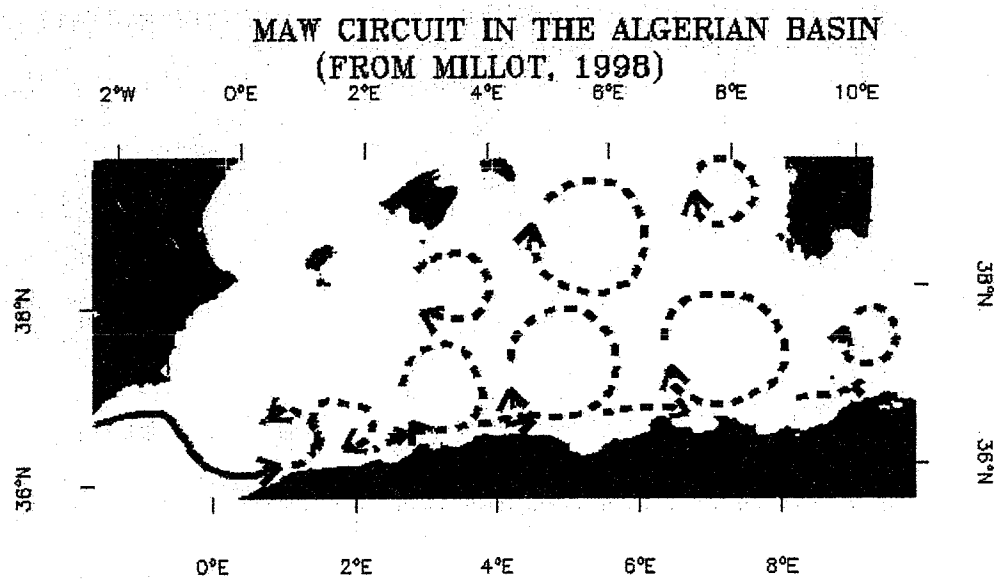

Figure 1. Circulation diagram of the Modified Atlantic water in the Algerian basin.

Figure 2. NOAA/AVHRR SST image of 16 October, showed the meander evolution and the deployment of the ARGOS buoys.

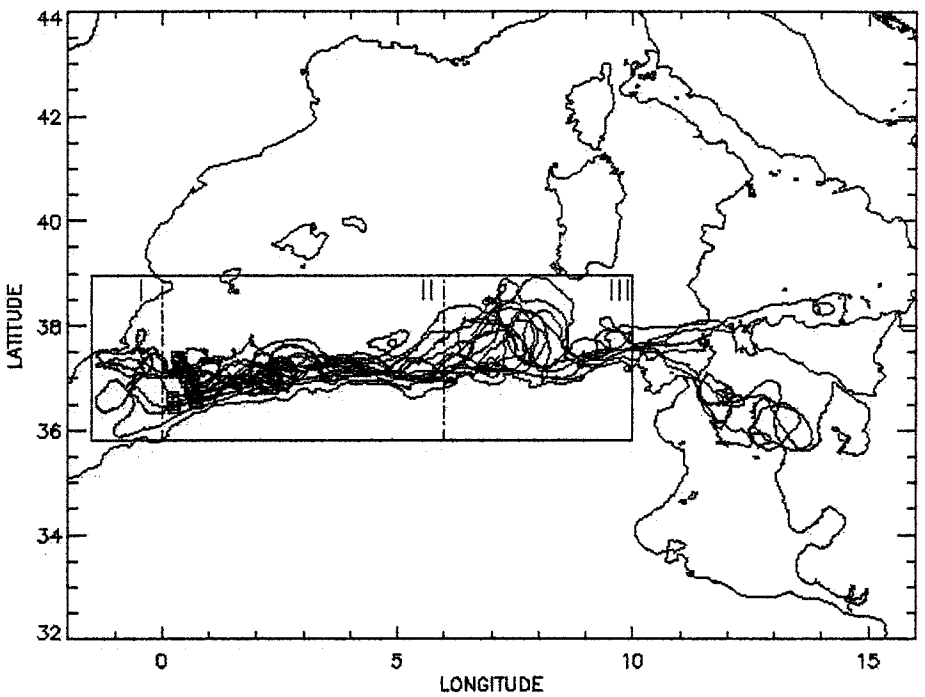

Figure 3. "Spaghetti" diagram of all 18 buoys. The boxes showed the three major features identified along the study. Box I, small scale eddies. Box 2, a meander evolving in a coastal anticyclonic eddy. Box3, an old eddy left the current and interacted with another one.

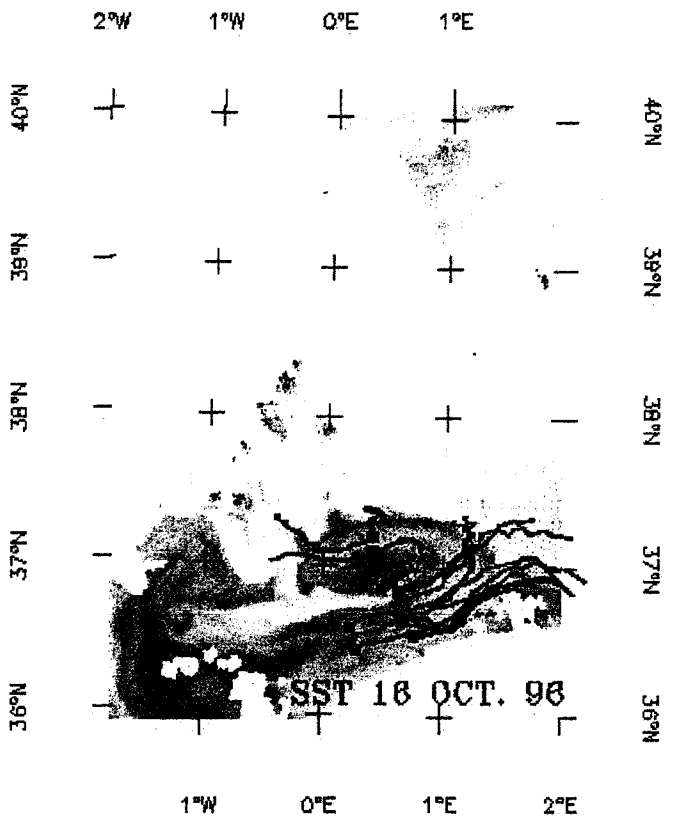

Figure 4. NOAA/AVHRR SST image of 16 October with superimposed buoy tracks of the first three days.

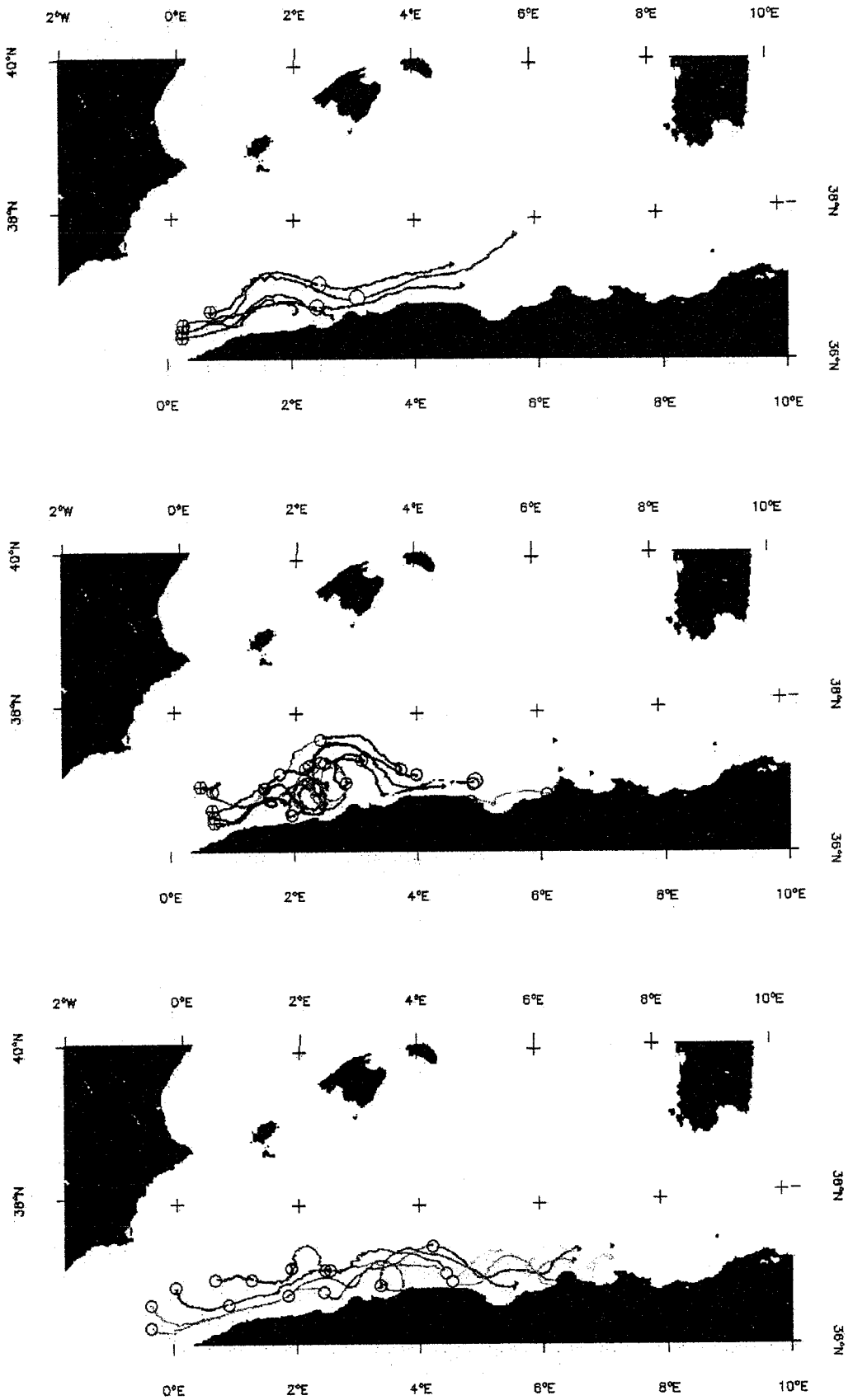

Figure 5. Clustered buoys, showed the meander evolution in a coastal anticyclonic eddy.

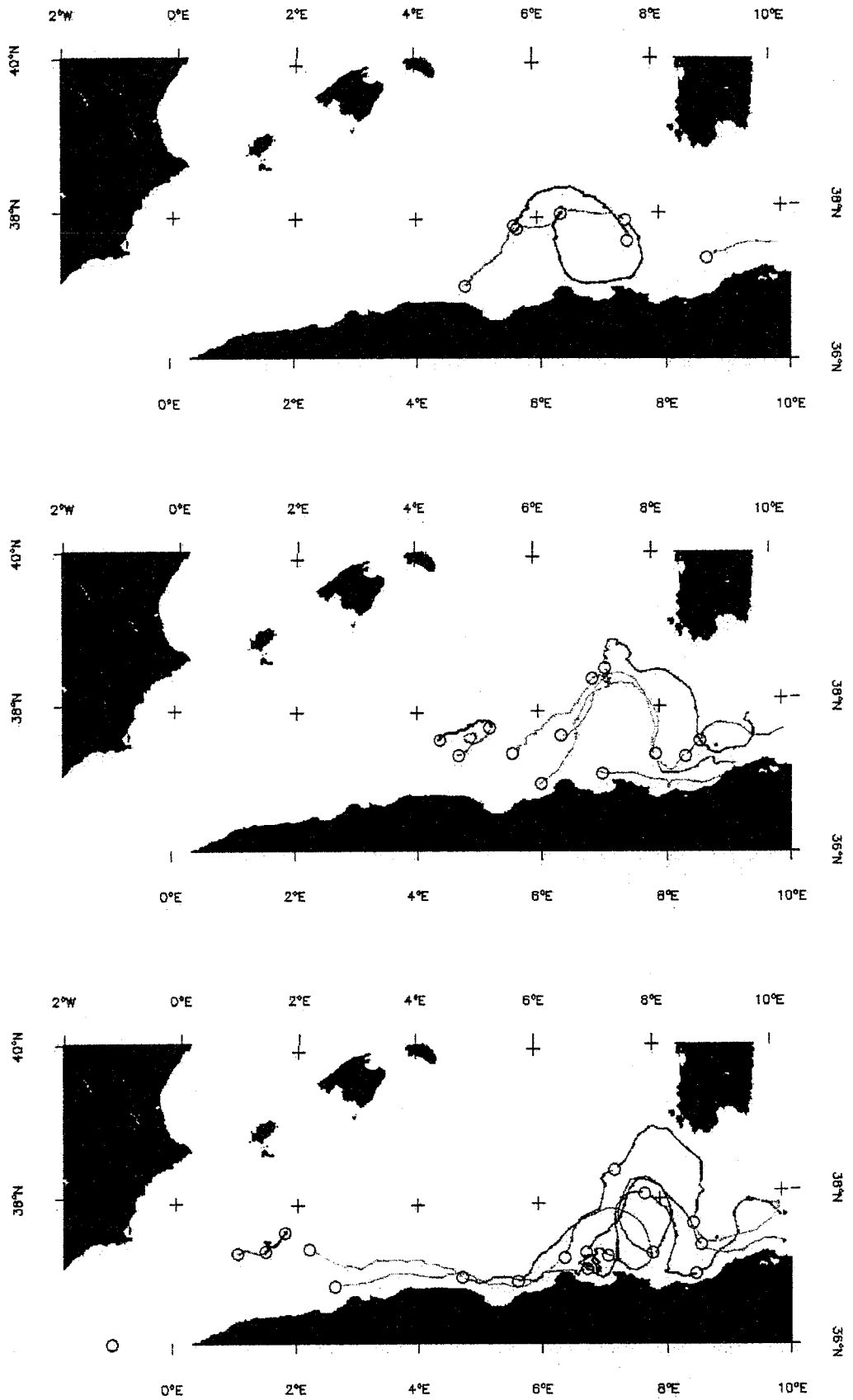

Figure 6. Clustered buoys, showed the meander evolution in a coastal anticyclonic eddy.

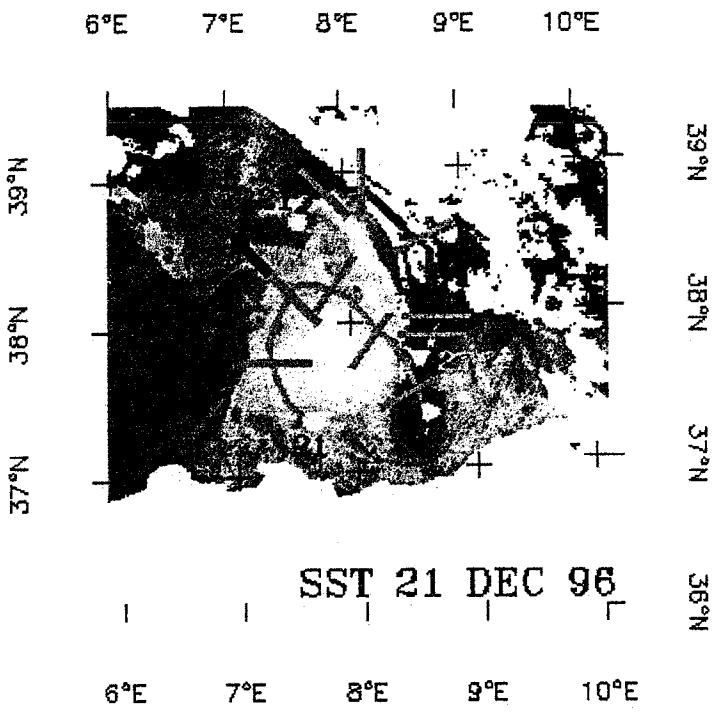

Figure 7. Northwestward circuit of the old eddy.

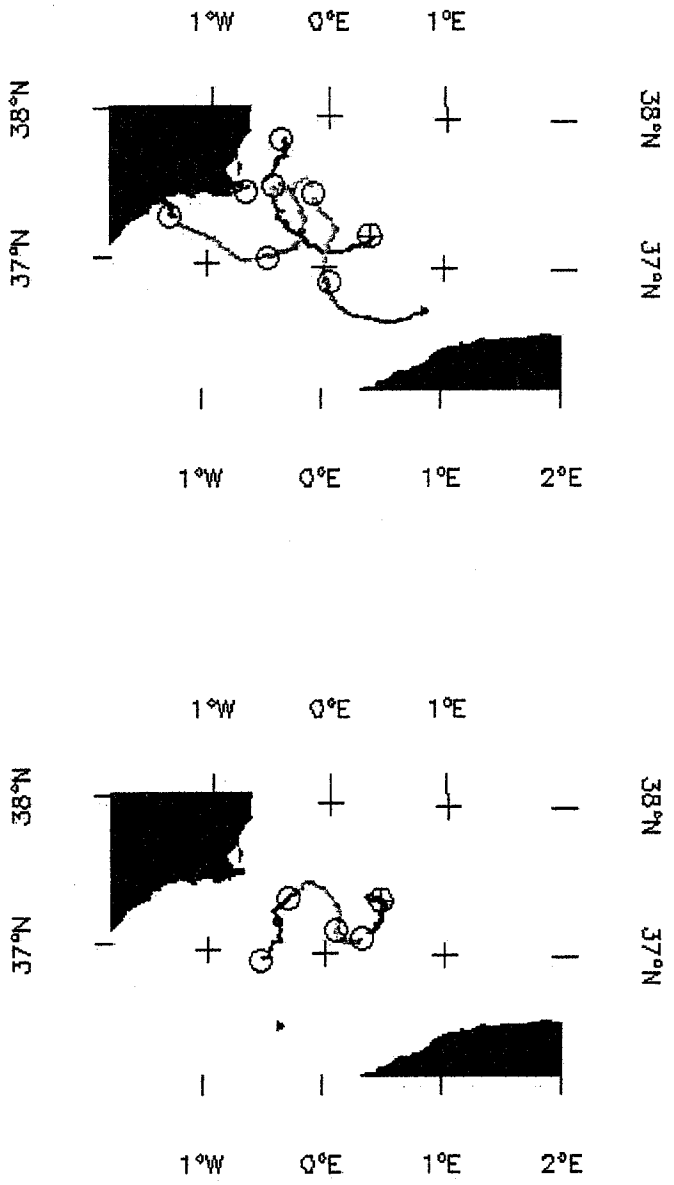

Figure 8. Clustered buoys showed the small scale eddies in the eastern boundary of the Alboran Sea. a) Buoy 15. b) Buoy 14.

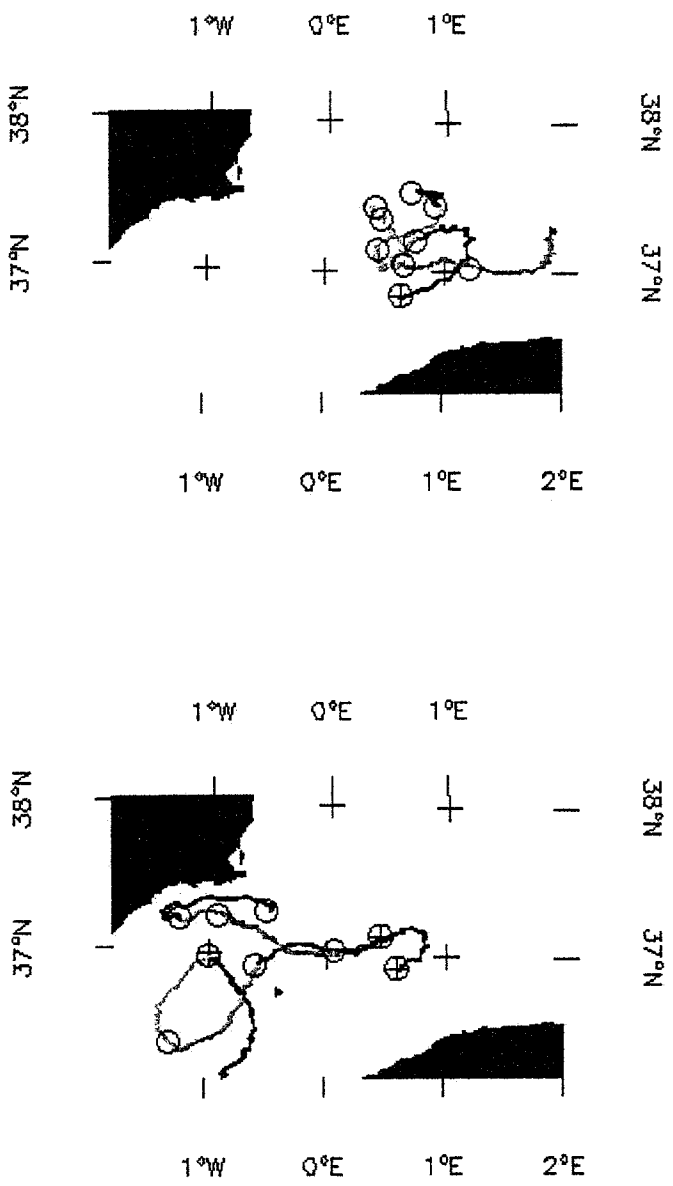

Figure 9. Clustered buoys showed the small scale eddies in the eastern boundary of the Alboran Sea. a) Buoy 16. b) Buoy 11 and buoy 12.

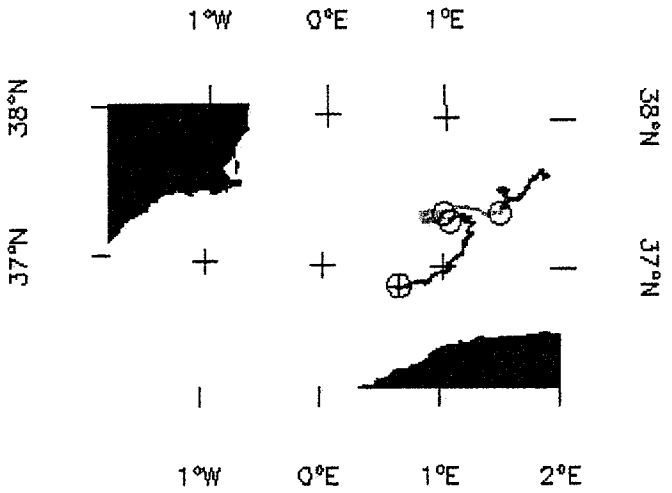

Figure 10. Buoy 13 showed a plume in the edge of the cyclonic eddy.

OVERALL ASSESSMENT ON THE EXPERIMENT AND THE USED ERS DATA SETS

The activities undertaken during ALGERS have produced new and significant results on the dynamics of the surface layer in the Algerian basin. Mesoscale structures are very important in the Mediterranean Sea, but especially decisive in the Algerian basin. Besides investigating some aspects of the physical-biological coupling related to these structures, mainly with *in situ* measurements, we have documented and quantified several characteristics of the temporal evolution of the anticyclonic eddies generated from the Algerian current. The synoptic and repetitive view offered by satellite remote sensing, has been a key point for the success of the project.

We cannot be completely satisfied with the contribution of ERS data in ALGERS. Although expected, some problems have appeared to be really hard and did not allow a full use of the data made available to us by ESA. The data sets were of good quality, received in reasonable delays, and any technical difficulty was rapidly and efficiently solved by ESRIN.

The maximum benefit has been obtained from altimeter data. The characteristics of ERS altimeter and satellite orbit provide an adequate spatial resolution for the study of the big offshore Algerian eddies, but not to resolve the temporal scales. The combination of ERS with Topex/Poseidon data in a series of sea surface anomaly maps gives a good product for mesoscale dynamics studies in this Mediterranean region.

The considerable amount of SAR scenes recorded and processed, in the best space and time windows available, have been quite disappointing. Unless most of the SAR images we analysed during our first ERS project, now we have not been lucky with the environmental conditions (wind) that strongly limit the formation of mesoscale structures in the radar images. We have to conclude that SAR, besides having proved to be able to image at a very high resolution structures related to surface currents, will not be an operative tool until a constellation of satellites can offer an adequate view of any ocean region. That means more than one image per day, to avoid the possible problems produced by unfavourable wind conditions.

As reported in our previous project, it is still easier to use NOAA infrared data than ATSR. We have analysed a few of them, and probably could have made an effort to increase this number, but as a general rule ALGERS has used infrared imagery from other sources than ERS.

Comparing to the original objectives, we can conclude that most of them have been achieved except for the modelling aspects. The modification of the circumstances (affiliation and involvement in projects) for some of the participant co-investigators has made difficult an adequate planification and co-ordination of the proposed activities.

Acknowledgements. We are recognised to ESA, who provided all the ERS data used in this study, to all the colleagues and other research projects that contributed in different aspects in the ALGERS activities, and to the funding agencies that made possible the proposed research.

PUBLICATIONS

These include ALGERS results, as well as results from our previous ERS project (*) published after November 1995:

Allen, J.T., Smeed, D.A., Crisp, N., Ruiz, S., Watts, S., Vélez, P.J., Jornet, P., Rius, O., Castellón, A. (1997).- *Upper ocean underway operations on B.I.O. Hespérides cruise OMEGA-ALGERS using SeaSoar and ADCP 30/9/96-14/10/96*, Southampton Oceanography Centre, Internal Document, 17, 52 pp.

Baldacci, A., Corsini, G., Diani, M., Chic, O., Font, J., Cipollini, P., Forrester, T., Guymer, T., Snaith, H. (1998).- *The OMEGA Atlas of Remotely Sensed Data,* http://radar.iet.unipi.it/OMEGA/ATLAS/atlas.htm, Printed version: Università degli Studi di Pisa, Pisa, 64 pp.

Bouzinac, C. (1997).- *Variabilité spatiale et temporelle de la circulation superficielle dans la région du courant Algerien.* Thèse de Doctorat, Université Pierre et Marie Curie, Paris VI, 131 pp.

Bouzinac, C., Font, J., Vázquez, J., Millot, C. (1997).- CEOF analysis of ERS and TOPEX/POSEIDON combined altimetric data in the Algerian Current region. In: *Space at the service of our environment. 3rd ERS 1 Symposium*, Ed. T.D. Guyenne , D. Danesy, ESA SP-414: 1497-1500, Noordwijk, ISBN 92-9092-656-2

Bouzinac, C., Vázquez, J., Font, J. (1997).- Análisis de datos altimétricos en el Mediterráneo occidental mediante Funciones Ortogonales Empíricas Complejas. In: *Teledetección: usos y aplicaciones*, Ed. J.L.Casanova, J.Sanz, Secr. Publicaciones e Intercambio Científico, Univ. Valladolid: 93-100 ISBN: 84-7762-693-6

Bouzinac, C., Vázquez, J., Font, J. (1998).- CEOF analysis of ERS-1 and Topex/Poseidon combined altimetric data in the region of the Algerian current. *J. Geophys. Res.*, 103(C4): 8059-8071

Chic, O., Font, J., García, Z. (1997).- Comparison between AVHRR real time and ERS-2 SAR near real time data in an oceanographic cruise in the western Mediterranean. In: *Oceans'97 MTS/IEEE* Proceedings on CD-ROM, Remote Sensing III - RADAR, ThF2.4 ISBN: 0-7803-4111-2

Chic, O., Font, J., Sandven, S. (1997).- The use of near real time infrared and SAR satellite imagery to update the sampling strategy of an oceanographic vessel. In: *Teledetección aplicada a la gestión de recursos naturales y medio litoral marino*, Ed. C. Hernández Sande, J.E. Arias Rodríguez, AET - Univ. Santiago de Compostela: 97-100 ISBN: 84-8498-351-X

Chic, O., Font, J., Sandven, S. (1997).- ERS-2 SAR near real time data used in the sampling strategy of an oceanographic cruise in the western Mediterranean. In: *Space at the service of our environment. 3rd ERS 1 Symposium*, Ed. T.D. Guyenne , D. Danesy, ESA SP-414: 1433-1438, Noordwijk,ISBN 92-9092-656-2

Font, J. (1997).- ALGERS'96 cruise in the western Algerian Basin. *MTP News*, 5: 8-9

Font, J., et al. (1996).- *OMEGA - ALGERS B.I.O. Hespérides*. Informe de campaña a la Comisión de Gestión, Barcelona, 219 pp.

Font, J., Millot, C., Julià, A., Salas, J., Chic, O. (1998).- The drift of Modified Atlantic Water from the Alboran Sea to the eastern Mediterranean. *Scient. Mar.*, 62 (in press)

Font, J., Shirasago, B., Martínez, J.J., Sánchez, D., Arbiol, R., Palà, V., Moreno, V., Martínez, A., Vázquez. J. (1996).- Evaluation of ERS-1 microwave sensors capability in the study of oceanic fronts. *Rev. Teledet*, 6: 27-36 (*)

Shirasago, B., Font, J. (1997).- Mesoscale structures detected with ERS-1 SAR in the Alboran Sea verified by ERS-1 ATSR and on site measurements. In: *International Seminar on the Use and Applications of ERS-1 in Latin America*, Ed. T.D. Guyenne, ESA Conference Proceedings series, ESA SP-405: 241-246 (*)

Shirasago, B., García-Górriz, E., Font, J. (1997).- Detección de estructuras de mesoescala en el Mediterráneo occidental mediante imágenes SAR del ERS-1 y datos oceanográficos. En: *Teledetección: usos y aplicaciones*, Ed. J.L.Casanova, J.Sanz, Secr. Publicaciones e Intercambio Científico, Univ. Valladolid: 101-108 ISBN: 84-7762-693-6 (*)

Vázquez, J., Font, J., Martínez-Benjamín, J.J. (1996).- Observations on the circulation in the Alboran Sea using ERS1 Altimetry and Sea Surface Temperature data. *J. Phys. Oceanogr.*, 26 (8): 1426-1439 (*)

PRESENTATIONS TO SCIENTIFIC SYMPOSIA

European Geophysical Society XX General Assembly
1995, April, Hamburg (Germany)
"Sea surface altimetric analysis and geostrophic dynamics in the western Mediterranean"
D.Sánchez, J.J.Martínez Benjamín, J.Vázquez, J.Font, J.M.Redondo (poster)

IAPSO XXI General Assembly
1995, August, Honolulu (USA)
"Circulation of the Western Mediterranean from satellite altimetry using ERS-1 and TOPEX/POSEIDON data"
J.Vázquez, J.Font, J.J.Martínez Benjamín

VI Reunión Científica de la Asociación Española de Teledetección
1995, September, Valladolid (Spain)
"Análisis de datos altimétricos en el Mediterráneo mediante funciones ortogonales empíricas complejas"
C.Bouzinac, J.Vázquez, J.Font

Operational Oceanography and Satellite Observation
1995, October, Biarritz (France)
"Observations on the variability of the Algerian current using altimetric data"
C.Bouzinac, J.Vázquez, J.Font, J.J.Martínez Benjamín (poster)

Second Workshop of the Mediterranean Targeted Project
1996, February, Iraklion (Greece)
"Variability in the Algerian basin and Sardinia channel using altimetric and in-situ data"
C.Bouzinac, J.Font (poster)

Recent Advances in Turbulence II
1996, June, Barcelona (Spain)
"Study of the Algerian current variability by satellite altimetry"
C.Bouzinac, E.García-Ladona, J.Font

3rd ERS Symposium
1997, March, Florence (Italy)
"ERS-2 SAR near real time data used in the sampling strategy of an oceanographic cruise in the western Mediterranean"
O.Chic, J.Font, S.Sandven (poster)
"CEOF analysis of TOPEX/POSEIDON and ERS-1 combined altimetric data in the region of the Algerian Current"
C.Bouzinac, J.Font, J.Vázquez, C.Millot

European Geophysical Society XXII General Assembly
1997, April, Viena (Austria)
"ALGERS cruise, October 1996: an interdisciplinary study of a mesoscale instability of the Algerian current"
J.Font and ALGERS Team (poster)
"Lagrangian observations of the Algerian current"
J.Salas, E.García-Ladona, J.Font, C.Millot

VII Congreso de la Asociación Española de Teledetección
1997, June, Santiago de Compostela (Spain)
"The use of near real time infrared and SAR satellite imagery to update the sampling strategy of an

oceanographic vessel"
O.Chic, J.Font, S.Sandven

MTP-MATER WP2 Workshop
1997, June, Barcelona (Spain)
Interdisciplinary study of the Algerian basin mesoscale instabilities"
J.Font

NATO Advanced Study Course on Ocean Forecasting
1997, July, Oristano (Italy)
"Analysis of drifting buoys in the Algerian current"
J.Salas, E.García-Ladona, J.Font

7th Annual International TeraScan User's Conference
1997, September, Boulder (USA)
"Comparison between AVHRR real time and ERS-2 SAR near real time data in an oceanographic cruise in the western Mediterranean"
O.Chic, J.Font, Z.García

OCEANS'97 Marine Technology Society / IEEC
1997, October, Halifax (Canada)
"Comparison between AVHRR real time and ERS-2 SAR near real time data in an oceanographic cruise in the western Mediterranean"
O.Chic, J.Font, Z.García

International Conference: Progress in Oceanography of the Mediterranean sea
1997, November, Rome (Italy)
"The interdisciplinary study of the Algerian basin mesoscale instabilities: MATER - ALGERS'96 cruise"
The ALGERS'96 Group (poster)
"Kinematic analysis of drifting buoy trajectories in the Algerian current"
J.Salas, E.García-Ladona, J.Font, C.Millot (poster)

European Geophysical Society XXIII General Assembly
1998, April, Nice (France)
"Statistical analysis of the surface circulation in the Algerian current using Argos buoys"
J.Salas, E. García-Ladona , J. Font (poster)
"Application of Topex/Poseidon altimeter data for CEOF and along-track analysis in the Atlantic Ocean and western Mediterranean sea"
J.J.Martínez-Benjamin, A.Guasch, D.Sariñena, R.Corredor

XXXV Congrés-Assemblée Plenière de la Commission Internationale pour l'Exploration Scientifique de la Méditerranée
1998, June, Dubrovnik (Croatia)
"Circulation variability in the channel of Sardinia observed from in-situ and altimetric data"
C.Bouzinac, J.Font, C.Millot, J.Vázquez
"ALGERS cruise, October 1996: an interdisciplinary study of a mesoscale instability of the Algerian current (western Mediterranean)"
J.Font and the ALGERS Group
"Drifter and satellite thermal observations of the Algerian current in autumn and winter 1996-97"
J.Salas, E.García-Ladona, J.Font, C.Millot